THE STRUCTURE OF SOME ATLANTIC ISLANDS AS DEDUCED FROM GRAVITY AND OTHER GEOPHYSICAL DATA

A thesis submitted

for

the degree of Doctor of Philosophy

by

Duncan John Macfarlane, B.Sc., D.I.C.

December, 1968

Geophysics Department,
Imperial College,
London, S.W.7.

ABSTRACT

The results of reconnaissance gravity surveys on twenty-five of the Atlantic oceanic islands are presented. Digital computer programs are developed for processing of the gravity data, notably for terrain correction and density determination. Fourteen of these land gravity surveys are used in conjunction with nearby marine gravity and seismic refraction data, to study the subsurface structure of the islands. All the islands are volcanic structures formed at centres along deep fissures in the earth's crust. They are characterized by high Bouguer anomalies ranging from 125 - 289 mgal of which about one third comes from a primary volcanic pipe or high-level magma chamber. The islands can be divided into two groups on the basis of gravity field, crustal structure and depth of magma generation. Those on the Mid-Atlantic Ridge have lower maximum and regional Bouguer anomaly values; they rise from shallower water depths, above a thinner crust which is underlain by lower density mantle material; the magma for the islands on the Ridge is believed to be generated at shallow levels and volcanic centres are regarded as

intrusions of differentiated, fused mantle material, while the volcanic centres of the other oceanic islands are probably high-level reservoirs for magma which is generated deep in the mantle.

CONTENTS

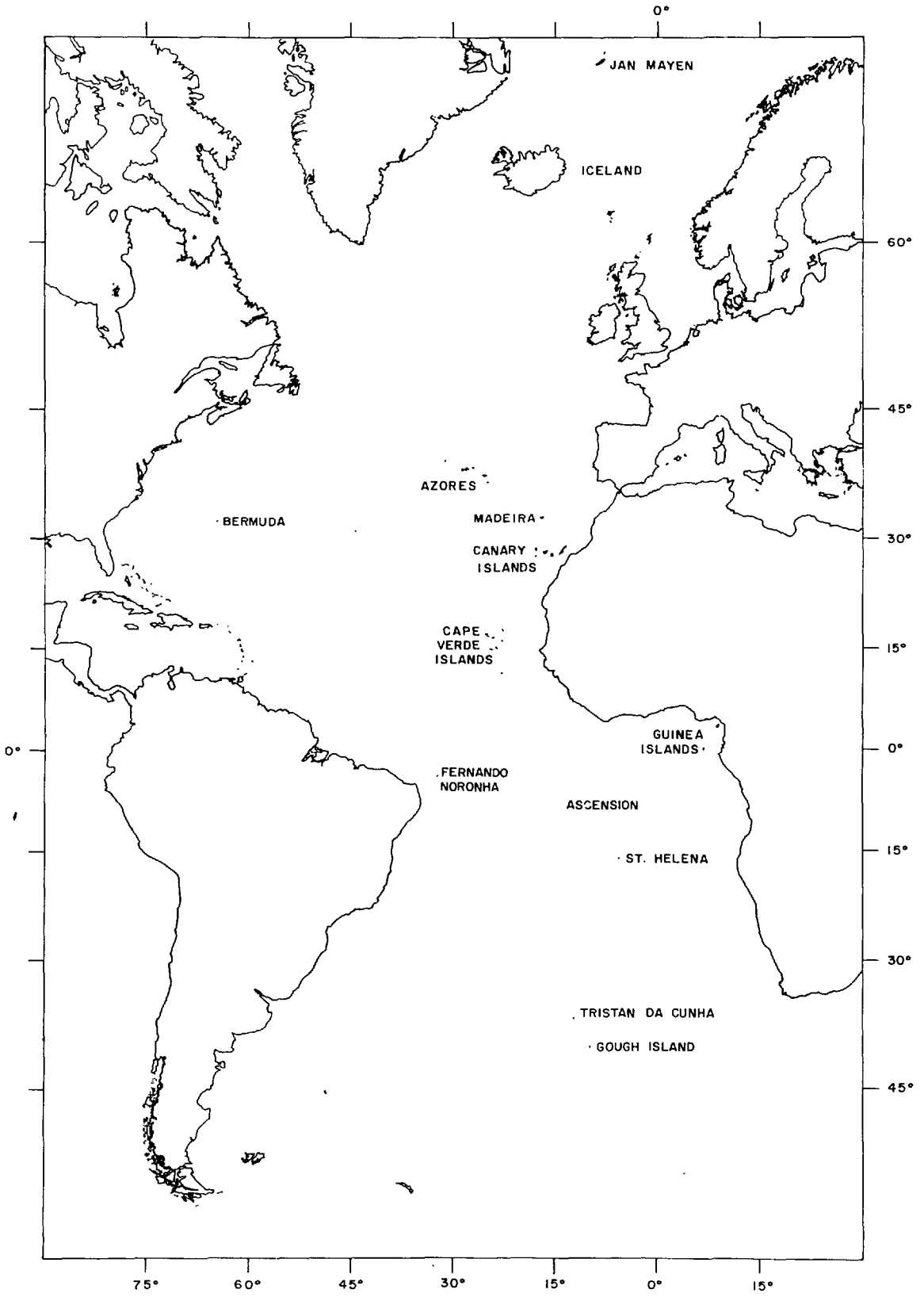

FIG. I-I. ATLANTIC ISLANDS

CHAPTER 1

INTRODUCTION

Oceanic islands were seized on by the early geologists as being the only accessible exposures of the vast area of the earth's surface that is covered by sea. While the rapid advances in marine geology and geophysics in recent years have brought the whole of the oceanic crust within direct or indirect reach, and have shown that the islands must be regarded rather as anomalies of the oceanic crust, scientific interest in these islands has increased rather than diminished. Much of this interest has been in the hope that study of the islands may indirectly yield information concerning the structure and history of the ocean basins but the islands are also regarded as of interest in their own right. In this thesis, an attempt is made primarily on the basis of original gravity data on many of the Atlantic islands named in Fig. 1.1 to define a common structure for oceanic islands and to deduce their possible evolution in the light of the known facts and present theories of the earth's crust.

In this introductory chapter, the geological environment of the islands, i.e. the Atlantic Ocean, is described and the

main facts and theories regarding oceanic islands are reviewed. The chapter closes with a brief summary of current theories of oceanic genesis and their bearing on the possible history of the islands.

1.1 Structure of the Atlantic Ocean Floor.

The structure of the ocean floor (see Fig. 1.2) can be considered in three main divisions : 1) the deep ocean basins, 2) the continental margins, and 3) the Mid-Atlantic Ridge.

1.1.1 The Deep Ocean Basins. These are large flat-bottomed areas of the deep-ocean floor lying between the continental margins and the Mid-Atlantic Ridge. Their smoothness appears to be due to a thick layer of sediments, since gravity and magnetic observations indicate that the sub-bottom relief is large. The small abyssal hills which border the basins on their seaward side are considered (Heezen et al, 1959) to represent the original topography buried beneath these abyssal plains.

Following current usage, the term "crust" is applied to the upper part of the lithosphere above the Mohorovicic discontinuity. At the Mohorovicic discontinuity or "Moho" the seismic velocities increase suddenly to 7.6 - 8.3 km/sec.

Worzel (1965b) presents from a compilation of all the seismic refraction data available up to 1964, an average crustal section for the ocean basins (see Fig. 2.7). This

FIG. I-2. Physiographic provinces in the Central Atlantic, after Heezen and Tharp, 1959 and 1961.

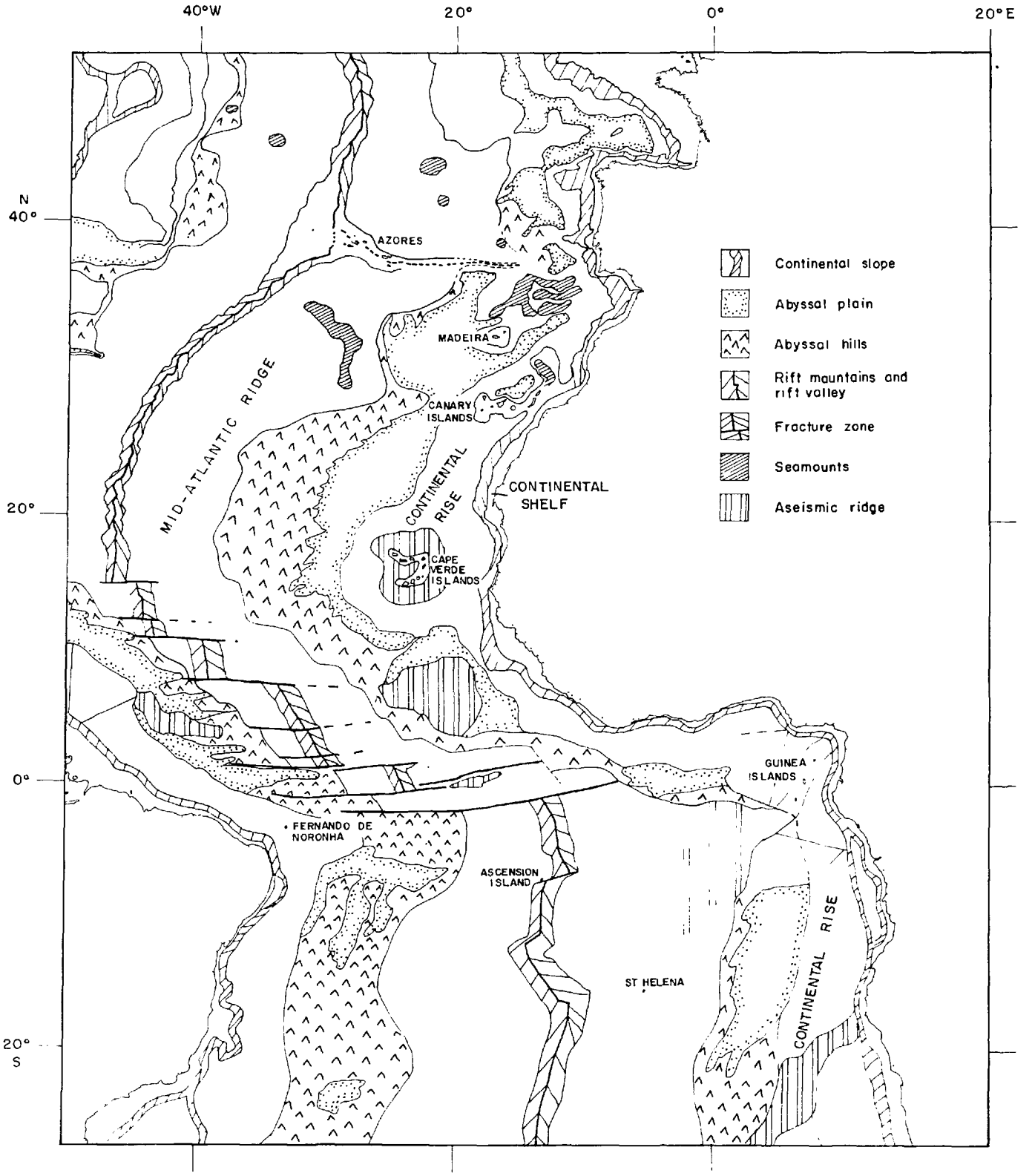

consists of 4.9 km of water, 0.7 km of sediments of density 2.3 gm/cc and velocity 2.5 km/sec, 1.7 km of layer 2, or "basement" of density 2.55 gm/cc and velocity 5.1 km/sec, and 4.2 km of layer 3 or "oceanic layer" of density 2.9 gm/cc and velocity 6.7 km/sec overlying mantle material of density 3.4 gm/cc and velocity 8.1 km/sec. Layer 2 is considered to be basalt (Hill, 1960) and layer 3 to be partially serpentinized peridodite (Hess, 1965; Nicholls, 1965). The total thickness of the ocean crust and the velocities for the different layers are markedly different from continental crust (Fig. 2.7).

1.1.2 Continental Margins. Adjoining the continents is the smooth gently-sloping continental shelf. Depths on the shelf are less than 450 metres and the width may vary from a few kilometres to over 350 km. The edge of the continental shelf is marked by a sharp increase in gradient as the relatively steep continental slope grades sharply down to about 2000 m. Below 2000 m a more gentle slope which Heezen et al (1959) have named the continental rise, links the continental slope to the abyssal plains at depths of greater than 7300 m (4000 fathoms). Except for submarine canyons and seamounts, the bathymetric relief is slight.

A summary of the structure of coastal margins by Worzel (1965a) indicates that the transition from continental crust of 20 - 30 km thickness to oceanic crust, occurs in a distance

of 100 - 200 km with the greatest part of the change occuring 30 - 50 km on either side of the 2000 m line. It appears that the continental-type basement layer wedges out towards the ocean with a major discontinuity in crustal structure at the base of the continental slope.

1.1.3 The Mid-Atlantic Ridge is part of a world-wide feature of mid-ocean ridges running through the Atlantic, Indian and Pacific Oceans. It is a broad rise 1000 - 3000 km wide occupying the centre third of the ocean and with its crest approximately following the median line of the ocean. The crest of the ridge rises 2 - 3 km above the ocean floor and while on average the rise is gently sloping, locally the relief may be very rough.

The Ridge can be separated into three structural units:- the Rift Valley, the High Fractured Plateau and the Flanks (Heezen et al, 1959). The crest of the Ridge is generally marked by a deep rift valley which is about 10 - 20 km wide at the bottom. The valley floor is rough and is bordered by peaks which rise 1000 to 2000 m above the level of the bottom. The depth to these crest peaks varies from about 1000 - 2000 m below sea-level. These peaks give way to high fractured plateaus where local relief is of the order of 500 - 1000 m. On either side of the plateau the flanks descend in a series of steps to join the abyssal hills.

The width of the individual zones varies considerably and the distinction between zones is not always clear. Even the rift valley is not always recognizable as a single well-developed valley. Topographic forms may also be confused by the east-west fractures and displacements which characterize the rise.

The crestal zone of the ridge may be considered to be defined by the 3000 m contour and within this region there is very little sedimentary cover even in the valleys (Ewing et al, 1966). On the flanks, the sediments are slightly thicker but are concentrated mainly in the valleys where they may be several hundred metres thick.

Dredge hauls from the peaks have obtained pillow olivine basalt-lava (Loncarevic et al, 1966) and metamorphic rocks have been dredged from the median valley (van Andel and Bowin, 1968) but the dominant rock type on the Mid-Atlantic Ridge is a tholeiitic basalt, (Engel and Engel, 1964). None of the dredged material was older than Tertiary and this is consistent with estimates of the ages of islands on the Mid-Atlantic Ridge.

The volcanic islands of Jan Mayen, Iceland, the Azores, St. Paul's Rocks, Ascension, Gough and Bouvet, and the Atlantis, Plato, Cruiser and Great Meteor seamounts all lie on the Ridge. These suggest that the Mid-Atlantic Ridge is an area of strong volcanic activity and this is supported by

heat-flow observations. High values of two to four times the average heat-flow in the Atlantic Ocean have been observed along a narrow band about 200 km wide centred on the crest of the Ridge (von Herzen and Langseth, 1966).

The crestal zone is also characterized by shallow focus (less than 60 km deep) earthquakes. Virtually all the seismic activity is concentrated in the rift valley.

1.2 The Oceanic Islands.

In this study a distinction is made between the oceanic islands and island arcs. The latter form arcuate groups located at or near continental margins, the shape being generally determined by the nearby coastal region. Typically the convex side faces seawards and is bordered by a deep trench with the islands capping parts of a submarine ridge on the concave side. Studies by Vening Meinesz (1948) and Worzel (1965a) suggest that these are linked to the continents in their structure.

The oceanic islands on the other hand, are purely oceanic features. They are, essentially, huge submarine volcanoes and represent only a small proportion of the several thousand marine volcanoes which are widely distributed throughout the oceans. The volcanoes which have never developed sufficiently to break the surface of the sea are termed seamounts. The bedrock of the seamounts is generally

basalt and their shapes are similar to volcanic archipelagoes. Guyots are flat-topped seamounts that are considered to be the roots of islands which have been truncated by wave erosion, before or during subsidence. Where conditions favour the growth of coral, an atoll may be formed as the island subsides.

The oceanic islands may be isolated, e.g. Fernando de Noronha; in small groups, e.g. Tristan da Cunha, Inaccessible and Nightingale; or part of a chain, e.g. the Azores Islands. The areas of the islands investigated in this report range from 18 square km for Fernando de Noronha to 2058 sq km for Tenerife. The maximum sub-aerial elevation ranges from about 300 m to 3718 m. The islands rise steeply from the sea floor and their total height including the submarine portion may be over 7000 m for the islands not on the Mid-Atlantic Ridge. The depth of the ocean floor is much less on the Ridge and the overall height of the islands there does not exceed 4000 m.

The dominant sub-aerial rock-type on the islands is olivine alkaline basalt. The subordinate rock types are largely alkali-andesite, rhyolite, trachyte, phonolite and salic pumice. Dredge hauls from the deep flanks of the islands and from the surrounding sea-floor yield samples of tholeiitic basalt. Engel et al, (1965), were prompted by these facts to suggest that these rocks represent successive

differentiation products of a primary magma. The suggested sequence of differentiation is primary magma → tholeiite → alkali basalt → andesite, rhyolite, trachyte, etc. McBirney and Gass (1967) noted that the degree of silica saturation of the basalts and the differentiatiates, decreases with distance from the Mid-Atlantic Ridge and shows a strong correlation with heat-flow from the ocean floor. They were lead to suggest that the magma is generated at shallow depths under the Ridge and at considerably greater depths in areas remote from the Mid-Atlantic Ridge.

The estimated maximum age of outcrop on any of the islands is Cretaceous and with the exceptions of the Cape Verde and Guinea islands, none of the islands appears to be older than Miocene. A remarkable feature is the occurrence of historic volcanic eruptions within almost every one of the groups of islands regardless of the apparent age of the group.

Darwin (1842) considered that subsidence was part of the normal development of oceanic islands irrespective of fluctuations in sea-level and the investigations of Wilson (1963b) suggested a rate of subsidence of 4 - 50 m/million years. Evidence of uplifted marine terraces and marine fossils on many of the Atlantic islands indicates that they appear to emerge after having subsided. Wilson (1963b) suggests tectonic disturbances as the cause of this unusual behaviour.

Much detailed geological work has been carried out on the surface of islands but it must be remembered that the accessible sub-aerial portion of the island forms less than five per cent of the total volume of the island volcano. In investigating the bulk of the island which lies underwater, earth scientists have turned with increasing success to geophysical methods.

One of the first geophysicists to turn his attention to oceanic islands was Vening Meinesz (1948) who made many measurements of the gravity field on and around islands. Assuming crustal densities of 2.937 and 3.07 gm/cc he calculated the isostatic anomalies for nine different islands for various crustal models and chose as correct that model which gave the smallest isostatic anomaly. This method lead him to conclude that of the Atlantic islands, Faial, S. Miguel and Tristan da Cunha were isostatically compensated by local variations in crustal structure, while Madeira, the Canary Islands, the Cape Verde Islands and Bermuda were regionally compensated on a scale measured in several hundreds of kilometres. It is of interest to note that the islands of the former group lie on the Mid-Atlantic Ridge and that those of the latter lie remote from it.

Woollard (1951) with a gravity survey of the island of Oahu in the Hawaiian islands, was perhaps the first to attempt the detailed investigation of the substructure of an oceanic

island. In his interpretation he adopted a mean specific gravity of 2.3 for the island block, on the basis of Nettleton's (1939) profiling method. With the help of marine pendulum gravity stations around the island he deduced a 500 km-wide regional minimum of - 70 milligals under the island that he suggested might be due to a combination of subsidence and the presence of a sub-crustal magma chamber. The gravity field on the island indicated a local anomaly of + 110 milligals associated with a major volcanic vent. This he interpreted as the effect of a plug of solid magmatic material, density 2.9 gm/cc and diameter 6 km extending to a depth of 8 km.

Since then gravity surveys have been made of many oceanic islands mainly in the Pacific Ocean. In his summary of the results from the Pacific Ocean island surveys, Woollard (1964) noted that one third of the total gravity field comes from primary volcanic pipes but that these pipe features are not present in every case. The observed Bouguer anomaly ranges from + 164 to + 330 milligals, the higher values occurring where the pipe effect is present.

From the early 1950's, gravity surveys have been supplemented by seismic refraction studies of islands and atolls (Officer, 1952; Raitt, 1954), and by airborne magnetic surveys, (Malahoff and Woollard, 1966). All these methods have been applied in the Hawaiian Islands where extensive geophysical investigations under the auspices of the Hawaiian

Institute of Geophysics and the University of Hawaii have revealed many features of the sub-structure of these islands. These Hawaiian studies represent the only systematic geophysical investigation of oceanic islands yet available. Despite the considerable differences between the islands of the Pacific and of the Atlantic oceans, the results from Hawaii provide a useful starting point in considering the Atlantic islands.

The Hawaiian Islands are the surface expression of a much larger submarine ridge known as the Hawaiian Swell, which consists of a pile of tholeiitic lavas 10 km thick and 2000 km long. On the basis of the observed seismic velocity, a density of 2.75 gm/cc is assigned to the bulk of the ridge as being submarine lava flows, (Strange et al, 1965). Seismic refraction and gravity data reveal that the crust has subsided under the load of this extruded material by some 2 - 3 km, giving rise to an upper layer 2 - 3 km thick of material which has been erupted above or near sea-level. This layer is assigned a specific gravity of 2.6, also from the observed compression wave velocity. The sub-aerial parts of the islands are considered to have an average bulk-density of 2.3 gm/cc.

Very large gravity and magnetic anomalies indicate rift zones and primary volcanic pipes extending downward at least to the Moho. Seismic refraction measurements over these

features have observed compression wave velocities similar to that of mantle material at depths as shallow as 1.8 km (Furumoto et al, 1965). It is concluded (Strange et al, 1965; Malahoff and Woollard, 1966) that the Hawaiian Swell and Islands have resulted from intrusions from the mantle along faults oriented either east-west or north-west south-east. At certain points, these intrusions escaped to the surface to provide the primary source of volcanic material. The estimated dimensions of the volcanic pipes which are possibly formed at the intersections of rifts of the two systems, range from 4 - 20 km in diameter and from 2 - 20 km in vertical length. Malahoff and Woollard (1966) consider that these may be composite volcanic plugs but the very high seismic velocities have also lead to the suggestion that they may be intrusions of mantle material.

Macdonald (1965) suggests a magma rich in olivine crystals and that the dense core indicated by seismic and gravity results may be cumulate material formed by the crystals lagging behind as the more fluid magma rise into a high-level magma chamber. The mass of this ultra-dense core will exert an outward pressure on the lower part of the confining structure, which may be sufficient to cause a splitting open of the volcano as a whole including one or more rift zones and the summit region. The fluid magma can then escape along these fissures, emptying the high level

magma reservoirs. Macdonald proposes the collapse of the summit into the void thus created as a possible mechanism of caldera formation.

Hypotheses of possible island sub-structure have been proposed from geological observations of the form of volcanoes on the continents and from the study of lavas erupted in an aqueous environment.

Nayudu (1962) proposes a three-stage development for submarine volcanoes:-

1) Fluid lava is erupted from fissures on the sea-floor to form a mound of tuff and breccia.
2) This mound is then intruded by later magma to form dykes, sills or laccolith-like bodies within the tuff, and more tuff and breccia where lava is extruded into the sea.
3) The sequence may stop there but is more likely to be repeated several times to form a composite body with a core containing a high proportion of solid lava surrounded by flanks of tuff, breccia and volcanic debris.

From the study of intra-glacial volcanoes on Iceland, Jones (1966) suggests that volcanic eruptions in deep water result in the quiet effusion of lava consisting entirely of pillow lavas and breccias forming cones with steep slopes of up to 30°. He considers that eruptions in shallow water or

just above sea-level are explosive and result in the formation of vitric tuffs. Because of the steep flanks of the pillow lava, gravitational collapse will occur very readily so that the eventual structure will be that of a core of pillow lavas surmounted and flanked by layers of basalt breccia and vitric tuff.

A feature common to both hypotheses is a core of higher density and evidence for such a core has been provided by seismic refraction observations on atolls in the Pacific, (Raitt, 1954, 1957) and on seamounts in the Atlantic (Laughton et al, 1960; Worzel, 1959).

Interpretations of island structure in this report are based very largely on gravity surveys. In view of the inherent ambiguity of gravity data, the above hypotheses and the results collected on the Hawaiian Islands are used as a framework for the interpretation of the gravity data from the Atlantic islands.

1.3 Theories of Oceanic Genesis.

It is necessary to consider the history of oceanic islands in the light of current theories of the origin of oceans and continents. In the last half-century, the focus of such theories has been the concept of continental drift. This concept has been examined at length in two recent volumes (Continental Drift; Editor S.K. Runcorn, Academic

Press, 1962; Symposium on Continental Drift, Phil. Trans. Roy. Soc. Ser A. 258, 1965, Editors Blackett, P.M.S., Bullard, E., and Runcorn, S.K.) and in recent review articles (Wilson, 1963a; Hurley, 1968) and it is proposed to give here only a brief outline of present ideas, concentrating on aspects of particular relevance to the Atlantic Ocean.

Several nineteenth century geologists, e.g. Snider (1858), were lead by the continuity of structure and stratigraphy on the opposing Atlantic margins to suggest that the Americas and Europe and Africa are the formerly contiguous parts of a much larger continental mass. However, it was not until F.B. Taylor in the U.S.A. in 1908 and A.L. Wegener in Europe in 1910 independently published theories of continental drift that the concept really gained widespread interest. In the years of vigorous geological debate which ensued, a mass of evidence has accumulated from many branches of the science and this evidence has been admirably reviewed by Westoll (1965). He concludes that "purely geological evidence piece by piece can neither prove nor disprove drift. The most useful information comes from the convergent evidence of many independent facts that may individually be regarded as having only a modest probability of being due to drift, but which in combination can hardly be explained in any other way."

One of the strongest arguments for movement of the continents arises from recent studies of rock magnetism. Results from palaeomagnetic measurements on rocks of the same ages on the different continents indicate that the continents have moved with respect to the present position of the magnetic pole and that they have moved independently of each other. The motions inferred are in accord with the older, purely geological evidence pointing to drift.

Wegener, in his theory of continents as rafts of sial floating on a sea of sima like icebergs in the ocean, failed to suggest a convincing mechanism to cause the break up and movement of the continents and the difficulty of finding such a mechanism which is compatible with the observed physical properties of the crust and mantle is the major weakness in the hypothesis of continental drift, (Jeffreys, 1952; Macdonald, G.J.F, 1965).

The most plausible mechanism is that of convection currents within the mantle as suggested by Holmes (1928), Griggs (1939) and Vening Meinesz (1948). This principle has been developed and refined by Dietz (1961) and Hess (1962). The convection currents, driven by radiogenic heating, are considered to be confined to the upper few hundred kilometres of the mantle. Hess (1965) suggests that they extend to a depth of 750 km, the vertical extent of earthquake foci. The hot current of the proposed convection cell rises to the

surface, producing uplift due to decrease in density by partial fusion and thermal expansion (Bott, 1965) to form ridges such as the Mid-Atlantic Ridge. At the surface the current splits and moves away from the ridge with equal velocity in both directions inducing tension and rifting along the ridge crest. Estimates of the velocity of horizontal translation are in the range of 1 cm/yr to several cm/yr.

The oceanic crust is considered to be a serpentinized peridodite, a hydrated form of upper mantle material (Hess, 1965; Nicholls, 1965). The convection theory supposes that new crust is generated by volcanism and dyke injection at the crest of the mid-oceanic ridges and is transported away from the ridges by the convection currents as it is formed.

Menard (1964) suggests that the crust is moved by viscous drag from the more rapidly flowing mantle convection current. By this theory, crustal buckling will occur where the convection current reaches the continent.

In the theory of Hess (1965) the newly formed oceanic crust moves away from the ridge at the same velocity as the underlying convection current until it reaches the downward flowing limb of the convection cell where it is resorbed by dehydration in the mantle. The location of the downflowing limb is considered to be indicated by the compressional features of the earth's crust, the recent mountain belts, deep trenches, island arcs, and deep earthquakes. By this

concept the trailing edge of a drifting continent remains undeformed but the leading edge becomes deformed when it reaches the downward flowing limb of the convection cell, e.g. the entire western cordillera of the Americas. In this respect the theory of Hess provides the better explanation for the observed features in the Atlantic Ocean.

The hypothesis of continental drift driven by mantle convection has been used to explain most of the observed features of the oceans: the mid-ocean ridges as zones of uplift, volcanism, shallow focus earthquakes and tension; the existence of transcurrent faults on the mid-ocean ridges (Wilson, 1965); the maintaining of the oceanic trenches out of isostatic equilibrium (Vening Meinesz, 1948); the lack of old rocks in the Atlantic ocean and the very small thickness of sediment on the Mid-Atlantic Ridge (Ewing and Ewing, 1967); the geological youth of oceanic islands, and sea-bottom cores and samples and their apparent increase in age with distance from the crests of the mid-ocean ridges (Wilson, 1963a); the high heat flow anomaly and low Bouguer anomaly over the mid-ocean ridges; and finally the linearity of the magnetic anomaly patterns parallel to the ridges (Vine and Matthews, 1963). This last feature, the linear magnetic pattern first detected by Mason and Raff (1961), has lead to results so striking that they have been hailed by Hurley (1968) as "the confirmation of continental drift."

Studies of rock magnetism have shown that the polarity of the earth's magnetic field has reversed many times at certain fixed times in the past and from measurements of the magnetism in basaltic rocks, Cox, Doell and Dalrymple (1964) proposed a reversal time scale for the last four million years. Vine and Matthews (1963) suggested that as the new crust generated at the crest of the mid-oceanic ridge, cools through the Curie temperature, it will be magnetized in the current direction of the earth's magnetic field. Then if crustal spreading is taking place, this crust will drift outward from the ridge. resulting in strips of alternately normal and reversely magnetized material parallel to the ridge. This theory was able qualitatively to explain the observed linear anomalies parallel to and symmetrical about the axis of the ridge.

The enthusiasm of Hurley (1968) was aroused by recent work which has been able to test quantitatively the predictions of the Vine and Matthews theory. Pitman and Heirtzler (1966) and Vine (1966) assumed the reversal time scale of Cox et al (1964) and a suitable rate of crustal spreading and computed magnetic anomaly profiles across the mid-ocean ridge crest according to the Vine and Matthews model. The agreement of the computed anomaly with the observed anomaly for several crossings of the mid-ocean ridge system is remarkable and the rates of drift which give the best correlation are

consistent with those required to account for continental drift. The results appear to indicate that crustal spreading rates vary along the length of the mid-ocean ridge system by at least a factor of four.

It is considered (Tozer, 1965; Ewing and Ewing, 1967) that the rate of radiogenic heat generation in the mantle is inadequate to maintain continuous convective motion and that convection will be intermittent with an active phase separating periods of quiescence several times longer. This hypothesis has been proposed as an explanation of the discontinuity of sediment thickness on the mid-ocean ridges. The axial portion of the ridges is characterized by a 100 - 400 km wide belt where the sedimentary cover is very thin and the width of this belt appears to relate to the spreading rate as determined by the magnetic methods of Vine, and Pitman and Heirtzler.

It has also been argued that there are more fundamental changes in convective motion of much longer period. Sutton (1963) has given these slower cycles the name of chelogenic zones: "a sequence of events controlled by mantle convection currents which begins with widespread orogenic events and passing through a period of drift dispersal and regrouping of the continental masses ends with a quiescent interval before the inception of the succeeding cycle." Runcorn (1962) has suggested that these longer cycles commence with a change

in the mantle convection pattern as a result of the increase in radius of the earth's core by separation of iron towards the centre.

Mantle convection is not the only proposed mechanism for continental movement. Several earth-scientists have considered the expansion of the earth as a possible cause of movement (Carey, 1958; Egyed, 1957; Heezen, 1962). By this theory, at an early stage of the development of an expanding earth, a sialic crust differentiated to form a solid, originally continuous, crust over the surface of the earth. Continued expansion disrupted this crust and the sima welled up into the gradually widening cracks. The sial blocks maintained approximately the same surface area and the sima solidified where it reached the surface to form the floor of a slowly widening ocean with continuous formation of new oceanic crust at the fractures in the crust along the median line of the oceans.

The fit of the continents on the surface of an earth of half the present radius is very good (Creer, 1965) but in other respects this theory does not account for as many of the observed features of the earth's crust as does the convection current hypothesis. The most telling objection to the expansion concept is that of time scale. According to the geological evidence, the whole Atlantic Ocean opened in the last 200 MY or so, but there is no known mechanism to

provide this rate of expansion. Also, palaeomagnetic results from Europe and Siberia (Cox and Doell, 1961) indicate that the radius of the earth has changed not at all or only very slightly since the Permian times.

While it may be premature to state that continental drift does occur and that the continental movement is due to convection currents in the upper mantle, this hypothesis does present the most convincing explanation of an increasing number of the observed features of the earth's crust.

1.4 History of the Atlantic Ocean.

If continental drift is assumed, the Atlantic Ocean is the archetypal example of an ocean formed by the splitting apart of a continental mass and an attempt has been made to trace the history of the ocean back to the Pre-Cambrian. Wilson (1966) suggests from geological evidence, that from the late Pre-Cambrian until the Middle Ordovician an open ocean existed in approximately the position of the present Atlantic Ocean. This ocean he considers to have closed by stages over about 100 MY and that from the Permian to the Jurassic no deep ocean existed in the North Atlantic region. The present Atlantic Ocean started to open in the Cretaceous along slightly different lines from before. This latter date is deduced from the continuous marine facies dating from earliest Cretaceous times which are exposed on the

Cape Verde Islands. This estimate is in reasonable agreement with the dates of 250 MY ago for the commencement of rifting and 190 MY for the first North Atlantic ocean basin deduced by Ewing et al (1966) from the ages of sediment cores from the ocean floors. It is quite possible that the continental separation was not synchronous along the length of the American-Eurafrican rift.

There have been attempts to deduce the more recent history of ocean spreading from the discontinuity in sediment distribution, age of outcrop and magnetic anomaly observed at the margins of the crestal region of the Mid-Atlantic Ridge. Van Andel and Bowin (1968) consider that spreading ceased prior to the Upper Miocene and recommenced in recent times after a long period of tectonic tranquillity. This hypothesis is on a time scale slightly different from a similar view expressed by Ewing and Ewing (1967) who suggested that the present cycle of spreading began 10 MY ago following a long period of quiescence estimated at 40 MY long.

The magnetic studies of Vine (1966) indicate spreading rates along the Mid-Atlantic Ridge of 0.95 cm/yr just south of Iceland and 1.9 cm/yr at 38°S. These contrast with the considerably higher estimates for the rate on the East Pacific Rise (4.4 cm/yr) and on the Pacific-Antarctic Ridge (4.5 cm/yr; Pitman and Heirtzler, 1966).

Wilson (1963a) was the first to note that the ages of the oceanic islands and of sediment cores from the ocean floor seem to increase with distance from the crest of the Mid-Atlantic Ridge. He proposed that the oceanic islands may be formed at the crest of the ridge and carried outwards on the continuously foundering flanks to the abyssal plain. By this theory and assuming steady state spreading, it is then possible to compute drift rates from the estimated ages of the islands and their distance from the Ridge. This test of the theory is severely handicapped in that age estimates for the islands are based on subaerial outcrops and thus may be much less than the age of origin of the entire island volcanoes. However, Vogt and Ostenso (1967) conclude from a detailed study of islands and guyots that the agreement of drift rates computed on Wilson's hypothesis with those deduced by other methods, is such as to lend considerable support to this theory.

Two possibilities have been put forward for the origin of islands in the area of new crust formation at the ridge crest. The first envisages a volcanic source located permanently at the crest and the lateral drift carrying volcanic piles off the ridge as they are formed. The second hypothesis is that the source of magma generated in the crestal region may move away from the ridge, so prolonging active volcanism for some distance from the ridge. Of the

two theories, the Recent volcanism on many islands remote from the Mid-Atlantic Ridge must favour the latter.

Clearly theories of the geological history of the Atlantic Ocean and of the islands therein remain fairly speculative. In this thesis, some of these theories are examined in the light of data from the Atlantic islands and are at the same time used to give direction to ideas of the origin and development of the oceanic islands.

CHAPTER 2

FIELD OPERATIONS AND DATA PROCESSING

2.1 Field Operations.

Field operations were adapted to suit the facilities available on each island and so vary in detail, but the general procedure followed the lines described below.

The surveys were of a reconnaissance nature only and in most cases the time available was limited. To obtain the best coverage, therefore, automobile transport was used, and stations were located close to the road wherever possible. The spacing between stations varied from one half to four kilometres. Where possible, stations were established at bench marks or spot heights, and when these were absent, at some point readily identifiable on the maps, such as road junctions and bridges.

On ten of the islands, maps on a scale of 1 : 25,000 or larger were used. These were recently compiled maps of good quality and with them it was possible to locate stations to better than 20 metres. Elevations were taken from the same maps, which were contoured at 10 metre intervals, or by reference to sea-level at coastal stations and, except where

the topography is very abrupt, are accurate to ± 10 m. On the other islands, Santa Maria, S. Miguel and Gran Canaria, elevations were determined by altimeter, resulting in much poorer elevation control, perhaps only ± 20 m for some stations.

Gravity measurements were carried out using Worden Geodetic gravimeter No. 241, which has a scale constant of 0.0851 (5) mgal/scale division. Drift control readings were made at the same station at the beginning and end of each day's operations and the observed values corrected on the assumption of linear drift. Temperature effects contributed largely to the observed drift and varied with the climatic conditions during the survey. On the Azores in winter, drift was less than 0.2 mgal/day, but in the large temperature range encountered in the Canary Islands in summer it sometimes reached 0.6 mgal/day. This drift may not be linear but the error involved in assuming linearity will not be more than 0.2 mgal.

On islands where a previously established gravity base was known to exist, this base was reconnected to continental bases and used in the survey. On the other islands, a new base station was established by connections either from continental bases or other island base stations.

2.2 Data Reduction.

The gravity contour map presented for each island is based on the Bouguer anomaly values at the established stations. In all cases, sea-level is chosen as the datum elevation and all the measured data are corrected relative to this plane. The corrections are an attempt to remove from the measured values various large influences whose causes are accurately known.

The first such influence is the variation of the gravitational field with latitude. Values of the theoretical gravity g_n for each station were calculated from the International Gravity Formula (Nettleton, 1940)

$$g_n = 978.0490\ (1 + 0.0052884\ \sin^2\phi - 0.0000059\ \sin^2 2\phi)$$

where ϕ is the latitude.

The "free-air" correction accounts for the decrease in the gravity field with increasing elevation, i.e. increasing distance from the centre of the earth. This correction varies slightly with the radius of the earth but may, with sufficient accuracy, be taken to be equal to 0.3086 mgal/m.

The simple Bouguer correction takes into account the attraction of the material between the datum and the individual station. This correction considers the effect as being due to an infinite slab of material between each station and the reference elevation. It is equal to $2\pi\rho Gh$, where G is the gravitational constant, ρ is the density and h the height

of station above datum, and is always opposite in sign to the free-air correction.

The choice of a value for the density in the Bouguer correction is not a simple matter and is discussed at length in Chapter 3. In practice the elevation correction in all cases was made using a mean density of 2.3 gm/cc for the islands.

Since both the free-air and simple Bouguer corrections are simple constants multiplied by the elevation differences, it is common practice to combine the two effects into a single factor, known as the elevation factor. For a density of 2.3 gm/cc, this factor is equal to

0.2123 mgal/m or 0.06471 mgal/ft.

On all the islands, the topography is rugged and for most stations departs considerably from the flat sheet assumed on the simple Bouguer correction. This can lead to large errors if not taken into account. The usual procedure for calculating the effect of rough terrain is the zone chart method which was presented by Hammer (1939). This chart is drawn on a transparent sheet to the same scale as the topographic map and is superimposed on the map with its centre at the gravity station to be corrected. The average elevation in a zone relative to the station is determined and the effect of the zone, in milligals, is taken from a set of tables.

The above procedure for terrain corrections was adopted for half the islands surveyed, using the chart and tables presented by Bible (1962). Since the elevations on the maps used were all in metres, the tables were converted to the metric system and also extended to include some of the very large elevation differences found in the islands surveyed. This table is included as Table 2.1. Bible's tables allow correction for the topographic effect out to Hammer zone M, i.e. out to 22 km. In the case of islands, which generally stand 3 - 5 km above the surrounding sea-floor, the correction for the bathymetry beyond zone M is considerable, so, still using a flat earth approximation, tables were prepared to extend the corrections to 239 km, beyond which any contributions from topography amount to less than 4 mgal. This table is presented as Table 2.2. It should be noted that the Hammer zones differ in radii from those of Hayford and Bowie (1912).

Both the Bouguer correction and the terrain correction neglect the curvature of the earth and it is appropriate to consider the error this introduces. Hayford and Bowie (1912) have shown that sufficient accuracy can be maintained if the earth be assumed flat up to the outer radius of their zone L (28.8 km) and if the sea-level surfaces in zones M (28.8 - 58.8 km), N (58.8 - 99.0 km) and O (99.0 - 166.7 km) are also considered flat parallel planes but 500 ft, 1600 ft, and

TABLE 2.1 TERRAIN CORRECTION TABLE FOR GRAVITY OUT TO 21.95 KILOMETRES (METRIC SYSTEM)

ZONES	B	C	D	E	F	G	H	I	J	K	L	M
COMPARTMENTS	4	4	8	16	16	16	16	16	16	16	16	16
INNER RADIUS (M)	2.0	16.6	53	170	390	895	1530	2615	4469	6652	9903	14742
OUTER RADIUS (M)	16.6	53.3	170	390	895	1530	2615	4469	6652	9903	14742	21945
CORRECTION IN MGAL	PLUS OR MINUS THE ELEVATION IN METRES											
0.00	0	2	6	16	25	45	59	77	114	139	169	207
0.005	1	4	10	29	44	78	102	134	197	240	293	358
0.01	2	6	15	42	63	111	145	190	279	340	415	507
0.02	2	7	19	54	81	144	188	245	361	440	537	655
0.03	3	9	23	65	97	171	223	291	427	521	635	775
0.04	4	10	26	74	110	194	253	330	485	591	720	879
0.05	4	12	30	83	122	215	280	365	536	653	797	972
0.06	5	13	32	91	134	235	305	397	583	711	867	1057
0.07	6	14	35	98	144	253	328	427	627	764	931	1135
0.08	7	15	38	106	154	270	350	455	668	814	992	1209
0.09	8	17	40	113	163	286	370	482	707	861	1049	1278
0.10	9	18	43	120	172	301	390	507	744	905	1103	1344
0.11	10	19	45	126	181	316	409	531	779	948	1155	1407
0.12	11	20	48	133	189	331	427	554	813	989	1204	1467
0.13	12	21	50	139	198	344	444	576	845	1028	1252	1525
0.14	13	22	53	146	206	358	461	598	877	1066	1298	1581
0.15	15	23	55	152	213	371	477	618	907	1102	1342	1635
0.16	16	25	57	158	221	384	493	639	936	1138	1385	1687
0.17	18	26	60	164	228	396	509	658	965	1173	1427	1738
0.18	20	27	62	171	236	409	524	677	993	1206	1468	1788
0.19	22	28	64	177	243	421	539	696	1020	1239	1507	1836
0.20	25	29	66	183	250	432	553	714	1047	1271	1546	1883
0.21	29	31	69	189	257	444	567	732	1073	1302	1584	1928
0.22	33	32	71	195	264	455	581	750	1098	1333	1621	1973
0.23	38	33	73	202	271	467	595	767	1123	1363	1657	2017
0.24	45	35	76	208	278	478	608	784	1148	1392	1692	2060
0.25	54	36	78	214	284	489	622	800	1172	1421	1727	2102

TABLE 2.1 TERRAIN CORRECTION TABLE FOR GRAVITY OUT TO 21.95 KILOMETRES (METRIC SYSTEM)

ZONES	B	C	D	E	F	G	H	I	J	K	L	M
COMPARTMENTS	4	4	8	16	16	16	16	16	16	16	16	16
INNER RADIUS (M)	2.0	16.6	53	170	390	895	1530	2615	4469	6652	9903	14742
OUTER RADIUS (M)	16.6	53.3	170	390	895	1530	2615	4469	6652	9903	14742	21945
CORRECTION IN MGAL	PLUS OR MINUS THE ELEVATION IN METRES											
0.26		37	80	221	291	500	635	816	1195	1449	1761	2143
0.27		39	83	227	297	510	648	832	1218	1477	1795	2184
0.28		40	85	233	304	521	660	848	1241	1504	1828	2223
0.29		42	87	240	310	531	673	864	1264	1531	1860	2263
0.30		43	90	247	317	542	685	879	1286	1558	1892	2301
0.31		45	92	253	323	552	697	894	1308	1584	1923	2339
0.32		47	95	260	330	562	710	909	1329	1610	1954	2376
0.33		48	97	267	336	573	721	924	1351	1635	1985	2413
0.34		50	100	274	342	583	733	938	1372	1660	2015	2450
0.35		52	102	281	349	593	745	953	1392	1685	2044	2485
0.36		54	105	288	355	603	757	967	1413	1709	2074	2521
0.37		56	108	295	361	613	768	981	1433	1733	2102	2555
0.38		58	110	302	367	622	779	995	1453	1757	2131	2590
0.39		60	113	310	374	632	791	1008	1473	1780	2159	2624
0.40		62	116	317	380	642	802	1022	1493	1804	2187	2657
0.41		65	119	325	386	652	813	1035	1512	1827	2215	2691
0.42		67	121	333	392	661	824	1049	1531	1849	2242	2723
0.43		70	124	341	399	671	835	1062	1550	1872	2269	2756
0.44		73	127	349	405	681	846	1075	1569	1894	2295	2788
0.45		76	130	357	411	690	857	1088	1588	1916	2322	2820
0.46		79	133	366	417	700	867	1101	1606	1938	2348	2851
0.47		82	136	374	423	709	878	1114	1625	1960	2374	2882
0.48		86	140	383	430	719	889	1126	1643	1981	2399	2913
0.49		90	143	392	436	728	899	1139	1661	2003	2425	2944
0.50		94	146	402	442	738	910	1151	1679	2024	2450	2974

TABLE 2.1 TERRAIN CORRECTION TABLE FOR GRAVITY OUT TO 21.95 KILOMETRES (METRIC SYSTEM)

ZONES	B	C	D	E	F	G	H	I	J	K	L	M
COMPARTMENTS	4	4	8	16	16	16	16	16	16	16	16	16
INNER RADIUS (M)	2.0	16.6	53	170	390	895	1530	2615	4469	6652	9903	14742
OUTER RADIUS (M)	16.6	53.3	170	390	895	1530	2615	4469	6652	9903	14742	21945
CORRECTION IN MGAL	PLUS OR MINUS THE ELEVATION IN METRES											
0.51			149	411	448	747	920	1164	1697	2045	2475	3004
0.52			153	421	454	757	931	1176	1714	2065	2500	3033
0.53			156	431	461	766	941	1188	1732	2086	2524	3063
0.54			160	441	467	776	951	1200	1749	2106	2548	3092
0.55			164	452	473	785	961	1213	1766	2127	2573	3121
0.56			167	463	479	794	972	1225	1784	2147	2596	3149
0.57			171	474	485	804	982	1236	1801	2167	2620	3178
0.58			175	485	492	813	992	1248	1818	2187	2644	3206
0.59			179	497	498	823	1002	1260	1834	2206	2667	3234
0.60			183	509	505	832	1012	1272	1851	2226	2690	3262
0.61			188	522	511	841	1022	1283	1868	2245	2713	3289
0.62			192	535	518	851	1032	1295	1884	2264	2736	3317
0.63			197	548	524	860	1042	1306	1901	2284	2759	3344
0.64			201	562	530	870	1052	1318	1917	2303	2781	3371
0.65			206	576	5	879	1062	132	1933	2322	2804	3398
0.66			211	591	543	888	1071	1341	1949	2340	2826	3424
0.67			216	606	550	898	1081	1352	1965	2359	2848	3451
0.68			221	622	556	907	1091	13	1981	2378	2870	3477
0.69			227	639	563	917	1101	13	1997	2396	2892	3503
0.70			232	656	570	926	1110	13	2013	2414	2913	3529
0.71			238	674	576	936	1120	1396	2029	2433	2935	3554
0.72			244	693	583	945	1130	1407	2044	2451	2956	3580
0.73			251	713	590	955	1139	1418	2060	2469	2978	3605
0.74			257	733	596	964	1149	1429	2075	2487	2999	3631
0.75			264	755	603	974	1159	1440	2091	2505	3020	3656

TABLE 2·2 TERRAIN CORRECTION TABLE, 21.95 TO 238.79 KILOMETRES

ZONES	N	O	P	Q	R	S
COMPARTMENTS	16	16	16	16	16	16
INNER RADIUS (KMS)	21.95	32.67	48.63	72.39	107.75	160.41
OUTER RADIUS (KMS)	32.67	48.63	72.39	107.75	160.41	238.79
CORRECTION IN MGAL	PLUS OR MINUS THE ELEVATION IN METRES					
0.005	357	436	532	649	792	966
0.01	619	755	921	1124	1371	1673
0.02	799	975	1189	1451	1770	2160
0.03	946	1154	1407	1717	2095	2556
0.04	1072	1308	1596	1947	2375	2898
0.05	1186	1446	1764	2152	2626	3204
0.06	1289	1572	1918	2340	2855	3483
0.07	1385	1689	2061	2514	3067	3741
0.08	1475	1799	2194	2676	3265	3983
0.09	1559	1902	2319	2829	3451	4211
0.10	1640	1999	2439	2975	3629	4427
0.11	1716	2093	2552	3113	3798	4633
0.12	1789	2182	2661	3246	3959	4830
0.13	1860	2268	2766	3373	4115	5020
0.14	1928	2350	2866	3496	4265	5203
0.15	1994	2430	2964	3615	4409	5379
0.16	2057	2508	3058	3730	4550	5550
0.17	2119	2583	3150	3841	4686	5716
0.18	2179	2656	3239	3950	4818	5877
0.19	2237	2727	3325	4055	4946	6034
0.20	2294	2796	3410	4158	5072	6187
0.21	2350	2864	3492	4259	5194	6336
0.22	2404	2930	3572	4357	5314	6482
0.23	2457	2995	3651	4453	5431	6624
0.24	2510	3058	3728	4547	5545	6764
0.25	2561	3120	3804	4639	5657	6901
0.26	2611	3181	3878	4729	5767	7035
0.27	2660	3241	3951	4817	5875	7167
0.28	2708	3300	4022	4905	5981	7296
0.29	2756	3357	4092	4990	6086	7423
0.30	2802	3414	4162	5074	6188	7548
0.31	2848	3470	4229	5157	6289	7671
0.32	2894	3525	4296	5238	6388	7792
0.33	2938	3579	4362	5318	6486	7911
0.34	2982	3632	4427	5398	6582	8028
0.35	3025	3685	4491	5475	6677	8144
0.36	3068	3737	4554	5552	6771	8258
0.37	3110	3788	4616	5628	6863	8370
0.38	3152	3839	4678	5703	6954	8481
0.39	3193	3889	4739	5777	7044	8591
0.40	3234	3938	4798	5850	7133	8699
0.41	3274	3987	4858	5922	7220	8806
0.42	3314	4035	4916	5993	7307	8912
0.43	3353	4082	4974	6063	7393	9016
0.44	3392	4129	5031	6133	7478	9120
0.45	3430	4176	5088	6201	7561	9222
0.46	3468	4222	5144	6270	7644	9323
0.47	3506	4267	5199	6337	7726	9422
0.48	3543	4313	5254	6403	7807	9521
0.49	3580	4357	5308	6469	7888	9619
0.50	3616	4401	5362	6535	7967	9716

4,500 ft respectively, vertically below the sea-level surface of the innermost zone. If we consider an elevation difference in the outer zones of 4 km, which is the approximate depth of water in the deep ocean, and calculate the terrain correction for these outer zones on the flat plane assumption and according to Hayford and Bowie's model, we find that the difference is only 3 mgal. Since this error is practically the same for all stations, it will have no effect on the interpretation of the anomalies.

The zone chart method of terrain correction as outlined above, is a very lengthy process. Consequently, a computer programme to perform this operation was developed, based on the evaluation of the attraction of the island structure at the station positions, using the formula developed by Talwani and Ewing (1960) for the gravitational effect of a three-dimensional body.

This procedure involved approximating the topographic and bathymetric contours by straight lines, to form closed polygons. The x, y coordinates of the corners of the polygons and of the station positions were then obtained using an electronic digital plotting table. With these as data, and using the programs discussed in detail in Section 2.3 the total terrain and bathymetric corrections could be computed directly.

If g_o = the observed value of gravity and g_n = the normal value of gravity at sea-level and T = the terrain correction, then the Bouguer anomaly at a station at an elevation h metres is given by

$$g = g_o - g_n + 0.3086h - 2\pi\rho Gh + T$$

where ρ = the density and G = the gravitational constant.

2.3 Gravimetric Terrain Correction by Digital Computer.

In the past few years, several workers have developed methods of terrain correction suitable for numerical techniques on computers. Bott (1959), Kane (1964), Gimlet (1964), Nagy (1966), Ehrismann et al (1966) and St. John and Green (1967) have all proposed methods which use a grid of one form or other for estimating average heights of topography. These have one serious disadvantage as regards the present application to reconnaissance survey work, namely the labour involved in digitizing the topographic map by this method. Unless the survey is fairly concentrated, little time is saved in comparison with manual methods, particularly since the contribution to the correction, of the area close to the station must still be estimated by graticule techniques, or by alternative techniques as suggested by Kane, unless the area of the grid sections are made so small as to be impractical for large areas.

The procedure adopted to overcome this difficulty is essentially that suggested by Talwani and Ewing (1960) who considered the gravitational attraction of three-dimensional bodies of arbitrary shape. In a recent paper Takin and Talwani (1966) describe a more sophisticated method based on the formula for the gravitational attraction of the frustrum of a cone, but as the procedure outlined below gives sufficiently accurate results for the present purpose, it was preferred on the grounds of its greater simplicity.

Talwani and Ewing (1960) represent the three-dimensional body by contours. Each contour is then replaced by a horizontal irregular n-sided polygonal lamina (Fig. 2.1). The gravity anomaly at any external point due to each lamina is determined analytically and plotted as a function of the height of the lamina. By interpolation, a continuous curve can be obtained relating the heights of the laminae with their gravity anomaly (Fig. 2.2). The total area under this curve represents the anomaly due to the entire body and can be obtained by numerical integration.

The expression used to calculate V, the gravity anomaly caused by the polygonal lamina per unit thickness, is that developed by Talwani and Ewing (1960). If x_i, y_i, z_i and x_{i+1}, y_{i+1}, z_{i+1} are the coordinates of two successive vertices of the polygon, V can be expressed as

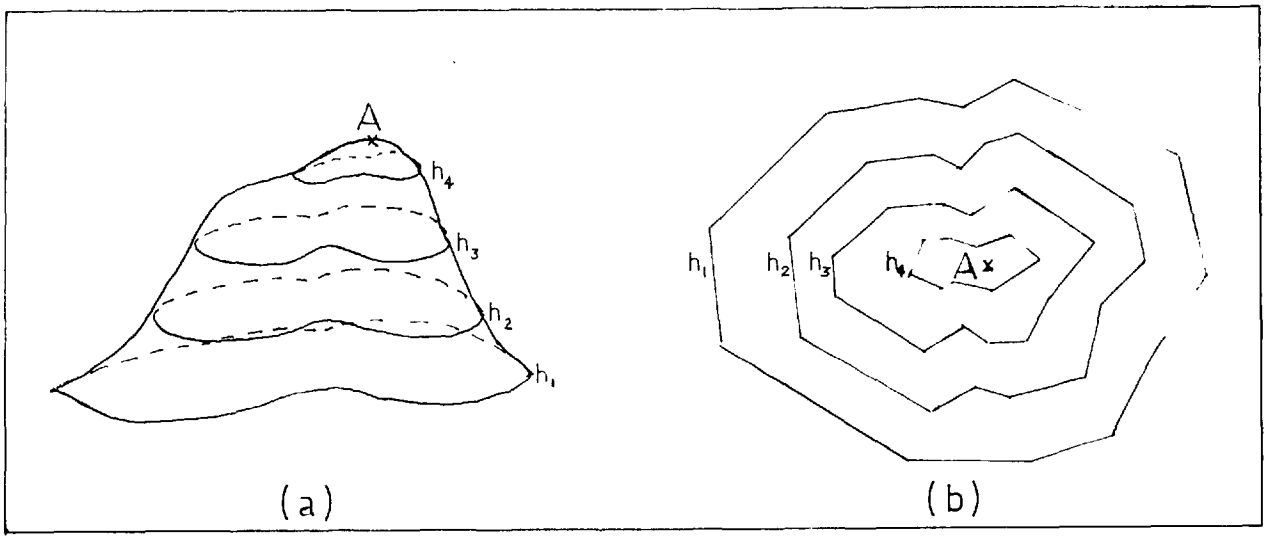

FIG. 2.1 (a) The three-dimensional body is represented by contours. (b) The contours replaced by horizontal polygonal laminae.

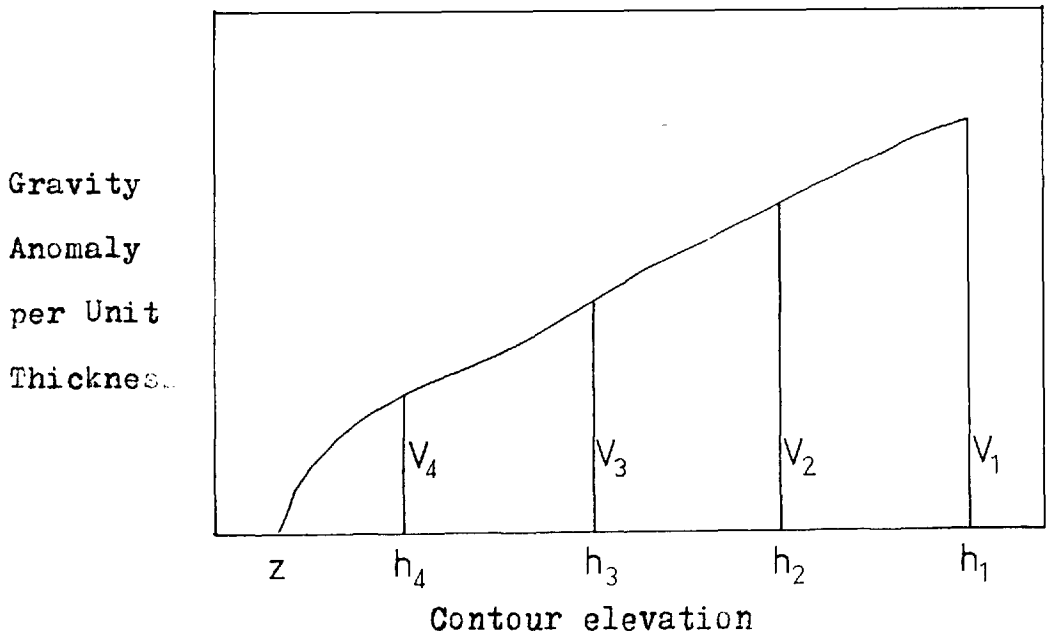

FIG. 2.2 The area under the curve is equal to the gravitational attraction of the body at the point A, elevation z.

$$V = k\rho\sum_{i=1}^{N}\left\{W\arccos\left\{(x_i x_{i+1} + y_i y_{i+1})/\sqrt{(x_i^2+y_i^2)(x_{i+1}^2+y_{i+1}^2)}\right\}\right.$$
$$\left. -\arcsin\frac{zq_i S}{(p_i^2+z^2)^{\frac{1}{2}}} + \arcsin\frac{zf_i S}{(p_i^2+z^2)^{\frac{1}{2}}}\right]$$

where $S = +1$ if p_i is positive, and -1 if p_i is negative

$W = +1$ if m_i is positive, and -1 if m_i is negative

$$p_i = \frac{y_i - y_{i+1}}{r_{i,\,i+1}} x_i - \frac{x_i - x_{i+1}}{r_{i,\,i+1}} y_i$$

$$q_i = \frac{x_i - x_{i+1}}{r_{i,\,i+1}} \cdot \frac{x_i}{r_i} + \frac{y_i - y_{i+1}}{r_{i,\,i+1}} \cdot \frac{y_i}{r_i}$$

$$f_i = \frac{x_i - x_{i+1}}{r_{i,\,i+1}} \cdot \frac{x_{i+1}}{r_{i+1}} + \frac{y_i - y_{i+1}}{r_{i,\,i+1}} \cdot \frac{y_{i+1}}{r_{i+1}}$$

$$m_i = \frac{y_i x_{i+1} - x_i y_{i+1}}{r_i \quad r_{i+1}}$$

$$r_i = +\,(x_i^{\,2} + y_i^{\,2})^{\frac{1}{2}}$$

$$r_{i+1} = +\,(x_{i+1}^{\,2} + y_{i+1}^{\,2})^{\frac{1}{2}}$$

$$r_{i,i+1} = \left((x_i - x_{i+1})^2 + (y_i - y_{i+1})^2\right)^{\frac{1}{2}}$$

The terrain correction can be split into two parts, the correction for the mass of the island above sea-level, hereafter called the land correction, and the bathymetric correction, necessary because of the mass deficiency produced by the presence of sea-water instead of land. For both parts the assumption of a flat earth was made, but as shown in Section 2.2 the error introduced is not a serious one.

The bathymetric and topographic contours must first be approximated by straight lines (Fig. 2.1). This approximation can be made as accurately as desired within the limits set by the scale of the topographic map simply by increasing the number of straight lines, but at the expense of computing time. Close fit of the contours is only important, however, when a portion of the contour lies close to a gravity station. By fitting only such portions of the curve very closely, accuracy can be maintained without increasing the computing time unduly.

A similar compromise between accuracy and computing time must be made in the choice of contour intervals. The interval used varied from island to island depending on the maximum elevation. For the land correction, it ranged from 250 m on islands with elevations greater than 1000 m to 60 m on Ascension Island where the maximum elevation is 859 m.

Having produced the polygons, the x and y coordinates of each of the vertices must be determined. The z coordinate of each point is simply the elevation of the contour. Similarly, the x, y and z coordinates of the gravity stations must be obtained, these two sets of coordinates, and the mean density of the island, forming the data from which the program can compute the terrain correction.

The land and bathymetry corrections were always made separately, since the programs differ in several details, chiefly in the methods of numerical integration.

The integration procedure used by Talwani and Ewing is to fit parabolas to successive sets of three points and then to find the area contained between the parabolas and the axis.

If V_0, V_1, and V_2 are the gravity anomalies per unit thickness caused by contours at heights Z_0, Z_1 and Z_2, then the gravity anomaly caused by the portion of the body lying between horizontal planes at depth Z_0 and Z_2 is given by

$$\int_{Z_0}^{Z_2} V dZ = \frac{1}{6}\left\{ V_0 \frac{Z_0-Z_2}{Z_0-Z_1}(3Z_1-Z_2-2Z_0) - V_1 \frac{(Z_0-Z_2)^2}{(Z_1-Z_2)(Z_0-Z_1)} - V_2 \frac{Z_0-Z_2}{Z_1-Z_2}(3Z_1 - Z_0 - 2Z_2)\right\} \qquad (3)$$

By choosing successive sets of three points, the integration can be carried out for all the contours and the total anomaly obtained.

In the land correction, the x, y coordinates of the gravity station lie outside all contours above the station elevation and for these contours V has a small negative value. The station will lie within ~~one contour for~~ all contours ~~levels~~ below the station so that for all such levels, V has a large positive value. Therefore the function V changes very rapidly near the station elevation and if an attempt is made to integrate the function using equation 3 large errors will result. Instead the follwoing method was

adopted. The value of V at an elevation one metre above the station elevation was made equal to the value of V for the nearest contour above it, and the value of V at the elevation of the station was made equal to the value of V for the nearest contour below it (Fig. 2.3). The area under the curve of V against contour elevation Z was then obtained by calculating the sum of the areas of the trapezoids formed by successive pairs of points including those at the station elevation and at one metre above it.

The same difficulty does not arise in the bathymetric correction. The station, being above sea-level, is enclosed by one contour for all the depths at and below sea-level, so that V is large and positive and a smoothly varying function for all contour depths. In this case Talwani's method of integration is quite suitable and was in fact used.

For the land correction the result calculated is the total anomaly at the gravity station caused by the part of the island above sea-level. Since the maximum dimension of any of the islands at sea-level was 85km it was not considered necessary to limit the area over which the attraction was computed. The land correction can then be obtained by subtracting the calculated anomaly from the Bouguer correction; the modulus of the result is the land correction.

i.e. $T_L = 2\pi\rho Gh - \Delta g$ (4)

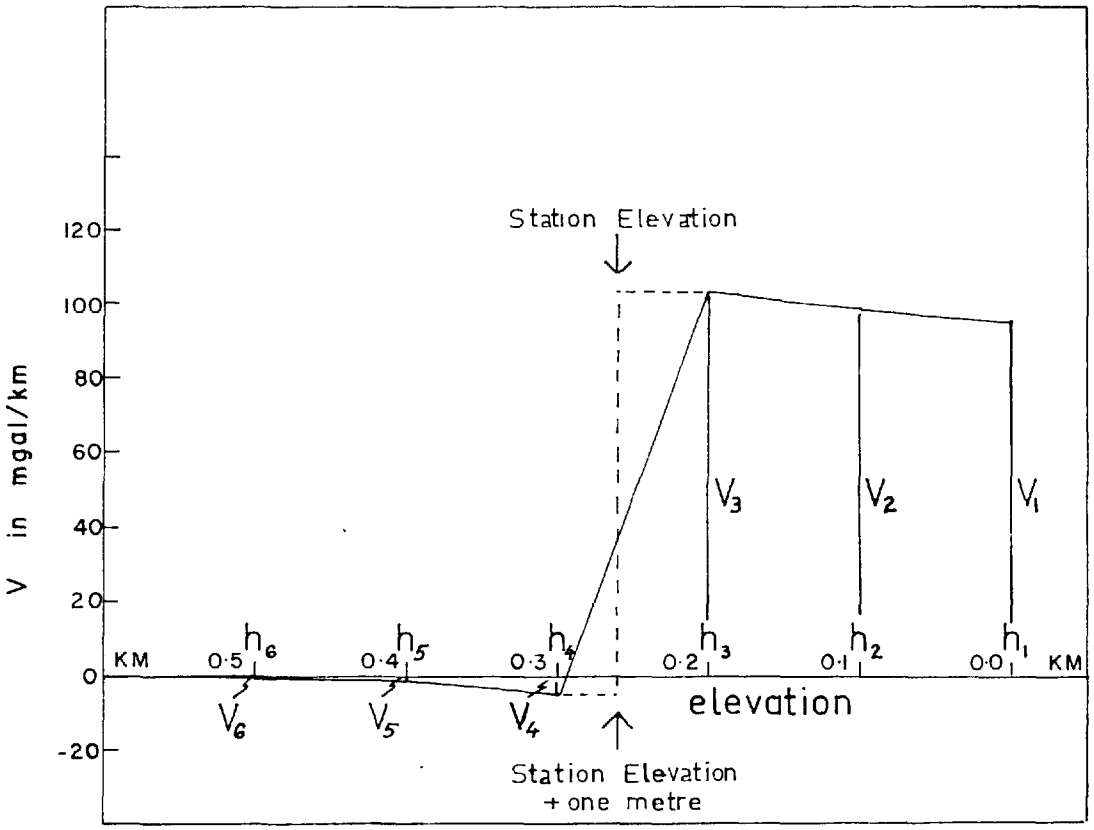

FIG. 2·3 Method of interpolation used in the integration procedure of the Land Correction program.

where T_L = land correction

Δg = calculated anomaly for the island above sea-level

ρ = density

h = elevation of the station

For the bathymetric correction, the anomaly due to the bulk of the island between sea-level and the level of the surrounding ocean floor is calculated. The correction is then the difference between the Bouguer correction for an infinite slab of this thickness and density equal to the island density, minus the density of sea water, and the calculated anomaly.

i.e. $T_B = 2\pi\sigma Gd - \Delta g$ (5)

where T_B = bathymetry correction

Δg = calculated anomaly due to the land between sea-level and depth d.

σ = density of island body - density of sea water, 1.03 gm/cc.

Then the total terrain correction is equal to the sum of the land and bathymetry corrections.

Advantages of the Method. (1) The input data consist of the topographic contours approximated by closed polygons. It was possible, using an electronic digitizer, to prepare the data for one island, topography and bathymetry, in about eight man-hours. (2) The data need be prepared only once for any number of stations in the area. (3) It is unnecessary to use manual methods to calculate the gravitational attraction of the area close to the station.

Bathymetric Correction Program

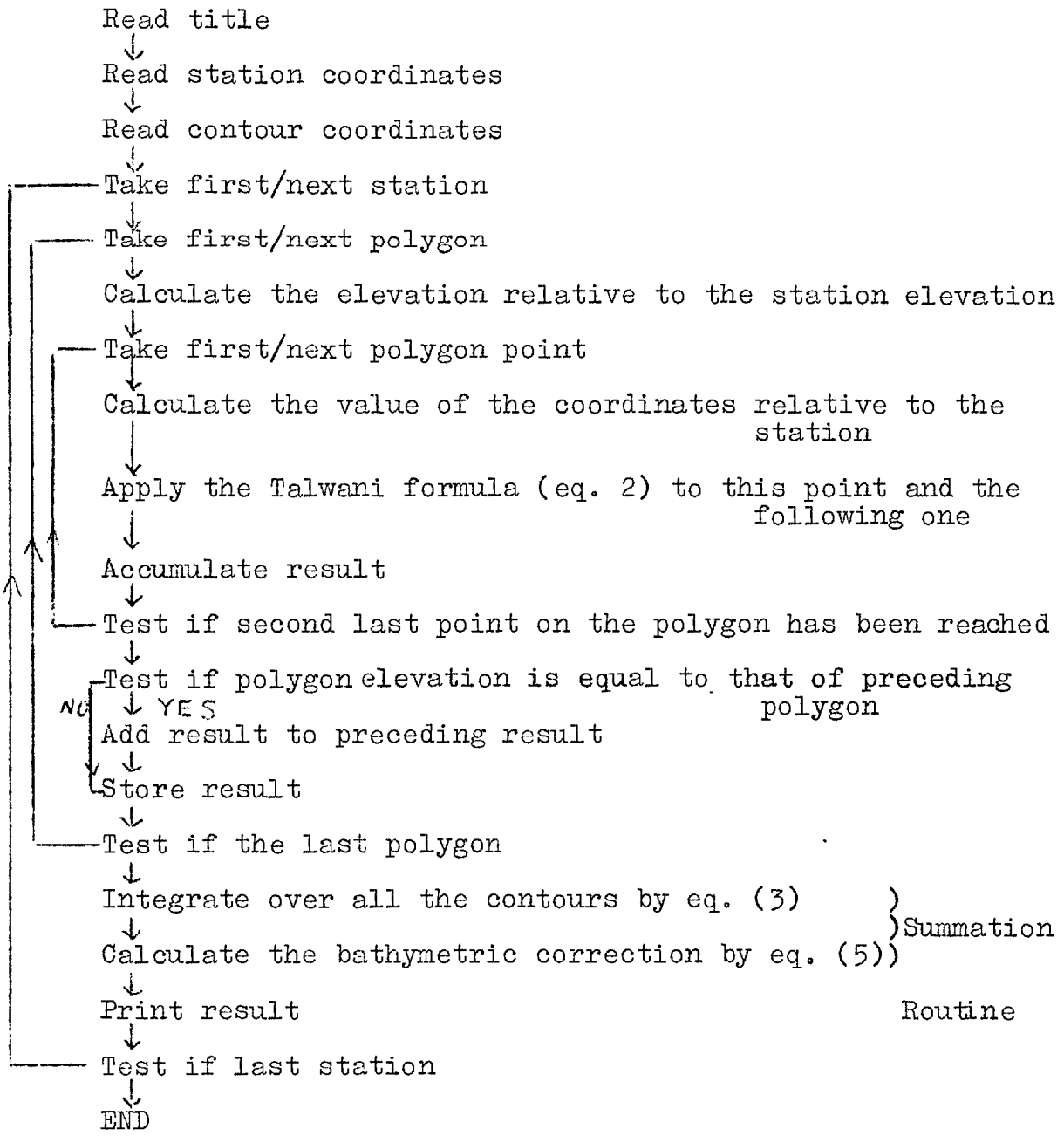

Fig. 2.4

FIG. 2.5 Land Correction Program

This program differs from the bathymetric correction program only in the numerical integration routine, for which the Flow Diagram is reproduced below.

The input consists of n elevations h_i and their corresponding gravity anomaly per unit thickness, V_i. Station elevation is z metres. V, K, D_i, and W_i are storage locations in the computer.

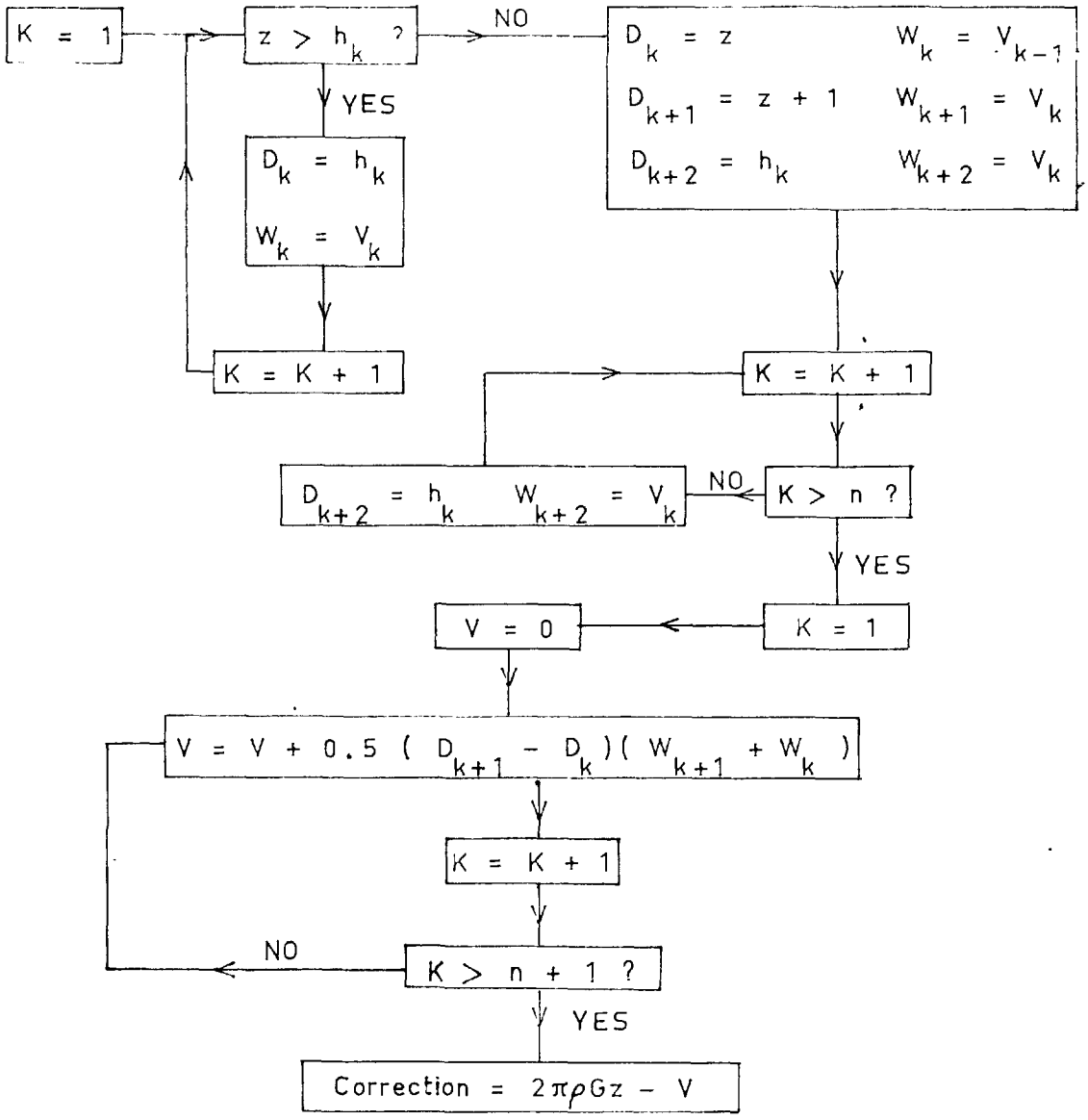

Disadvantages of the Method. (1) It is very difficult to include the effects of the earth's sphericity. (2) Every polygon must be closed so that the number of contours in the vicinity of the station cannot be increased without greatly increasing the number of polygon points and hence computer time.

Accuracy. The terrain corrections calculated by computer are compared in Table 2.3, with those calculated manually for all the stations on the island of Santa Maria. The land corrections for several stations on other islands are also compared in Table 2.4 to investigate the effect of different contour intervals. Of the latter group of stations, several were selected for checking because of the proximity of very rugged topography to the station. Hence the difference between the corrections by the two methods in these cases indicate the maximum difference to be expected in any of the other terrain corrections which were made by computer. This maximum difference is 3.0 mgal and is observed in the case of the highest station occupied in any of the surveys, which was at an elevation of 2727 m.

The observed differences are mainly one-sided, being on average one milligal higher for the computed results. Since the manual method can be affected by operator bias in estimating the average heights within the zonal compartments, it cannot be said that the computed results are definitely

Accuracy of Terrain Correction. SANTA MARIA

Station No.	Elevation	Total Terrain Correction	Terrain Correction	Difference	% Difnce.
0	100 m	15.1 mgal	12.5 mgal	+2.6 mgal	17.2
1	113	13.4	12.2	+1.2	9.0
2	87	14.4	13.8	+0.6	4.2
3	7	11.5	10.8	+0.7	6.1
4	95	12.4	11.7	+0.7	5.6
5	193	13.8	12.0	+1.8	13.0
6	420	20.3	20.3	+0.0	0.0
7	565	29.8	27.5	+2.3	7.7
8	220	15.3	15.2	+0.1	0.7
9	178	14.5	13.1	+1.4	9.7
10	2	14.7	13.1	+1.6	10.9
11	44	12.7	12.5	+0.2	1.6
12	1	12.4	12.0	+0.4	3.2
13	87	13.5	12.6	+0.9	6.7
14	4	14.1	13.5	+0.6	4.3
15	108	14.0	12.7	+1.3	9.3
16	85	14.8	13.6	+1.2	8.1
17	40	14.9	14,3	+0.6	4.0
18	252	14.8	13.5	+1.3	8.8
19	150	14.1	13.4	+0.7	5.0
20	195	14.0	12.7	+1.3	9.3
21	230	14.4	13.4	+1.0	6.9
22	245	14.8	14.6	+0.2	1.4
23	260	15.8	16.4	-0.6	-3.8
24	218	15.2	14.9	+0.3	2.0
25	260	16.9	17.2	-0.3	-1.8
26	145	15.7	16.4	-0.7	-4.5
27	250	17.4	17.9	-0.5	-2.9
28	7	17.7	16.1	+1.6	9.0
29	108	12.8	11.9	+0.9	7.0
30	425	21.1	20.5	+0.6	2.8
31	333	18.8	17.7	+1.1	5.9
32	310	20.0	19.8	+0.2	1.0
33	255	20.8	20.3	+0.5	2.4
34	3	21.0	18.4	+2.6	12.4
35	230	25.0	24.6	+0.4	1.6
36	237	21.0	20.3	+0.7	3,3
37	275	20.2	20.2	+0.0	0.0
38	273	19.8	18.6	+1.2	6.1
39	298	20.8	18.1	+2.7	13.0
40	1	20.5	18.5	+2.0	9.8
41	205	20.4	18.6	+1.8	8.8
42	481	25.5	26.0	-0.5	-2.0
		Mean = 16.98	Mean = 16.13	Mean = 0.85	+5.2%
			Root Mean Square = 1.21		= 7.1%
			Standard deviation = 0.8617		= ±4.9%

Manual Estimate by Template

Table 2.3

Terrain Correction Accuracy with Differing Contour Intervals

Land correction only

	Cntr. Int.	Stn. No.	Elvtn	By Computer	Manually by Template	Diff.	% Diff.
				mgal	mgal		
Ascension Island	200'	199	1608'	5.9	6.2	-0.3	-5.1
		200	1147'	3.4	3.4	0.0	0.0
Flores	100m	13	503m	4.6	4.2	+0.4	8.7
		18	8m	3.1	2.7	+0.4	12.9
		27	63m	10.1	10.7	-0.6	-5.9
Madeira	250m	14	1818m	37.9	39.2	-1.3	-3.4
Hierro	250m	4	1m	9.2	8.7	+0.5	5.4
		9	652m	16.5	14.4	+2.1	12.7
		28	48m	9.7	8.4	+1.3	13.4
Tenerife	250m	6	289m	8.0	7.2	+0.8	10.0
		13	3m	4.2	3.2	+1.0	23.8
		17	825m	14.5	11.7	+2.8	19.3
		40	403m	4.2	2.9	+1.3	30.9
		66	4m	1.5	0.8	+0.7	46.7
		73	312m	4.0	2.9	+1.1	27.0
		82	546m	10.0	7.8	+2.2	22.0
		87	585m	9.3	8.1	+1.2	12.9
		105	2727m	36.7	33.7	+3.0	8.2
		117	122m	3.8	2.9	+0.9	23.7
		143	1589m	24.2	22.2	+2.0	8.3
For Tenerife only				Mean		1.545	21.21

Root Mean Square Diff = 1.73

Standard Deviation = 0.82

Table 2.4

in error by this much. Even if this were the case, a one-sided error of this magnitude would not have any serious effect on the interpretation of the Bouguer anomaly. The standard deviation of the differences is of more interest and for both the 100 m and 250 m contour intervals this is less than one milligal. This accuracy is quite adequate for the reduction of reconnaissance survey data.

The machine time required on the University of London Atlas computer was 3.6 seconds per gravity station in the case of Lanzarote, where the topography and bathymetry were defined by polygons with a total number of 1450 sides. The number of sides is the controlling factor as far as machine time is concerned and in this, Lanzarote is typical of the islands to which this process was applied.

2.4 Regionals and Residuals.

The present surveys have station spacing greater than two kilometres and an accuracy in the Bouguer anomaly of $\pm$ 3 mgal on most of the islands. This means that only major anomalies with a wave length greater than 4 km and an amplitude of more than 6 mgal can be detected. On two of the smaller islands, Ascension and Faial, closer station spacing and increased accuracy enable smaller anomalies to be recognized, although strongly masked by the effects due to larger anomalies. The study of these smaller anomalies is

facilitated if the effects due to the larger anomalies can be removed. This is the well-known problem (Nettleton, 1954) of separating narrow anomalies with relatively high curvature (the 'residual' field) from broader anomalies with relatively low curvature values. This latter field is known as the regional field and is the interpreter's concept of what the Bouguer anomaly would be if the smaller anomalies were not there. As such, the choice of the regional field is subjective, but several attempts have been made to find an objective method of defining the field, and these have led to the application of convolution filtering to gravity maps (Byerly, 1965; Dean, 1958; Mesko, 1965).

The method adopted in the present case is that due to Simpson (1954) in which the regional field over the area of interest is assumed to be a smooth surface. In a mathematical sense this means that the equation of the surface is a polynomial of low degree.

Simpson's method consists of approximating the Bouguer anomaly over the area of interest to a low order polynomial in x and y, by the method of least squares. This field is considered as the 'regional' field and is subtracted from the observed field to leave the 'residual' gravity.

With access to a high-speed computer, the order of the polynomial fitted to the observed field can be raised to any reasonable order. Regional fields up to the 5th order were

calculated for the island of Faial and are illustrated in Fig. 2.6. As the order increases, the calculated regional effect clearly contains elements of the field it is wished to observe and, therefore, on the two islands where residuals were computed, they represent the gravity values corrected for a first or second order regional trend.

The mathematics of the method for a second order regional field are as follows. Given gravity values g (x,y) at discrete points over a pattern P in the x, y plane. Let these be approximated by a polynomial

$$G(xy) = C_{00} + C_{10}x + C_{01}y + C_{20}x^2 + C_{11}xy + C_{02}y^2$$

The Cij are chosen such that

$$I(Cij) = \sum_P (g(xy) - G(xy))^2 = \sum_P R^2(xy)$$

assumes a minimum value. R(xy) may then be considered as the gravity value corrected for a second order regional trend.

$$I(Cij) = \sum_P \left\{ \sum_{i=0}^{2} \sum_{j=0}^{2-i} \sum_{k=0}^{2} \sum_{l=0}^{2-k} C_{ij}C_{kl}\, x^{k+i}\, y^{l+j} \right\} - 2\sum_P g \sum_{i=0}^{2} \sum_{j=0}^{2-i} C_{ij}\, x^i\, y^j + \sum_P g^2$$

To minimize I, differentiate partially with respect to Cij and equate to zero.

i.e. $$2 \sum_{k=0}^{2} \sum_{l=0}^{2-k} C_{kl} \sum_P x^{k+i}\, y^{l+j} - 2\sum_P g x^i y^j = 0$$

$$\text{or} \sum_{k=0}^{2} \sum_{l=0}^{2-k} C_{kl} \sum_P x^{k+i}\, y^{l+j} = \sum_P g x^i y^j$$

where i = 0, 1, 2 and j = 0, 1, 2 - i,

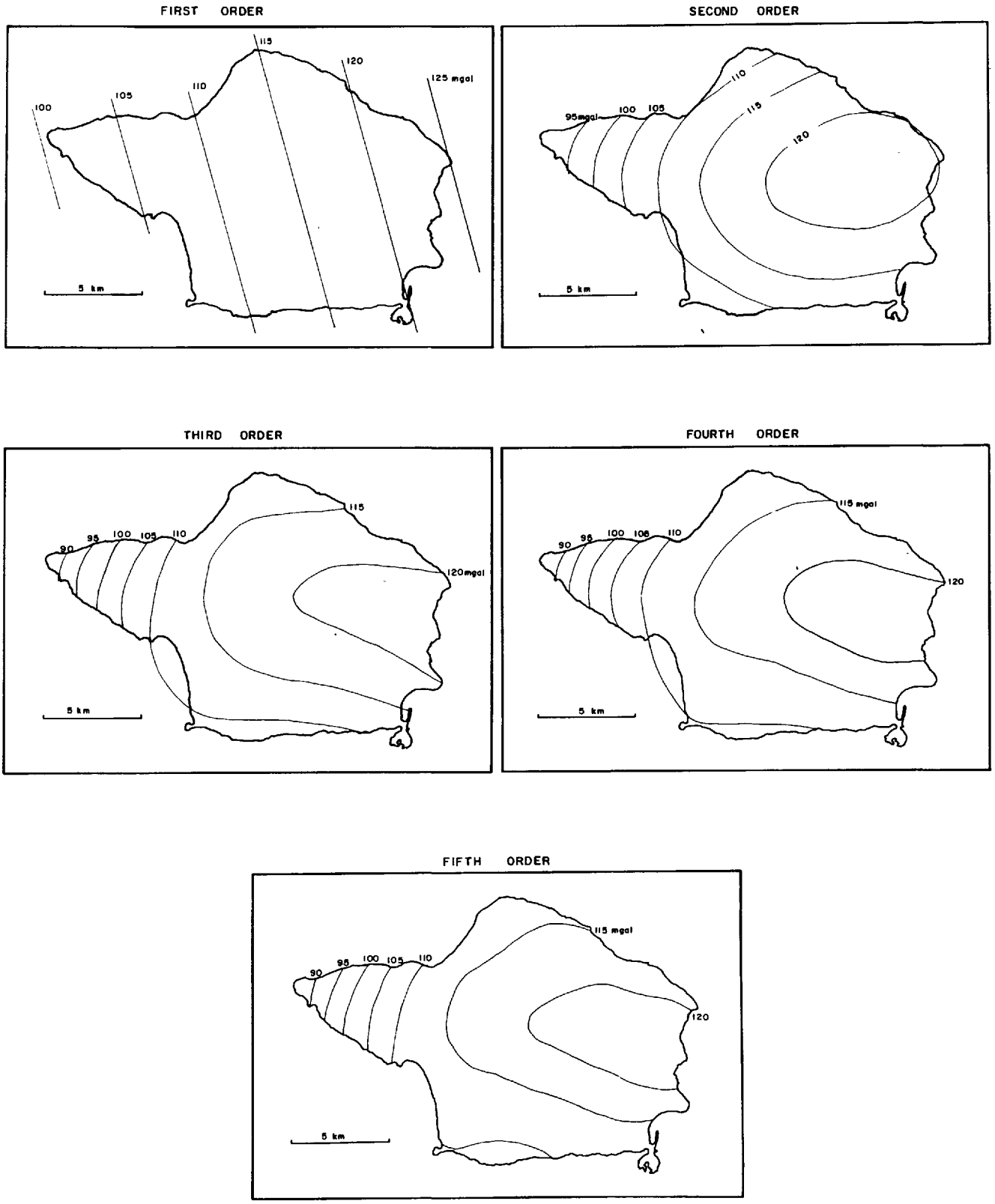

FIG 2·6 Regional field on Faial obtained by fitting polynomials of degree 1 to 5 to the Bouguer anomaly.

or in matrix notation

$$\left[\sum_{\rho} x^{k+i}\, y^{l+j}\right]\left[C_{kl}\right] = \left[\sum_{\rho} g x^{i} y^{j}\right]$$

whence the solution is

$$\left[C_{kl}\right] = \left[\sum_{\rho} x^{k+i} y^{l+j}\right]^{-1}\left[\sum_{\rho} g x^{i} y^{j}\right] \qquad (1)$$

The residual at the station (xy) is therefore

$$R(xy) = g(xy) - G(xy)$$

2.5 Estimation of Anomalous Mass.

While gravity measurements alone cannot uniquely determine the distribution of anomalous mass, they can provide a unique estimate of the total anomalous mass, if the anomaly is sufficiently well defined. From Gauss's Theorem, Hammer (1945) and La Fehr (1965) show how the total anomalous mass can theoretically be estimated from the expression

$$M = (1/2\pi G)\int_{S} g_z \, dS \qquad \text{——————} \qquad (2.9)$$

where M is the anomalous mass, G the gravitational constant, g_z the vertical component of attraction and S is the plane of observation. In practice this plane will compromise the area of measurements and the integration will be replaced by summation. Two special cases can be noted. When the anomaly possesses approximately radial symmetry, if r is the radial distance from the centre of the anomaly, then

$$M = (1/G)\int_{0}^{\infty} g_z(r)\, r\, dr \qquad \text{——————} \qquad (2.10)$$

or in summation form

$$M \approx (\Delta r/G)\sum_{i=0}^{n} g_z(r_i) r_i \qquad \text{——————} \qquad (2.11)$$

where Δr is the interval of integration. For r and Δr in kilometres and g_z in milligals

$$M = 0.15 \times 10^{15} \Delta r \sum_{i=0}^{n} g_z(r_i) r_i \quad \text{gm} \qquad (2.12)$$

For the case where the anomaly can be considered two-dimensional, the mass per unit length M_l is given by

$$M_l = (1/2\pi G) \int_{-\infty}^{\infty} g_z \, dx \qquad (2.13)$$

or

$$M_l = 2.386 \times 10^{8} \int_{-\infty}^{\infty} g_z \, dx \qquad (2.14)$$

where g_z is in milligals and x, the distance along the profile is in kilometres.

In practice, the integration cannot be extended to infinity, nor in many cases to a distance where the effect of the anomalous mass is effectively zero. In such cases it is possible to calculate only a percentage of the total mass. La Fehr (1965) has shown that the percentage calculated for a given gravity coverage, and hence the correction which must be applied, depends upon the depth and the distribution of the anomalous mass and he presents a series of curves which show this dependence for several two-dimensional and three-dimensional mass distributions. As will be demonstrated in the following chapters, these curves permit improved estimates of the total mass.

2.6 Marine Gravity Data Processing.

In addition to the gravity data on the subaerial parts of the island, a considerable amount of marine gravity data in the vicinity of several of the islands were made available to the author. The data processing techniques are different and are described separately.

Marine gravity data can be in two forms, as measurements made with pendulum apparatus on submerged submarines or as continuous gravity profiles obtained by a surface ship using a specially designed gravimeter on a gyro-stabilized platform. The result in both cases is the value of observed gravity at the sea surface and from this the free-air anomaly can be calculated by subtracting the normal gravity field computed from the International Gravity Formula.

This free-air anomaly can yield some information, but it is more helpful in demonstrating the effect of the sub-bottom structure if the Bouguer anomaly is computed by correcting for the deficit caused by the water layer. For gravity measurements located close to any of the islands this correction can be made using the bathymetric correction program already described in Section 2.3. Away from the islands, accurate knowledge of the bathymetry is generally only two-dimensional, consisting of the soundings observed during the ship's passage, or at the time of measurement in the case of pendulum data. The Bouguer anomalies can then be computed,

assuming two-dimensional bathymetry, by the computer program described by Talwani et al (1959). This method is based on the evaluation of the gravitational attraction due to a two-dimensional body of arbitrary shape by approximating it to an n-sided polygon. In the same paper, Talwani et al show how, having made some assumptions as to the composition of the crust, it can be adapted to obtain an estimate of the thickness of the oceanic crust.

In the present calculations, the standard crustal sections assumed (Fig. 2.7) are those described by Worzel (1965b). The standard oceanic crust consists of 4.9 km of water, density 1.03 gm/cc, 0.7 km of sediments of density 2.3 gm/cc, 1.7 km of "layer 2" of density 2.55 gm/cc and 4.2 km of "layer 3" of density 2.9 gm/cc above a mantle of density 3.4 gm/cc. This column is in isostatic balance with the sea-level continental column 33 km thick and of mean density 2.9 gm/cc. In all subsequent discussion the crust is taken as the layers bounded at the bottom by the Mohorovicic discontinuity, i.e. the boundary above the 3.4 gm/cc layer. This sub-Moho material is termed the mantle.

Except for this different assumption as to the standard crustal columns, the procedure used for pendulum station profiles was exactly as described by Talwani et al (1959) and only the adaptation used for continuous gravity profiles will now be described.

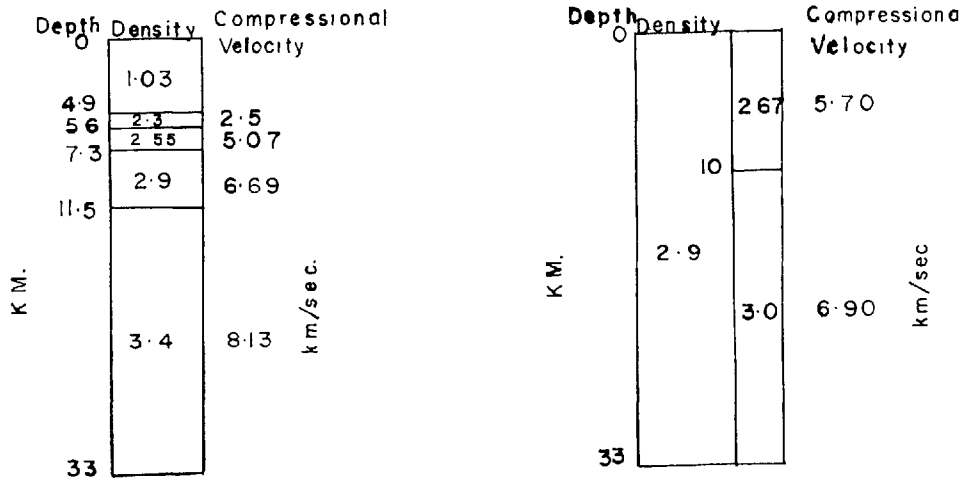

FIG. 2·7 Standard crustal sections after Worzel (1965)

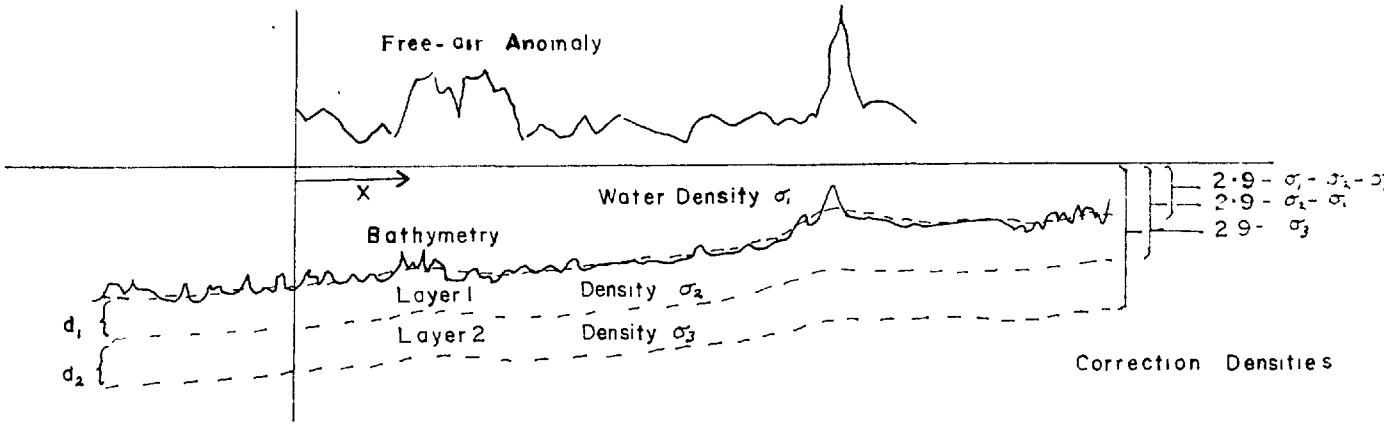

FIG. 2·8 Correction of marine gravity data

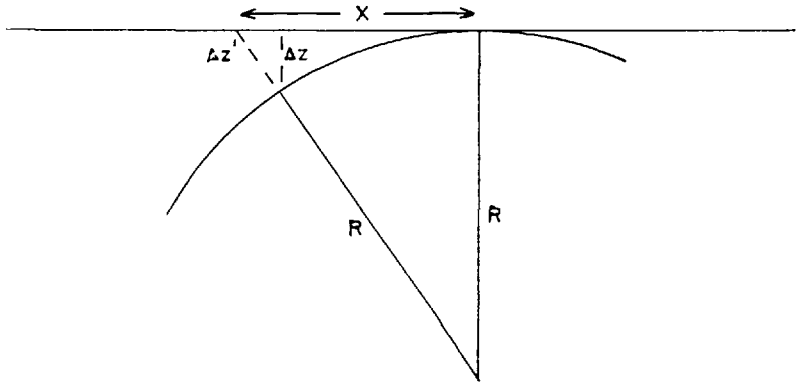

FIG. 2·9 Diagram illustrating the curvature correction

The gravity data (see Fig. 2.8) consists of the free-air anomaly taken at 5 km intervals, and the bathymetric data of depths d(x) to changes of slope and their distance (x) along the profile. As the water correction is made to a range of 200 km on either side of each gravity point, the bathymetric data must extend 200 km beyond either end of the gravity profile.

In correcting for the water layer and the crustal layers out to 200 km, the effect of the curvature of the earth becomes significant and it is necessary to lower the depth coordinates of the surfaces of the various layers to account for it. The amount of this lowering can be derived with sufficient accuracy as follows (see Fig. 2.9). For x = 200 km and R the mean radius of the earth, equal to 6368 km, Δz can be taken equal to $\Delta z'$ with an error of less than 1 in 2000. Then

$$z = \sqrt{x^2 + R^2} - R$$

$$= R(1 + x^2/R^2)^{\frac{1}{2}} - R$$

$$= R + \tfrac{1}{2}\, x^2/R - 1/8\, x^4/R^3 + \ldots - R$$

$$\approx \tfrac{1}{2}\, x^2/R \quad \text{neglecting terms in } 1/R^3 \text{ and over}$$

i.e. If there is a point depth z at a distance x, its depth corrected for curvature will be

$$z' = z + x^2/2R$$

i.e. $z' = z + 0.0000785\, x^2$ where x and z are in kilometres.

The flow diagram for the program as prepared for the Atlas computer is presented in Fig. 2.10 and the divisions of the program are briefly described below.

In part I, the bathymetry is approximated by a tenth order polynomial in x using least squares. The smooth curve having been obtained, its depth, increased by the appropriate amount, is used in part II to represent the configuration of the surfaces of the upper sub-bottom layers of the crust.

In the following discussion, the term "crustal anomaly" is used to describe the anomaly corrected for the mass deficit due to the water layer and crustal layers 1 and 2. It is this anomaly and the Bouguer anomaly which are calculated in part II of the program. The thicknesses of layers 1 and 2 are taken as the mean of the results obtained by seismic refraction surveys in the area of interest. If these thicknesses are d_1 and d_2 the lower surfaces of layer 1 and layer 2 are represented by the smoothed bathymetry curve, its depth increased by d_1 and $d_1 + d_2$ respectively. The density used in the Bouguer correction for the water layer is the assumed density of the upper crust minus the density of sea-water. In calculating the crustal anomaly it is the density differences between the respective densities of the water layer and layers 1 and 2 and the value of 2.9 gm/cc of the standard continental column, which are used.

Marine Bouguer Anomaly and Depth to Moho
Program Flow Diagram

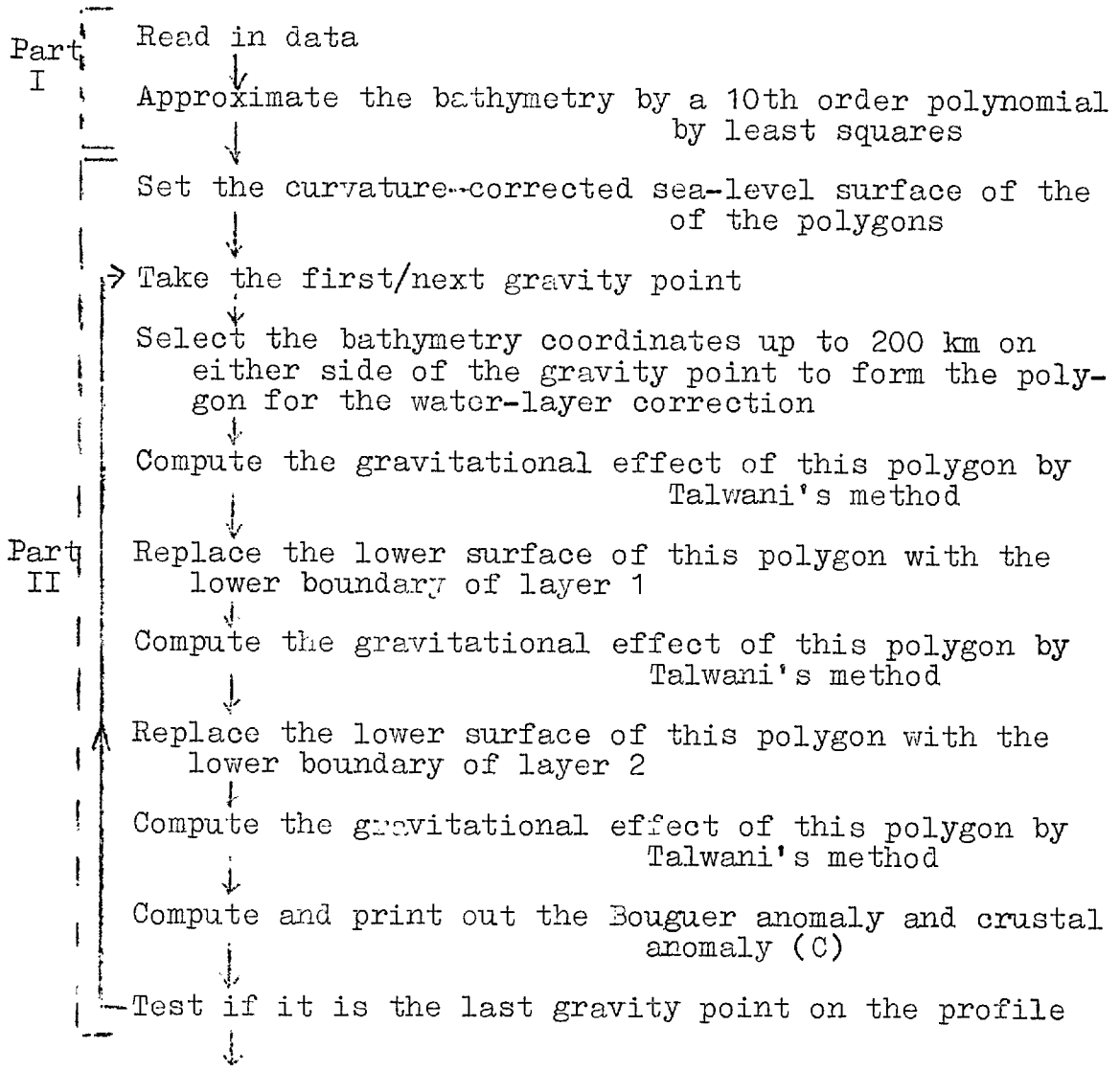

Fig. 2.10 (continued overleaf)

Fig. 2.10 (continued)

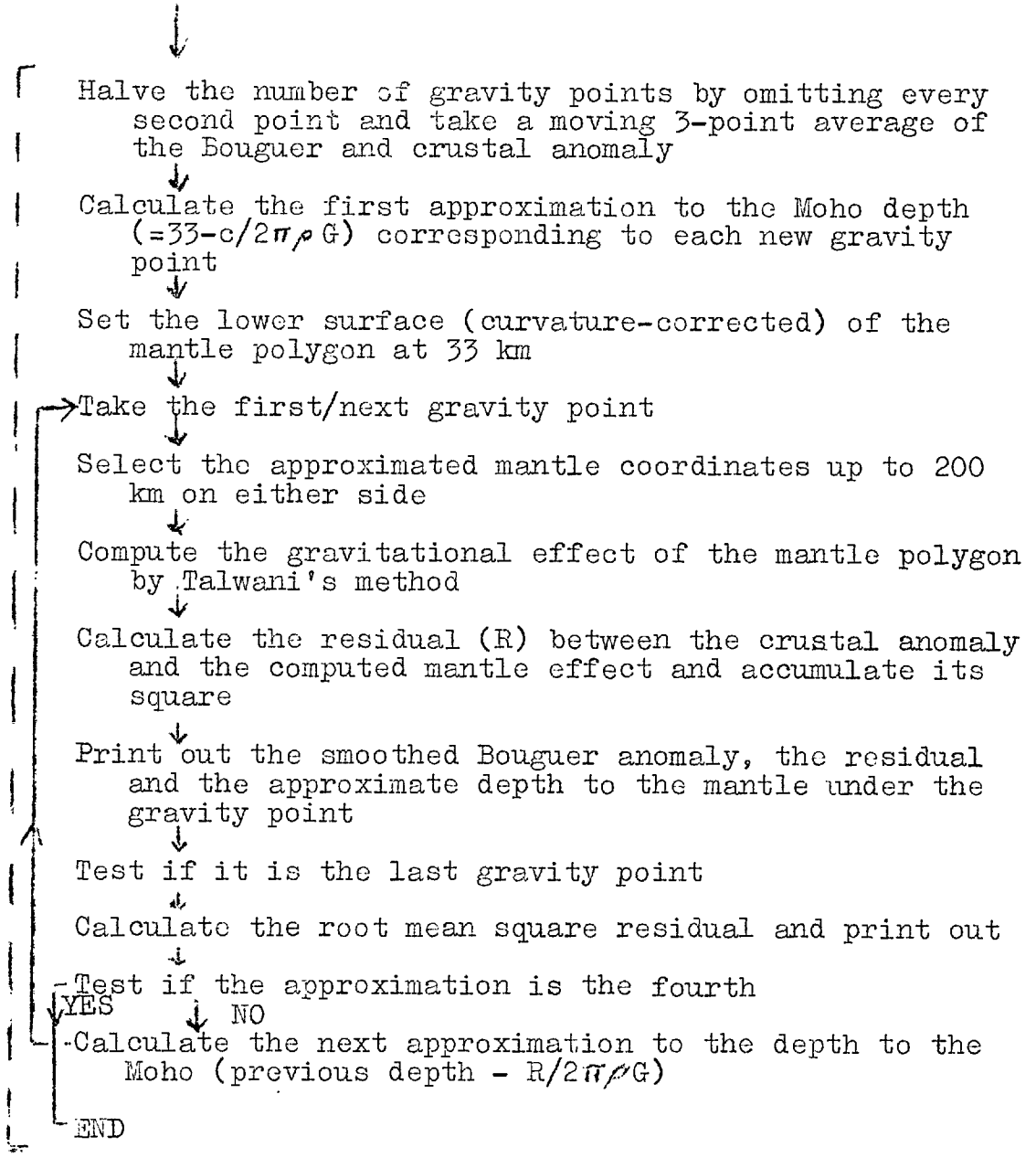

The three layers under the gravity point are first approximated by n-sided polygons extending 200 km on either side of the point. It makes the program more efficient if, instead of calculating the effect of each layer separately, the three polygons each have sea-level as their upper surface, the lower surfaces then being respectively, the bathymetry (unsmoothed) and the lower boundary of layer 1 and layer 2. The contribution of individual layers can then be obtained by subtraction, but this is unnecessary. The Bouguer anomaly is simply the free-air anomaly plus the correction for the water layer, and the crustal anomaly (C) is equal to the free-air anomaly plus the sum of the corrections for all three polygons when the densities used are as shown in Fig. 2.8.

The sea-level surface, corrected for sphericity, is approximated by straight lines, 20 km long. As the co-ordinates of this surface remain the same for all the polygons and all points on the gravity profile, they are set up before the main cycle in part II begins.

Part III consists of a series of successive approximations to the depth of the Moho. The number of gravity points is first reduced to one every 10 km by taking a moving three-point average of the Bouguer anomaly and crustal anomaly (C). The thickness (t) of the horizontal infinite slab of density 0.5 gm/cc (3.4 - 2.9 gm/cc) is calculated. As in the Bouguer reduction, $C = 2\pi\rho Gt$, where ρ = 0.5 gm/cc and G =

gravitational constant. Then the depth 33 - t km is taken as the first approximation to the depth of the Moho. The gravitational effect of the mantle between this depth and 33 km is then calculated as in part II. If the difference between the crustal anomaly and this calculated mantle effect is R, then a better approximation to the depth of the Moho is given by

$d - R/2\pi\rho G$, where d is the former depth.

With the recomputed depths, the mantle effect is then re-calculated.

It was found that the root mean square of R(x) calculated for each approximation, decreased very slowly after the fourth successive approximation. As the residuals for the fourth cycle are less than the magnitude of the errors inherent in the calculation of the crustal anomaly, there is little to be gained by using more than four successive approximations.

CHAPTER 3

DETERMINATION OF THE DENSITY TO BE USED IN THE BOUGUER CORRECTION

3.1 Introduction

For the sake of simplicity and uniformity and also in order that comparisons between the islands might be drawn more readily, the same mean density was used in the Bouguer corrections in all cases. This is not to imply that the bulk density is exactly the same for each island, but in assuming one mean value for a whole island, the average is taken over a number of rock types in a number of physical forms and one can expect that this average will not differ widely from island to island.

Three lines of evidence were considered in choosing the density value to be used. These were, (1) direct measurement of rock samples from the islands, (2) seismic information around the islands and on other similar islands, and (3) estimates of the density from the observed gravity values.

3.2 Direct Measurement of Rock Samples.

Rock samples are normally collected for geological purposes and as such are taken from fresh, solid material.

But on the volcanic islands, rocks are often deeply weathered, much of the lava is scoriaceous and vesicular, and there is normally a considerable proportion of tuffs, breccias and other pyroclastic material. Thus a density derived from the average of rock sample densities would have an artificially high value. However the specific gravities of individual rock types are able to provide some estimate as to the value of density to be expected.

With one or two exceptions, the rocks on the islands are entirely volcanic in origin, in the range basalt - trachyte - rhyolite and their associated pyroclastic materials, tuffs, ignimbrites and breccias. Their specific gravities range from 2.9 - 3.0 for solid olivine-basalt through 2.6 for trachyte, 2.5 for rhyolite, to less than 1.0 for pumice. The values for a basaltic lava flow can further range from 2.9 - 1.5 depending on the percentage of vesicles present. The mean density of the island will depend on the main rock type, the vesicularity of the lava and the proportion of pyroclastic material, and direct measurement of specific gravity is useful only in so far as it enables us to set an upper and lower limit to the probable mean density of the island.

A range of 1.0 - 3.0 gm/cc is not realistic since none of the islands is entirely pumicious or entirely solid lava; one can also say that most of the island rocks fall in the

range 2.0 - 3.0 gm/cc, since this includes many of the compacted pyroclastic rocks. The probable mean density on a volcanic island can therefore reasonably be limited to the range 1.8 - 2.6 gm/cc.

3.3 Estimation from Observed Compressional Velocities.

One of the best sources of indirect evidence as to the density of the subsurface rocks is seismic information. This is most useful in that it also gives some clues as to the density of the island body below sea-level.

As far as is known, no seismic work of any kind has been carried out on any of the Atlantic islands with which we are concerned, so we must consider seismic data around the islands, on other volcanic islands and also on seamounts on the assumption that the latter are basically similar structures which have not quite broken surface. This data is summarized in Table 3.1 and Fig. 3.1.

For surveys on the island surface, there is the data on Iceland (Bäth, 1960; Pálmason, 1963), the Faroes (Pálmason, 1965) and on Hawaii (Furumoto et al, 1965). These all show a top layer approximately one kilometre thick, with a compressional velocity of 2.8 - 3.9 km/sec. This layer is absent from the atolls and has possibly been stripped by marine erosion as the islands slowly subsided. The rocks of the second layer are below sea-level and have most probably

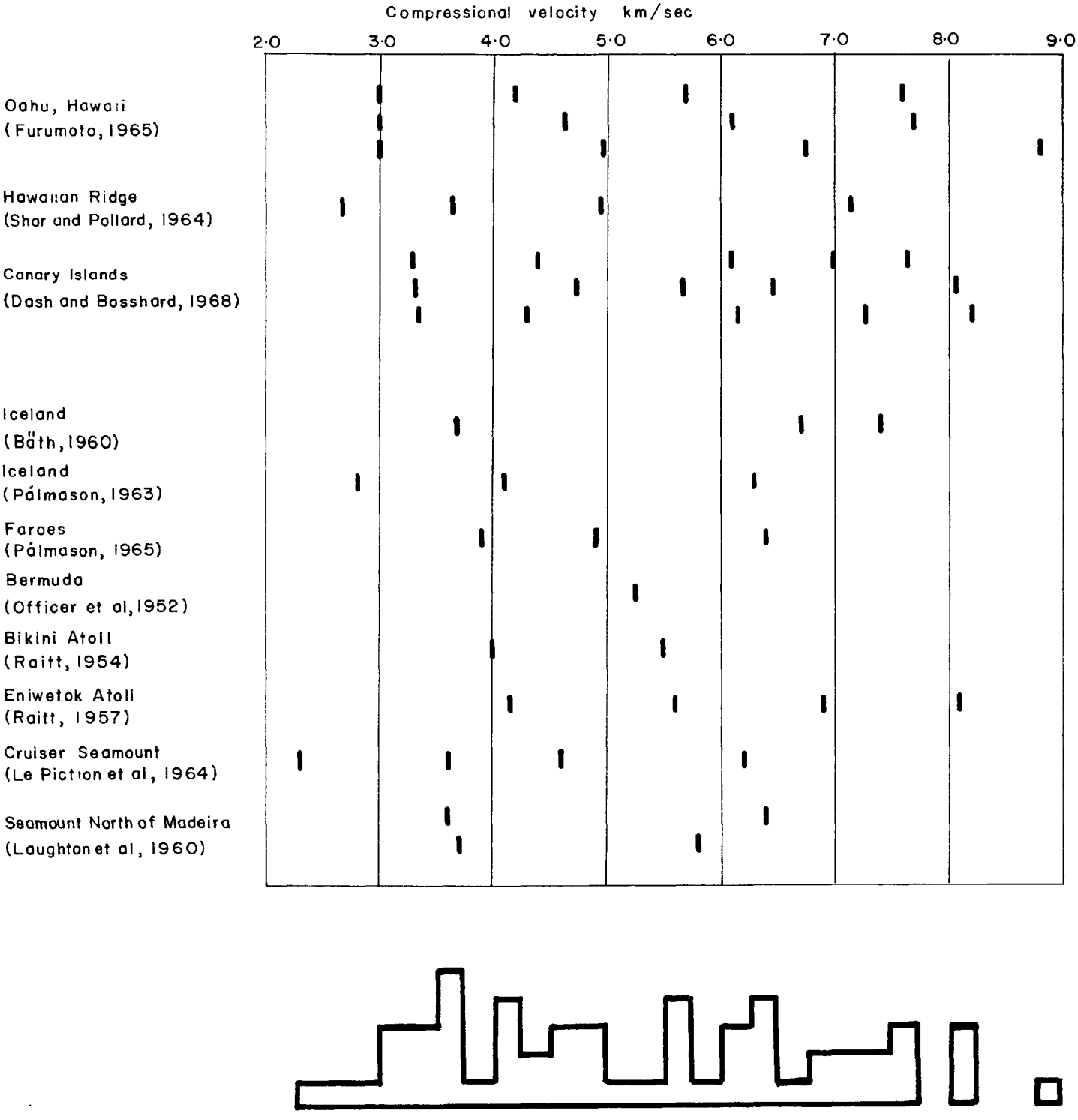

FIG. 3.1. Summary of seismic refraction studies on islands and seamounts.

Seismic Velocities and Thicknesses of
Island and Seamount Seismic Stations.

Region	Velocities km/sec							Thicknesses km				
	a	b	c	d	e	f	Water	a	b	c	d	e
Iceland (Bäth, 1960)		3.69			6.71	7.4	0		2.1		15.7	10.0
Iceland (Palmason, 1963)		2.8	4.1	5.0	6.3							
Faeroes (Palmason, 1963)		3.9	4.9	6.4					0.5-0.8	2.0-2.5		
Bermuda (Officer, 1952)				5.25								
Cruiser Seamount (Le Pichon & Talwani, 1964)	2.3	3.6	4.6	6.2				0.2	0.5	4.0		
Seamount N of Madeira (Laughton et al, 1960)		3.6 3.7		6.4 5.3					1.2 2.2			
Bikini Atoll (Raitt, 1954)			4.0	5.5						3.0		
Eniwetok Atoll (Raitt, 1957)	Coral and Limestone		4.15	5.59	6.90	8.09				1.5-2.0	3.0	6.0

Oahu		3.0	4.2	5.7		7.6			1.2	2.6	1.6		
(Furumoto, 1965)		3.0	4.63	6.1		7.7			0.7	1.0	2.9		
		3.0	4.97		6.75	8.8			2.15	7.4		11.0	
Hawaii	2.68	3.65	4.96		7.15	8.10	0.52	0.83	1.4	5.9		5.3	
(Shor and Pollard, 1964)							1.20	1.01	0.2	7.7		2.2	
Canary Islands		3.30	4.40	6.10	7.00	7.65	3.52		2.09	2.57	3.32	3.21	
(Dash and Bosshard,		3.35	4.30	6.15	7.28	8.20	2.96		2.31	2.92	1.13	5.28	
1968)		3.31	4.73	5.67	6.45	8.07	2.21		2.34	1.30	3.17	2.20	
							3.09		1.79	2.70	1.11	2.75	

Table 3.1

been erupted in a sub-aqueous environment. Hence data from seamounts and from the areas immediately surrounding the islands also become relevant. In all cases, the low velocity layer is underlain by a layer of considerably higher velocity, at a depth below sea-level which is above that of the sea-floor in the surrounding ocean. With the exception of Bermuda, a seamount north of Madeira and Bäth's results from Iceland, the velocity of this layer is between 4 - 5 km/sec and its thickness between 1.0 and 4.0 km. Below this is a further layer with velocity 5.1 - 6.4 km/sec, very similar to "layer 2" of the oceanic crust.

Seismic evidence must be treated with some caution since special care must be exercised in interpreting velocity information in terms of density. Manghani and Woollard (1965) have shown that the velocity-density relationship is strongly affected by porosity and the amounts of glass and olivine present in the rock, and in these respects several differences between the oceanic rocks and the commonly encountered continental-type igneous rocks must be considered.

Oceanic basalts tend to be vesicular and even where the lava is solid, a lava flow will often have bands of vesicular lava at its base and at its top. Moore (1965) has shown that this is true only of lava erupted above or little below sea-level. In lavas erupted under water, vesicularity appears to decrease with increasing depth and pressure until below 800 m there are essentially no vesicles.

Lavas extruded at some depth in a sub-aqueous environment tend to be in the form of breccias or pillow basalt, (Nayudu, 1962; Moore, 1965; Jones, 1966; McBirney, 1963) with a glassy outer shell about one centimetre thick and poorly developed columnar jointing perpendicular to the outer surface. Void spaces between successive flows of the pillow lava or breccia produce porosity in the volcanic pile persisting down to much greater depths than is possible by vesicularity, and thus lower the density and velocity of the rock.

These factors can result in velocities much lower than are normally associated with volcanic rocks and, more important, the presence of glass and fine cracks in the lava results in a lower velocity for a given density than one might otherwise expect.

For the material above sea-level, where the conditions for the formation of glass and pillow lava exist only in lakes, the velocity-density relationship is little changed. From the curve presented by Nafe and Drake (1963) relating compressional velocity and density, the 2.8 - 3.9 km/sec velocities obtained for the upper layer correspond to densities between 2.15 and 2.35 gm/cc. From the same curve, the velocities of 4.0 - 5.0 km/sec for the second layer would correspond to a density range of 2.35 - 2.55 gm/cc. However, on the assumption that this second layer corresponds to breccia and pillow lava, with a high percentage of glass and

possibly olivine and also with some porosity remaining, these velocities were considered to correspond to a density of 2.6 gm/cc, somewhat higher than predicted by Nafe's curve.

3.4 Estimation from Surface Gravity Data.

Several methods have been suggested for the determination of the bulk density from the gravity data. The basic method is that due to Nettleton (1939) whereby gravity profiles are calculated for various assumed values of the density of the underlying formations. The value which makes the profile correlate least with the topographic section is selected as the true mean density of the surface rocks. Nettleton's original method is graphical, but Jung (1953) has pointed out that it can be translated into exact mathematical language by putting the correlation coefficient between the Bouguer anomaly and elevation equal to zero. Parasnis (1952) proposed another method similar in principle, where the free-air anomaly computed for various stations at different elevations is plotted against - 0.04191h + T (h = elevation in metres, T = terrain correction for unit density) and the slope of the line determined by least squares, is adopted as the true density.

A necessary condition before Nettleton's system or the variations upon it can be applied, is that the topography is not correlated with the subsurface structure. This is seldom

the case on oceanic islands. The maximum elevations frequently occur at the main centre of volcanic activity or along volcanic fissures, so that the topography is very closely connected with the subsurface structure and therefore the Bouguer anomaly.

Before any of the profile methods can be applied, the gravitational effect of the main subsurface structures must be removed from the observed Bouguer anomaly. The removal of this field can be very conveniently combined with an extension of the method developed by Legge (1944) for the determination of the bulk density from gravity data. His method consisted in developing the Bouguer anomaly values observed at discrete points over an areal pattern, as a second order polynomial in x and y by least squares and then choosing that density for the Bouguer correction which reduced the sum of the squares of the residual values to a minimum. In applying Legge's method to all the stations distributed over each island, polynomials of up to the seventh order in x and y were used to approximate the observed field. The main subsurface structures being fairly deep, their effects should be adequately approximated by an nth order polynomial. The residuals, once this polynomial has been removed, will then have zero correlation with the topography.

The main assumption of the density profiling method has been expressed differently by Le Pichon and Talwani (1964) as follows "if there is any subsurface anomalous distribution of mass, its wavelength is either much shorter or much longer than the dimensions of the body studied." The removal of an nth order regional field is equivalent to submitting the gravity data to a high-pass filter, removing all the long-wavelength components. The wavelengths of the field remaining are then much shorter than the dimensions of the area studied. The assumption of the profiling method is then true for the residual field, and the method can be applied.

The extended version of Legge's method described below allows the digital filtering and the density determination to be performed in one operation.

The Bouguer anomaly is equal to

$$g_i = g_o + 0.3086h - \rho(0.04191h - T)$$

where g_o = difference between the observed and normal gravity

h = elevation in metres

ρ = density

T = terrain correction for unit density.

Let the corrected Bouguer anomaly over the pattern P be approximated by an nth order polynomial in x and y so that

$$g_i \approx \sum_{i=0}^{n} \sum_{j=0}^{n-i} a_{ij} x^i y^j$$

Then choose ρ and the a_{ij} such that

$$I(a_{ij},\rho) = \sum_P \left[g_o + 0.3086h - \rho(0.04191h - T) - \sum_{i=0}^{n} \sum_{j=0}^{n-i} a_{ij} x^i y^j \right]^2$$

be a minimum

Let $g_o + 0.3086h = f$ and $0.04191h - T = d$

$$I(a_{ij},\rho) = \sum_P (f^2 - 2f(\rho d + \sum_{i=0}^{n} \sum_{j=0}^{n-i} a_{ij} x^i y^j) + (\rho d + \sum_{i=0}^{n} \sum_{j=0}^{n-i} a_{ij} x^i y^j)^2)$$

To minimize $I(a_{ij},\rho)$, differentiate partially with respect to a_{ij} and ρ and equate to zero.

$$\sum_P (\boxed{}^{i}_{j} x^i y^j (\sum_{i=0}^{n} \sum_{j=0}^{n-i} a_{ij} x^i y^j + \rho d) = \sum_P f(\boxed{} x^i y^j)$$

etc.

and $\sum_P fd = \sum_P d(\rho d + \sum_{i=0}^{n} \sum_{j=0}^{n-i} a_{ij} x^i y^j)$.

In matrix notation this becomes

$$\begin{bmatrix} N & \Sigma x & \Sigma y & \cdots & \Sigma y^n & \Sigma d \\ \Sigma x & & & & & \\ \Sigma y & & & & & \\ & & & & & \\ \Sigma y^n & & & & & \\ \Sigma d & & & & & \Sigma d^2 \end{bmatrix} \begin{bmatrix} a_{00} \\ a_{10} \\ a_{01} \\ \vdots \\ a_{0n} \\ \rho \end{bmatrix} = \begin{bmatrix} \Sigma f \\ \Sigma fx \\ \Sigma fy \\ \\ \Sigma fy^n \\ \Sigma fd \end{bmatrix}$$

i.e. $[X][A] = [F]$ say

Hence the solution is

$$[A] = [X]^{-1}[F]$$

This method was applied to the data of all the islands on which terrain correctionshad been made and the results are shown in Table 3.2. The order of the polynomial required to adequately define the field due to the main structures will depend on the dimensions of the island and on the number and complexity of the structures. Values of N from 3 to 7 were used and while the results show that the value of the density obtained depends upon the order of the polynomial to some extent, the values for the 5th, 6th and 7th orders differ by less than 0.1 gm/cc in all cases where the number of stations is large enough to justify using such high orders. Since for 5th, 6th and 7th order polynomials, there are respectively 22, 29 and 37 coefficients to be determined, the data from the islands of Fernando de Noronha (20 stations) and Madeira (23 stations) are insufficient to warrant the use of these high orders.

For the sake of comparison, the value of the density was also calculated by the Parasnis method. In all cases, the values obtained by the extended Legge method, using the mean of the 5th, 6th and 7th order values, were lower than those calculated by the Parasnis method, the average difference being 0.39 gm/cc. The mean specific gravity for the islands excluding Madeira and Fernando de Noronha, is 2.31 with a range from 2.10 to 2.58 by the extended Legge method, and 2.80 ranging from 2.46 to 3.06 by the Parasnis method.

Density Values Calculated from the Gravity Data

Island	Extended Legge Method 3rd	4th	5th Orders	6th	7th	Mean of 5th, 6th and 7th	Parasnis Density	Diff. P-L
S. Maria	2.19	2.23	2.18	2.24	2.10	2.17	2.49	+0.32
S. Miguel	2.70	2.55	2.61	2.55	2.58	2.58	2.90	+0.32
Terceira	2.04	2.02	2.11	2.08	2.12	2.10	2.75	+0.65
Pico	2.57	2.49	2.22	2.28	2.30	2.27	2.61	+0.34
Faial	2.17	2.17	2.19	2.09	2.08	2.12	2.50	+0.38
S. Jorge	2.63	2.38	2.25	2.25	2.38	2.29	2.59	+0.30
Flores	2.25	2.27	2.30	2.24	2.34	2.29	2.46	+0.17
Lanzarote	2.42	2.06	2.64	2.33	2.57	2.51	3.06	+0.55
Tenerife	2.65	2.53	2.45	2.38	2.40	2.41	2.90	+0.49
Hierro	2.43	2.39	2.37	2.37	2.35	2.36	2.76	+0.40
Ascension	2.17	2.42	2.39	2.35	2.30	2.35		
Madeira	2.23	2.15	2.18	2.26	2.36	2.27	2.57	+0.30
Fernando de Noronha	1.84	1.64	1.27	1.06	1.17	1.17	1.20	+0.03

Table 3.2

It can readily be seen why the Parasnis method yields values which are too high. The Bouguer correction is $-2\pi\rho Gh$, where ρ = density, h = elevation, and G = gravitational constant. In circumstances where the high gravity anomaly is associated with high elevations, as happens on most of the oceanic islands, the Parasnis method will attempt to remove this genuine correlation between elevation and Bouguer anomaly by increasing the Bouguer correction, i.e. by assigning an artificially high value to the density.

The former value of 2.31 gm/cc is in excellent agreement with both geological and seismic evidence and on these bases a density of 2.3 gm/cc was adopted for the Bouguer reduction and land correction of all the islands.

As the order of the regional field removed is increased, the magnitude of the residuals approaches the limits of accuracy of the observations. For this reason and because the stations are generally small in number and not closely or regularly spaced, one hesitates to place an absolute reliance on the calculated densities for the individual islands, but discussion as to the possible significance of the difference between the islands must be deferred to a later chapter.

3.5 Density of the Island below Sea-Level.

So far, we have considered the density only of the tip of the island which shows above sea level. For the great bulk of the island which lies below sea-level, the density can be inferred from dredgings from the island slopes, from seismic evidence and from marine gravity work.

Dredgings from several seamounts, Retreiver Peak (Shurbet and Worzel, 1955), Caryn Peak (Miller and Ewing, 1956), Jasper Seamount (Harrison and Brisbin, 1959) and a seamount north of Madeira (Laughton et al, 1960) have obtained vesicular and altered basalts of low density. A sample from Jasper Seamount had a density of 2.05 gm/cc and a velocity of 3.7 km/sec, and vesicular samples recovered from the seamount north of Madeira had dry densities ranging from 1.61 - 1.85. Assuming complete porosity their respective vesicularities of 43 - 35 per cent would yield a wet density of from 2.05 - 2.23 gm/cc.

Moore (1965) sampled lavas along the rift zones off the coast of the island of Hawaii and found that the vesicularity and the bulk density showed a systematic change with depth; the density increased from 2.2 gm/cc at the surface to 2.9 gm/cc at one kilometre below sea-level, then more slowly, until it reached 3.0 gm/cc at 4 km. Since these are lavas, they set an upper limit for the specific gravity of the sub-aqueous material, which will consist also of pyroclastics,

sediments and volcanic debris from eruptions nearer the surface, or even sub-aerial eruptions. Compaction will also play a part with increasing depth but a density between 2.0 and 2.6 gm/cc seems reasonable for the material forming the flanks of the islands. However, it is probable that the core of the island has a considerably higher density than the flanking rocks. Nayudu (1962) from the observed occurrence of tholoids, suggests a core of lavas intruded into the body of the island in the form of dykes, sills, or a laccolith-like structure. Such lavas would be non-vesicular, due to their depth of intrusion, with a density in the region 2.6 - 3.0 gm/cc and would increase the bulk density of the island considerably.

The seismic data, as has already been discussed, show a 2.3 gm/cc layer underlain by 2.6 gm/cc material at a depth below sea-level which is above that of the surrounding sea-floor. This is clearly consistent with the above hypothesis of the island structure.

Nettleton's profiling method cannot be applied to the marine gravity data for the same reason which ruled out the use of his method for the surface gravity measurements. Since a magma chamber or some form of compensation may be expected, of similar dimensions to the island itself, the requirement that the topography have no correlation with any subsurface anomalous distribution of mass cannot be satisfied.

When marine gravity stations exist close to land where there is a well established gravity trend, however, this trend should be continued by the marine measurements without any sharp change between the land and marine Bouguer anomaly values. Such marine stations exist in Tenerife (line HH', Fig. 6.4) and on S. Miguel (line CC', Fig. 5.5) Bouguer anomaly. Profiles are shown in these figures for several assumed values of density and in both cases are smoothest for a density value between 2.2 - 2.4 gm/cc. This would imply that the bulk density of the island, down to a depth of about 3 km at least, falls within this range and that the core forms only a small part of the island body.

On these bases, the mean density of the island was taken to be 2.4 gm/cc for the purpose of the bathymetric correction.

CHAPTER 4

A GRAVITY SURVEY OF ASCENSION ISLAND

4.1 Introduction

A gravity survey was conducted as part of the investigations of the Oxford Expedition to Ascension in July 1964 (Atkins et al, 1964). The gravity base station WA6049 established by Woollard (Woollard and Rose, 1963) was used as the primary base for the survey. His description of this stations follows,

WA6049. At the weather station, in the centre of the operations room floor.

07^{o} 58.5'S 14^{o} 24.4'W 259 feet 978294.3 mgal

4.2 General Geology

Ascension Island (Fig. 4.1) is situated in the South Atlantic Ocean and rises some 100 km west of the axis of the Mid-Atlantic Ridge at 7^{o} 57'S, 14^{o} 23'W. Roughly triangular in outline and some 97 km^2 in area, it rises from a depth of 3400 m, where its basal diameter is approximately 80 km, to a maximum elevation of 859 m above sea-level.

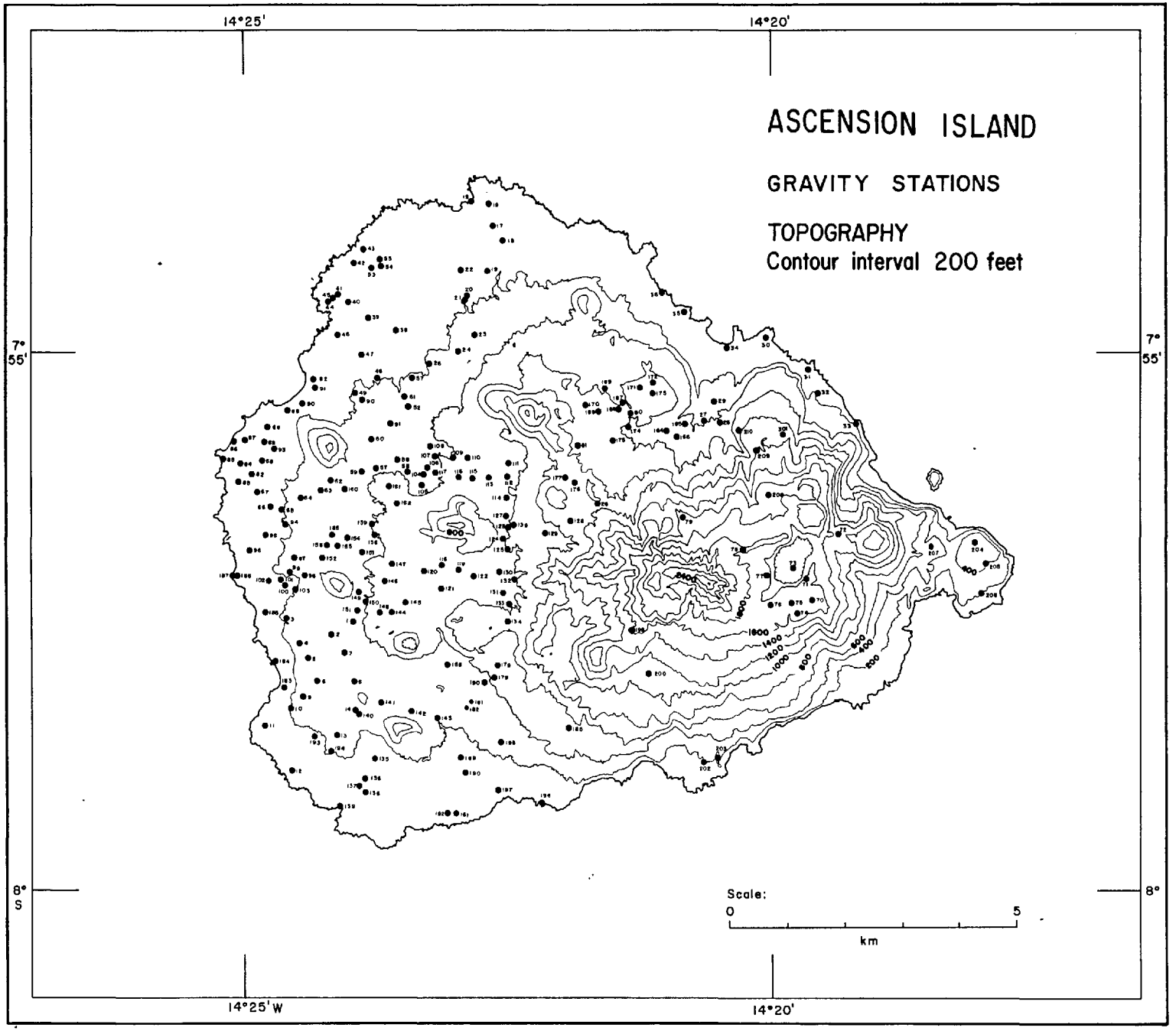
14°25'
14°20'
ASCENSION ISLAND
GRAVITY STATIONS
TOPOGRAPHY
Contour interval 200 feet
7° 55'
8° S
Scale:
0
5
km
14°25' W
14°20'

FIG. 4·1

The trend of the surface topography is continued in the bathymetry. The body of the island slopes away steeply in the NE and SE with gradients of between 15° and 25°. In the east, the slope is gentler, between 8° and 15°, and in the west the depth increases slowly down to 200 fathoms, forming a shelf some 5 km wide beyond which the gradient changes to 10°, as in the east.

With the exception of thin local deposits of wind-blown sand and beach rock, it is entirely volcanic in origin with lava types ranging from basalt to rhyolite, though the main lava types are basalt and trachyte (Atkins et al, 1964; Bell, 1965). The principal trachyte masses occur in the eastern part while basalt predominates in the west in the form of basalt flows and cones. There are also large deposits of pyroclastic material in many parts of the island. In the eastern part there is a small caldera-like structure ascribed to a combination of explosive activity and of subsidence following the protrusion of nearby large trachytic bodies (Bell, 1965). Apart from one clear case of fissure eruption to be seen bisecting the eastern peninsula, eruptions have been mainly of the central variety.

There is no recorded historical eruption but two of the lava flows, one in the north west, the other in the south-west, are clearly very young. In recent K-Ar and Rb-Sr dating, one trachyte sample yielded an age of 1.5 MY, but the

other six rocks dated were all much younger (Bell, personal communication).

4.3 Details of Survey.

A Worden Pioneer Gravimeter No. 628 was used, which enabled the value of gravity to be measured to ± 0.1 mgal. Stations were located to within 20 m using the 1964 U.S. Naval 1 : 2400 map. Elevations were determined from the same map, which was contoured at 10 ft intervals, or by reference to sea-level at coastal stations, and are accurate to ± 10 ft. Topographic corrections were calculated by computer, using a contour interval of 200 ft, and should be accurate to ± 2 mgal. The uncertainty in elevation corresponds to an error of 0.6 mgal. The error due to tidal effects is much less than this, and was neglected, so that the total error in the Bouguer anomaly is less than ± 3 mgal.

4.4 Regional

Although no data are to hand from continuous gravity measurements, Worzel (1965b) published the details of a large number of pendulum gravity stations around Ascension Island and these are shown in Fig. 4.2. The first question to be answered concerns the isostatic adjustment of the island. One approach (Vening Meinesz, 1948) is to calculate the isostatic anomaly using various assumed models for the crust and to accept that model as true which brings the anomaly

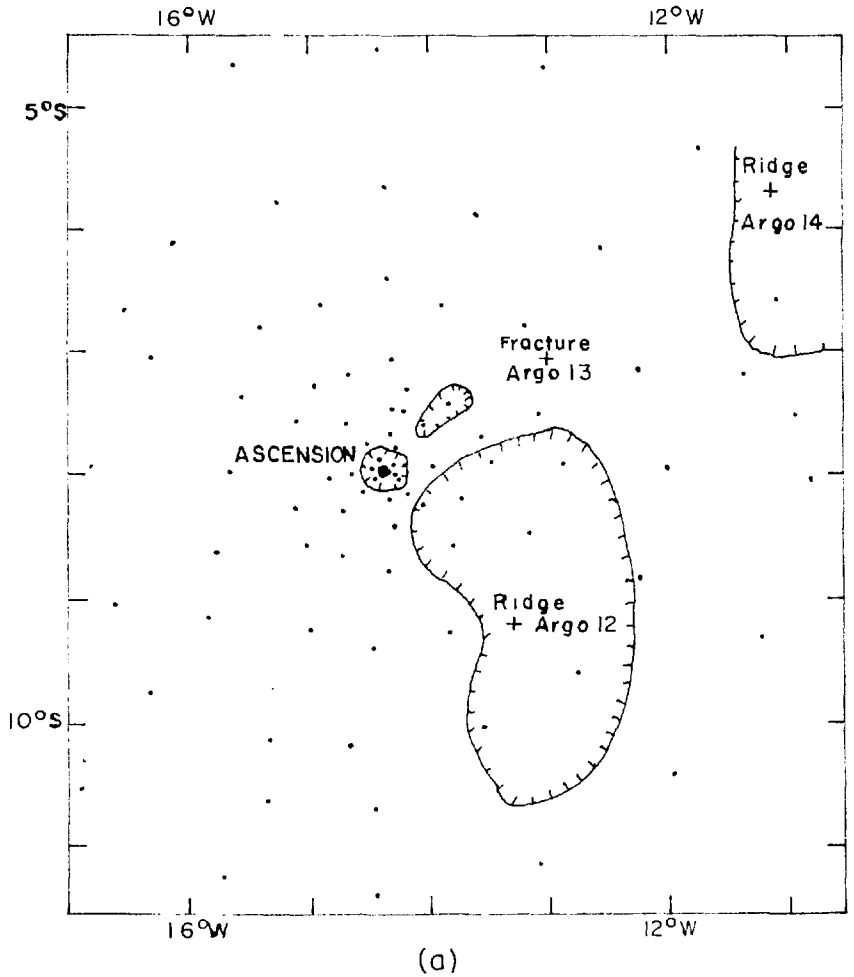

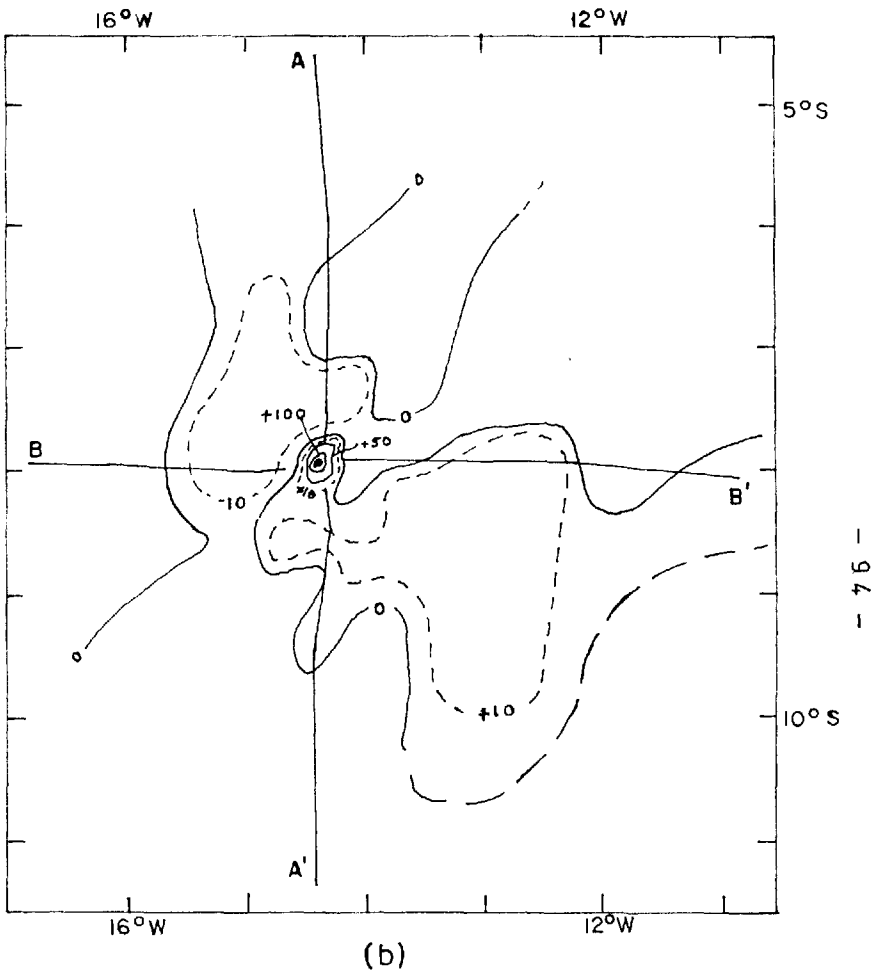

FIG.4·2. Pendelum gravity data around Ascension Island (after Worzel, 1965)

(a) Gravity stations and Bouguer anomaly

Contours enclose areas where the Bouguer anomaly is <200 mgal

(b) Free-air anomaly

closest to zero. This is not only an extremely tedious process, it is also easy to be misled by studying isostatic anomalies that are based on assumed densities, and dimensions of the compensating mass which may well be in error.

It is well-known that over a broad, isostatically compensated region the free-air anomaly will average zero. This needs only that the field be adequately defined over a broad area and requires no assumptions as to density or shape of the subsurface compensating masses.

Islands represent a load on the oceanic crust but, because of the strength of the crustal material, isostatic adjustment does not take place immediately under the island. Instead, it is spread over a wide area of the order of 100 km radius (Vening Meinesz, 1948). The Airy hypothesis of isostasy is of a rigid crust floating on a denser plastic substratum and bending under the load (the island in this particular case) in the same way as an elastic plate floating on a liquid bends under the weight of a superimposed load. The down-bending displaces the denser material and causes a mass deficiency equal to the imposed mass. In the same way, the island in isostatic equilibrium would have a broad root of less dense material thrusting down into the mantle with a mass equal to that of the island superimposed on the oceanic crust.

The gravity field due to the island will thus have two components, a broad shallow negative effect due to the deep island root and a sharp positive effect due to the excess mass of the island body protruding above the surrounding sea-floor. A gravity profile across an island in isostatic equilibrium might appear as in Fig. 4.3.

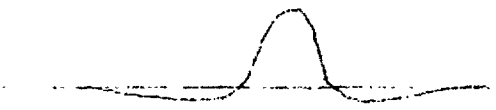

Free-Air Anomaly

Fig. 4.3

As one approaches the island, the deeper and wider compensating mass first produces a negative free-air anomaly which changes to a much larger and sharper positive free-air anomaly as the more local effect of the island body itself becomes predominant. Then if the surrounding structures are also in equilibrium, so that the mean free-air anomaly of the background field is zero, the integral of the free-air anomaly on and around the island must be zero.

This pattern can be seen in Fig. 4.2 and more clearly in Fig. 4.4 where the large positive value of free-air anomaly on and in the immediate vicinity of the island changes rapidly to negative values which practically surround the island. Thus qualitatively it can be said that the island is compensated to some degree. Quantitatively,

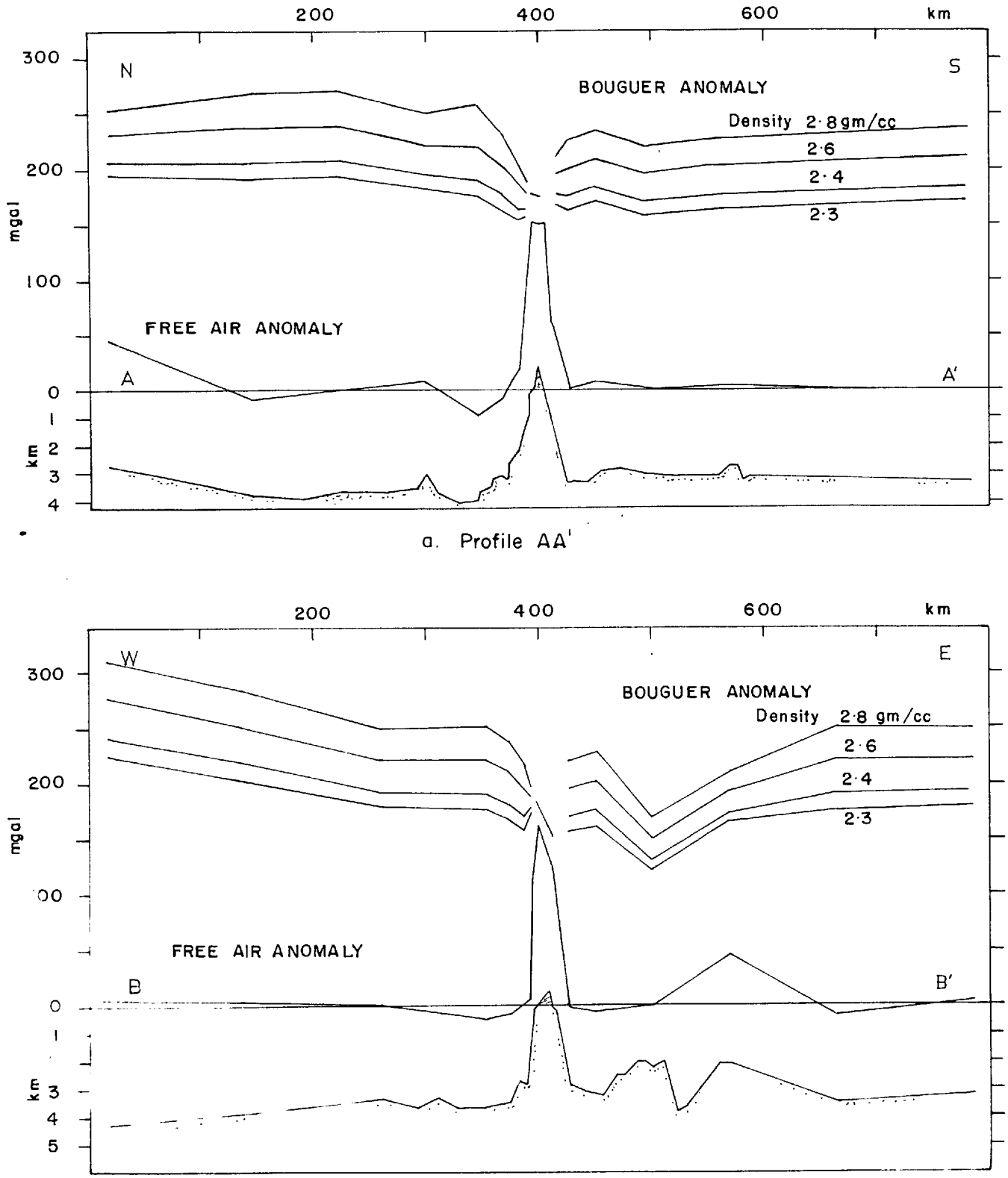

FIG. 4·4 Free-air and Bouguer anomaly profiles across Ascension Island
The locations of the profiles are shown in Fig. 4·2.

complications arise from the island's position on the Mid-Atlantic Ridge and from the proximity of the east-west fracture zone shown in the chart for this area (Heezen and Tharp, 1961) and in the profile 13 in the paper by Vacquier and Von Herzen (1964). The bathymetric data in this area (National Hydrographic Office, Collected Soundings Sheet No. 275) are very scanty and the positions of the Mid-Atlantic Ridge and the fracture zone as determined by Vacquier and Von Herzen (1964), shown on the map, are the best evidence we have as to the location of these features.

Both the mid-ocean ridge and the fracture zone can be expected to have gravity anomalies associated with them. Work by Talwani et al (1961; 1965) and also the gravity profiles across the Mid-Atlantic Ridge shown in Figs. 5.3 and 5.4 indicate that the Ridge is generally associated with a positive free-air anomaly and a low Bouguer anomaly. A continuous gravity profile across the Romanche fracture zone (Heezen et al, 1964) shows a broad region of positive free-air anomaly about 160 km wide with a narrow (25 km) negative anomaly in the middle, corresponding to the trench of the fracture zone.

Similar patterns can be seen in Fig. 4.2, where a north-south trending region of positive free-air anomaly and low Bouguer anomaly, which coincides with the position of the Ridge as determined by Vacquier and Von Herzen (1964), can be seen south of 8^{o}S.

This area is terminated to the north by an ENE-WSW band of negative free-air anomaly extending eastwards from Ascension Island. The low Bouguer anomaly of one station in the east of the map, coupled with the position of the axis of the ridge as determined by Vacquier at 5.7°S, 11.1°W suggest that the ridge continues northwards from about 7°S, having been displaced right-laterally some 200 km. The position of the postulated fracture is at variance with its position as obtained by Vacquier and it may be that there is more than one fracture, arranged en echelon as in the Chain and Romanche fracture zones (Heezen et al, 1964). On these bases, it is suggested that Ascension Island lies at the western end of an approximately east-west fracture zone.

In an attempt to place the question of isostatic equilibrium on a quantitative basis, an approximate integration of the free-air anomaly was calculated for progressively increasing distances from the island. The area around Ascension was divided into approximately 12 km squares and the free-air anomaly in each square assigned by interpolation. With the island as the centre, the free-air anomaly was then summed over all the squares, with increasing area of integration. The results are shown in Table 4.1 and indicate that, if anything, the island is slightly overcompensated and that the radius of compensation is approximately 70 km

Integration of the Free-Air Anomaly around the Island.

The size of each square is 11.7 x 11.7 = 136 km^2

Area of Integration	Integrated Free-air Anomalies	Anomaly/ Square	Radius of Integration
1 x 1 squares	160 mgal	160	5.8 km
3 x 3	520	57.78	17.5
5 x 5	563	22.52	29.2
7 x 7	450	9.18	40.9
9 x 9	295	3.64	52.6
11 x 11	127	1.05	64.3
13 x 13	-124	-0.73	75.9
15 x 15	-350	-1.56	87.6
17 x 17	-529	-1.83	99.3
19 x 19	-489	-1.35	111.0

Table 4.1

Fig. 4.4 shows also the Bouguer anomaly along the north-south and west-east profiles AA' and BB' indicated in Fig. 4.2b. These Bouguer anomalies have been calculated as described in Section 2.6 for several island densities but the resulting profiles are a good example of the failure often encountered of Nettleton's (1939) method to yield a value for bulk density.

The west-east Bouguer anomaly profiles (Fig. 4.4b) show a gravity minimum located some 100 km to the east of the island. This coincides with the suggested position of the Ridge axis and is consistent with other gravity profiles across the Mid-Atlantic Ridge (Fig. 5.3 and 5.4) which also indicate a Bouguer anomaly minimum over the crest of the ridge.

4.5 Local Anomaly

The distribution of the gravity stations established in the course of the survey is shown in Fig. 4.1. The chief characteristic of the Bouguer anomaly as it is contoured in Fig. 4.5 is a pronounced east-west gradient across the island, decreasing from a maximum value of 194 mgal in the south-west to a value of 156 mgal in the extreme east. The maximum gradient is 7 mgal/km, which occurs in the south-west, and the mean east-west gradient is 2.2 mgal/km. Other major features are the gravity maxima, one in the north-west, the other in the south-west, and the slight depression in the Bouguer anomaly which runs east-west across the middle of the island. This latter feature may be associated with the fissure line which Bell (1965) suggested might run westwards from the eastern peninsula, but the poor distribution of stations in the eastern half of the island makes it impossible to determine that this is not merely a gravity col between the north-west and south-west anomalies.

The smaller anomalies are masked by the strong east-west gradient in Fig. 4.5, and can be seen more clearly on the residual gravity map, Fig. 4.6. This map was obtained by removing the second order regional field in the manner described in Chapter 2, Section 4. For convenience, a constant value was added to the residuals in order to make the lowest value zero. The accuracy of the Bouguer anomaly is

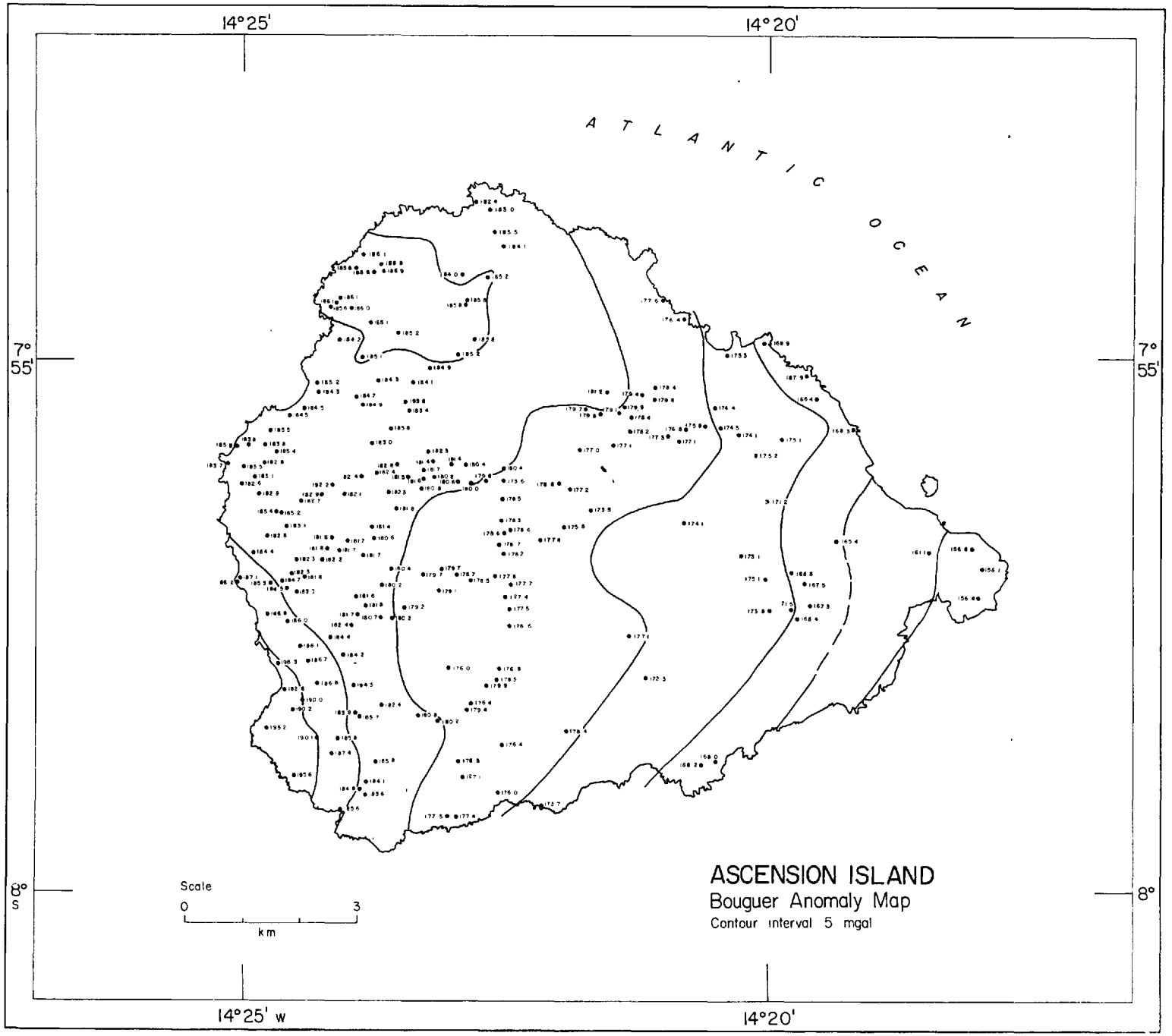
14°25'
14°20'
7° 55'
8° S
14°25' w
ATLANTIC OCEAN
Scale
0
3
km
ASCENSION ISLAND
Bouguer Anomaly Map
Contour interval 5 mgal

FIG. 4·5

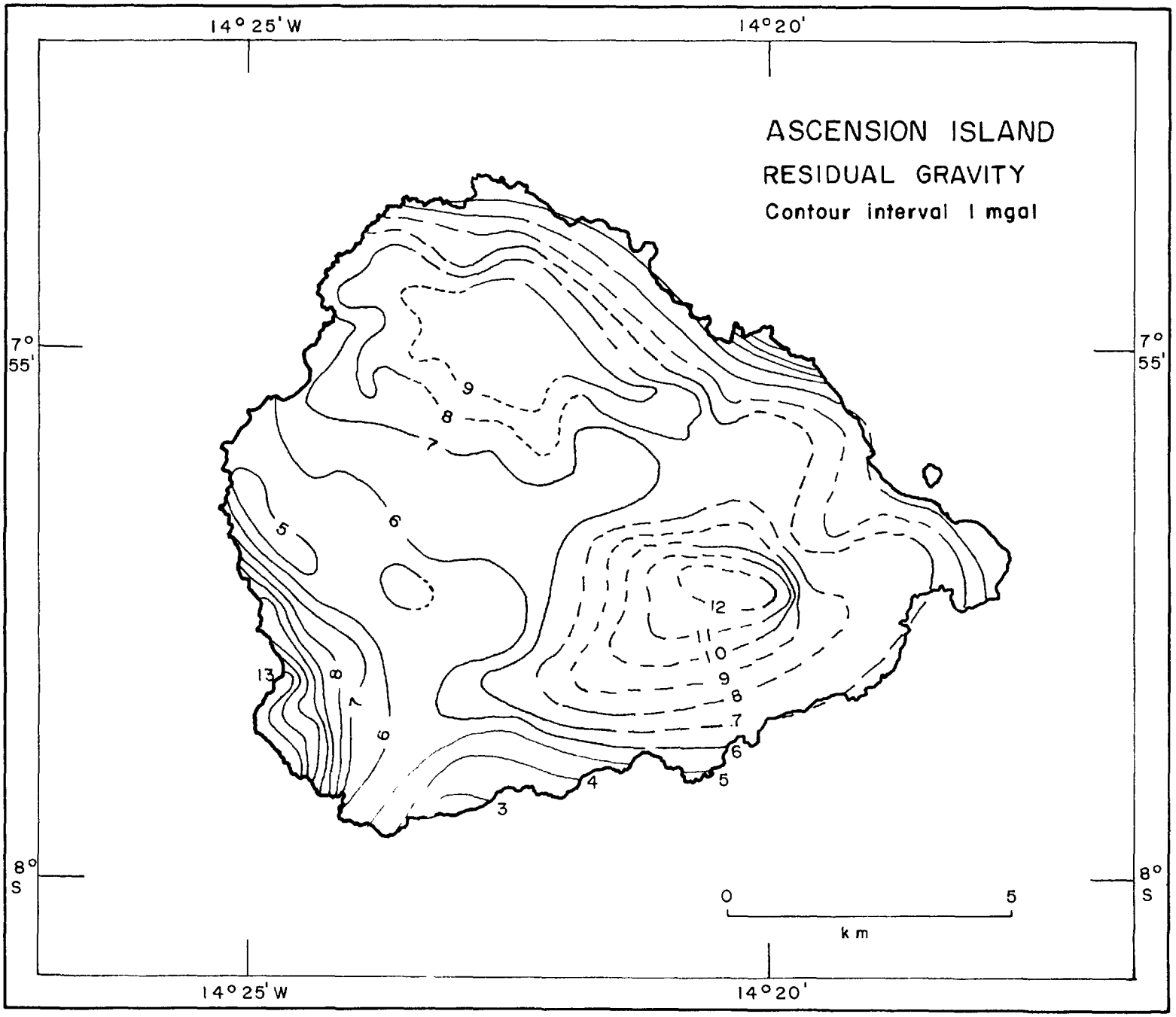
14° 25' W
14° 20'
ASCENSION ISLAND
RESIDUAL GRAVITY
Contour interval 1 mgal
7° 55'
8° S
9
8
7
6
5
12
11
10
9
8
7
6
5
4
3
13
8
7
6
0
5
km

FIG. 4·6

only ± 3 mgal, and the contours drawn at one milligal intervals have been smoothed slightly. That the smoothing required was only slight bears out the accuracy of the methods of elevation determination and terrain correction.

The residual map shows a large positive anomaly in the centre of the island with noses pointing east, north-west and south-west, the last two towards two other positive centres in the north-west and in the south-west respectively. Gravity stations are too few in the north and east to accurately define the anomalies in those areas, so that the contours there must be considered highly conjectural. As drawn, the eastern positive anomaly is located over the older trachytic centre of the island, the north-west anomaly is near one of the centres of most recent activity in the island and the anomaly in the south-west appears to be centred 3 km west of the other centre of recent activity (Atkins et al, 1964).

The configuration of Bouguer anomaly contours in Fig. 4.5 suggests a large mass excess near the west coast of the island and two additional smaller masses in the north-west and south-west. Considering first the large anomaly, the one-sided gravity gradient implies that the centre of the anomalous body must be displaced to the west of the island. The slight gradient at the western end of the island may be due to the effects of the two anomalies to the north and south, and does not necessarily require that the body be centred off-shore.

With gravity coverage limited to the island surface, it is impossible to determine the value of the background gravity field. The depths and positions of the pendulum gravity stations near the island are inconsistent with the bathymetry shown on the Admiralty chart No. 1691. This makes it impossible to compute the Bouguer anomaly of these stations with any accuracy, with the result that the marine gravity data are of little assistance in estimating the background gravity field. Experience on other islands (see Chapters 5 and 6) indicates that the regional field is generally 20 - 30 mgal less than the lowest gravity value observed on the island and for this reason a value of 130 mgal was adopted as the background Bouguer anomaly over the island. The amplitude of the gravity anomaly over the main centre is then 52 mgal.

Corollary 1.1 of Bott and Smith (1958) states that for the gravity field due to a three-dimensional body, if $g(x)$ and $dg(x)/dx$ are respectively the gravity anomaly and the gravity gradient at a point x, then the maximum depth to the upper surface of the anomalous body is given by

$$1.5\ g(x) \Big/ \frac{dg(x)}{dx} \qquad (4.1)$$

In the present case this formula yields a limiting depth of 10 km.

With a gravity anomaly of + 52 mgal and a maximum possible depth of 10 km, the anomalous body must clearly be a

large mass of high density material. In a volcanic environment, this mass is likely to take the form of a volcanic plug, a dense dyke swarm or a crustal magma chamber. Any one of these, if it produces an anomaly of 50 mgal, will indicate a major volcanic centre. There is only one such anomaly on Ascension Island and it is interpreted as indicating the primary volcanic centre which has built up the bulk of the island structure as it stands above the level of the sea-floor.

The anomaly is centred well to the west of the apparent mountainous core of the island, but this position is quite consistent with the bathymetry, which shows that the summit area of the volcanic edifice extends 5 km west of the present island. The young basaltic lavas and cinder cones in the western half of the island obscure any geological traces of this main centre, but it is probable that the shallow shelf to the west of the island is an abrasion surface created by the marine erosion of the summit of this primary volcano.

The elongation of the Bouguer anomaly contours in an easterly direction suggests that the island as it now stands may have been built up along an east-west trend by lateral offshoots from the main volcanic centre. This trend may be a continuation of the fracture zone which displaces the axis of the Mid-Atlantic Ridge at this latitude.

The westerly position of the main volcano centre may indicate that trachytic highlands in the east of the island represent an eastward shift of volcanic activity with time. This would be in accord with the very young basalt found in the eastern peninsula. The recent though not historic activity which has occurred in the west may result from a reactivation of the primary volcanic centre.

The three positive anomalies shown in the residual map have similar magnitudes and dimensions. The anomaly to the south-west is the best defined, and appears to have an amplitude of between 12 and 15 mgal. The maximum depth to the anomalous body can be estimated from equation 4.1 and is equal to 1.5 km. Similar results are found for the other two residual anomalies.

Stearns and Macdonald (1946) found in the island of Hawaii that the summit of each volcanic centre is underlain by a dyke complex or a composite volcanic plug which measures up to 6 km in diameter, and the residual gravity anomalies on Ascension Island may be due to similar structures on a smaller scale.

The eastern centre on the residual gravity map is located under great outcrops of trachyte and may indicate a high-level, predominantly trachytic, magma chamber. The gravity noses which extend from this anomaly suggest that the other trachyte domes and plugs on the island are

offshoots from this secondary centre.

4.6 Conclusions

(1) It is suggested from the marine gravity data that Ascension Island lies at the western end of an east-west series of en echelon fractures which displace the Mid-Atlantic Ridge right-laterally about 200 km. The island lies some 100 km to the west of the ridge axis, being located to the south of this fracture zone.

(2) It is considered that the island is in isostatic equilibrium and that the compensation is regional in character with a radius of regionality of between 70 and 100 km.

(3) The gravity data on the island surface show that the present island has been constructed along an eastern extension from the primary volcanic centre, which is located in the west of the island. Three smaller gravity anomalies are associated with old and recent centres of volcanism and are considered to be due to high level magma chambers or dyke complexes at a depth below the island surface of less than 1.5 km.

CHAPTER 5

GRAVITY SURVEYS OF SOME OF THE AZORES ISLANDS

5.1 Introduction

5.1.1 Introduction. During January, February and March 1965, gravity surveys were carried out with a Worden Geodetic Gravimeter on seven of the nine Azores islands as a follow-up on the work done the previous summer on Ascension Island. In view of the central role of the Mid-Atlantic Ridge in current theories of the history of the Atlantic Ocean, (Hess, 1962; Dietz, 1962; Wilson, 1963a) the unique position of the Azores Islands relative to the ridge and the possibility that they may be the crest of an Azores-Gibraltar ridge makes them of outstanding interest in any study of the Atlantic islands.

5.1.2 Gravity base stations used and established. The base value used for the whole archipelago was that for Santa Maria airport, established by Bettac and Schulte in 1961 with a gravity tie to the Lisbon national gravity base. This station was connected to the Lisbon Airport lower gravity station twice in the course of the survey. The value obtained agreed with that of Bettac and Schulte to within 0.1 mgal

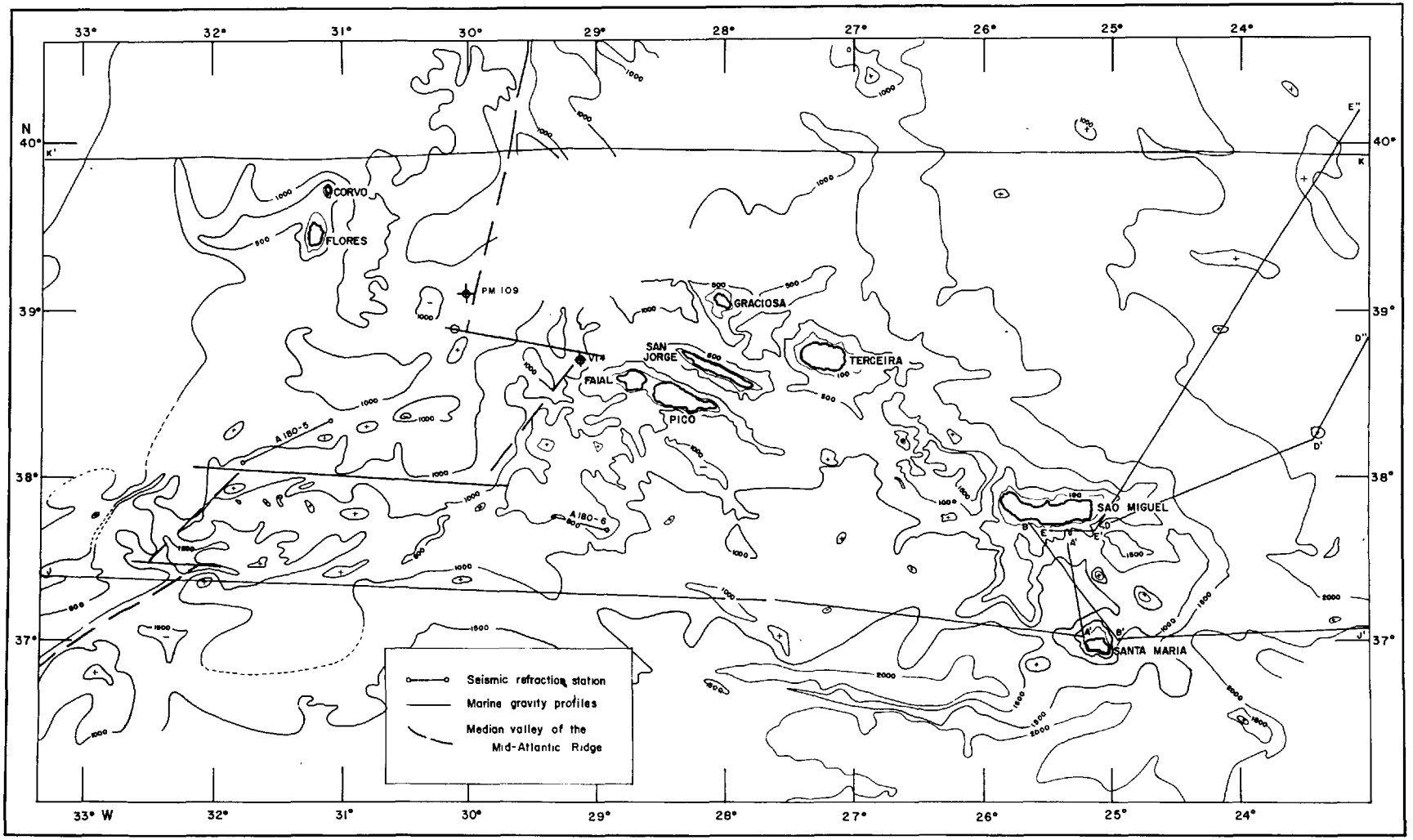

FIG. 5.1. AZORES ARCHIPELAGO. BATHYMETRY from collected soundings by the National Hydrographic Office Contours East of 30° by B.W. Creed of the National Institute of Oceanography.

and the mean value of 980117.3 mgal was adopted. One other base station established by Bettac and Schulte and described in the "Rapport National Sur les Travaux Geodesiques de Portugal 1963" was approximately reoccupied and again the results were found to be in good agreement.

The descriptions and values of these bases and other previously established stations used in the survey are included in the following list with the new bases set up in the course of the survey. The interconnections are shown in Fig. 5.2.

Earlier Gravity Bases

London Heathrow Airport (Woollard and Rose, 1963)

Street side of terminal at the foot of Channel 9 down escalator.

51° 28.1'N; 00° 27.0'W : 74 feet : 981200.3 mgal

Lisbon Airport Lower Gravity Station

By a bolt in the floor outside SITA (teleprinter) Office and across from customs baggage exit on Lowest level of terminal.

31° 46.1'N; 9° 07.7'W : 361 feet : 980080.2 mgal

Santa Maria Airport (Bettac and Schulte)

In the south corner of the Customs Room

36° 57.7'N; 25° 09.9'W : 100 m : 980117.3 mgal

S. Miguel (Bettac and Schulte)

Alfonso Chaves Meteorological Observatory, Ponta Delgada.

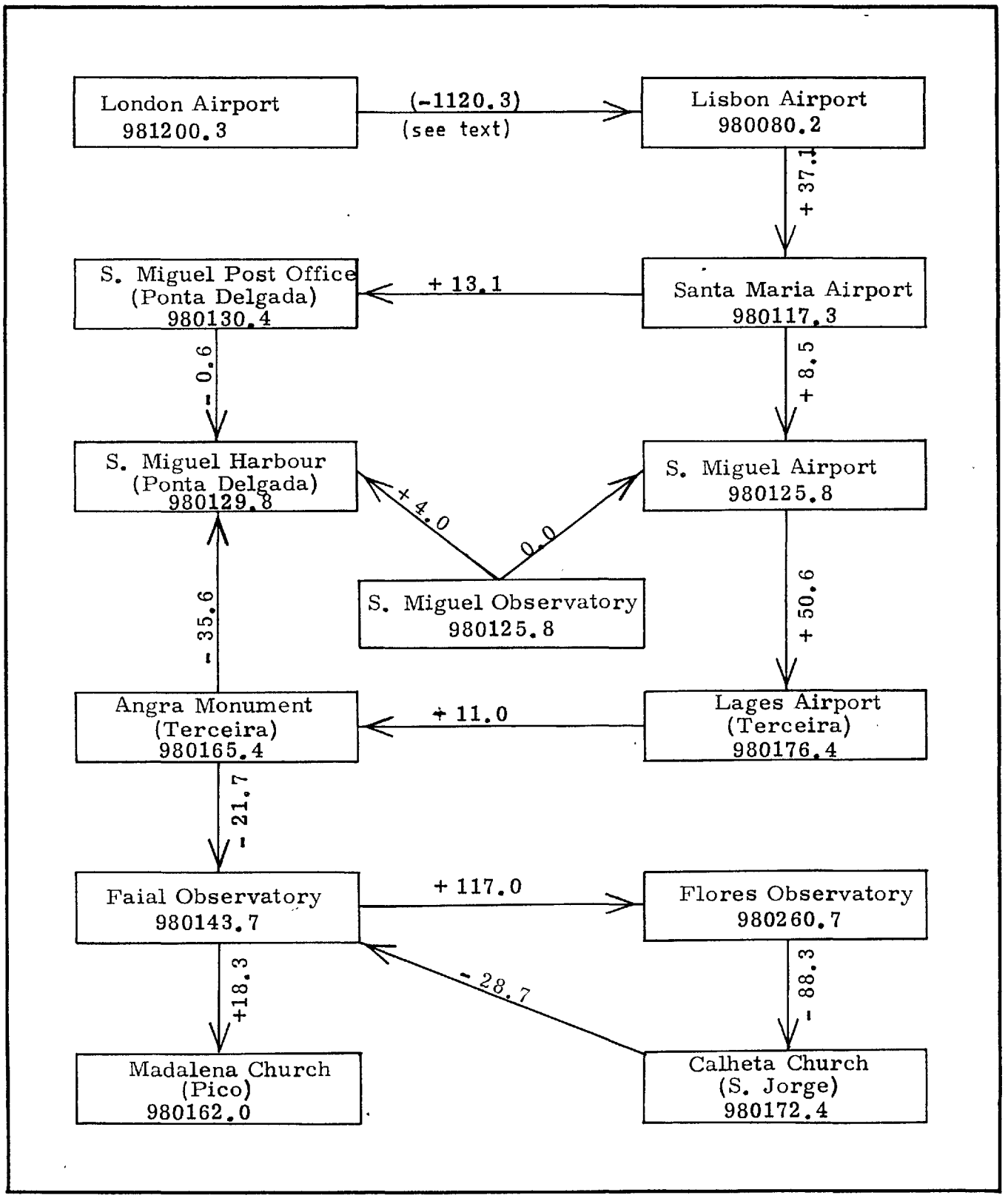

Fig. 5.2. Gravity Base Interconnections, Azores Islands.

In a half-buried outbuilding to the north of the observatory, by a pillar on which a recording gravimeter for studying earth tides is installed.

37° 44.6'N; 25° 39.8'W : 31 metres : 980125.8 mgal

New Gravity Bases

S. Miguel Santana Airport

In the air terminal building in the north-west corner of the Departure Lounge.

37° 48.1'N; 25° 33.5'W : 60 metres : 980125.8 mgal

S. Miguel Ponta Delgada Post Office

In the Post Office, in the alcove to the left on entering the main door.

37° 44.2'N; 25° 40.2'W : 6 metres : 980130.4 mgal

S. Miguel Ponta Delgada Harbour

At the foot of the stairway by the bend in the pier.

37° 44.0'N; 25° 39.8'W : 3 metres : 980129.8 mgal

Terceira Lages Airport

In the Air Terminal Departure Lounge, placed centrally by the foot of the large mural on the south wall.

38° 45.2'N; 27° 05.6'W : 55 metres : 980176.4 mgal

Terceira Angra do Heroismo Monument

By the obelisk overlooking the park, on the small bronze plaque (NP 86.626) on the western side of the monument.

38° 39.5'N; 27° 13.2'W : 86.6 metres : 980165.4 mgal

Faial Meteorological Observatory, Horta

On the concrete apron at the base of the triangulation pillar in the Observatory garden.

38° 31'36.4"N; 28° 37'47.5"W : 59 metres : 980143.7 mgal

Flores Meteorological Observatory, Santa Cruz

One foot to the North of the triangulation pillar located 50 yards to the West of the Observatory.

39° 26.9'N; 31° 07.5'W : 41 metres : 980260.7 mgal

S. Jorge Calheta Church

On the doorstep of the rear door of the church, on the northern side between two towers.

38° 36.1'N; 28° 00.8'W : 15 metres : 980172.4 mgal

Pico Madalena Church

In the alcove at the right of the porch of the main (west) entrance, placed centrally close to the wall.

38° 32.1'W; 28° 31.7'W : 8 metres : 980162.0 mgal

The observed gravity difference between London Airport and Lisbon Airport was in error by 0.2 mgal. This is an error of only 1 part in 6000 and is not enough to justify altering the calibration constant of the gravimeter.

5.1.3 General Geology. The Azores Archipelago (Fig. 5.1) consists of nine islands strung out over 600 km in the middle of the Atlantic Ocean, some 1300 km west of Portugal. The islands are the tips of large volcanoes which rise from the Azores Plateau, an area of 135,000 square km of sea-floor

where the depth is less than 1000 fathoms (1828 m). The total area of the islands is 2294 km^2, the largest being S. Miguel with 746 km^2. The maximum elevation reached is 2351 m on Pico, which is more than twice as high as any of the other islands.

The islands are oriented ESE-WNW along a topographic trend which is continued as an ill-defined ridge running from the eastern end of the Azores to the Straits of Gibraltar. This Azores-Gibraltar Ridge as it has been called, is seismically active and largely on this basis has been described by Heezen et al (1959) as "structurally and topographically similar to the Mid-Atlantic Ridge". Krause (1965) on the other hand, from considerations of bathymetry, seismicity and magnetic anomaly, sees the Azores as being associated with a large fracture zone which crosses the Atlantic from New England to Gibraltar passing through the Kelvin Seamount chain and the Azores.

The Azores Plateau is divided into two parts by the crest of the Mid-Atlantic Ridge, which at this latitude changes direction from a general WSW to a northerly trend, and passes between the islands of Flores and Faial. Because of this change of direction and because of the presence of the Azores Plateau, there is some uncertainty as to the precise position of the crest of the ridge. However, the crest does seem to be a structural boundary. Krause suggests

that the West Azores fracture zone, i.e. west of the median valley of the Mid-Atlantic Ridge, has a right lateral displacement while in the east zone a left lateral movement seems indicated: also that, though the fracture zones have probably been active from the Mid-Mesozoic, only the eastern zone is active at present, the west zone perhaps having been quiescent since Cretaceous or early Tertiary times. The structural trends show a ~~familiar~~ similar division. In the east, sea-floor trends are ESE-WNW, parallel to the known tectonic and volcanic trends, but in the west are N-S, parallel to the main trends of the Mid-Atlantic Ridge.

A review article on the geology of the Azores (Hadwen and Walker, in press) has recently been completed by the geologists who accompanied the gravity survey, and the following outline of the general geology is abstracted from this article.

The rocks are lavas and pyroclastics of the alkali basalt-trachyte suite. Apart from beach deposits, sedimentary rocks and associated submarine volcanic material are found only on Santa Maria, the most easterly of the islands. Of the basalt products, lava flows predominate and pyroclastics probably form less than one third of the total volume. Few of the lava flows exceed 10 m in thickness. The trachyte, which is found on all the islands except Santa Maria and Pico, occurs as lavas, domes and as pyroclastic sheets.

Eruptions have been mainly of the fissure type, with an ESE-WNW trend, giving rise to the elongated shapes of the islands. Machado (1965) also points out apparently concentric or radial patterns of fissures around the summits of Faial and Pico. There appear to be two generations of faults; the younger, trending WNW-ESW, is visible on Pico and Faial, while the older faults seen on Santa Maria and Flores have a N-NE trend.

Nine major calderas appear on the islands, all apparently with mainly basaltic sub-structures and all interpreted by Machado (1965) as collapse structures. There are also deep troughs located between several of the islands along the same tectonic trends as the islands. Many of these have earthquakes associated with them and it is possible that they also are collapse structures.

Historic eruptions have occurred on São Miguel, Terceira, S. Jorge, Pico and Faial, and hot springs and fumaroles exist on all the islands, except Corvo and Santa Maria. There is a tendency on each of the islands east of the Mid-Atlantic Ridge for the age of the volcanic activity to decrease towards the west.

No radiometric age determinations have been published on the Azores and the only firm indication as to the age of the older formations are the Upper Miocene fossils found in the sedimentary rocks of Santa Maria, overlying its volcanic

core. Largely on the basis of morphology, Santa Maria, Flores and the western part of S. Miguel are described as old and the remaining islands as relatively young.

5.1.4 Other Geophysical Data in the Area. The results of two seismic stations in the area have been published (Ewing and Ewing, 1959). Their positions are indicated on Fig. 5.1 and the data obtained are tabulated below.

Profile	Velocity km/sec			Thicknesses, km		
	sedi-ment	base-ment	anomalous mantle	Water	sedi-ment	base-ment
A 180-5	(1.80)	4.86	7.24	1.72	0.58	1.77
A 180-6	3.15	5.42		0.70	1.66	

There are also several continuous gravity tracks in the area. Tracks JJ' and KK' are gravity measurements carried out by the Geodetic Institute of the Delft Technological University on board Hr. Neth. Ms. Snellius during the Navado III programme, 1965, and very kindly made available for this present research. Profiles DD' and EE' were made by R.S.S. Discovery in 1965 and used for this survey by courtesy of the Department of Geodesy and Geophysics, University of Cambridge. The Bouguer anomaly was computed for these profiles by means of the two-dimensional correction program detailed in Chapter 2, and results are presented as Figs. 5.3, 5.4, 5.5 and 5.6.

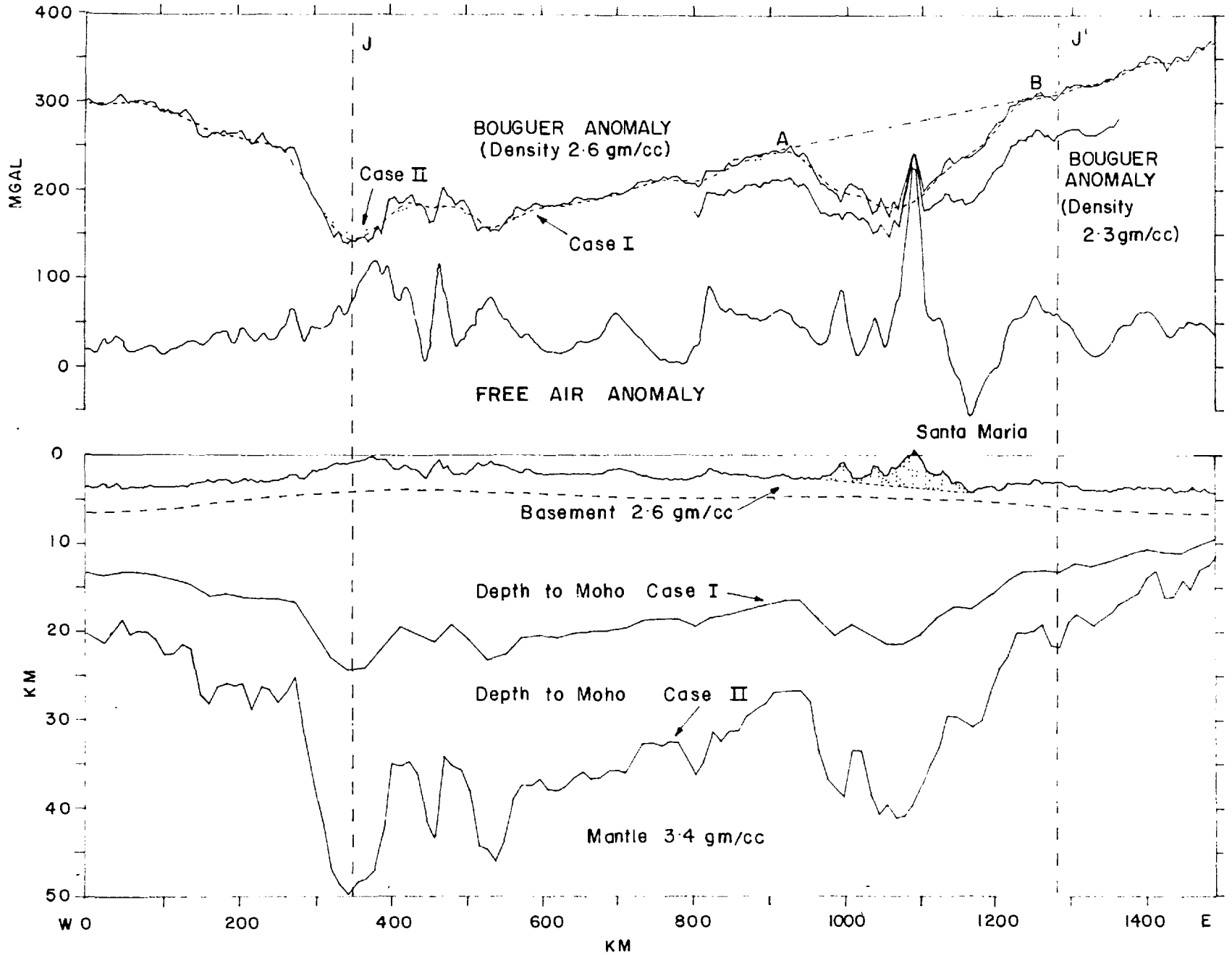

FIG. 5.3. Gravity profile J J' and possible structure sections across the Mid-Atlantic Ridge and Santa Maria island. Case I for normal oceanic crust; Case II for axial zone crust.

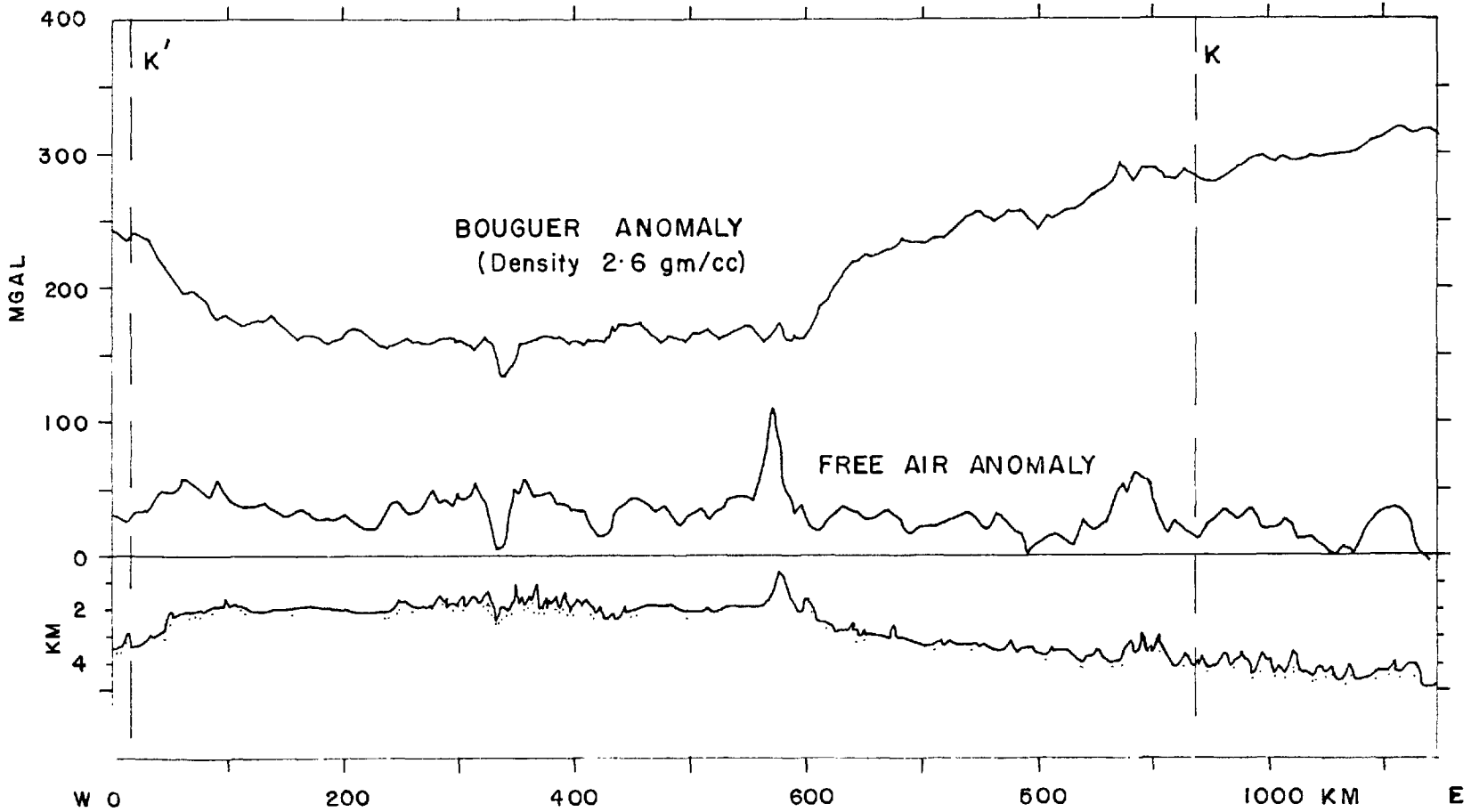

FIG. 5.4. Continuous gravity and topographic profile KK′ across the Mid-Atlantic Ridge. The track of the crossing is shown in Fig. 5.1.

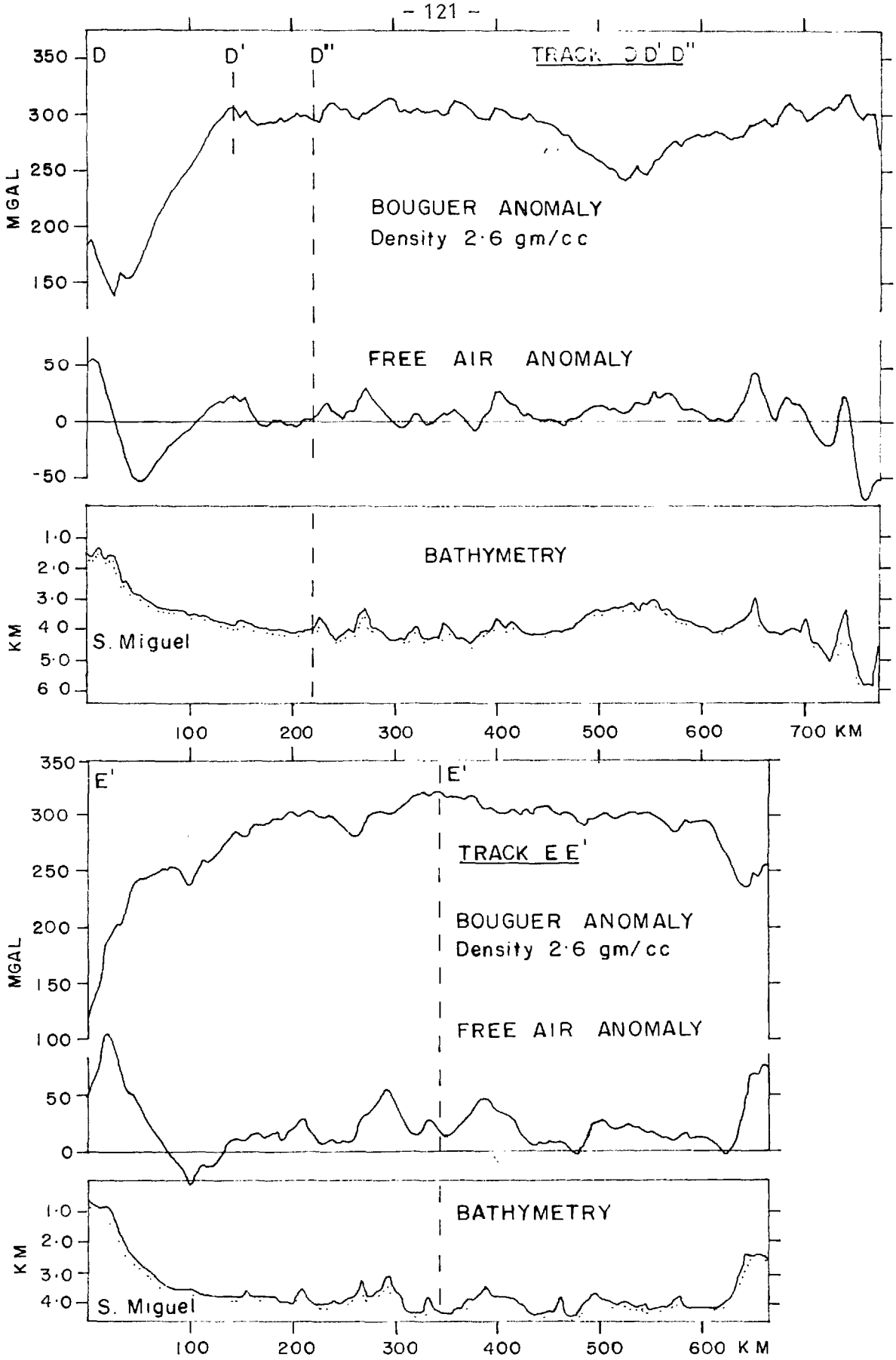

FIG.5.5. Continuous gravity and topographic profiles to the NE of S. Miguel.

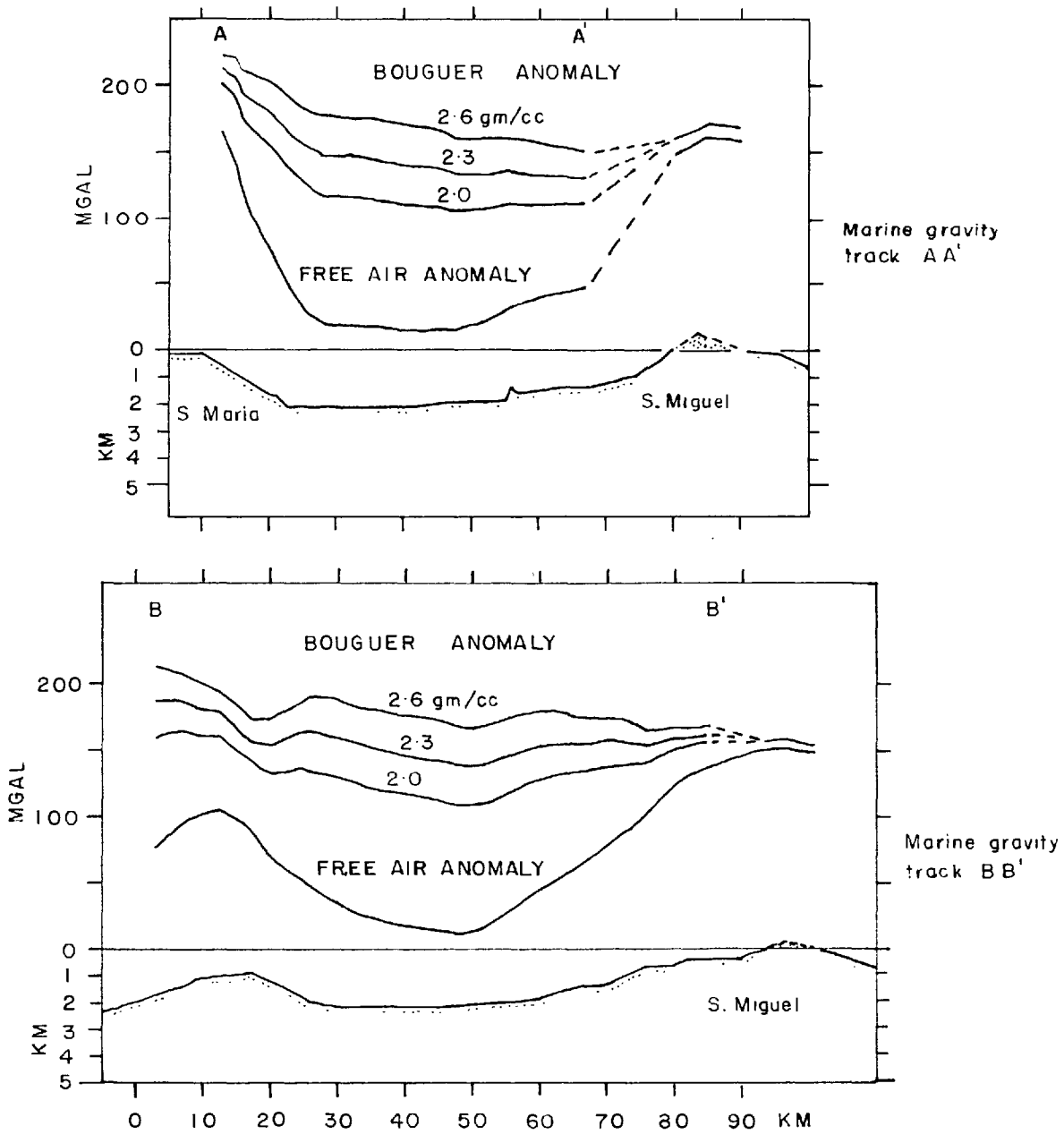

FIG. 5.6. Free air and Bouguer anomaly profiles between S. Maria and S. Miguel for three possible densities for the upper layers of the crust.

Magnetic data were available for the same tracks and were used in conjunction with the bathymetry to determine the position of the axis of the Mid-Atlantic Ridge. The position of the axis of the ridge as determined from magnetic data is shown at two other points. V14 is from Lamont data published by Heirtzler et al (1965) and PM 109 is the position indicated by a Project Magnet profile as published by Keen (1963).

The bathymetry around the Azores is drawn from collected soundings on the National Hydrographic Office 1:1,000,000 plotting sheets Nos. 58 and 59 and from the Admiralty Chart No. 1865. The contours of the eastern half (sheet 59) are mainly due to B.W. Creed of the National Institute of Oceanography.

5.2 A Gravity Survey of Santa Maria.

5.2.1 Introduction. Santa Maria, 37.0°N, 25.1°W, is situated on the edge of the Azores plateau and at the eastern end of a ridge which extends westwards to join the crest mountains of the Mid-Atlantic Ridge and which also marks the southern edge of the plateau. The bathymetry reveals that the island is also the southern end of another rise which trends north-eastwards and includes the Formigas rocks, some 32 km to the north-east. On the plateau side, the island slopes down to 1800 m but to the south and east the depth increases to 3700 m with gradients as high as 20°.

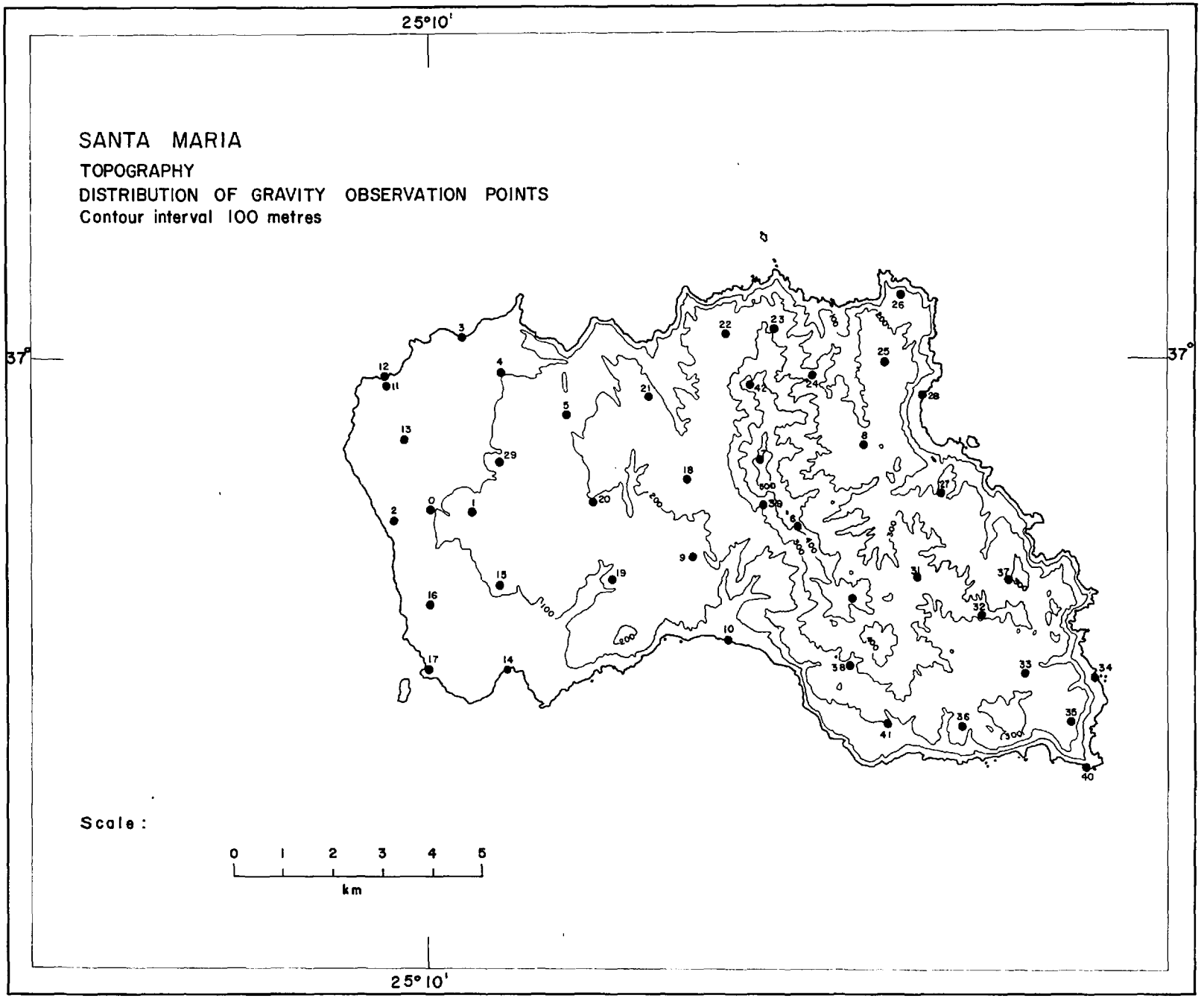
SANTA MARIA
TOPOGRAPHY
DISTRIBUTION OF GRAVITY OBSERVATION POINTS
Contour interval 100 metres
25°10'
37°
Scale :
0 1 2 3 4 5
km

FIG. 5.7.

The maximum elevation on the island is 590 m and its surface area is 96 km^2. A broad shelf of about half this area, where the depth is less than 200 m lies immediately to the north of the island.

5.2.2 General Geology. Two periods of volcanic activity are represented in the rocks on the island (Hadwen and Walker, in press). The older rocks found in the central ridge and underlying the western platform are thin ankaramitic subaerial lavas and tuffs cut by a dense swarm of ankaramite dykes. The rocks are often considerably altered. The younger series forms a peripheral belt of uplifted sedimentary rocks and submarine volcanic material around the central upland core. This sequence, of maximum thickness 150 - 200 m and resting discordantly on tilted ankaramite lavas, consists of boulder beds, palagonite breccias and basaltic pillows with interstitial calcareous mud, tuffaceous sandstones and highly fossiliferous limestones.

It is clear that there has been some variation of sea-level relative to the land. The early ankaramites are of subaerial origin down to the present sea-level, while the later subaqueous products are now found as high as 330 m above sea-level. The elevation of occurrence of the younger rocks decreases towards the south and east, suggesting that the island has suffered tilting as well as uplift.

The bathymetry, and the thickening of the tuff beds towards the north, suggest that the volcanic source may well be in the north of the present island, or even offshore on the flat shelf adjoining the north coast.

This island is alone amongst the Azores in having sedimentary rocks, and in the evidence for change of sea-level. Fossils from the calcareous rocks have been used by Zbyszewski (1961a) to date the periods of volcanic activity as Miocene and Quaternary. No radiometric dating has been published.

Olivine basalt from the Formigas rocks with limestone-filled cavities has also been dated as of Miocene age and in all other respects is very similar to the rocks found on Santa Maria.

5.2.3 Details of Survey. Stations were located to within 40 m using the 1965 1:50,000 map. Elevation determination was from the same map, supplemented by altimeter readings or by reference to sea-level at coastal stations, and is accurate to ± 10 m. The data-reduction procedure was as described in Chapter 2. The terrain corrections were calculated by computer and by manual methods and the latter were used in the calculation of the Bouguer anomaly. The elevation error corresponds to an inaccuracy in the Bouguer anomaly of ± 2 mgal. Tidal effects are much less, and are neglected.

Errors in terrain correction contribute a further 2 mgal (Table 2.3), so that the Bouguer anomaly values are accurate to ± 4 mgal.

5.2.4 Regional Gravity Field. Track JJ' (Fig. 5.1) provides a continuous gravity profile across the Mid-Atlantic Ridge and across Santa Maria. The Bouguer anomaly shown in Fig. 5.3, 5.4, 5.5 and 5.6, is calculated for a density of 2.6 gm/cc for the upper crust. The bathymetry profile in Fig. 5.3 clearly shows the position of the island at the edge of the plateau. The mean depth for 100 km to the west of the island is 2.34 km and for 100 km to the east is 3.75 km.

The free-air anomaly is strongly positive over the plateau to the west of the island, the mean value between 930 and 1030 km being + 43 mgal. In the east there is a marked negative anomaly which decreases to - 55 mgal. This is the same pattern as exists around Ascension Island (Fig. 4.2), and the same arguments as to isostatic equilibrium apply. Whilst it can be said that some form of compensation must be present, the analysis adopted for Ascension Island cannot be used here since the mean background field is not nearly zero.

Instead, the Bouguer anomaly is used. The Bouguer anomaly curve shows an almost linear gradient of 0.19 mgal/km, decreasing towards the crest of the Mid-Atlantic Ridge. This is different from the Bouguer anomaly for track KK' (Fig, 5.1), which shows an almost uniform Bouguer anomaly across the

whole width of the ridge, with steep gradients at the edges. It is, however, very similar to the Bouguer anomaly obtained in the ridge crossing at 32°N on Vema cruise 17 (Talwani and LePichon, 1965).

The smooth gravity gradient of track JJ' is disrupted by a 350 km wide negative anomaly of -100 mgal amplitude centred on Santa Maria. Santa Maria is itself marked by a much sharper positive anomaly of width 60 km and amplitude 60 mgal. The Bouguer anomaly calculated with a density of 2.3 gm/cc for the upper crust is also shown and demonstrates that the form of the anomaly does not change with changing density.

This anomaly shows that there is a sub-surface mass deficiency of wide extent associated with Santa Maria and an estimate of the total anomalous mass causing the anomaly can be obtained using Gauss's Theorem (Equ. 2.9). If the mass is equal to the mass excess of the island as a load on the oceanic crust, then isostatic equilibrium can be said to prevail.

The anomalous mass was calculated (a) as being radially symmetrical (equ. 2.12) and (b) as being approximately two-dimensional (equ. 2.14). The truth should lie somewhere between the two. The regional Bouguer anomaly was approximated by a linearly varying field, gradient 0.188 mgal/km, shown as AB on Fig. 5.3, and the resulting residual anomaly

is shown in Fig. 5.8. The residual anomaly for the 2.3 gm/cc anomaly is also shown in Fig. 5.8, after a regional gradient of 0.153 mgal/km has been removed. The smoothed curves, drawn by omitting the local anomalies due to seamounts and the island, and shown dotted in Fig. 5.8, are practically symmetrical about the island, suggesting that the subsurface anomaly is associated with the island, or that both the anomaly and the island are associated with the edge of the plateau.

From the 2.6 gm/cc curve, the anomalous mass was calculated to be -78×10^{18} gm for radial symmetry, and -4.5×10^{12} gm/cm for the two-dimensional case. The 2.3 gm/cc curve yielded a value of -72×10^{18} gm for radial symmetry, demonstrating that the result is not seriously affected by any reasonable change of density.

To the north, the shape of the island is lost in the Azores plateau below 1000 fathoms so that is it impossible to obtain an accurate estimate of the volume and hence the mass of the island body. If the width of the island in an east-west direction at 2000 fathoms is adopted as the basal diameter and the island is approximated by a truncated cone, upper radius 12 km, lower radius at a depth of 4 km, 60 km, and excess density equal to 1.57 gm/cc, the value of 29×10^{18} gm is obtained as a rough estimate of the mass of the island. For this model, the basal diameter of the island must be at

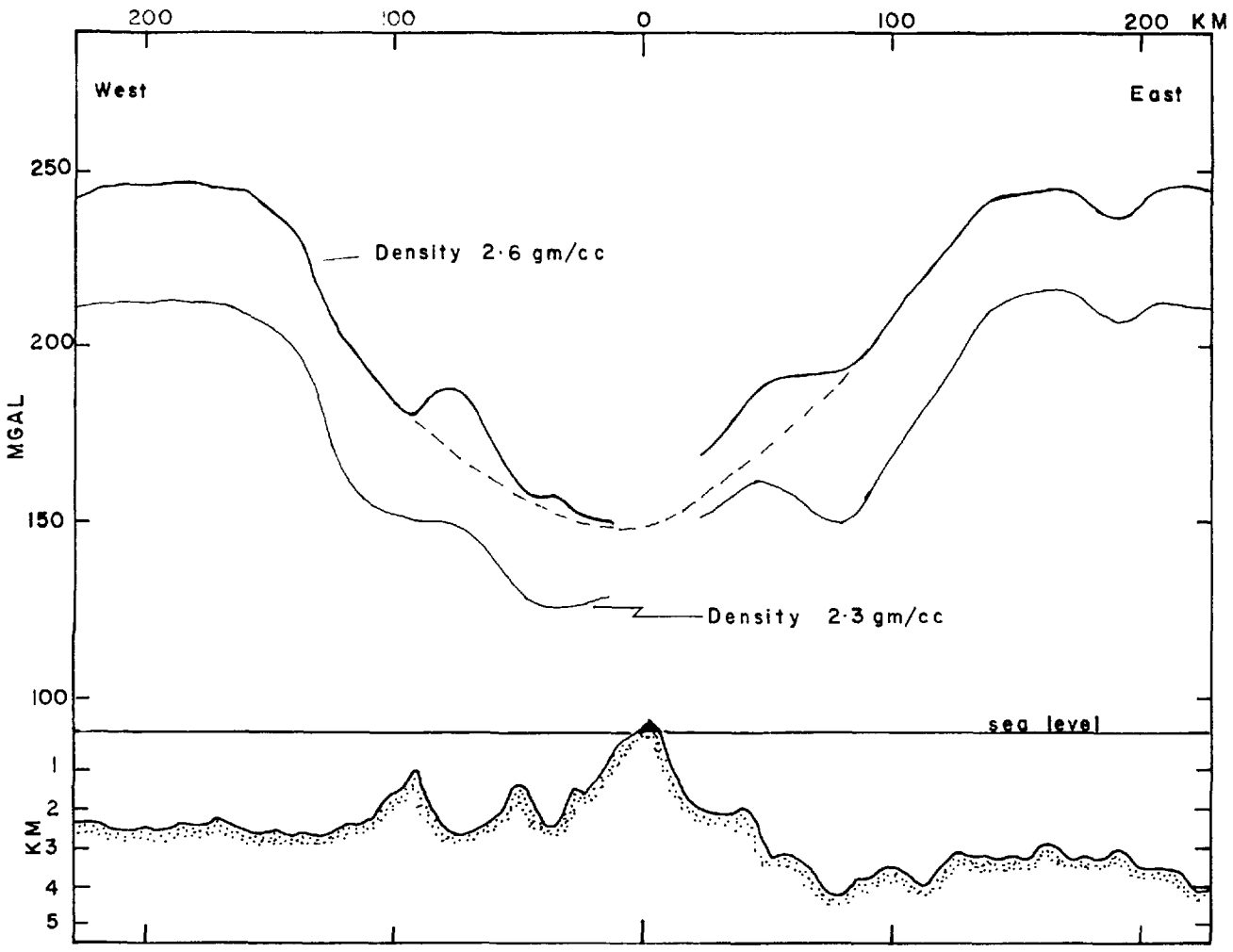

FIG. 5·8 Residual Bouguer Anomaly over Santa Maria after subtraction of a linear regional field of 0·188 mgal/km.

least 200 km before the island mass is approximately equal to the anomalous mass calculated on the assumption of radial symmetry. Therefore on a radial symmetry model the island would appear to be over-compensated.

In calculating the excess mass per unit length from the bathymetric profile, the island area was extended to include the seamounts to the west of Santa Maria and is shown as the shaded portion of Fig. 5.3. Again using the excess density of 1.57 gm/cc, this excess mass per unit length is equal to 4.65×10^{12} gm/cc. Considering the inaccuracies inherent in the method, this agrees very well with the value of the anomalous mass obtained from the gravity profile. Therefore, on an assumption of two-dimensionality, Santa Maria overlies a negative anomalous mass which is approximately equal in value to the load on the crust of the north-south Santa Maria ridge. Santa Maria can thus be said to be in isostatic equilibrium, but the compensation is probably associated with the Santa Maria - Formigas ridge complex and the edge of the Azores plateau rather than with the island alone.

The northern extension of the region of low gravity is clearly shown by tracks AA' and BB' (Fig. 5.1). The Bouguer anomaly (Fig. 5.6) was computed using three values of density 2.0, 2.3, 2.6 gm/cc, but the same features persist with all three, only the value of the Bouguer anomaly changing. Considering only the 2.6 gm/cc curve, since it is to be

compared with the JJ' profile, both tracks show the gravity anomaly decreasing from the local high of 210 - 220 mgal at Santa Maria to a value of 150 - 170 mgal at S. Miguel. For track BB', which trends north-westerly, part of this decrease may be due to decreasing distance from the axis of the Mid-Atlantic Ridge. Assuming that the gradient is the same as for track JJ', this effect would account for a drop of 13 mgal over the whole length of profile BB'. For track AA' this effect is only 3 mgal. Hence, the low gravity field shown by profile JJ' to be centred on Santa Maria, extends northward as far as S. Miguel, possibly becoming even lower under the eastern portion of S. Miguel. The assumption of two-dimensionality in the calculations of the anomalous mass is therefore quite valid.

The form which the mass deficiency takes is a matter for speculation, as there are an indefinite number of mass distributions which can produce the observed gravity anomaly. However, the maximum possible depth to the upper surface of the anomalous body can be determined from the gravity data and this sets one constraint on possible solutions. A further constraint is that the density contrasts must be geologically feasible.

Bott and Smith (1958) show that for two-dimensional density distributions, the maximum depth h for all x, is given by $h = A(x) / \frac{dA(x)}{dx}$ (5.1), where x is the distance along the

profile and A(x) is the gravity anomaly at x due to the anomalous body. For the maximum gradient of 0.52 mgal/km, which occurs at A(x) = 35 mgal, this equation yields a value of 67 km for the maximum depth.

A different approach due to Skeels (1963) uses the maximum value of the anomaly, the half-width, the three-quarter width, and the maximum permissible density contrast, to find the maximum depth and the dimensions of the rectangular prism of infinite length which could give rise to the anomaly. By this method, the maximum possible depth is 67 km to the upper surface of a prism 155 km wide and 7 km thick,

The anomalous mass may consist of (i) a greatly increased thickness of low density sediment around the island ridge (ii) some low density material in the crust or (iii) some low density material in the mantle, or any combination of (i), (ii) and (iii). These possibilities are now considered in turn.

A minimum value for the density of the sediment overlying the 2.6 gm/cc basement layer would be 1.9 gm/cc. For this density contrast of -0.7 gm/cc, a sediment thickness of more than 4 km is required to account for the anomaly of -96 mgal. There is no seismic refraction or seismic profiler work in the area to confirm or deny the existence of such a layer, but from the rugged bathymetry around the island it seems unlikely that such a depth of sediment can be present.

For sediment of this thickness, compaction at depth would lead to a density considerably higher than 1.9 gm/cc, and this in turn would require an even greater depth of sediment to account for the anomaly.

A low-density mass in the basement and oceanic layers requires that the density of the anomalous mass be appreciably less than 2.9 gm/cc. Of the rocks found on the island, the lowest density possible would be for a body of fused trachytic magma, to which an approximate density of 2.6 gm/cc might be assigned. There are two strong objections to such a body, from the geological evidence. In any such magma chamber, basalt, as the major rock type found on Santa Maria, is likely to predominate. The magma is unlikely to be in a molten state, since there is no evidence for extensive volcanic activity on Santa Maria in recent times. The density for a solid basaltic magma chamber would be approximately 3.0 gm/cc, having a slight positive density contrast with the oceanic layer and a strong positive contrast with the basement layer.

One form of mass deficiency in the mantle could be the depression of the crust into the mantle by isostatic adjustment under the load of the island ridge. The resulting configuration of the crust-mantle interface can be computed using the method detailed in Section 2.7. The major difficulty is the uncertainty as to the composition of the crust

and mantle under Santa Maria. Seismic refraction studies on the Mid-Atlantic Ridge indicate that in a zone across the axis of the ridge the crust is different from the rest of the oceanic crust (Le Pichon et al, 1965). In this "axial zone" crust the basement or "layer 2" is underlain by a layer which has a velocity of 7.2 - 7.6 km/sec, intermediate between the velocity of the normal oceanic layer and that of the normal upper mantle. Le Pichon et al. found that the boundary of this "axial zone" could be approximated by the 3.5 km isobath. Thus Santa Maria may occupy a position in the region of transition from normal crust to axial crust.

Fig. 5.3 shows the depth of the Moho calculated for both normal and axial zone crust on the assumption that the mass deficiency is due to a thickness of the crust. The results of 20 seismic refraction stations on the ridge between 30^{o} and 40^{o}N (Le Pichon et al, 1965) show that in all cases the depth of sediment is small, and therefore the sediment layer was included with the basement layer of 4.0 - 6.0 km/sec material for the purposes of the present calculations. The mean observed thickness of the sediment and basement layers together is 2.56 km, and this was the thickness used for the basement layer for both normal and axial zone type crust. From Nafe and Drake's (1963) velocity-density relationship, a density of 2.6 gm/cc was ascribed to this layer. In the normal crust this basement layer overlies the

2.9 gm/cc oceanic layer which is in turn underlain by the 3.4 gm/cc mantle. In the axial zone crust, the anomalous mantle to which Talwani et al (1965) ascribe a density of 3.15 gm/cc takes the place of this oceanic layer.

The calculated configuration of the Moho under Santa Maria shows a thickening of the crustal material by about 6 km for normal crust and 17 km for axial zone crust.

A second possible cause of mass deficiency in the mantle may be a decrease in the density of the sub-crustal material. This would be achieved if Santa Maria was underlain by an offshoot of anomalous mantle material flanked on the east and west by normal mantle. If, as suggested by Bott (1965), the anomalous mantle material is partially fused mantle rock, such material under the island would provide a magma source for the volcanic eruptions which have built up the island, but an explanation is then necessary as to why volcanic activity on the island has now ceased.

Several possible sources of the mass deficiency have been described singly, but these may combine in a variety of ways to produce the observed anomaly. Until more detailed marine gravity and magnetic surveys and seismic refraction studies have been carried out, the actual deep structure of the island must remain a matter for speculation.

5.2.5 Local Anomaly. The location of the gravity stations and their Bouguer anomaly values are shown in Fig. 5.7 and

Fig. 5.9, respectively. The centre of the Bouguer anomaly high as contoured on Fig. 5.9 coincides with the uplands of the ancient core of the island. A broad region of high Bouguer anomaly extends westwards to another centre which appears to be located offshore to the north-west of the island. This latter anomaly may indicate the position of the volcanic centre which gave rise to the subaqueous volcanic products found on the island. The geology and the bathymetry are both in agreement with such a possibility. A gravity nose extends south-eastwards from the main anomaly centre, and presumably indicates the rift zone which produced the NW-SE alignment of the topography and of the dyke swarms in that area.

With a density of 2.4 gm/cc for the island body and applying three-dimensional Bouguer corrections to the marine gravity values located a short distance from the island, a value of 175 mgal was obtained for the background field of the island. The regional field cannot be uniquely determined as it will vary with the density chosen in making the Bouguer correction, for example, from 190 mgal for a density of 2.6 gm/cc to 160 mgal for a density of 2.2 gm/cc. Such changes do not alter the shape of the anomaly in so far as it is determined from the surface data, and for any reasonable density will not radically affect a more detailed analysis.

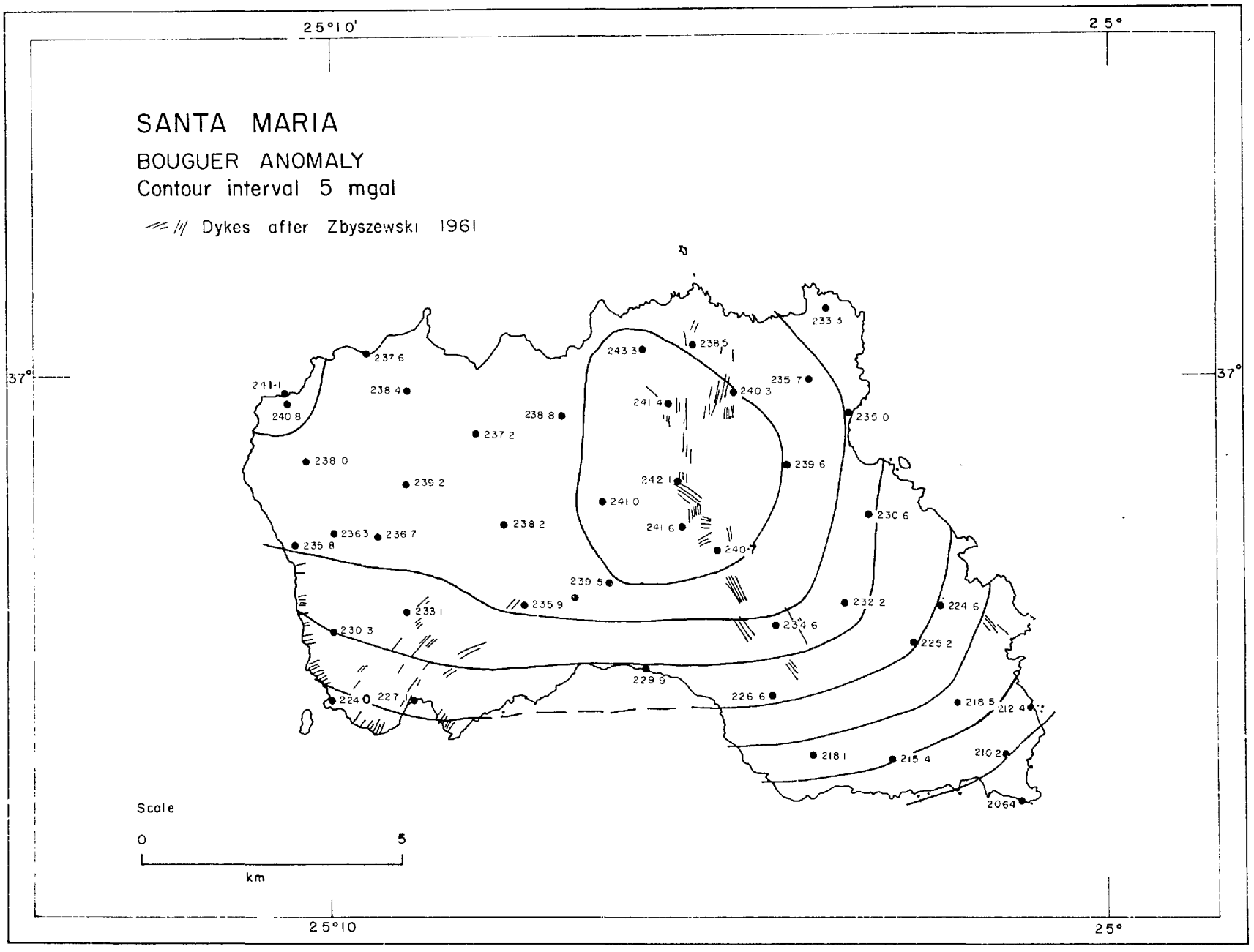
25°10'
25°
SANTA MARIA
BOUGUER ANOMALY
Contour interval 5 mgal
Dykes after Zbyszewski 1961
37°
237 6
241-1
238 4
240 8
238 8
237 2
238 0
239 2
238 2
2363
236 7
235 8
233 3
238,5
243 3
235 7
240 3
241 4
235 0
239 6
242 1
241 0
241 6
240·7
230 6
239 5
235 9
233 1
230 3
232 2
224 6
234 6
225 2
229 9
226 6
224 0
227,1
218 5
212 4
218 1
215 4
210 2
2064
Scale
0
5
km
25°10
25°

FIG. 5.9

5.3 A Gravity Survey of São Miguel.

5.3.1 Introduction. São Miguel lies in the North Atlantic between 37°40' and 37°55'N and between 25°10' and 25°50'W. It is 746 km^2 in area and elongated in an east-west direction with a length of 65 km and widths ranging between 8 and 15 km.

The maximum elevation is 1105 m above sea-level and in the north and east the island block slopes steeply down to depths of 3300 m with angles of slope of up to 10°. To the south, in the direction of Santa Maria, the depth decreases to only 2200 m, while from the western end of the island a ridge extends for 50 km in a southerly direction with depths of less than 550 m. Notable features of the bathymetry are two deeps in line with the tectonic trend of the Azores ridge; one lies to the north-west of the island, the other to the south-east, and both have slopes of 17° down to depths of 3000 m. The east-west trend of the island topography is continued in the bathymetry in the form of ridges extending west and east from the ends of the island.

5.3.2 General Geology. The island consists essentially of four volcanoes. Three volcanoes, aligned approximately east-west, form the uplands in the eastern half of the island, and are linked by a narrow waist of low-lying ground to the fourth volcano in the west. The eastern volcano is deeply dissected and is regarded as the oldest of the four (Hadwen and Walker, in press). Each of the four volcanoes is

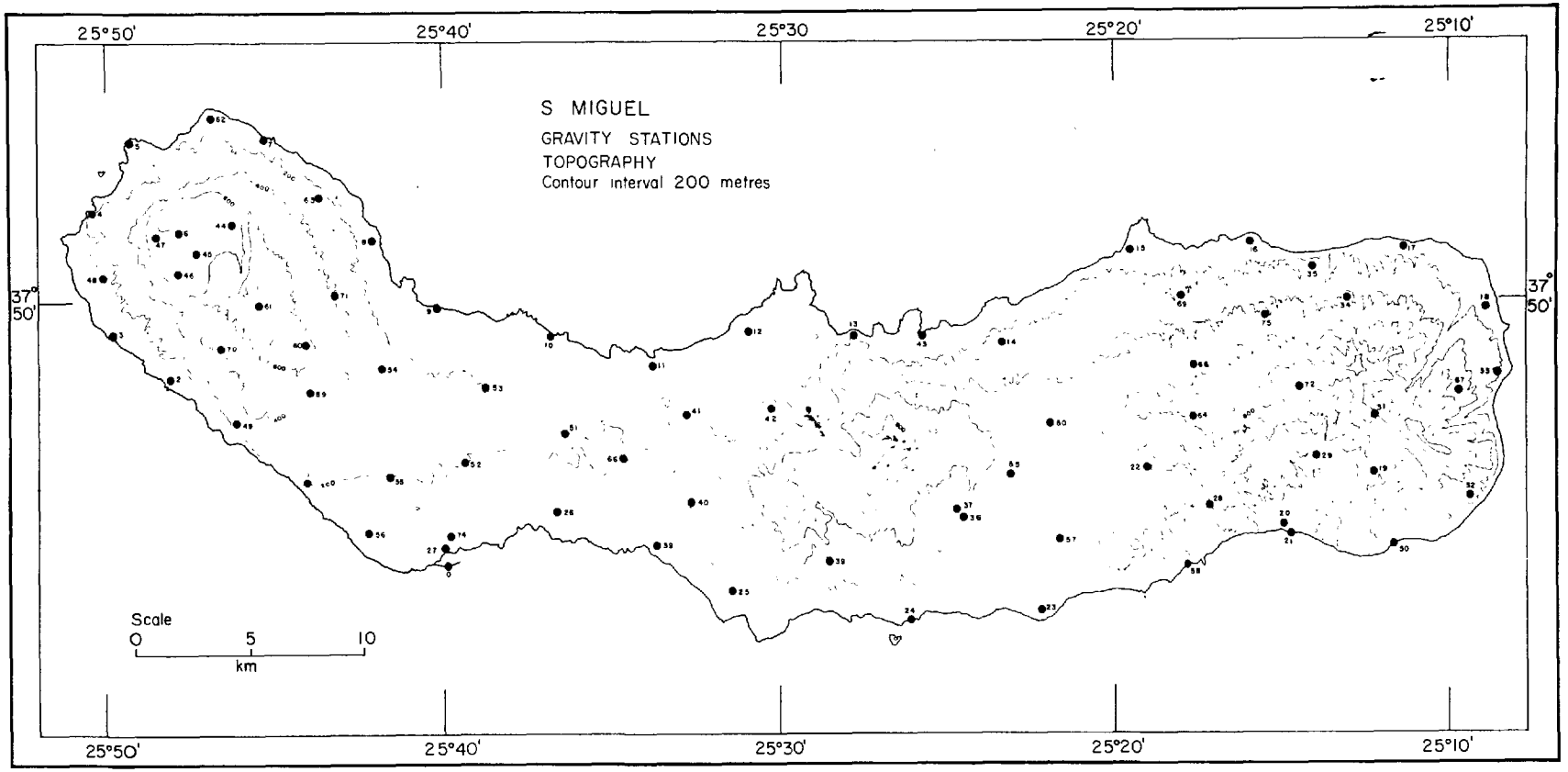
S MIGUEL
GRAVITY STATIONS
TOPOGRAPHY
Contour interval 200 metres
25°50'
25°40'
25°30
25°20'
25°10'
37° 50'
Scale
0 5 10
km

FIG. 5.10.

marked by a caldera and the western volcano is associated with a fissure zone extending south-eastwards parallel to the NW-SE elongation of the volcano. Evidence of historic submarine eruptions suggests that this fissure zone extends to the north-west beyond the shores of the present islands.

The rocks are basaltic lavas and trachytic lavas and pyroclastics, the last including an extensive mantle of trachytic pumice over much of the island.

Historic eruptions have been recorded in the three western volcanoes, and fumaroles are present in the two central calderas. No accurate dates are available for the oldest rocks on the island.

5.3.3 Details of the Survey. Field procedure and data reduction were carried out as described in Chapter 2. Stations were located to within 80 m using the 1941 1:50,000 map. As this map is quite old, and contoured at only 25 m intervals, elevations were determined using an altimeter, except for coastal stations and stations located at bench marks. For the altimeter stations, the elevation error is $\pm$ 20 m which corresponds to an error of $\pm$ 4 mgal in the Bouguer anomaly. Terrain correction was carried out by manual methods and will contribute a further error of about 1 mgal. Tidal effects and errors in drift correction are negligible by comparison, so that the total inaccuracy in the Bouguer anomaly is $\pm$ 5 mgal.

5.3.4 Regional Anomaly. Several marine gravity tracks end near S. Miguel (Fig. 5.1) but they are not particularly well located for determining regional trends around the island. These tracks (Fig. 5.5 and 5.6) have anomaly patterns similar to those already studied for Santa Maria and Ascension Island. The anomaly changes from a sharp positive of as much as +100 mgal near the island to a broad negative which has its minimum value between 50 and 80 km from the island. Further from the island this negative trough gives way to shorter wavelength anomalies of smaller amplitude. On EE', the mean value of the anomaly for this latter part of the track is 22 mgal, and over the same distance on DD'D" is 7 mgal. This difference probably reflects the closer proximity of the former profile to the axis of the Mid-Atlantic Ridge. On the short tracks AA' and BB', the free-air anomaly drops to small positive values between the islands of S. Miguel and Santa Maria. The generally low free-air anomaly over the region shows that compensation is to a very large extent complete. It can be inferred from the form of the free-air anomaly on the same grounds as have already been discussed in Chapter 4 that some manner of regional isostatic compensation exists under S. Miguel.

The Bouguer anomalies were calculated by the two-dimensional correction method in Chapter 2, using a density of 1.57 gm/cc for the water-layer correction, and show a

marked gravity low associated with the island. The minimum value indicated by profiles EE' and DD' is between 140 and 150 mgal and this is confirmed by the short profiles AA' and BB', which indicate a Bouguer anomaly of approximately 150 mgal in the vicinity of S. Miguel.

The Bouguer anomaly clearly demonstrates that a considerable mass deficit is associated with S. Miguel, as must be the case if the isostatic balance inferred from the free-air anomaly exists; whether or not complete equilibrium prevails cannot be established from the limited data which are available.

The Bouguer anomaly minimum on track DD' coincides with the eastward extension of the S. Miguel tectonic trend and demonstrates that this trend continues at depth some distance to the east of the island.

The amplitude of the negative anomaly as determined from the profiles EE' and DD'D" is 160 mgal, and is much larger than the 100 mgal anomaly observed over Santa Maria. It may well be that a large part of this anomaly is associated with the edge of the Azores plateau, in so far as it is also the edge of the axial zone of the Mid-Atlantic Ridge. The edge effect of the ridge can be seen very clearly on profile KK' (Fig. 5.4) and at the western end of profile JJ' (Fig. 5.3).

At the edge of the axial zone of the mid-ocean ridge, the Bouguer anomaly on tracks JJ' and KK' increases with a gradient of about 2 mgal/km from a value of approximately 150 mgal to between 200 and 250 mgal, at which point the gradient falls off rapidly to less than 0.4 mgal/km. This is almost exactly the shape of the anomaly on track EE', but on DD' the gradient of 2.0 mgal/km is maintained to a value of 300 mgal before decreasing to effectively zero as the ship's heading changes to parallel the Mid-Atlantic Ridge. This resemblance to the Mid-Atlantic Ridge Bouguer anomaly pattern strongly suggests that the crustal structure under the Azores plateau is very similar to that under the Mid-Atlantic Ridge. From the difference between DD'D" and EE' tracks it is apparent that the transition from plateau or axial zone type crust becomes more abrupt with increasing distance from the axis of the ridge.

The maximum depth to the upper surface of the anomalous body is 35 km when calculated on a three-dimensional basis from Corollary 1.1 of Bott and Smith (1958) (equ. 4.1), and is 23 km when the body is assumed two-dimensional (equ. 5.1). Otherwise the problem is the same as has already been discussed in the case of Santa Maria. Regional compensation has been inferred, and may be due to a thickening of the crust, a magma chamber in the upper mantle, or the presence of the "anomalous mantle" proposed by Talwani et al (1965) to provide the compensation for the Mid-Atlantic Ridge at these latitudes.

The configuration of the anomalous body cannot be uniquely determined from the gravity data alone, and further geophysical data, preferably from seismic refraction studies, are required before we can discriminate between the possible solutions. The general form of possible crustal structures will be similar to those deduced for Santa Maria, but until further information becomes available as to the composition of the crust under the island precise calculations of possible density models are valueless.

5.3.5 Local Anomaly. The distribution of the gravity stations and their Bouguer anomaly values are shown in Fig. 5.10 and 5.11 respectively. The main features are two centres of high Bouguer anomaly aligned in an approximately east-west direction. The larger centre is located near the geologically oldest volcano on the island (Zbyszewski et al, 1958) and has a maximum value of 203 mgal. The background field indicated by the marine gravity data is 140 -150 mgal so that the amplitude of the anomaly is approximately 60 mgal. This is similar to the 67 mgal observed for the Santa Maria local anomaly. In the west, the anomaly is centred to the south-east of the well-defined caldera of the western volcano, and has a Bouguer value of 172 mgal. This difference between the maximum values may be due at least in part to an east-west gradient in the regional field.

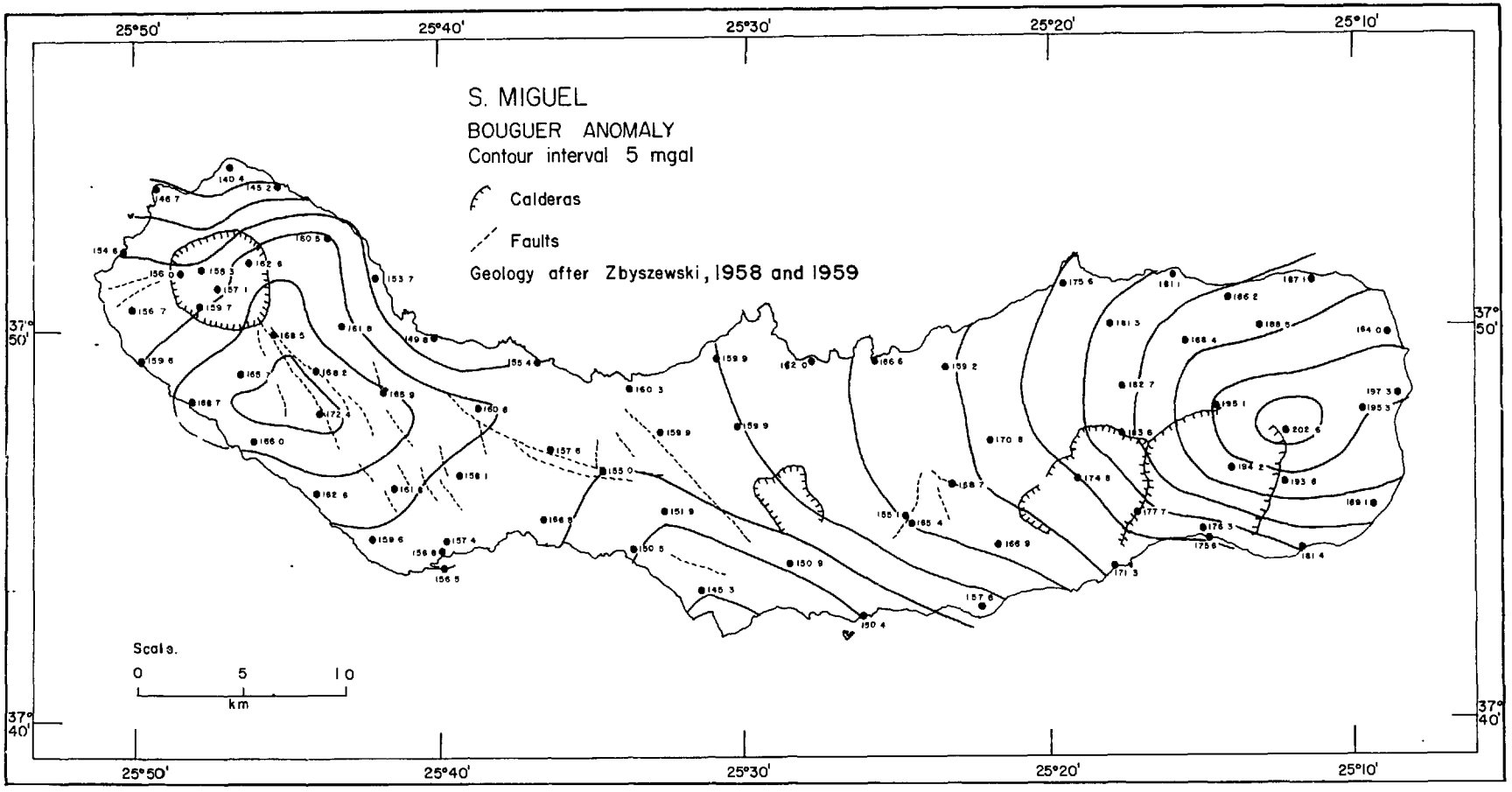
S. MIGUEL
BOUGUER ANOMALY
Contour interval 5 mgal
Calderas
Faults
Geology after Zbyszewski, 1958 and 1959
25°50'
25°40'
25°30'
25°20'
25°10'
37° 50'
37° 40'
Scale
0
5
10
km

FIG. 5.11.

The elongations of the Bouguer anomaly contours conform to the east-west trend of the eastern volcanoes, and in the western volcano, to the NW-SE trend of the faults and fissures there. The absence of major anomalies associated with the two more westerly volcanoes of the eastern group suggests that they are lateral offshoots from the oldest and principal centre and do not extend to any great depth.

There is a region of low Bouguer anomaly across the west-centre of the island, with a NW-SE trend parallel to the direction of the faults and fissures in the western half of the island. This belt of low anomaly may represent a NW-SE trending fracture zone. Such a possibility is in excellent agreement with the topographic and fault trends on either side of this low-lying central tract, and with the numerous adventive volcanic cones in this area.

The sparseness of the gravity data and the strong masking effect of the two main anomalies make it difficult to discern the effects of the calderas on the gravity field. The best documented caldera, that in the west, is associated with a slight decrease of perhaps 5 mgal in the Bouguer anomaly. This caldera is occupied by two large lakes, and these together with other low-density infilling material, could easily account for an anomaly of this magnitude. The two eastern calderas also appear to be connected with slightly lowered gravity values. Yokoyama (1963) had divided calderas

into three categories on the basis of their gravity anomaly. These are (i) high anomaly, (ii) no anomaly, and (iii) low anomaly. He considers that those calderas in the third category have all been formed during gigantic eruptions of pumice and that the negative anomalies over the caldera indicate the existence of coarse material filling the caldera to a depth of a few kilometres. This category corresponds to the calderas of Krakatoa type of Williams (1941), which are considered to have been formed by collapse following the eruption of a tremendous amount of pumice. The slightly low gravity values and the widespread mantle of pumicious material surrounding the calderas on S. Miguel suggest that the calderas belong to this type.

5.4 A Gravity Survey of Terceira.

5.4.1 Introduction. Terceira (Fig. 5.12) is an oval island, situated at 38°45'N, 27°15'W. Its maximum dimensions are 29 km east-west, and 18 km north-south, and its area is 398 km^2. The maximum elevation is 1021 m. The main bathymetric feature is a ridge, apparent on either side of the island, trending W20°N along a line which runs across the centre of the island. Another ridge extends due eastward from the island and is reflected in the bathymetry for 150 km. In the north-east and south-west the depth increases quite rapidly to 1400 m, with slopes of 10°, then more slowly to

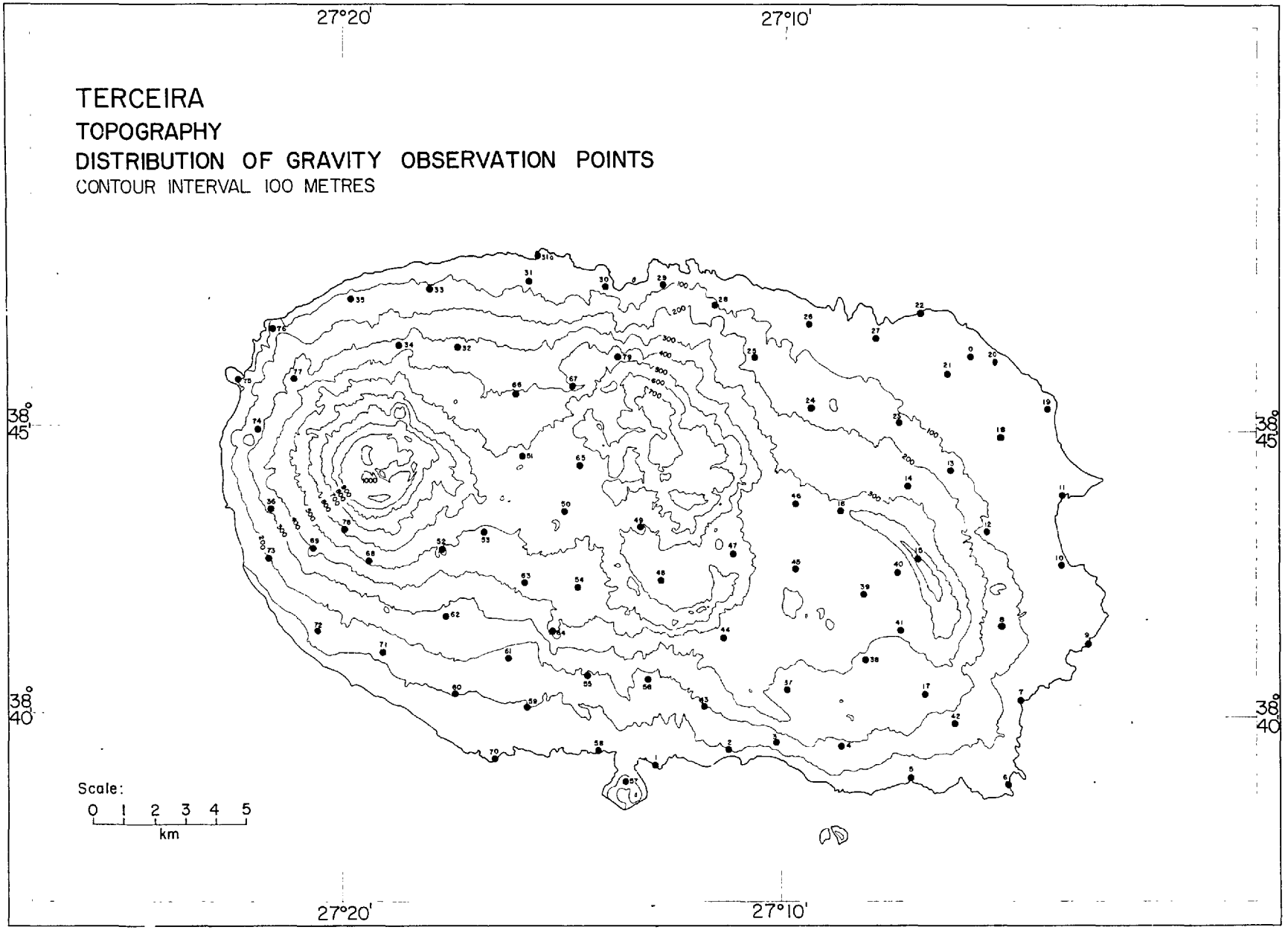
27°20'
27°10'
TERCEIRA
TOPOGRAPHY
DISTRIBUTION OF GRAVITY OBSERVATION POINTS
CONTOUR INTERVAL 100 METRES
38° 45'
38° 40'
Scale:
0 1 2 3 4 5
km

FIG. 5.12.

the general plateau level of approximately 1800 m. The width of the island at 1400 m is 60 km.

5.4.2 General Geology. The main features are two large calderas in the east and centre and a much smaller caldera associated with a large volcano in the north-west, all aligned in a WNW-ESE direction across the centre of the island. In the north-east, a graben structure strikes in a NW-SE direction.

Trachytic lavas and pyroclastic material are widespread. The oldest rocks, which are found in the east, are highly altered ankaramites, and these are succeeded by relatively young feldspar basalts and trachytes. Olivine basalts are also widespread.

An eruption of basaltic lava occurred in 1761, and hot springs exist in the centre of the island. No absolute age determinations are available for the oldest rocks, but on general grounds the eastern caldera is considered the oldest and the western volcano the youngest major structure.

Machado and Forjaz (1964) have interpreted a negative anomaly in the earthquake intensity of a seismic shock on San Jorge as being due to the presence of a magma chamber under Terceira at an estimated depth of 5 km.

5.4.3 Details of the Survey. Field procedure and data reduction were carried out as described in Chapter 2. Stations were located to within 40 m using a 1959, 1:25,000

military map. Elevations were determined from the same map, which was contoured at 10 m intervals, or by reference to sea-level at coastal stations, and are accurate to ± 10 m. Terrain corrections were computed using manual methods, and are accurate to ± 1 mgal.

The inaccuracy in the elevation corresponds to an error of ± 2 mgal in the Bouguer anomaly. Errors due to mislocation of the station and to neglecting tidal effects are negligible in comparison, so that the total inaccuracy in the Bouguer anomaly values is ± 3 mgal.

5.4.4 Local Anomaly. The island topography and the distribution of the gravity stations are shown in Fig. 5.12. The Bouguer anomaly as contoured in Fig. 5.13 reflects the WNW-ESE trend of the island topography and bathymetry and confirms the existence of an active belt which follows this trend across the centre of the island.

The gravity relief is small; the observed Bouguer anomaly ranges from 118 to 140 mgal with the higher values in a WNW-ESE belt across the island. Within this belt the two eastern calderas are marked by relatively low values of the Bouguer anomaly. The distribution of gravity stations around the western volcano is poor, due to difficulty of access, but the volcano appears to represent a gravity high. It may be that it is a younger, smaller version of the eastern caldera, where a region of high gravity encloses a

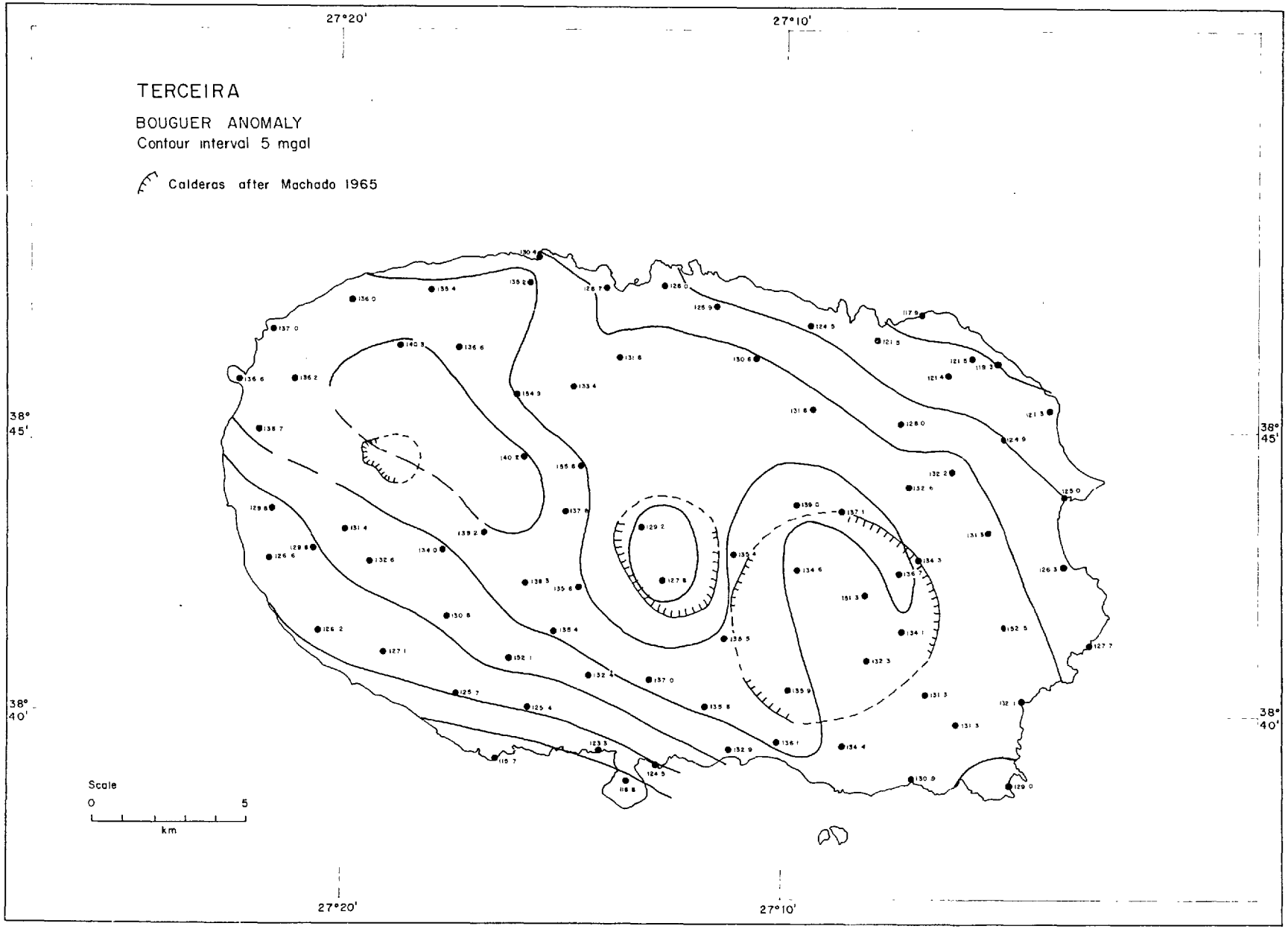
TERCEIRA
BOUGUER ANOMALY
Contour interval 5 mgal
Calderas after Machado 1965
27°20'
27°10'
38° 45'
38° 40'
Scale
0
5
km

FIG. 5.13.

smaller area of lower Bouguer anomaly. These low gravity values and the large quantity of ignimbritic deposits surrounding the calderas suggest that these calderas belong to the same category as those on S. Miguel, i.e. the Krakatoa type of Williams (1941), and have been formed by collapse following the explosive eruption of an enormous amount of pyroclastic material.

The anomalies due to the eastern calderas are approximately radial and when the mass deficit which they represent is calculated on this basis using Gauss's Theorem as described in Section 2.5, estimates of between 3.5 and 4.5 x 10^{15} gm are obtained for both anomalies. The estimates are roughly similar, even though the eastern caldera appears to be much larger in areal extent. The present survey stations are too widely spaced to permit detailed studies of the calderas, which are clearly fruitful areas for further gravity work on the island.

5.5 A Gravity Survey of San Jorge.

5.5.1 Introduction. San Jorge ($38^{o}40'N$, $28^{o}33'W$) is the northern member of a group of three islands, San Jorge, Faial and Pico, which occupies the centre of the Azores plateau. It is elongated in a NW-SE direction along the main tectonic trend of the Azores, with a length of 54 km and a maximum width of 7 km. The area of the island is 240 km^2 and the maximum elevation is 1053 m.

The sheer sea cliffs which typify the subaerial topography are not continued under water. In the north there is a shelf 1 - 2 km wide where the water is shoaler than 100 m. South of the island, this shelf is present only at the eastern end. Below 100 m, the depth increases rapidly to 1100 m, with slopes of 20 - 25° in the western half of the island but only half as steep in the east.

To the south-west, S. Jorge is separated from Pico by a flat-bottomed rift 1300 m deep and some 10 km wide. In the north, the water depth increases more slowly below 1100 m to a maximum value of approximately 2800 m in the submarine pits to the east and west of Graciosa.

5.5.2 General Geology. The island can be divided broadly into two parts, the boundary between the two parts being a north-south trending fault zone which crosses the island east of centre (Machado and Forjaz, 1964). This fault zone is marked by a saddle 2 km wide, and it is suggested that there has been lateral movement along this zone. The alignment of the faults and the volcanic cones, as well as the shape of the island, suggest that it has been built along a NW-SE fracture zone.

The eastern part of the island is considered the older, on the basis of the degree of dissection of the topography, and is comprised of basic basaltic lavas overlain by a sequence of basaltic lavas and pyroclastics in which highly altered pyroclastics predominate above 250 m.

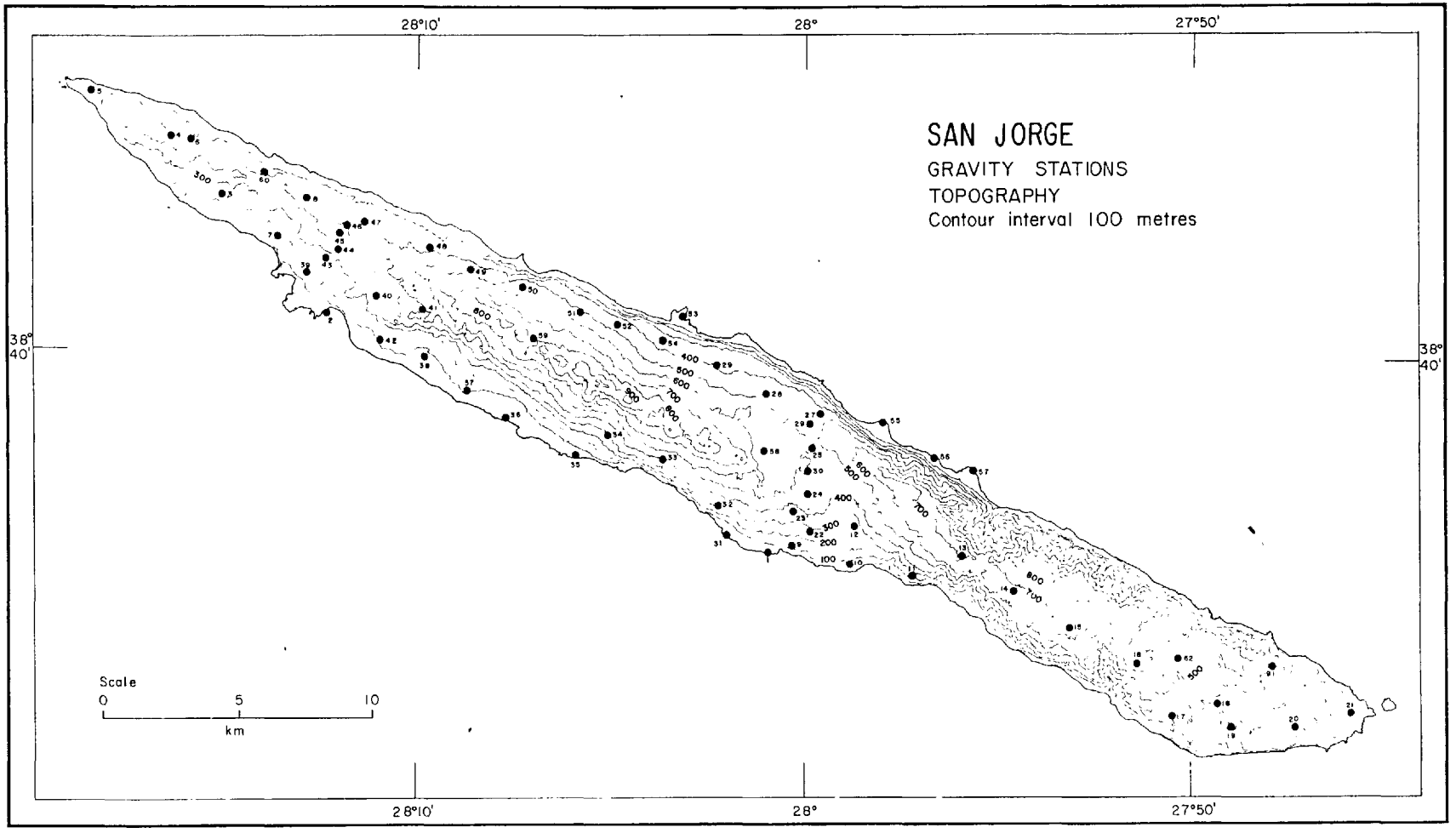
28°10'
28°
27°50'
38° 40'
SAN JORGE
GRAVITY STATIONS
TOPOGRAPHY
Contour interval 100 metres
Scale
0 5 10
km

FIG. 5.14.

In the central area, young basaltic lavas from a long narrow active zone along the spine of the island have overflowed the cliffs and built up coastal platforms along the south coast, and at one or two points in the north. All lavas west of the N-S fault appear to have a south-westerly dip, as though they originated from vents to the north of the islands. Hadwen and Walker (in press) suggest that the north coast is a fault scarp, the part of the island previously to the north having foundered either by down-faulting or large-scale land-slipping. The dips of the rocks in the eastern part of the island suggest an independent history.

In general, the rocks on the island are almost entirely basaltic lavas and pyroclastic rocks, with the latter, often highly altered, dominant above 250 m.

Historic eruptions have occurred in the central portion of the island, but no age determinations have been published for the oldest exposed rocks.

Several severe earthquakes have been recorded, one in 1964. In their analysis of this seismic swarm, Machado and Forjaz (1964) identify three types of shock, (1) in the central region of the island, with epicentres between 4 and 7 km deep, (2) near the south coast, at depths between 10 and 20 km, and (3) with epicentres near the north coast of Pico at a depth of approximately 20 km. In the same article, Machado and Forjaz have suggested, from a study of the

earthquake intensities on the surrounding islands, that magma chambers at a depth of approximately 5 km exist under S. Jorge, Terceira, Pico, Faial and Graciosa.

5.5.3 Details of the Survey. As described for Terceira.

5.5.4 Local Anomaly. The topography of the island and the distribution of gravity stations are shown in Fig. 5.14. The Bouguer anomaly values and contour map are presented as Fig. 5.15.

The highest observed Bouguer anomaly value is 149 mgal and the lowest, observed in the north-west, is 108 mgal.

The lowest value at the south-east end of the island is 123 mgal, and there is possibly an east-west gradient along the island due to the Mid-Atlantic Ridge, but as the gravity field is still decreasing rapidly at this point the data is insufficient to justify applying any such regional correction.

There are too few gravity stations in the central highlands to be able to state definitely that no major gravity anomaly exists there, but the main feature of the observed gravity field is a gravity high in the centre of the eastern and geologically older part of the island. The northern and southern boundaries of this centre are largely conjectural, since the nature of the terrain restricts the gravity stations to a narrow belt along the spine of the island.

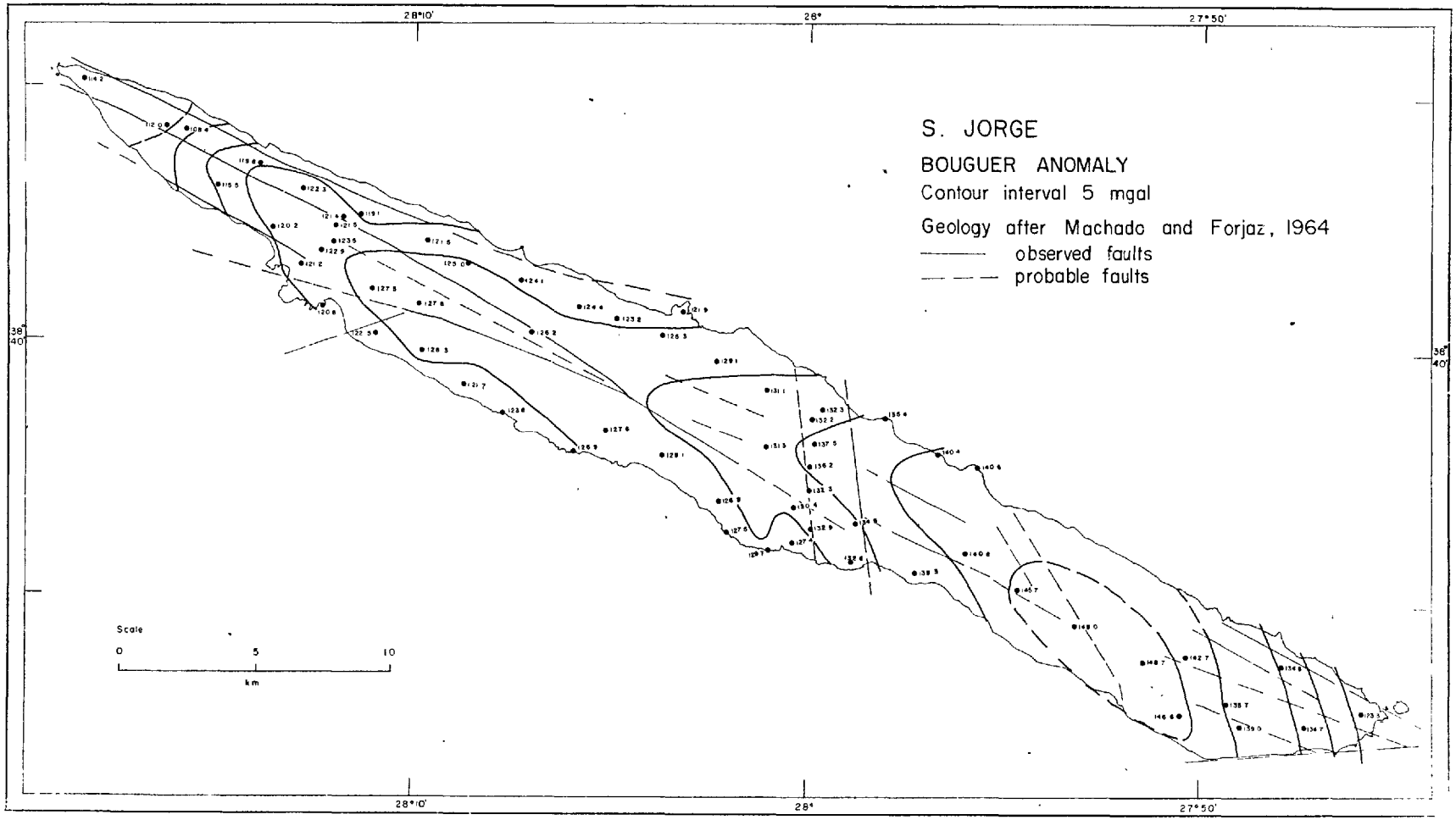
28°10'
28°
27°50'
38°40'
S. JORGE
BOUGUER ANOMALY
Contour interval 5 mgal
Geology after Machado and Forjaz, 1964
observed faults
probable faults
Scale
0
5
10
km

FIG. 5.15.

East of this centre, the gravity anomaly decreases rapidly and evenly, but to the north-west the gravity contours are elongated along the topographic trend of the island. This is consistent with the geological picture of the island having been built along a volcanic fissure system, perhaps following the eruption of a volcanic centre in the south-west.

There are, unfortunately, few data points across the north-south fault zone in the east-centre, but there is some evidence that there has been right-lateral movement in this area, though further west than is indicated by Machado and Forjaz (1964).

5.6 A Gravity Survey of Pico.

5.6.1 Introduction. Pico (Fig. 5.16) is situated in the Azores plateau at 38°28'N, 28°17'W, some 19 km south-west of S. Jorge. Its area is 433 km^2, with a maximum length of 45 km and a maximum width of 16 km. The island is dominated by the majestic volcanic cone of Pico de Pico which attains an elevation of 2351 m, by far the highest point in the archipelago. The maximum depth of the narrow channel between Pico and the island of Faial to the west, is only 100 m and the two islands are clearly one structural unit. The WNW-ESE trend of Pico is also continued eastwards in the form of a submarine ridge which can be traced for 100 km. In the north, the island is separated from S. Jorge by a 1300 m trench, and

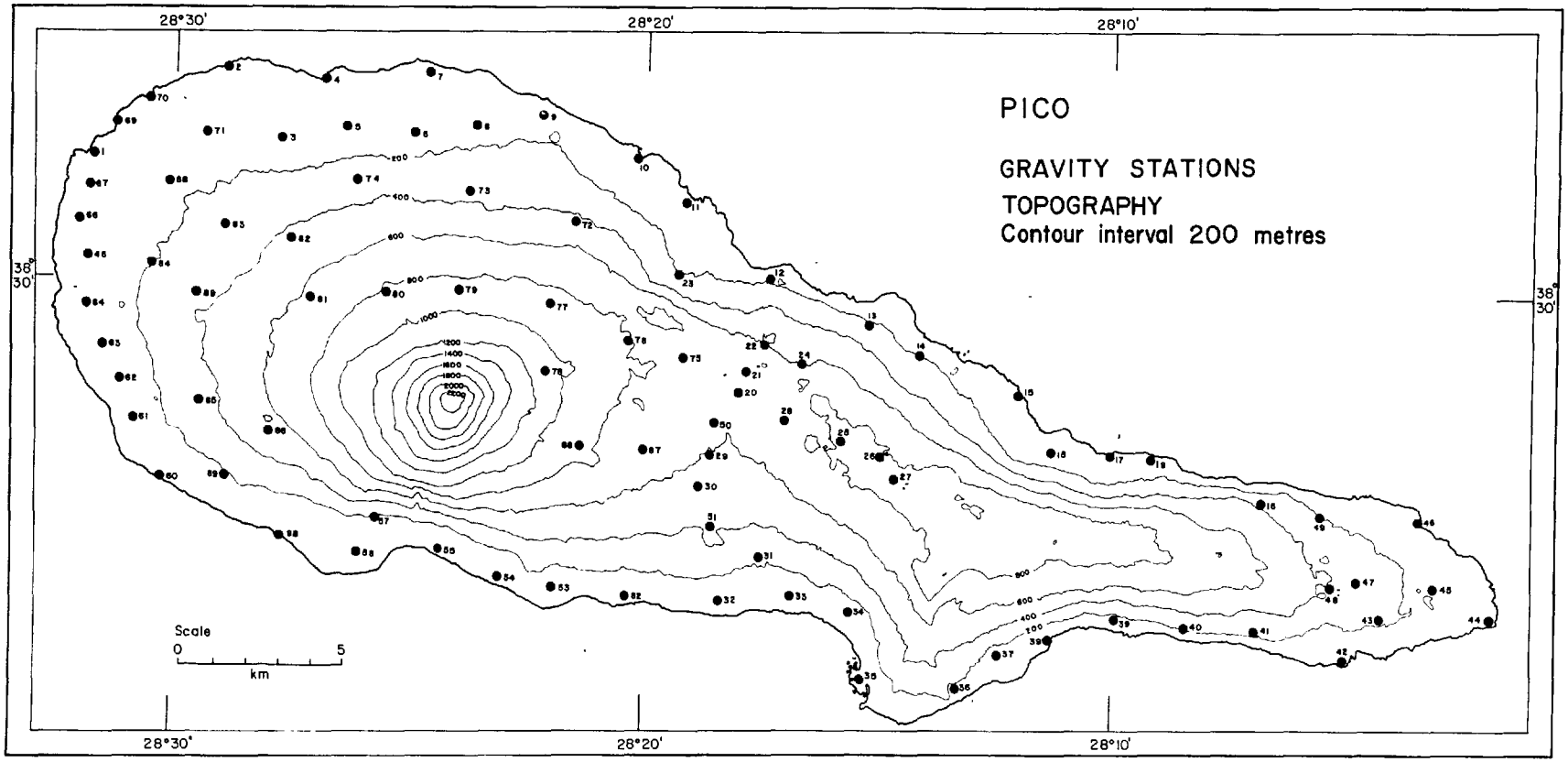
28°30'
28°20'
28°10'
38°30'
PICO
GRAVITY STATIONS
TOPOGRAPHY
Contour interval 200 metres
Scale
0
5
km

FIG. 5.16.

in the south the island flanks slope at an angle of 10^{o} down to 1100 m, then more gently down to the general level of 1800 m. The elevated Faial-Pico block is continued to the south-west as a large rugged area called the Princess Alice Bank, where the depth is less than 1000 m.

5.6.2 General Geology. Two separate trend lines are visible on the island, an east-west trend in the eastern portion of the island and, in the west, a NW-SE alignment. The eastern part is long and narrow and built along an east-west fissure zone marked by many small cones. The chief feature in this area occurs where this east-west zone intersects the NW-SE fracture zone of the western part of the island, and is considered (Zbyszewski et al, 1962) to be the oldest volcano on the island. Almost the whole of this eastern region is covered by young basaltic lavas. The only older rocks exposed are ankaramitic lavas. The western region consists almost entirely of the steep-sided cone and the more gently sloping lower flanks of the gigantic volcano Pico de Pico. Young basalt lavas and pyroclastic rocks are the only rocks which are exposed. The alignment of cones and fissures is NW-SE, in continuation of similar features on the island of Faial. An eruption in 1718 issued from a NW-SE trending fissure on the north-west flank of this cone, and two other historic eruptions occurred in the central saddle between the two parts of the island.

The western platform is subject to severe earthquakes, which have their epicentres in the channel west and north of Pico. From seismological investigations, Machado (1954) and Machado and Forjaz (1964) suggest the presence of two interconnected magma chambers under the island at a depth of approximately 5 km, one located under the north-west flank of the main cone, the other under the saddle area between the east and west regions.

5.6.3 Details of the Survey. As described for Terceira.

5.6.4 Local Anomaly. The topography of the island and the distribution of the gravity stations are shown in Fig. 5.16 and the Bouguer anomaly values and contour map in Fig. 5.17.

The two main features of the Bouguer anomaly map are (1) a centre of high anomaly with a maximum observed value of 147 mgal, located over the oldest centre of volcanism, and (2) another high anomaly centre, with a maximum observed value of 140 mgal, which is situated just to the east of the main volcanic cone. The exact position and shape of both anomalies are ill-defined, due to the paucity of gravity stations in their vicinity.

In the east of the island the gravity contours reflect the east-west topographic trend and confirm the rift-zone origin of this part of the island. A gravity nose from the eastern centre extends towards the west-central anomaly. It is possible that an offshoot from a magma chamber under the

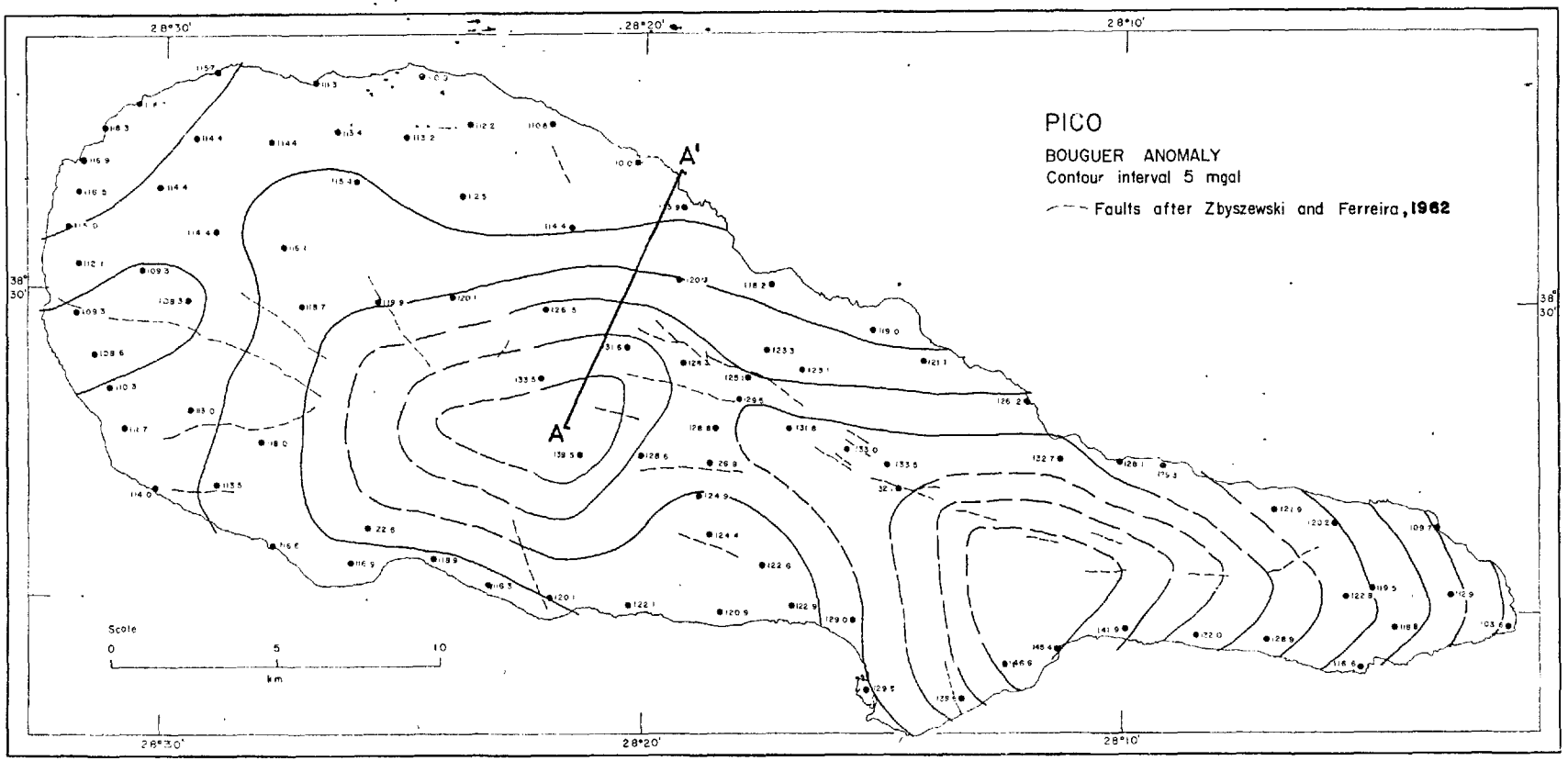
PICO
BOUGUER ANOMALY
Contour interval 5 mgal
Faults after Zbyszewski and Ferreira, 1962
A
A'
28°30'
28°20'
28°10'
38° 30'
Scale
0
5
10
km

FIG. 5.17.

eastern anomaly extends northwestwards along a line of weakness associated with the tectonic trends of the western half of the island, and is distending the island in this area. Such a possibility offers a satisfactory explanation for the faults, fissures, adventive cones and historic eruptions which characterize this part of the island.

Another gravity nose extends northwestwards from the western anomaly towards the Faial channel, and another smaller gravity high centred off the east coast of Faial (see also Fig. 5.20).

5.7 A Gravity Survey of Faial.

5.7.1 Introduction. Faial is situated on the Azores plateau at $28^{o}35'$N and $28^{o}43'$W. Its area is 172 km^2 and its maximum dimensions are 25 km by 14 km. The Faial channel between Pico and Faial has a maximum depth of 100 m, and the two islands form a single structural unit. In the north, east and south the bathymetry is the same as was described for Pico. In the west, the trend of the island is continued as a submarine ridge which swings south of west and eventually joins the western mountains of the Mid-Atlantic Ridge, which here trends north-south. The axis of the ridge, as determined from the bathymetry and from the magnetic data obtained on Vema cruise 14 (Heirtzler and Le Pichon, 1965), is some 25 km to the west of the island and takes the form of a valley

10 - 15 km wide with a depth of between 1900 - 2000 m to the valley floor.

5.7.2 General Geology. The island is a symmetrical volcano with a 2 km diameter caldera and is extended westwards along a WNW-ESE fissure zone by a line of overlapping cones. The eastern flank of the volcano is characterized by a series of NW-SE fault scarps, traces of which can be seen continued on Pico (Zbyszewski et al, 1962).

The rocks are largely feldspar-rich basalt lavas and pyroclastics. Trachyte occurs as dykes and plugs, and also as a mantle of trachyte pumice which thins away from the caldera.

Historic eruptions have occurred in the west, decreasing in age westwards. The last eruption in 1957-58 increased the length of the island in a westerly direction by 1 km.

Slight seismic tremors are often felt having epicentres located either to the west of the island, or between Faial and Pico. Machado (1954) and Machado and Forjaz (1964) interpret seismological observations in the area as indicating a magma chamber at a depth of approximately 5 km in the west of Faial.

5.7.3 Details of the Survey. As described for Terceira.

5.7.4 Regional Anomaly. The topography of the island and the distribution of gravity stations are shown in Fig. 5.18 and the Bouguer anomaly values and contour map in Fig. 5.19.

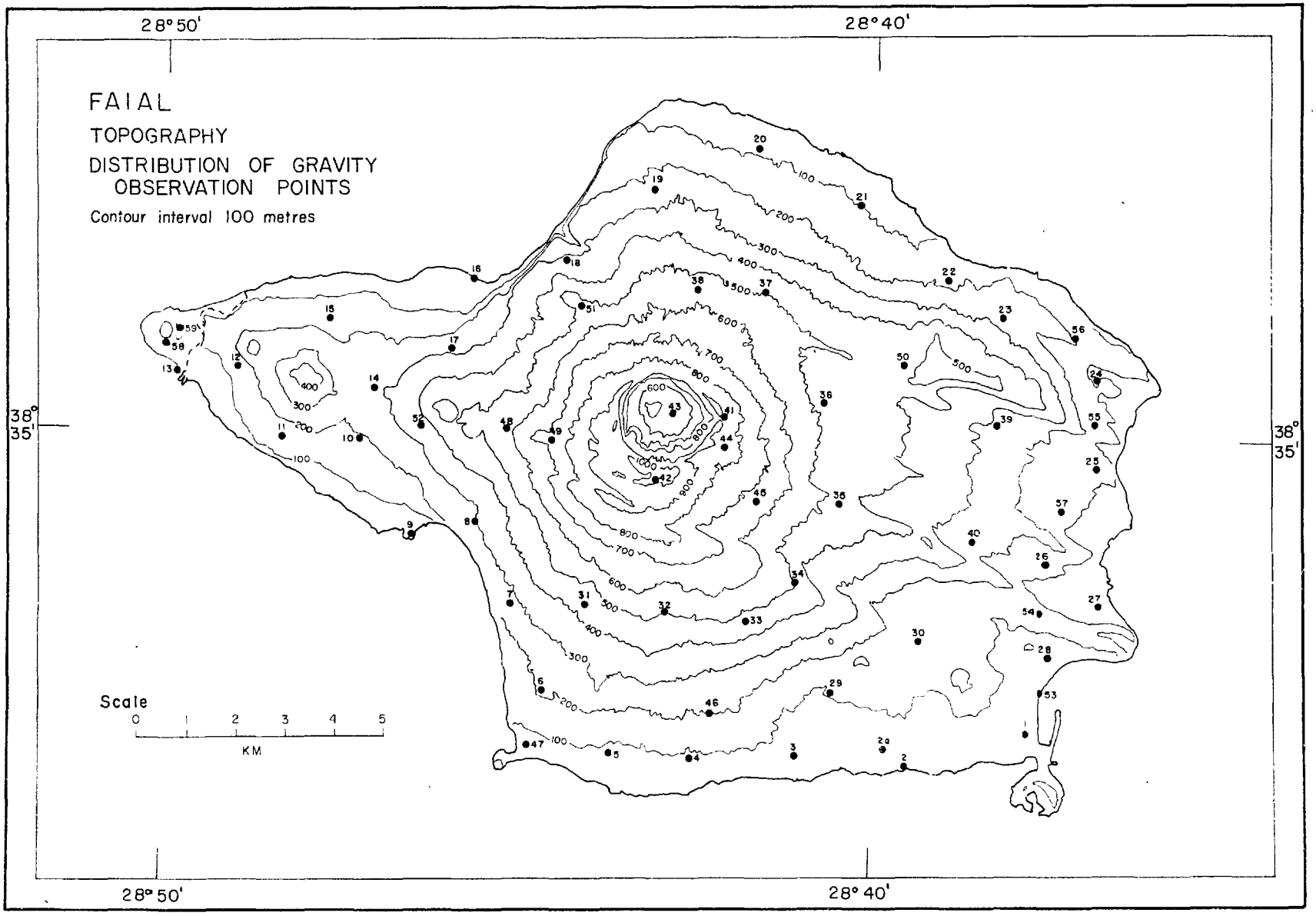
28°50'
28°40'
FAIAL
TOPOGRAPHY
DISTRIBUTION OF GRAVITY OBSERVATION POINTS
Contour interval 100 metres
38° 35'
Scale
0 1 2 3 4 5
KM

FIG. 5.18.

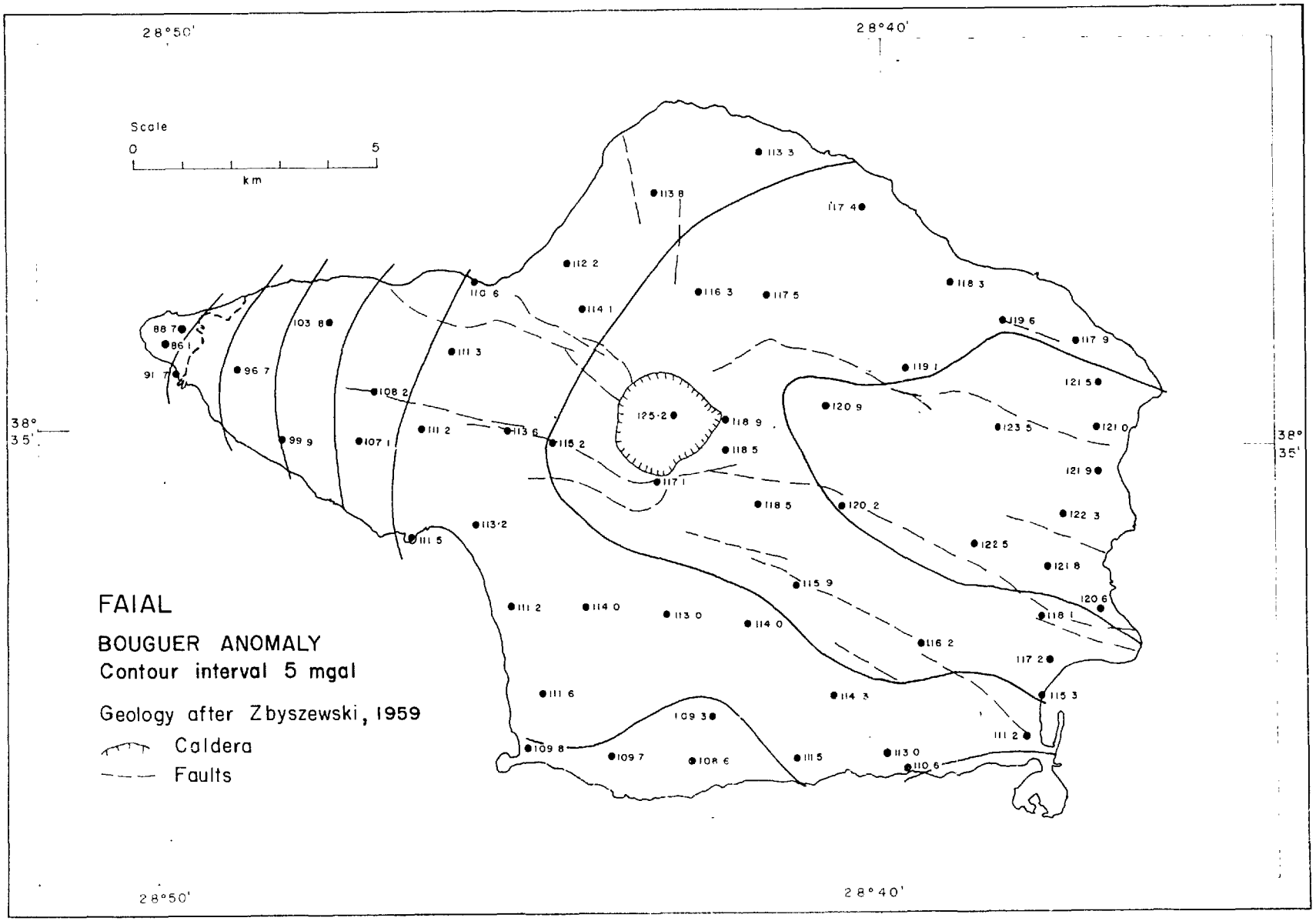
28°50'
28°40'
Scale
0
5
km
38° 35'
FAIAL
BOUGUER ANOMALY
Contour interval 5 mgal
Geology after Zbyszewski, 1959
Caldera
Faults
113 3
113 8
117 4
112 2
110 6
116 3
117 5
118 3
114 1
119 6
117 9
88 7
86 1
91 7
96 7
103 8
111 3
119 1
121 5
108 2
125·2
118 9
120 9
123 5
121 0
99 9
107 1
111 2
113 6
115 2
118 5
121 9
117 1
118 5
120 2
122 3
113·2
111 5
122 5
121 8
115 9
120 6
111 2
114 0
113 0
114 0
118 1
116 2
117 2
111 6
114 3
115 3
109 3
111 2
109 8
109 7
108 6
111 5
113 0
110 6

FIG. 5.19.

Faial is linked so closely with Pico that it cannot be considered in isolation, and the gravity anomaly on the three islands Faial, Pico and S. Jorge is presented as Fig. 5.20.

The principal feature of the Bouguer anomaly map is a pronounced east-west gradient whereby the gravity field is reduced from 124 mgal in the east to 86 mgal in the west. This minimum value is almost 20 mgal less than the minimum value observed at the eastern extremity of Pico, and this, and the westward decrease in the maximum values of the gravity centres on Pico and Faial, suggests that a regional eastward gradient is present, perhaps becoming steeper towards the west and the axis of the Mid-Atlantic Ridge. If the centres of high gravity have approximately similar amplitudes, the decrease in their maximum Bouguer anomaly values from 147 mgal in the east to 140 mgal in the centre and 124 mgal in the west would suggest a gradient increasing from 0.4 mgal/km in the west to 0.6 mgal/km in the centre. It is impossible to separate this regional gradient from the local gradient in the west of Faial but it may possibly be as high as 2.0 mgal/km. In an attempt to remove the masking effects of this gradient on the gravity anomaly, a first order regional field was fitted by least squares (see Fig. 2.6) and removed from the Bouguer anomaly to leave the residual anomaly which is shown in Fig. 5.21.

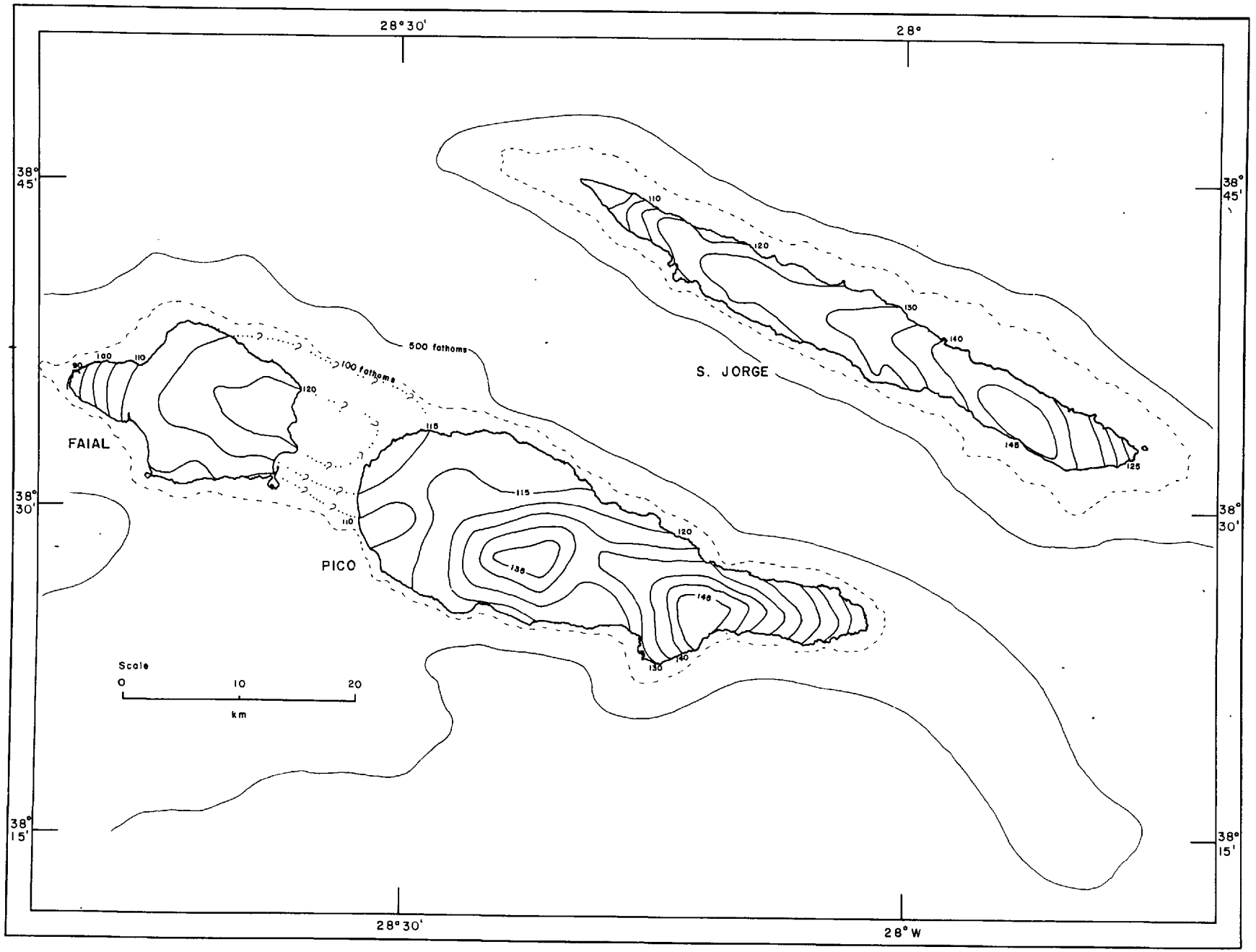

FIG. 5.20. Bouguer gravity anamaly map of Faial, Pico and S. Jorge. Contour interval 5 mgal.

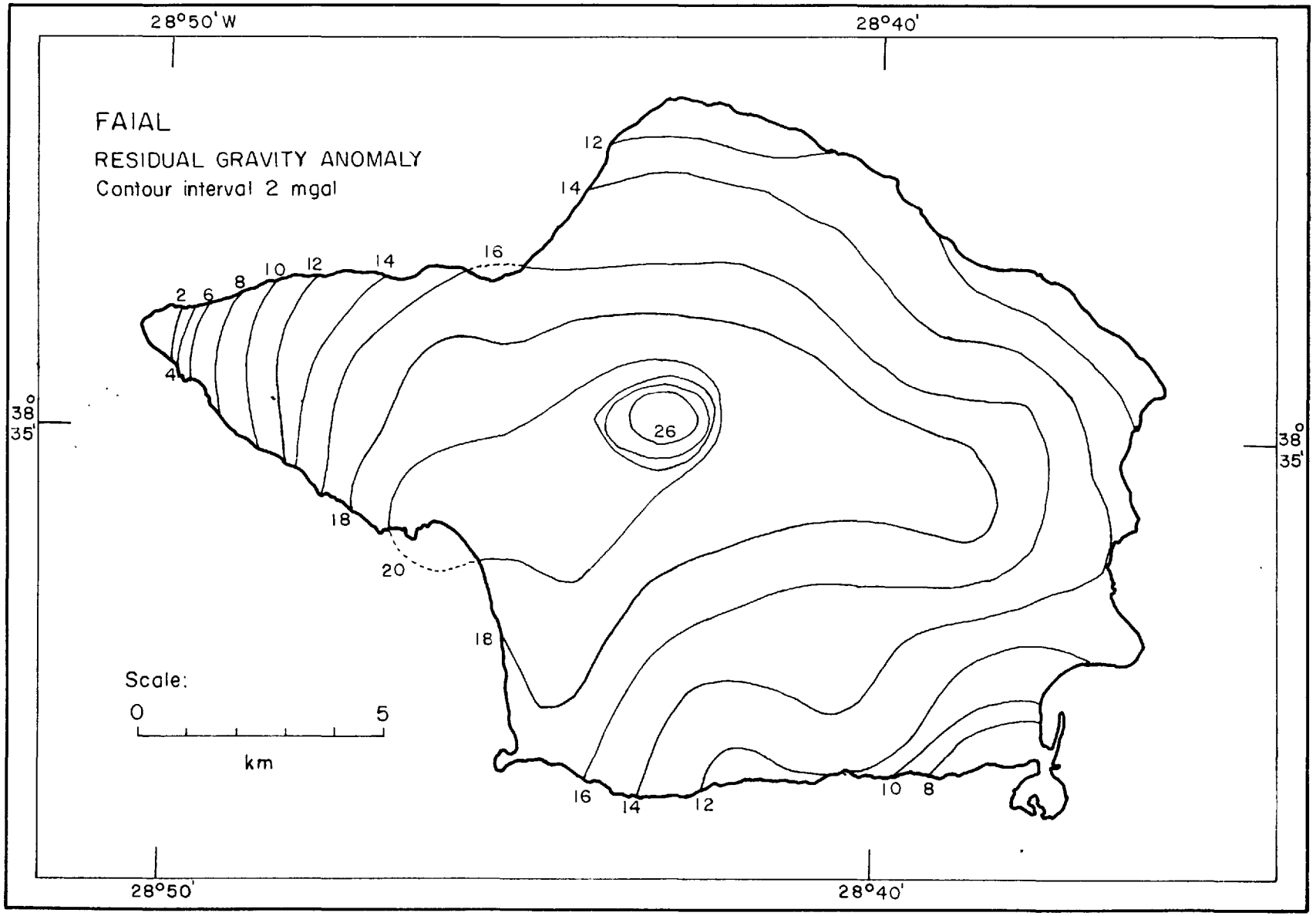
28°50'W
28°40'
FAIAL
RESIDUAL GRAVITY ANOMALY
Contour interval 2 mgal
12
14
16
10
12
14
2
6
8
4
26
18
20
18
Scale:
0
5
km
16
14
12
10
8
38° 35'
28°50'
28°40'

FIG.5.21

The gradient of the regional field is 1.25 mgal/km, and together with the steep gradients of the residual anomaly on the western peninsula supports the suggestion that the regional gradient increases towards the axis of the Mid-Atlantic Ridge.

Marine gravity profile JJ' (Fig. 5.3) and several published continuous gravity profiles across the Mid-Atlantic Ridge (Talwani et al, 1965; Van Andel et al, ~~in press~~ 1968) show a regional gravity gradient towards a minimum at the median valley. In most of these the observed gradients increase towards the ridge. The maximum gradient observed by Talwani et al (1965) in their profile which crosses the ridge at 32°N, perpendicular to its main trend, was 0.57 mgal/km adjacent to the ridge crest.

At 28°N, Van Andel and Bowin (1968) observed gradients ranging from 0.13 to 0.4 mgal/km, and gradients between 0.04 and 0.27 mgal/km at 22°N. In both cases the higher gradients occur closer to the crest. In a detailed geological survey of a section of the Mid-Atlantic Ridge near 45°N, Loncarevic et al (1966) observed a Bouguer anomaly gradient at the edge of the median valley of 5 mgal/km, decreasing rapidly to less than 2 mgal/km within 10 -- 15 km from the valley.

In the latitude of Faial, the axis of the ridge as determined from the bathymetry and the magnetic records

obtained on Vema cruise 14 (Heirtzler and Le Pichon, 1965) is some 25 km west of the island.

There is thus almost certainly a considerable gravity gradient across the island, probably becoming steeper in the west, but it is unlikely that it accounts for the full 5 mgal/km gradient observed on Faial, as this would imply a Bouguer anomaly of almost zero over the axis of the ridge. As it is, the value of the Bouguer anomaly, and the gradient at the western extremity of Faial, point to a value of not more than 80 mgal for the Bouguer anomaly in the median valley. This is over 50 mgal smaller than the values observed in the JJ' and KK' profiles (Fig. 5.3 and 5.4), and over 100 mgal smaller than the Bouguer anomaly over the median valley observed by Loncarevic et al (1966) near 45°N, and Talwani et al (1965) at 32°N. This low Bouguer anomaly has wide implications concerning the structure of the Azores, but these will be discussed later when the islands are considered as a group.

5.7.5 Local Anomaly. When the regional gradient is removed, the residual anomaly (Fig. 5.21) obtained has a centre of high anomaly over the summit caldera. The contours show the region of high gravity extending eastwards along the zone of faults and graben structures, and westwards along the rift zone which has given rise to the western peninsula. A gravity nose extending southwards to the trachytic plug at

the extreme south-west corner of the island suggests that a rift zone extends from the central vent to this point.

The high gravity anomaly observed at the caldera bottom is unique among the Azores calderas studied in this survey, although the mantle of trachytic pumice over the island is similar to those associated with the calderas on other islands. The possibility that the Bouguer anomaly is in error cannot be dismissed since there is no other gravity station to confirm this value, but if the observed value is assumed to be correct it requires a very high-density mass close to the surface of the caldera to account for it. If 3.15 gm/cc, the density of the "anomalous mantle" of Talwani et al (1965), is adopted as the density of this mass, then the gravity anomaly in the immediate vicinity of the caldera can be reproduced by a vertical cylinder of diameter 1 km, (the diameter of the bottom of the caldera) extending from the surface of the caldera floor down to 4 km.

5.8 A Gravity Survey of Flores.

5.8.1 Introduction. Flores ($39^{o}27'N$, $31^{o}12'W$) is the most westerly island of the Azores archipelago and with the island of Corvo some 18 km to the north forms the northern end of a north-south submarine ridge. The maximum elevation on the island is 915 m, its maximum dimensions are 17 km north-south, 12 km east-west, and its area is 142 km^2.

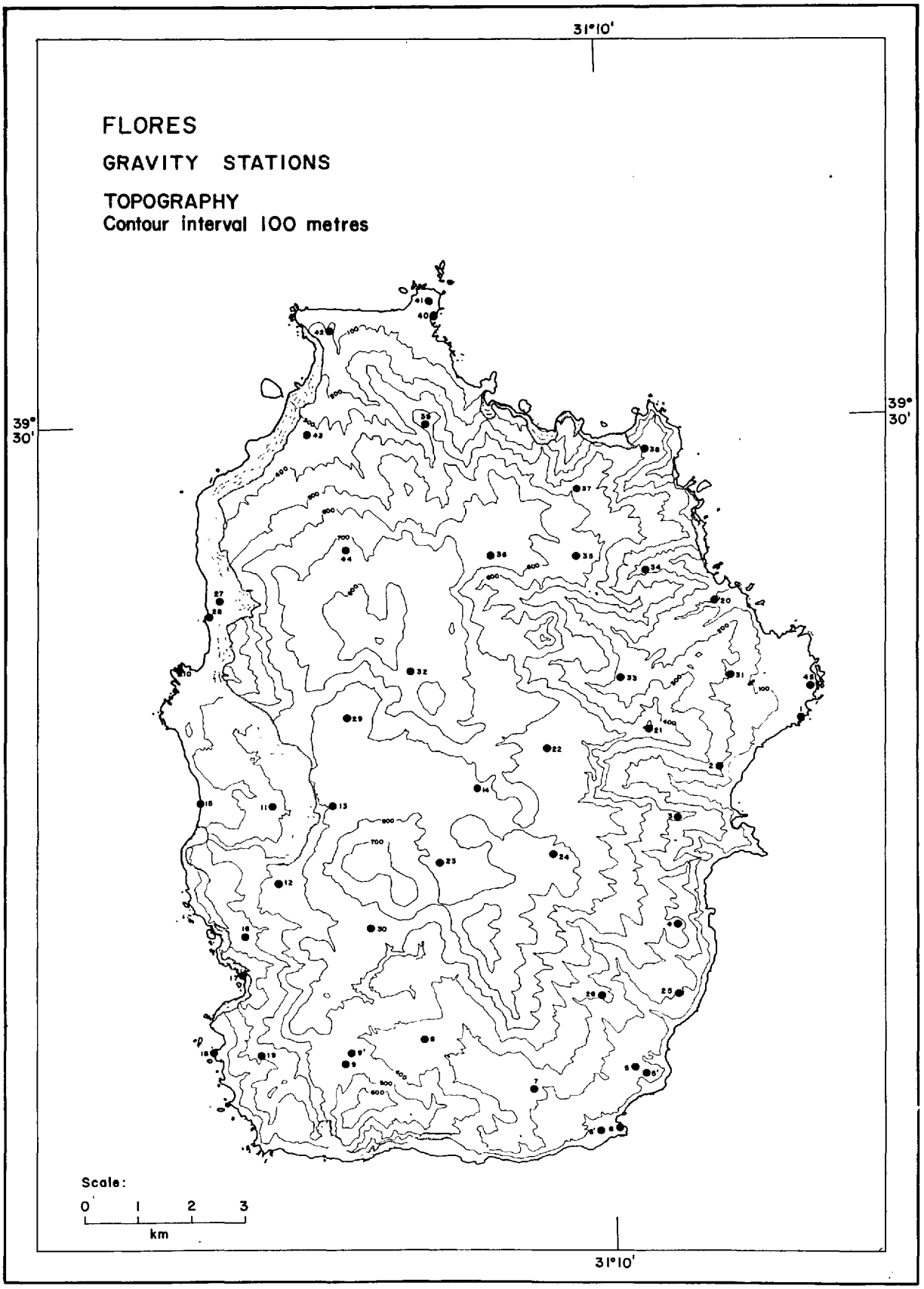
31°10'
FLORES
GRAVITY STATIONS
TOPOGRAPHY
Contour interval 100 metres
39° 30'
39° 30'
Scale:
0 1 2 3
km
31°10'

FIG. 5.22.

The island lies in line with the Pico-Faial tectonic trend and about 150 km west of the axis of the Mid-Atlantic Ridge, which in this latitude runs in an approximately north-south direction. The island is surrounded by a broad shelf, where the depth is less than 200 m. The minimum width of this shelf is 2 km along the east coast, but it extends to over 7 km towards Corvo in the north. Below 200 m the depth increases rapidly to 1500 m, then more slowly to the general 1800 m level of the Azores plateau.

5.8.2 General Geology. The highest point occurs north-west of centre and takes the form of a pyroclastic cone with fairly young basaltic lavas on its north-west slopes. To the south of it, there is a large shallow basin, 5 km in diameter, containing seven deep, water-filled craters, and in the middle a pair of volcanic cones 150 m high.

High cliffs practically surround the island, and some of these may be due to collapse (Hadwen and Walker, in press). Rock types range from olivine-basalt lavas and pyroclastics to trachyte plugs, lavas and tuff

Hot springs occur at sea level in the south-west but there are no recorded historic eruptions, and few young volcanic features are visible. Only one earthquake has been recorded.

No age determinations have been published for this island.

5.8.3 Details of the Survey. These are as described for Terceira, except that terrain and bathymetric corrections were calculated by the computer method described in Chapter 2. A contour interval of 100 m was used in approximating the topography, which was taken from a 1:25,000 1965 military map. The bathymetry was obtained from the Admiralty Chart No. 1946 and the 1:1,000,000 plotting sheet of collected soundings No. 58 produced by the National Hydrographic Office. The accuracy of the terrain corrections is therefore reduced to ± 2 mgal (see Table 2.3), and the total error in the Bouguer anomaly becomes ± 4 mgal.

5.8.4 Local Anomaly. The island topography and distribution of the stations are shown in Fig. 5.22 and the Bouguer anomaly values and contour maps in Fig. 5.23.

The Bouguer anomaly map is remarkable for its low relief, the lowest observed value being 146 mgal and the highest 161 mgal. This is possibly accounted for by the fact that the land surface represents only the inner part of the summit of the volcano which forms the island structure. The summit area must also include the wide marine terrace which surrounds the island.

No major gravity centre is visible, though a broad area of high Bouguer anomaly is associated with the uplands in the northern half of the island. The high anomaly is continued southwards in the form of a half circle open to the

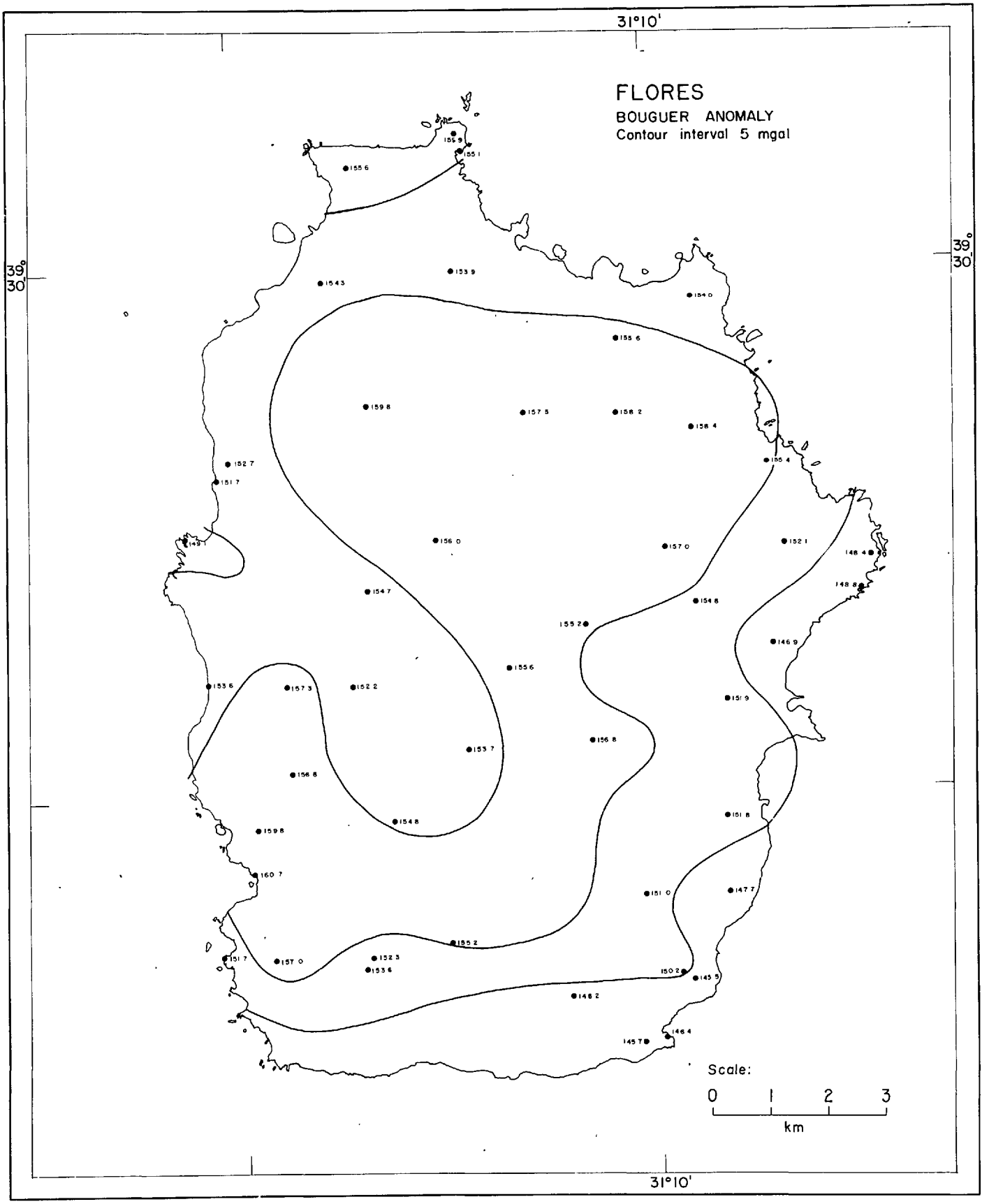
FLORES
BOUGUER ANOMALY
Contour interval 5 mgal
31°10'
39° 30'
155.9
155.1
155.6
153.9
154.3
154.0
155.6
159.8
157.5
158.2
158.4
155.4
152.7
151.7
149.1
156.0
157.0
152.1
148.4
148.8
154.7
154.8
155.2
146.9
155.6
153.6
157.3
152.2
151.9
153.7
156.8
156.8
154.8
151.8
159.8
160.7
151.0
147.7
155.2
151.7
157.0
152.3
153.6
150.2
145.9
148.2
146.4
145.7
Scale:
0 1 2 3
km

FIG. 5.23.

north-west and partially encircling a region of low gravity anomaly. The low anomaly is associated with the basin characterized by the seven deep craters and relatively young volcanic features. This half circle of high anomaly crosses the coast in the south-west, where fumarolic activity can be seen and where the Bouguer anomaly attains its maximum value.

5.9 General Discussion.

The general map of the gravity surveys of the Azores is presented in Fig. 5.24, and the gravity results are summarized in Table 5.1.

The WNW-ESE trend of the gravity contours on most of the islands emphasises the predominantly fissure nature of the eruptions, but with two exceptions the islands are also characterized by one, and sometimes two central-type volcanoes. It is probable that the central eruptions have arisen at points along the fissures of particularly weak crust, and the islands may owe their existence as sub-aerial structures to these centres. Terceira has no major centre of high anomaly and consists instead of a broad belt of high anomaly trending WNW-ESE across the island. Three smaller gravity features along the centre of this belt suggest that the island has been built by the coalescing of three adjacent minor volcanic centres located along a fissure. The low gravity relief on Flores distinguishes it from all the

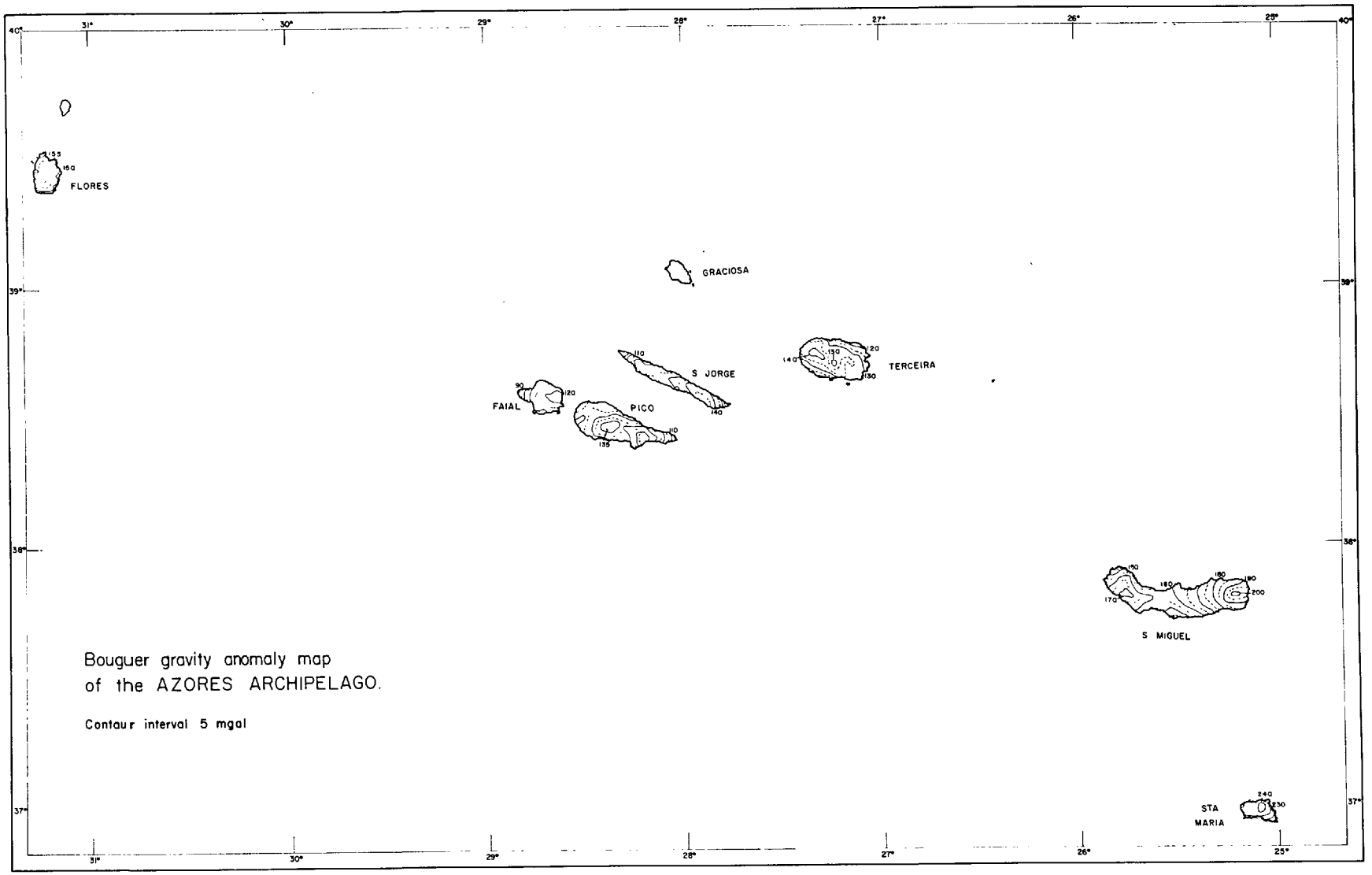
FLORES
GRACIOSA
S JORGE
TERCEIRA
FAIAL
PICO
S MIGUEL
STA MARIA
Bouguer gravity anomaly map
of the AZORES ARCHIPELAGO.
Contaur interval 5 mgal

FIG. 5.24.

Summary of Gravity Results in the Azores Islands.

Island Name	Distance from Mid-Atlantic Ridge to Nearest point	Distance from Mid-Atlantic Ridge to anomaly centre	Maximum Bouguer Anomaly	Amplitude	Maximum Gradient	Maximum Depth	Minimum Bouguer Anomaly	Estimatd Regional Field
	km	km	mgal	mgal	mgal/km	km	mgal	mgal
S.Maria	391	400	242	68	6.5	9.0	206	175
S.Miguel E	300	360	203	ca. 60	5.0	10.3	140	ca.145
S.Miguel W		309	175	ca. 60	4.9	10.0		ca.115
Terceira	220	225	140	ca. 40	6.0	5.0	115	ca.100
Flores	120	130	161		6.0		146	
S.Jorge	79	113	149	ca. 50	5.0	8.0	108	ca.100
Pico E	52	84	147	ca. 60	4.5	5.0	104	ca. 90
Pico W		68	140	ca. 55	5.0	9.0		ca. 85
Faial	26	44	125	ca. 50	5.0	8.0	86	ca. 75

Table 5.1

islands to the east of the Mid-Atlantic Ridge. A similar though somewhat smaller area of low gravity relief can be seen on the north-west of Santa Maria, and it may be that marine erosion has so reduced Flores that the present land surface represents only the summit region of a much larger central volcano.

The amplitudes of the central anomalies cannot be accurately estimated from the island surface data; even if marine gravity data are available the uncertainty is still considerable because of possible error in the density used for the Bouguer corrections of the marine data. The amplitudes and the regional field values listed in Table 5.1 may be in error by 10 - 20 mgal, but if this is borne in mind there does appear to be a slight tendency for the amplitudes to increase with distance from the Mid-Atlantic Ridge. No similar trend is visible in the maximum observed gradients, which range from 4.5 to 6.5 mgal/km.

The uncertainty in the amplitudes of the anomalies is reflected in the calculated maximum possible depth to the disturbing bodies. This depth is estimated from Corollary 1.1 of Bott and Smith (1958) (see equ. 4.1) and varies from 5.0 to 10.5 km. As the anomalous mass must have a higher density than the surrounding rocks, it will almost certainly lie in the crust. The calculated depths confirm this and

show that the anomalous body need not be within the body of the island standing above the level of the sea-floor.

Two central-type anomalies associated with the calderas on Terceira are gravity lows. These anomalies are of small amplitude and indicate lower density masses located closer to the surface than 1.5 km. The calderas on S. Miguel are also associated with low Bouguer anomalies. They have all been described by Machado (1965) as being of the Krakatoa type of Williams (1941), and as such are consistent with the classification of Yokoyama (1963), who noted that such calderas have negative gravity anomalies. The gravity high measured at the bottom of the Faial caldera may possibly be in error, but it may also be that Yokoyama's classification does not apply to calderas which originate in the heart of the volcanic centre. The other calderas on Terceira and S. Miguel are to one side of the major volcanic centres.

The estimated regional field Bouguer anomaly values, the minimum values on the islands, and the maximum values of the Bouguer anomaly centres, are plotted in Fig. 5.25 against their distance from the Mid-Atlantic Ridge. The position of the Mid-Atlantic Ridge is defined by the bathymetry and by the magnetic profiles V14 (Heirtzler and Le Pichon, 1965) and P109 (Keen, 1963). Distances are measured along the WNW-ESE trend of the islands. The corresponding sections of the marine Bouguer anomaly profile KK' is shown for comparison.

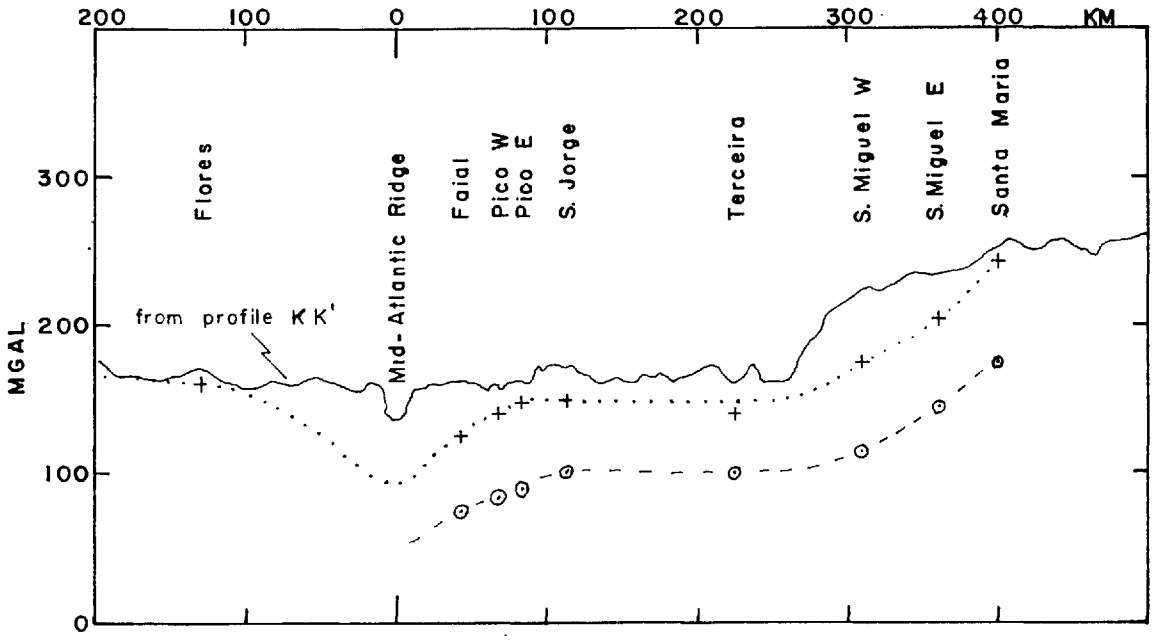

FIG.5·25 Variation of gravity field with distance from the Mid-Atlantic Ridge. + Maximum Bouguer anomaly observed on the island. ⊙ Estimated regional Bouguer anomaly. The corresponding section of the marine Bouguer anomaly profile from fig. 5·4 is shown for comparison.

The form of the two island curves is similar to the marine profile KK'. The anomaly decreases rapidly by 50 - 70 mgal over the outer islands of Santa Maria and S. Miguel to a level which is maintained over the Azores plateau until it again decreases steeply within 100 km from the axis of the Mid-Atlantic Ridge.

The regional Bouguer anomaly over the archipelago is in general 60 - 70 mgal less than on the marine gravity profiles to the north and south. The value of the regional field in the west of Faial, only 25 km from the axis of the Mid-Atlantic Ridge, may be as low as 70 mgal. With the gradients of 2 mgal/km and 5 mgal/km observed by Loncarevic et al (1966) over the axial zone of the ridge at 45°N this may mean a Bouguer anomaly of about 30 mgal over the median valley. This is 100 mgal less than the value observed on the KK' profile and is nearer the values observed on Iceland which lies across the Mid-Atlantic Ridge. Einarrson (1954) measured Bouguer anomaly values of -35 mgal over the axial zone in the centre of Iceland, increasing to +60 mgal on the edge. Seismic refraction work by Båth (1960) discovered that a 6.0 - 6.7 km/sec layer extended to 17 km depth under the centre of Iceland and was underlain by 7.4 km/sec material. This latter velocity probably corresponds to the anomalous mantle material considered by Talwani et al (1965) to underlie the axial zone of the Mid-Atlantic Ridge. The very low

regional field over the Azores islands clearly indicates a considerable mass deficiency and it may be that this deficiency also comprises a thickened crust underlain by anomalous mantle material.

Since it is probable that the Azores and the axial zone of the ridge to the north and south are underlain by anomalous mantle material (Le Pichon et al, 1965), the extra mass deficiency compared with the rest of the Mid-Atlantic Ridge which is implied by the Bouguer anomaly must arise from (1) a thickening of the crust as on Iceland, or (2) a thickening of the anomalous mantle layer as shown in Fig. 5.3, or (3) a decrease in density of the underlying anomalous mantle material. If the anomalous mantle material is partially fused mantle, as suggested by Bott (1965), the extensive fracturing in the Azores area may easily lead to increased fusion and consequent decrease in density of the sub-crustal material. Only seismic refraction studies can differentiate between the three possibilities, but the existing seismic refraction profiles in the area throw little light on the matter.

In the case of Santa Maria, the negative regional gravity anomaly has an amplitude of about 90 mgal and a width of 300 km (see Fig. 5.3), and it was shown in Section 5.2 that this anomaly indicates a mass deficiency which provides complete isostatic compensation for the island. In the same

way, the mass deficit under the Azores Archipelago indicates a degree of compensation, but there are insufficient data to show to what extent isostatic equilibrium has been achieved, or exactly what form the mass deficiency takes.

The track KK' (Fig. 5.1 and 5.4) crosses the Mid-Atlantic Ridge almost at right-angles, and the bathymetry profile shows clearly the median valley in the centre of a 500 km wide plateau where the water depth is less than 2000 m. This plateau can be divided into two parts according to the nature of the terrain. The inner part forms a belt 200 km wide of extremely dissected sea-floor, and this is flanked on either side by 150 km of much smoother bottom topography.

None of these features appears very clearly on the JJ' profile (Fig. 5.3) which crosses the ridge at an angle of approximately 60°. The bathymetry profile shows that the axial zone of the Mid-Atlantic Ridge consists of very wide and high mountains which extend for 150 km on either side of the median valley. The rest of the shallow terrain extending as far as Santa Maria is the southern flank of the Azores plateau.

It is worth noting that on both profiles there is a distinct topographic feature at the eastern edge of the uplifted portion. Le Pichon and Talwani (1964) carried out a gravity survey of a seamount located similarly at the western edge of the axial zone at 35°N and noted then that

the seamount marks the limit of the ridge and is connected with an important change in the crust and upper mantle. They amplified this statement later (Talwani et al, 1965) and showed that the edge of the axial zone of the ridge is the boundary between normal oceanic crust, underlain by normal mantle, and the axial region where the crust is underlain by anomalous mantle material, with sub-normal velocity and density.

The gravity anomaly profiles also are quite different. On the KK' track the Bouguer anomaly maintains approximately the same value of 165 mgal over the 500 km width of the axial zone, except for a -30 mgal anomaly over the median valley. The JJ' Bouguer anomaly has a strange W-shape but the low anomaly area is only some 200 km wide.

East of Santa Maria the JJ' track continues close to the line of the proposed Azores-Gibraltar Ridge, and may even cross it, but there is no continuation of the low Bouguer anomaly to indicate a mass deficiency similar to that over the Azores plateau. Thus, although there is considerable seismicity (Heezen et al, 1959) along it, this ridge does not appear to be associated with the low Bouguer anomaly which is characteristic of mid-ocean ridges.

If the positions of the axis of the ridge as determined on V14 and P109 are correct, then an east-west left-lateral transverse or dextral-transform (Wilson, 1965) fault is

indicated at approximately 38°40'N latitude. It also seems more probable that the east-west trench at 38°N is a right-lateral or sinistral transform fault than that the ridge should change direction through 45°. The ridge does however appear to change direction slightly in the area of the Azores from a NE-SW trend at 37° to a NNE-SSW trend at 40°.

If the above observations are viewed in the light of the crustal spreading hypothesis as suggested by Hess (1962) and Dietz (1962), and recently updated by Vine (1966), several points emerge.

(1) The abrupt change in the submarine topography between the inner and outer ridge on the KK' bathymetry profile may indicate a sudden change in drift rate or an abrupt change in sediment thickness. Fortunately, Ewing and Ewing (1967) published a tracing of seismic profiler records made during a traverse of the ridge at about 40°N, and this tracing shows a clear discontinuity in sediment thickness at about 125 km from the axis of the ridge. Ewing and Ewing interpreted this abrupt change in sediment thickness which they observed on many other profiler crossings of mid-oceanic ridges, as indicating a break in the crustal spreading activity lasting from the late Mesozoic or early Cenozoic until 10 MY ago. The earlier spreading was considered to have moved the continents to roughly their present positions and to have had essentially the same ridge-axis as the present spreading cycle.

(2) The Ewing and Ewing hypothesis leaves unexplained the apparent disparity in width of the ridge north and south of the Azores. The width of the axial zone at 37°N suggests that the spreading rate has been only half as much as in the north, or that the present elevated area corresponds to only one of the two most recent postulated spreading cycles. There is no indication on the magnetic data along the JJ' track of a decrease in wavelengths compared to the KK' track which would support the former conclusion, nor is there any evidence for sedimentation on the axial zone of the southern profile. It may be that the section of the ridge to the south of the right-lateral transverse fault was inactive for all or part of the previous spreading cycle. If this fault is the right-lateral fault which Krause (1965) infers in the west Azores, then the above interpretation would account for its quiescence since Cretaceous or early Tertiary time. If the present crustal spreading rate is the same north and south of the transverse, or rather transform fault, there will be no relative displacement except in the part between the two ends of the ridge. The left-lateral transverse fault to the north of Faial may also be the left-lateral fault which Krause (1965) suggests exists in the east Azores and gives rise to the trend of the islands and the Azores-Gibraltar Ridge.

(3) The above-mentioned transform faults and possibly a few other minor ones not apparent from the limited data available, may accomodate the change in direction of the Mid-Atlantic Ridge between 38°N and 40°N. Crustal spreading will mean that the east Azores is a region of tensile stress. The large-scale fracturing which results is orientated preferentially along the existing directions of weakness caused by the transform faulting. These fractures under tensile stress will be easily invaded by magma to produce the fissure eruptions which are so characteristic of this region.

While the crust to the east of the ridge is under tension, to the west it is under compression. Conditions are therefore unfavourable for volcanism and this may account for the disparity in scale of volcanic activity east and west of the ridge.

(4) Minor volcanic activity occurs fairly randomly over the islands, but there is a strong tendency for the main shield-building volcanism to decrease in age towards the ridge, both across the whole archipelago and on individual islands. This clearly is true on S. Miguel, S. Jorge, Terceira and Pico. There is only one shield volcano on Faial but, as on Ascension Island, the shape of the island indicates that the recent volcanism is extending the island in the direction of the ridge. Looking at the archipelago as a whole, Santa Maria and the eastern volcano on S. Miguel appear to be

extinct, suggesting that volcanism ceases at the edge of the plateau or axial zone, and also that the order of extinction of the islands may occur along the island chain towards the axis of the Mid-Atlantic Ridge. The decrease in age of the volcanism towards the ridge may indicate that the islands are drifting over the magma source as suggested by Wilson (1963a) but the contemporaneity of active volcanism throughout the archipelago makes it more probable that this may reflect a tendency for fracturing and tensile stress to be greater on the ridge side of an already established centre. If the latter possibility is true, then there may be one magma source for the whole Azores Archipelago, and this magma may be the cause of the low Bouguer anomaly. The rapid west-east increase in Bouguer anomaly over S. Miguel and Santa Maria suggests that the volcanoes have become extinct because they have drifted beyond the eastern boundary of this magma chamber. The magma may be the partially fused mantle material which, as suggested above, may underlie the crust in this region.

The proposed origin of the islands along fractures associated with the change in direction of the axis of the Mid-Atlantic Ridge means that, although crustal spreading will still move the islands away from the ridge, the island structure need not have been initiated at the axis of the ridge as suggested by Wilson (1963a), and their age of origin need bear no relation to distance from the axis.

5.10 Conclusions.

(1) The islands are built along volcanic fissures and are characterized by central anomalies of about 60 mgal amplitude and maximum gravity gradient 5.5 mgal/km.

(2) The volcanic fissures arise in an area of crustal tension caused by a change in direction of the ridge axis and are aligned along an east-west fracture zone which is the basis of the Azores-Gibraltar Ridge.

(3) The islands are isostatically compensated to some extent and it is suggested that this compensation is provided by partially fused mantle material which underlies the crust and which is the magma source for the archipelago.

(4) All the data acquired are consistent with current theories of crustal spreading.

CHAPTER 6

GRAVITY SURVEYS OF SOME OF THE CANARY ISLANDS

6.1 Introduction.

Following the gravity surveys on the Azores Archipelago and Ascension Island it was decided to investigate other oceanic island groups well removed from the Mid-Atlantic Ridge so that comparisons might be drawn and any distinctive differences or similarities be noted. Accordingly, in June 1965 reconnaissance gravity surveys were made of four of the Canary Islands, viz. Lanzarote, Gran Canaria, Tenerife and Hierro. The almost unique position of the Canary Islands, strung out in a line from the continental slope to the ocean floor also raised questions which it was hoped these surveys might go some way to answering. (1) Are these islands truly oceanic, are they continental fragments (Hausen, 1959) or were they some admixture of the two? (2) If they are oceanic in character, what is the reason for their presence in an otherwise uniform continental slope?

6.1.2 Base Stations used and Established. Although the Spanish Insititio de Geografia y Cadastral had already established base stations on each of the Canary Islands,

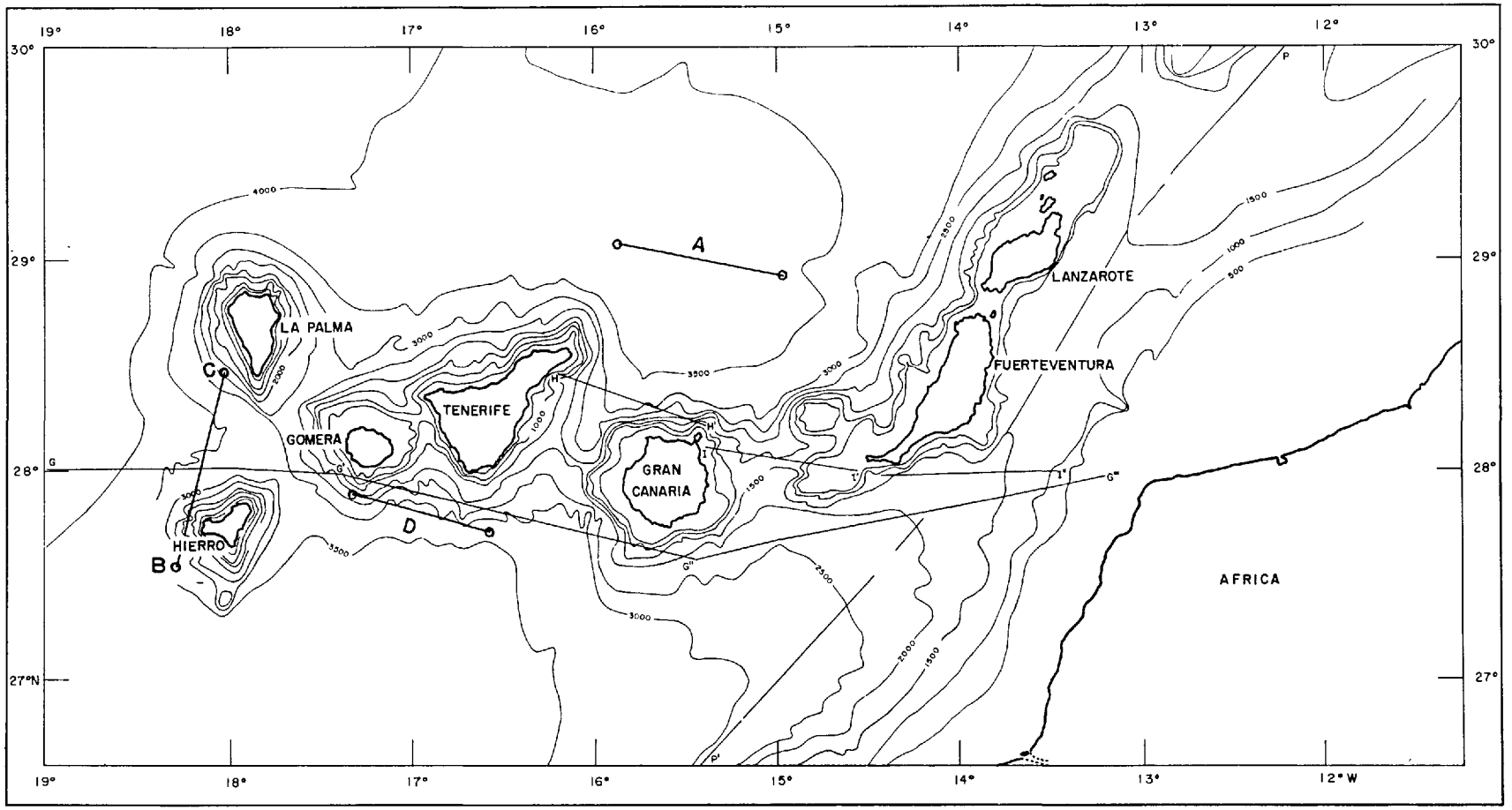

FIG. 6.1. CANARY ISLANDS. BATHYMETRY by E Bosshard from collected soundings Contour interval 500 metres.

——— marine gravity track

o——o seismic refraction profiles (Dash and Bosshard, 1968)

their exact locations were not known to the author at the time of the survey. It was therefore necessary to set up a new chain of base stations which was tied to the European Gravity Network through Madrid on the outward journey and Lisbon on the return journey.

In Madrid, the base used was the major gravimeter base in the Instituto Geografico y Cadastral building where the value was taken as 979970.2 mgal. The Lisbon base was the Airport Terminal Station (Martins and Morelli, 1962) the value of which was obtained by combining the value of 980090.69 mgal for the E.G.N.I. Lisbon station and the Martins and Morelli value of -11.39 mgal for the difference between this station and the Airport Terminal to give 980079.3 mgal.

The observed gravity difference between London Airport and Madrid Airport and between Lisbon Airport and London Airport was in error by 0.3 and 0.4 mgal respectively. This error of only 1 part in 3500 was not considered enough to justify altering the calibration constant of the gravimeter.

When Gran Canaria Airport was connected to these two stations the gravity values obtained were

(1) Madrid → Gran Canaria g = 979377.0 mgal

(2) Gran Canaria → Lisbon g = 979377.6 mgal

The difference is attributed to the temperature drift of the gravimeter and as no reason existed for discriminating

between the two ties, the mean value of 979377.3 mgal was adopted for the primary base in the Canary Islands from which all the other base values were calculated.

None of the base stations established by the I.G.C. was reoccupied exactly, but by chance five of the new stations were quite close to I.G.C. bases. For these five stations the I.G.C. values are from 0.9 to 1.3 mgal higher than the present values. On this evidence the primary base values may be in error by 1 mgal but an error of this magnitude does not in any way affect the validity of the present surveys.

The descriptions and gravity values of the base stations used and established in the course of the surveys are given in the following list and the interconnections are shown in Fig. 6.2.

Previously Established Gravity Bases.

London, Heathrow Airport (Woollard and Rose, 1963)

On the street side of the Terminal at the foot of Channel 9 down-escalator.

51°28'N, 00°27'W; 74 feet; 981200.3 mgal

Madrid, Instituto Geográfico y Cadastral

By the plaque on the floor of the gravity room Number 61 in the basement of the main building

979970.3 mgal

Lisbon, Airport Terminal Station (Martins and Morelli, 1962)

At the entrance of the Terminal building for arriving

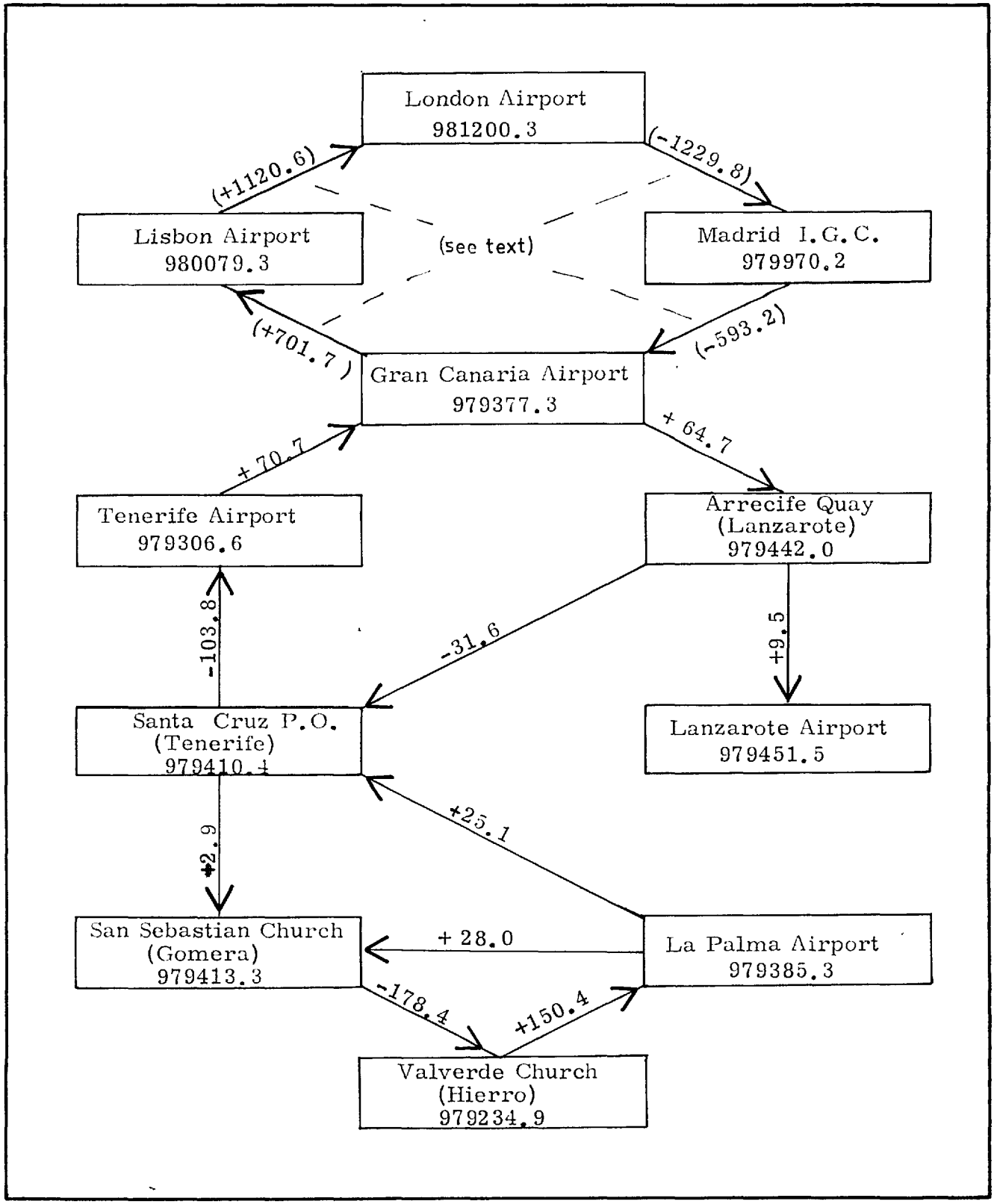

Fig. 6.2. Gravity Base Interconnections, Canary Islands

passengers, by the brass plate on the step which runs along the western face, i,e, the runway side, of the building in front of the column dividing the two doors.

38°46'N, 9°07.7'W; 361 feet; 980079.3 mgal

New Gravity Bases.

Gran Canaria, Gando Airport.

In the Terminal building, in the Cash Exchange hall to the right of the main entrance, between two doors on the airfield side wall.

27°56'22"N, 15°23'07"W; 22 metres; 979377.3 mgal

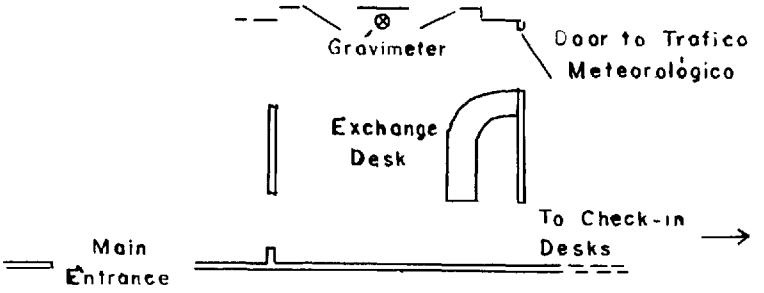

Tenerife, Los Rodeos Airport.

In the Terminal building, on the runway level, in the corridor marked 'Jefe de Aeropuerto' leading from the waiting room.

28°28.8'N, 16°20.3'W; 630 metres; 979306.6 mgal

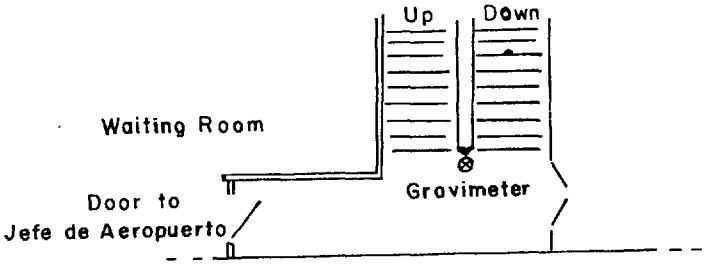

Tenerife, Santa Cruz Post Office

Inside the Post Office vestibule, in the corner immediately to the right of the door.

28°27'29"N, 16°14'16"W; 6 metres; 979410.4 mgal

Lanzarote, Guasimeta Airport

In the Terminal building waiting room in the corner by the telephone booth.

27°57.0'N, 13°36.5'W; 38 metres; 979451.5 mgal

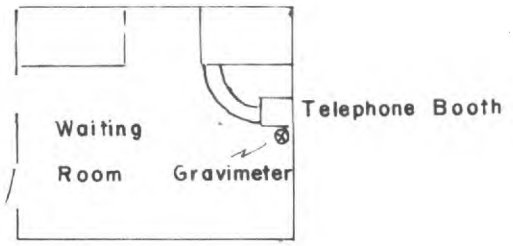

Lanzarote, Arrecife Harbour

By the landward door of the DISA building on the wharf.

28°57.9'N, 13°31.8'W; 4 metres; 979442.0 mgal

Gomera, San Sebastian Church

Asuncion Church, in the near corner of the buttress to the left of the main door.

28°04'59"N, 17°16'05"W; 20 metres; 979413.3 mgal

Hierro, Valverde Church

On the left hand end of the stone ledge to the right of the church door.

27°48'23", 17°54'47'W; 571 metres; 979234.9 mgal

La Palma, Buenavista Airport

Outside the Terminal building to the right of the entrance to the waiting room.

28°40'N, 17°47'W; 385 metres; 979385.3 mgal

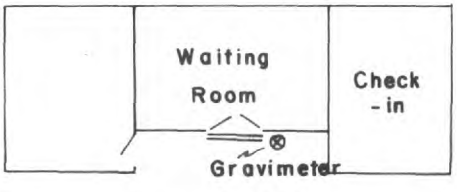

6.1.3 General Geology. The Canary Archipelago (Fig. 6.1) comprised of seven major and five minor islands totalling 7545 km^2 in area, forms a great half circle open to the north with its eastern end some 100 km from the coast of Morocco and its western end projecting 500 km into the Atlantic. The five western islands are great volcanic peaks which coalesce to form a broad east-west ridge rising from a depth of 3500 m. The two eastern islands of Lanzarote and Fuerteventura lie on a NNE-SSW trending shallow platform on the upper continental rise and are separated from the African mainland by a trench no more than 1250 m deep.

Hausen has published general accounts of the geology of Tenerife (1965), Fuerteventura (1958), Lanzarote (1959) and Gran Canaria (1962), and shorter reports on Gomera (1965) and Hierro (1964) in which he also summarises the contributions of previous workers in the region. Most of the following outline of the island geology is abstracted from these papers.

The islands all consist of great piles of mainly basaltic lavas and pyroclastics with minor intrusives and, with the exception of Gomera, are characterized by adventive cones with recent and sometimes historic lava flows. The only sedimentary materials of non-volcanic origin other than surficial deposits are a fringe of coastal limestone around Gran Canaria and a 30 m thickness of probably lacustrine

limestone which is found intercalated into a mighty pile of basaltic lavas on Lanzarote. The oldest formation in the archipelago consists of a mighty spilitic complex, with ultrabasic and other intrusives, which is found beneath a marked unconformity in Fuerteventura, Gran Canaria, Gomera and La Palma.

Igneous rock types are in the range tholeiite-basalt-trachyte-phonolite-rhyolite with basalts predominating.

While no accurate dating has been performed on the spilitic 'basement complex' which Hausen (1959) has suggested might owe its deformation to Hercynian orogenic activity, radiometric K-Ar dating in conjunction with palaeomagnetic studies (Abdel-Monem et al, 1967) tentatively places the maximum age of the lavas found above the major unconformity at 16 MY. The lavas were found on Gran Canaria but similar volcanic sequences on islands as far apart as Lanzarote and Gomera have also been dated as at least 12 MY old. Volcanic activity has continued intermittently from that date to the present day.

The main fault and fissure lines trend NNW-SSE and NE-SW and are conformable with the trends of the adjacent African continent. Several authors have suggested a genetic relationship between the Canary Islands and the extensive tectonic activity of the Atlas Mountain region (Hausen, 1959). Hausen (1962) has proposed the hypothesis that the islands

represent the remnants of an old headland of the African continent. Recent work on Lanzarote (Tinkler, 1966) found little evidence however, of the tectonic instability which this would seem to imply.

6.1.4 Other Geophysical Data in the Area. In the summer of 1967, members of the Department of Geophysics, Imperial College, on board F.S.S. Meteor carried out seismic refraction studies in the Canary region. The preliminary results are used here by courtesy of Dr. B.P. Dash and E. Bosshard. The Station positions are indicated in Fig. 6.1 and the data obtained as follows.

Seismic Refraction Results after Dash and Bosshard (1968)

Profile	Velocity km/sec Crustal layers 1	2	3	4	Man-tle	km Water Depth	Thicknesses/km Crustal layers 1	2	3	4
A	3.3	4.4	6.1	7.0	7.7	3.52	2.09	2.57	3.32	3.21
B	3.3	4.7	5.7	6.45	8.1	2.21	2.34	1.36	3.17	2.20
C						3.09	1.79	2.70	1.11	2.75
D	3.35	4.3	6.15	7.3	8.2	2.96	2.31	2.92	1.13	5.28

The depth to the Moho of 15 km to the north and south of Tenerife and of 11.3 km to the west of Hierro suggests that the crust is thinning towards the ocean basin. Of the low-velocity layers, layer 1 is probably composed of sediment and volcanic debris and layer 2 is probably pillow basaltic lava.

There are also several continuous marine gravity tracks in the area. The tracks GG', HH', and II' shown in Fig. 6.1

are gravity measurements carried out by the Geodetic Institute of the Delft Technological University on board Hr. Neth. Ms. Snellius during the Navado III programme in 1965, and very kindly made available for the present research. Passage data acquired on board H.M.S. Protector is used by courtesy of the Geology Department of the University of Birmingham and is indicated in Fig. 6.1 by the track PP'. The Bouguer anomaly was computed for these profiles by means of the two- and three-dimensional correction programs discussed in Chapter 2 and is presented in Fig. 6.3 and 6.4.

The bathymetry around the archipelago is drawn from collected soundings on the National Hydrographic Office 1:1,000,000 plotting sheet No. 104 supplemented by soundings obtained by F.S.S. Meteor in 1967, and from Admiralty Charts Nos. 1869 and 1870.

6.2 A Gravity Survey of Lanzarote.

6.2.1 Introduction. Lanzarote, 29°0'N, 13°35'W, is the most easterly island of the Canary archipelago and lies on a submarine platform trending NNE-SSW approximately 100 km from the coast of Africa. Its area is 796 km^2 and it has a maximum length of 60 km, a maximum width of 21 km and a maximum elevation of only 671 m. The trend of the island is continued by Fuerteventura in the south and by the small islands of Graciosa and Alegranza in the north to form a

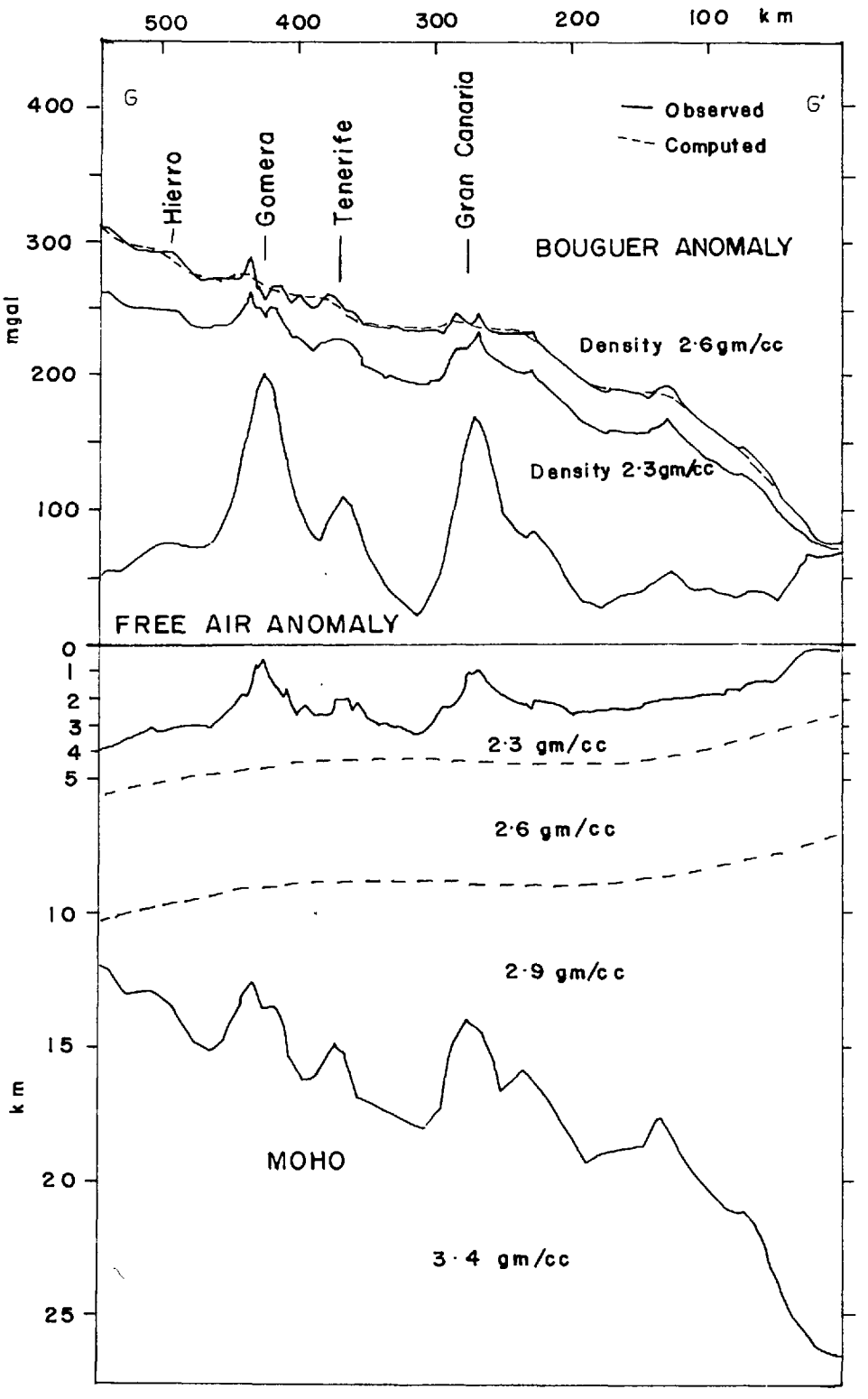

FIG. 6·3. Gravity profile GG′ and possible East-West structure across the Canary Islands. (see Fig. 6.1)

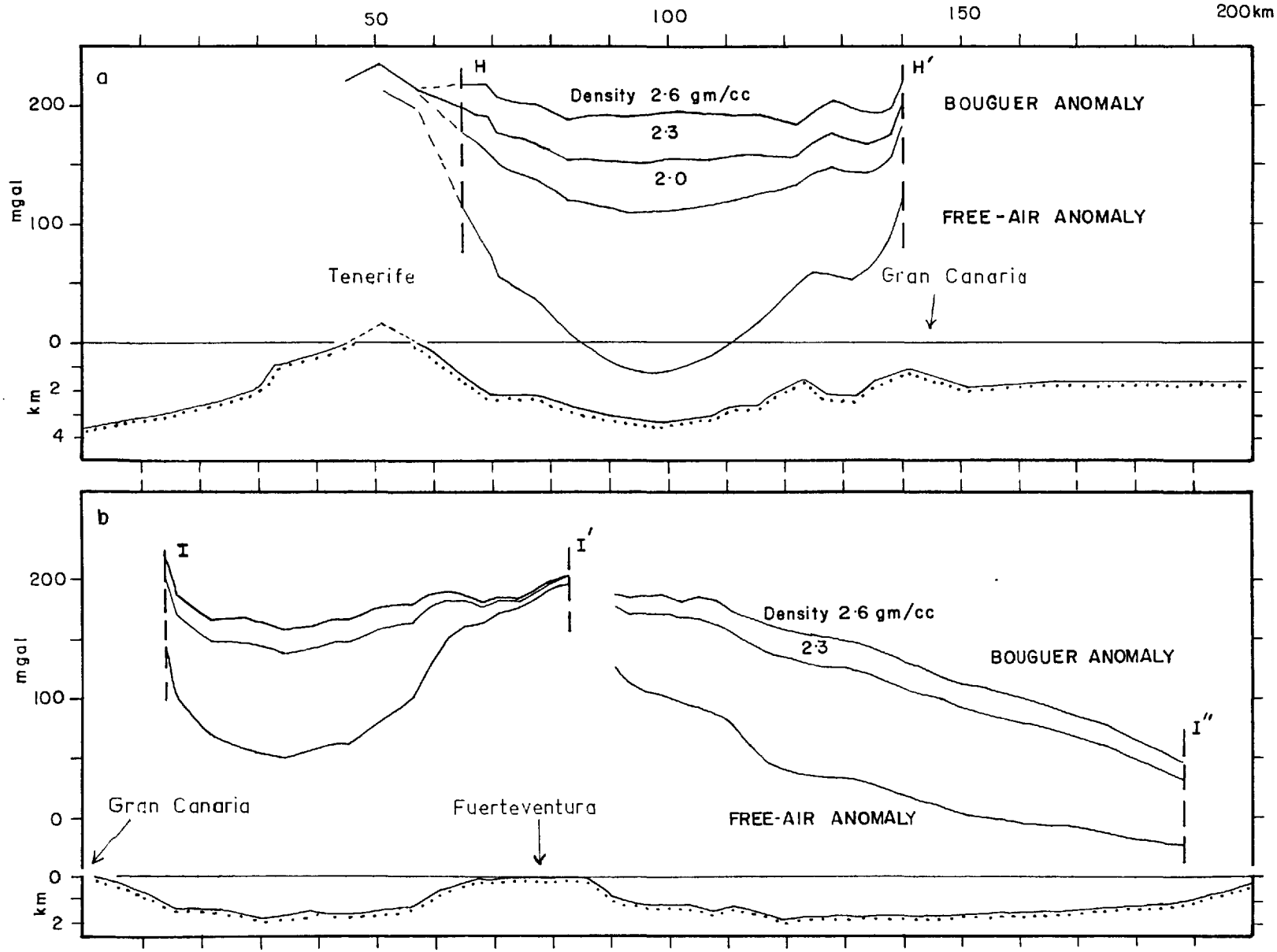

FIG. 6·4. Short free-air and Bouguer anomaly profiles in the Canary Islands. a. Marine gravity track HH'. b. Marine gravity track II'I''.

large submarine platform, 250 km in length, parallel to the trend of the African continental shelf. A relatively shallow trench, 1250 m deep, separates this platform from the continent but towards the Atlantic the island slopes steeply down to 3400 m with gradients of 1 in 10.

6.2.2 General Geology. The outstanding features are two older dissected upland areas in the north and south, separated by a broad lower-lying region where most of the later volcanic activity has occurred. These uplands are composed of sheets of olivine basalts, flows, tuffs and agglomerates and comprise the table-land series (Hausen, 1959), which Hausen considers to have covered the entire island at one time but to have since been faulted to form the tectonic graben structure of the lower central portion of the island. This central portion is occupied by later olivine-basaltic lavas and cones aligned along ENE-WSW trends and it is in this belt that the historic volcanic activity has taken place. The rocks on the island are throughout of a monotonously olivine-basalt composition.

Several raised beaches can be seen, at levels of 55, 35, 25, 15, 6 and 1 m and have been attributed to Quaternary eustatic changes in sea-level (Tinkler, 1966). On the basis of the continuity of these raised beaches around the island, Tinkler argues that the island must be a region of tectonic stability and attributes the form of the island to regional

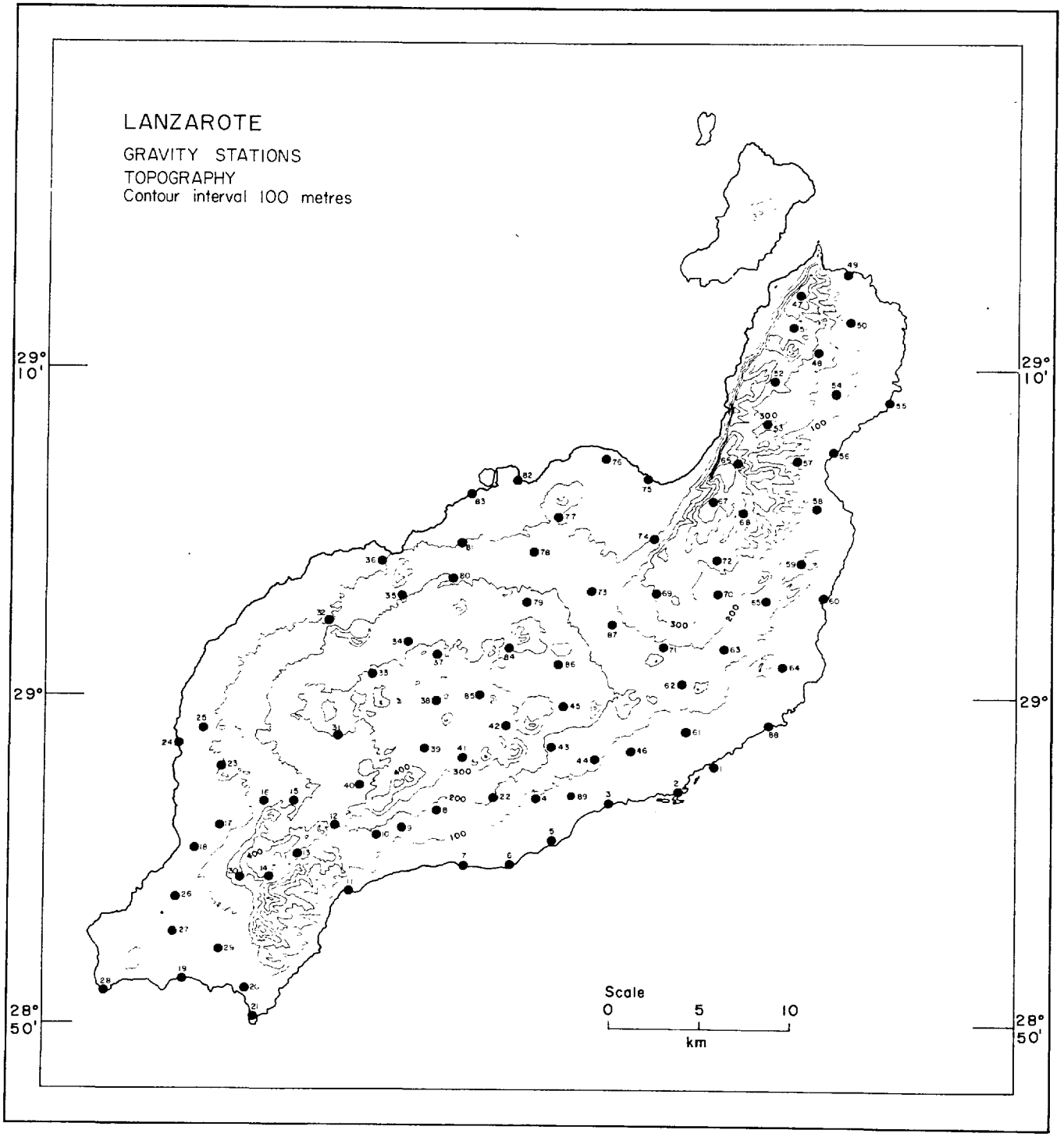
LANZAROTE
GRAVITY STATIONS
TOPOGRAPHY
Contour interval 100 metres
29° 10'
29°
28° 50'
Scale
0 5 10
km

FIG. 6.5.

inequality of the eruptions which formed the 'tableland' series, and the steep escarpments of the north and south uplands to long continued marine erosion from the west.

The island is still volcanically active, the last recorded eruption being in 1824. K-Ar dating of the tableland series (Abdel-Monem et al, 1967) suggests that this region has been intermittently active since at least 12 MY ago.

6.2.3 Details of the Survey. Field operations and data reduction were carried out as described in Chapter 2. Stations were located to within 40 m using the 1949-56, 1:25,000 military map of the island. Elevations were taken from the same map, which was contoured at 10 m intervals, or by reference to sea-level at coastal stations. Terrain corrections were calculated by computer as described in Chapter 2; topographic contours at 100 m intervals were approximated by polygons from the 1:100,000 map of the island. Bathymetric contours were obtained from a slightly revised version of the National Hydrographic Office 1:1,000,000 plotting sheet No. 104 as contoured by A.S. Laughton and D.G. Roberts of the National Institute of Oceanography.

The elevations are accurate to $\pm$ 10 m, which corresponds to an error of $\pm$ 2 mgal in the Bouguer anomaly. Errors in terrain correction contribute a further $\pm$ 2 mgal. Inaccuracies due to mislocation of stations, to assuming linear drift

and to neglecting tidal effects are much smaller and are neglected. The Bouguer anomaly values are therefore accurate to ± 4 mgal.

6.2.4 Regional Anomaly. The island is situated on the upper continental slope about 90 - 100 km distant from the edge of the continental shelf so that the main regional trend in the gravity field is the change associated with the transition from continental to oceanic crust. Profile GG' (Fig 6.3) crosses the continental slope and shows this change admirably. A possible crustal structure section has been calculated in the manner described in Chapter 2 to conform to the gravity profile and the seismic refraction data of Dash and Bosshard (1968), and is also shown in Fig. 6.3. For the sake of simplicity the 4.5 and 6.0 km/sec layers have been considered as one layer of density 2.6 gm/cc and thickness 4.6 km. Densities of 2.3 gm/cc and 2.9 gm/cc respectively are ascribed to the 3.3 km/sec and 7.0 km/sec layers from the velocity-density curves of Nafe and Drake (1963). The value used for the thickness of the 3.3 km/sec layer is 2.1 km, which is the mean from the seismic refraction results. The computed depth to the mantle increases from a depth of 12 km west of Hierro to almost 27 km under the continental shelf. The short wavelength variations in the depth to the Moho are considered not to be real but to be the expression of much shoaler

crustal structures. Thus the trend of the Moho may be as indicated, but the interface is likely to be rather smoother.

A small gravity high can be seen on the free-air and Bouguer anomaly curves of profile GG' at a distance of 125 km from its eastern end. When the profile is projected perpendicular to the trend of the continental shelf this feature is almost exactly the same distance from the continental shelf break as is Lanzarote, suggesting that the SSW trend of the Lanzarote-Fuerteventura platform is continued southwards beyond its apparent end at 28^{o} latitude.

There is clearly a strong gravity gradient over this part of the continental slope, most probably acting perpendicular to the trend of the continental shelf. Its value cannot be accurately assessed from the GG' profile because of the above-mentioned anomaly but must be between 0.6 and 1.0 mgal/km. The calculated depth to the mantle under the gravity high is between 17 and 19 km and with a density of 2.4 gm/cc for the Bouguer corrections the Bouguer anomaly is 125 mgal.

Another marine gravity profile, PP' (for position see Fig. 6.1) passes between Lanzarote and the African mainland, roughly parallel to the trend of the island and some 30 km from it. There is a marked free-air anomaly minimum of 20 mgal amplitude opposite Lanzarote and, as the sea-floor is fairly level along this part of the profile, the same

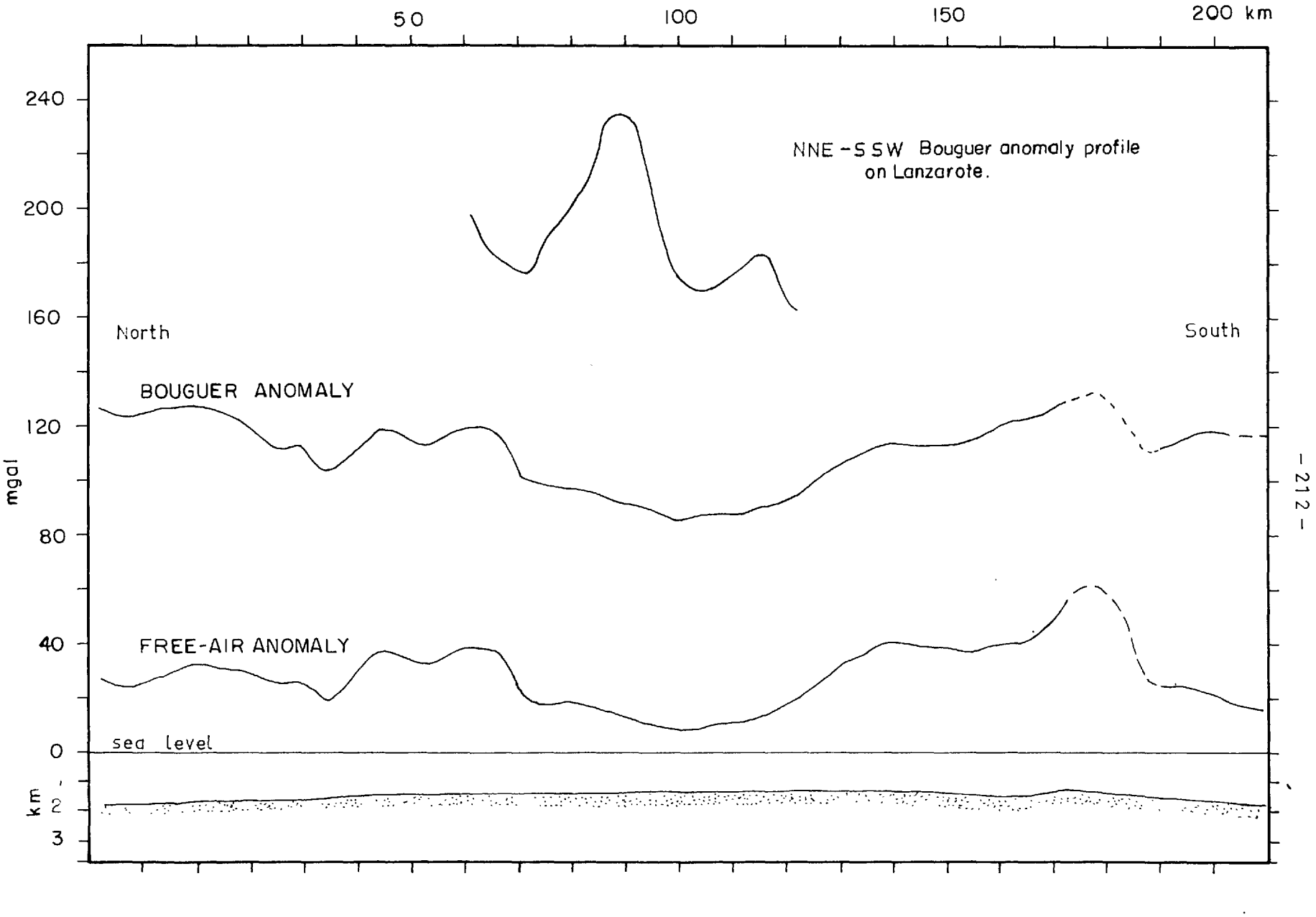

FIG. 6.6. Marine gravity profile PP′ between the Lanzarote-Fuerteventura platform and the African mainland.

minimum appears in the Bouguer anomaly. The section of the PP' profile opposite the Lanzarote-Fuerteventura platform is drawn on a larger scale in Fig. 6.6 together with the NNE-SSW gravity section on Lanzarote, (Fig. 6.7) projected onto PP' perpendicular to the main trend of the island.

The sharp decrease in the Bouguer anomaly at 70 km coincides with a slope reversal in the island gravity field. The topography and geology of the island suggest that the central part of the island has been downfaulted between the uplands in the north and south to form a graben structure (Hausen, 1959) and it is probable that the steep slope in the marine gravity anomaly represents the northern margin of the seaward extension of this graben. The flatness of the bathymetry along the profile at this point may indicate a fairly thick layer of sediment which would explain the absence of any bathymetric expression of the graben. The low anomaly belt on the island lies across the middle of the northern uplands and while there is a pronounced col at this point, it is about 8 km north of the more obvious graben border. Detailed geological work may indicate a fault at this point but this location suggests that the graben of the low Bouguer anomaly may be formed by reverse faulting.

No sharp increase in the Bouguer anomaly is observed at the southern margin of the suggested graben. Instead it coincides with the minimum gravity anomaly value in this

part of the PP' profile. This may be a result of lateral displacement which has taken place along the graben margin. This lateral movement is inferred on two grounds. Firstly, the NNE trending scarp visible in the northern uplands, appears to have been displaced 15 - 20 km westwards in the south of the island; and secondly, the areas of high Bouguer anomaly which extend along the NNE-SSW trend of the Lanzarote-Fuerteventura platform are similarly displaced south of a belt of low Bouguer anomaly which crosses the island at this point. A gravity gradient of between 0.6 and 1.0 mgal/km was deduced from the GG' profile and attributed to thinning of the crust towards the ocean. If then a right-lateral displacement has taken place, to the south of the fault the crust will be relatively thicker and the gravity field less than to the north so tending to cancel the increase in gravity at the edge of the horst block.

Other features of the PP' gravity profile coincide with the ends of the Lanzarote-Fuerteventura platform and with the northern end of Lanzarote. Regrettably, there is a gap in the marine gravity data at the southern edge of the platform but clearly the latter represents a distinct structural feature. The features on the gravity profile are interpreted as being the expression of tectonic structures, though it is impossible to say if any lateral movement has occurred. It is possible that a ENE-WSW striking drop-fault forms the

southern end of the Lanzarote-Fuerteventura platform and such a possibility is consistent with the apparent continuation of the island trend observed on profile GG'. However, with the present data, such suggestions remain highly speculative.

Hausen (1962) has expressed the possibility that the Canary Islands are the remnants of a "Pre-Canarian basalt-covered headland of the sial block of Africa", and while there is evidence of considerable tectonic activity in this area, the observed gravity values make such an origin for the islands appear unlikely. In profile GG' the Bouguer anomaly increases from a fairly typical continental value of 25 mgal over the continental shelf to over 250 mgal west of Hierro. In the computed crustal section the depth to the Moho decreases from a depth of 26 km under the continental shelf to 12 km at the western end of the section.

If the archipelago was a fractured headland, a presumably down-faulted portion such as the trench between Lanzarote and Africa, would be underlain by a continental thickness of crust and the Bouguer anomaly would, because of the downfaulting, have a value lower than that over the continental shelf.

In fact, the Bouguer anomaly computed from the Protector profile averages 96 mgal opposite Lanzarote, which on the GG' crustal section would imply a crustal thickness at least 5 km less than under the continental shelf.

The possibility that the islands of Lanzarote and Fuerteventura represent continental fragments separated from the African mainland must also be considered. Again, the Bouguer anomaly values argue against such an origin for the islands. Combining the Bouguer anomaly observed on the Protector track 30 km east of the island and the gradient of 0.8 mgal/km observed on the GG' profile, an estimate of approximately 120 mgal is obtained for the background gravity field over the island. Again, from the GG' section, this gravity value implies a crustal thickness of some 19 km, clearly not a typical continental thickness for the crust. The assumption of a gravity gradient similar to that observed on the GG' profile is consistent with the Bouguer anomaly on the island and it is unlikely that the regional anomaly is less than 100 mgal over the island. If the background field did have a continental value of approximately 25 mgal, the resulting amplitude of the island anomaly is over 200 mgal which though not impossible is quite unprecedented.

The regional gravity data available are insufficient to warrant any consideration of isostatic equilibrium.

6.2.5 Local Anomaly. The topography of the island and the distribution of gravity stations are shown in Fig. 6.5, and the Bouguer anomaly values and contours in Fig. 6.7. The dominating feature in the Bouguer anomaly map is the gravity high which occupies a position in the centre of the island

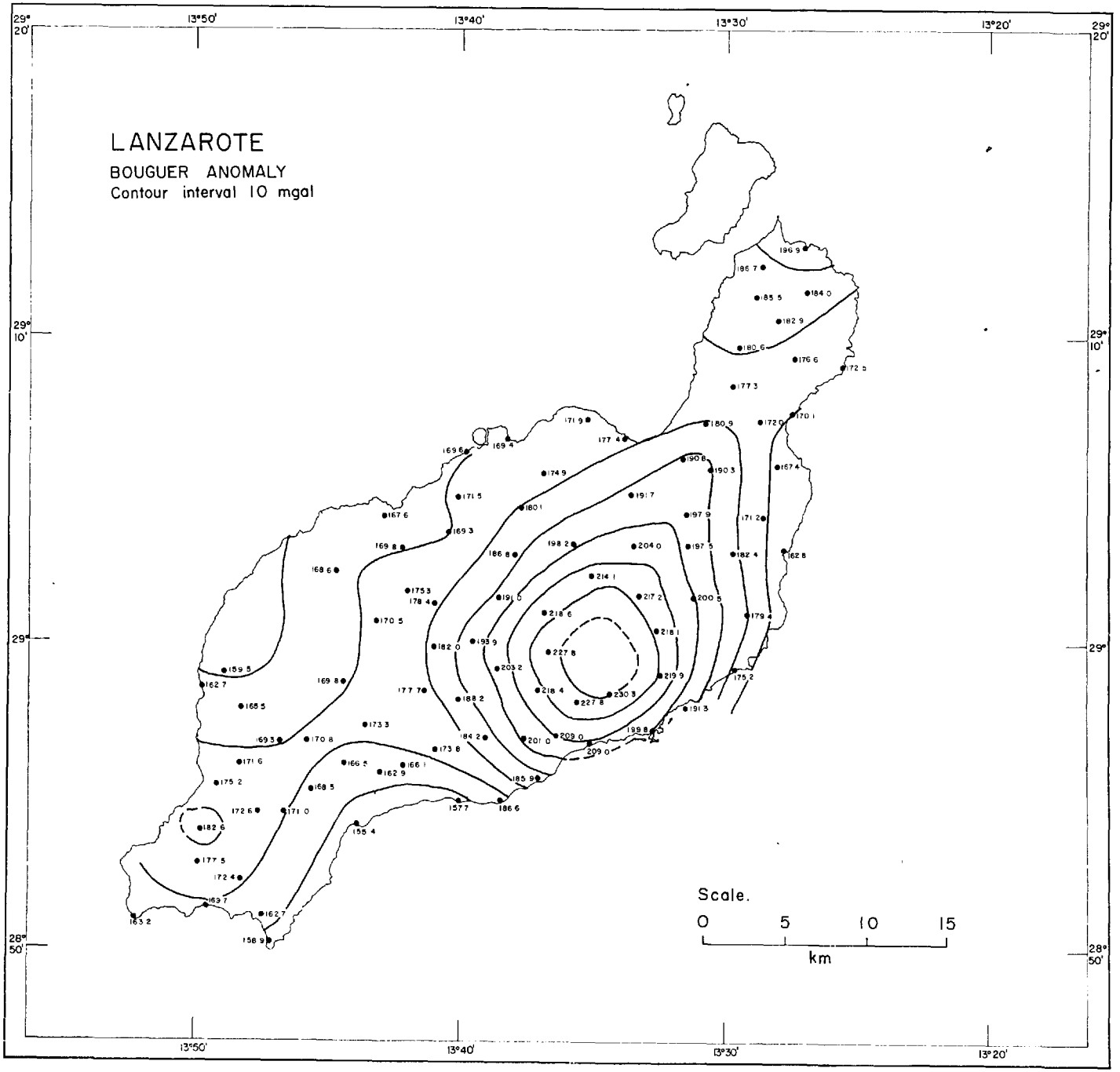
LANZAROTE
BOUGUER ANOMALY
Contour interval 10 mgal
29° 20'
13°50'
13°40'
13°30'
13°20'
29° 10'
29°
28° 50'
Scale.
0 5 10 15
km

FIG. 6.7.

quite near the only cone of the tableland series (Hausen, 1959) preserved in the central graben. It is centred in line with the NNE-SSW trending scarp of the northern uplands and it may be that this volcanic centre has arisen in an area of weak crust created at the intersection of two fault systems, namely the NNE-SSW faults which caused the north scarp and the NW-SE faults of the graben. This gravity high is interpreted as being the main volcanic centre in the island, and its elongations towards the northern and southern uplands as the results of extension of volcanic activity along a NNE-SSW rift zone.

The gravity features shown on the PP' profile can be expected to have a considerable influence on the Bouguer anomaly on the island and Fig. 6.8 shows a NNE-SSW gravity profile across the island after the removal of a regional field consisting of the PP' profile in Fig. 6.6 increased by 25 mgal to account for the WNW-ESE gravity gradient across the island. The amplitude of the resulting anomaly is 118 mgal and its half-width is approximately 25 km. Two smaller maxima can be seen to the north and south of the main anomaly. These may represent smaller volcanic centres in the north and south of the island but they may also be a result of a larger throw of the graben on the island than at the point where H.M.S. Protector passed. The amplitude of the main anomaly is very similar to the anomaly over the summit

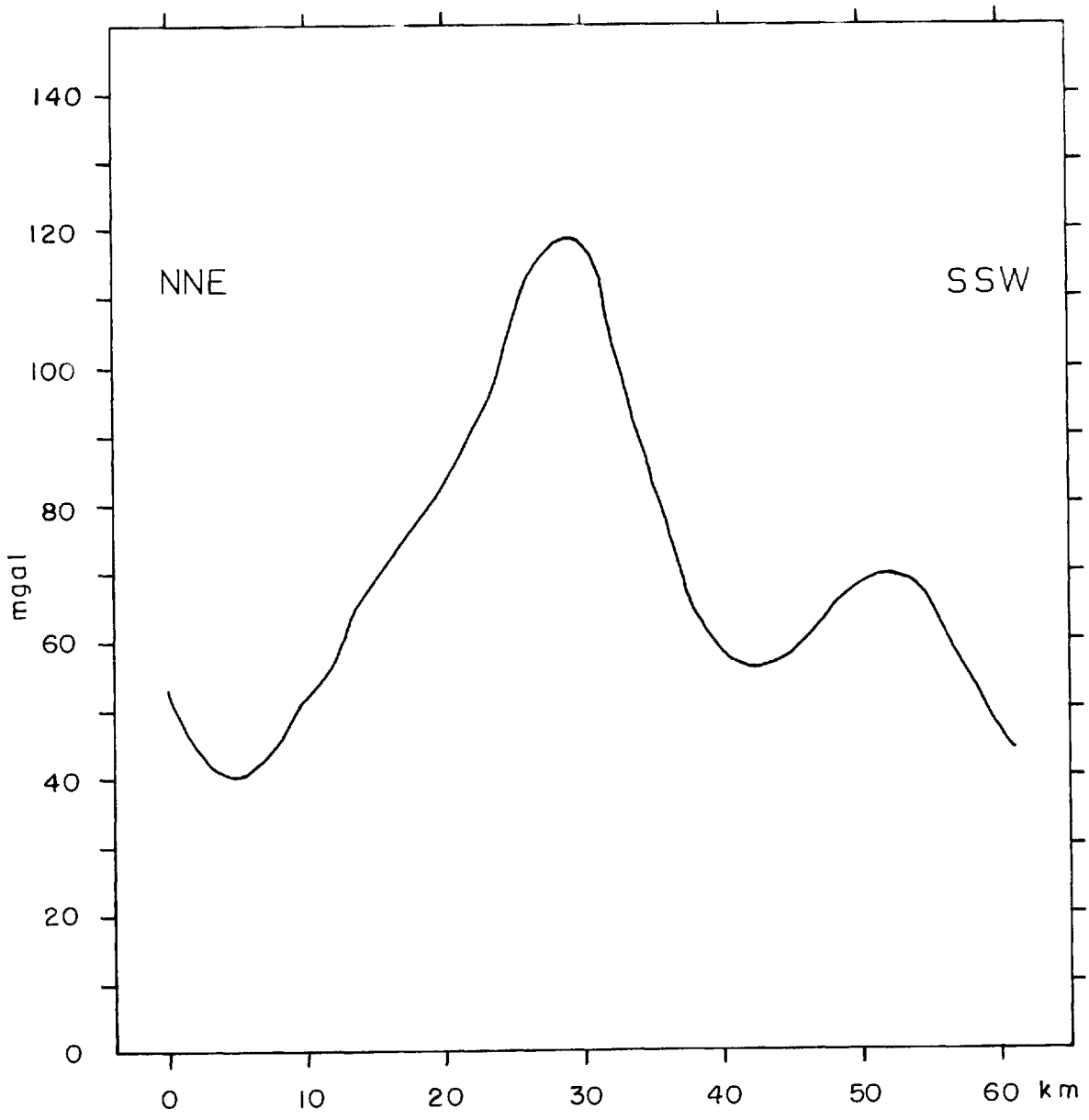

FIG. 6·8. NNE—SSW gravity section on Lanzarote with the regional field removed.

caldera on Tenerife (Fig. 6.12) and it can reasonably be assumed that the volcanic centre which the Lanzarote anomaly is taken to represent, at one time built up a major cone with ridges along the NNE-SSW rift zone similar to the topographic structure now visible on Tenerife (Fig. 6.11). On Lanzarote, only the ridges remain as horst blocks, the central cone having subsided between them and been covered by younger volcanic material. The topographic gradients around the summit cone of Tenerife suggest that such a cone on Lanzarote may have stood over 2,000 m above the present level, so that the vertical movement of the graben on the island may be quite considerable, certainly greater than the 500 m which is enough to account for the anomaly observed on the PP' profile. In fact it would require a throw of some 1,000 m to reverse the anomalies observed over the northern and southern uplands.

Other features of the local field, such as the westward displacement of the anomaly contours associated with the rift zone on the south, have already been mentioned in the regional field section.

The recent volcanism has taken place in a broad low-lying area in the west of the island. In the gravity map this is represented by an area of low relief with a gravity nose extending westward from the main anomaly. This suggests that

the more recent volcanism is moving to the west, probably along the NW-SE lines of crustal weakness.

6.3 A Gravity Survey of Gran Canaria.

6.3.1 Introduction. Gran Canaria is a great shield volcano situated 250 km from the African continent at 27°55'N, 15°35'W. It measures approximately 46 km in diameter and has a total area of about 1500 km^2. The maximum elevation on the island is 1950 m and below sea-level the island slopes down to depths of 3600 m in the north and south. In the east and west, Gran Canaria is connected to Fuerteventura and Tenerife respectively by narrow ridges with depths of less than 1500 m. Except in the north, the island is surrounded by a broad shallow marine terrace.

6.3.2 General Geology. The island represents a huge pile of volcanic strata accumulated on a basement which is also volcanic. The island is characterized by fairly mature erosion topography and the basaltic tableland series of Hausen (1962), which is the oldest series so far dated by radiometric methods, has been estimated as being between 12 and 16 MY old (Abdel-Monem et al, 1967). This series is found chiefly in the cliffs along the north-west coast and appears to have originated from some great shield volcano to the west of the present coastline (Hausen, 1962).

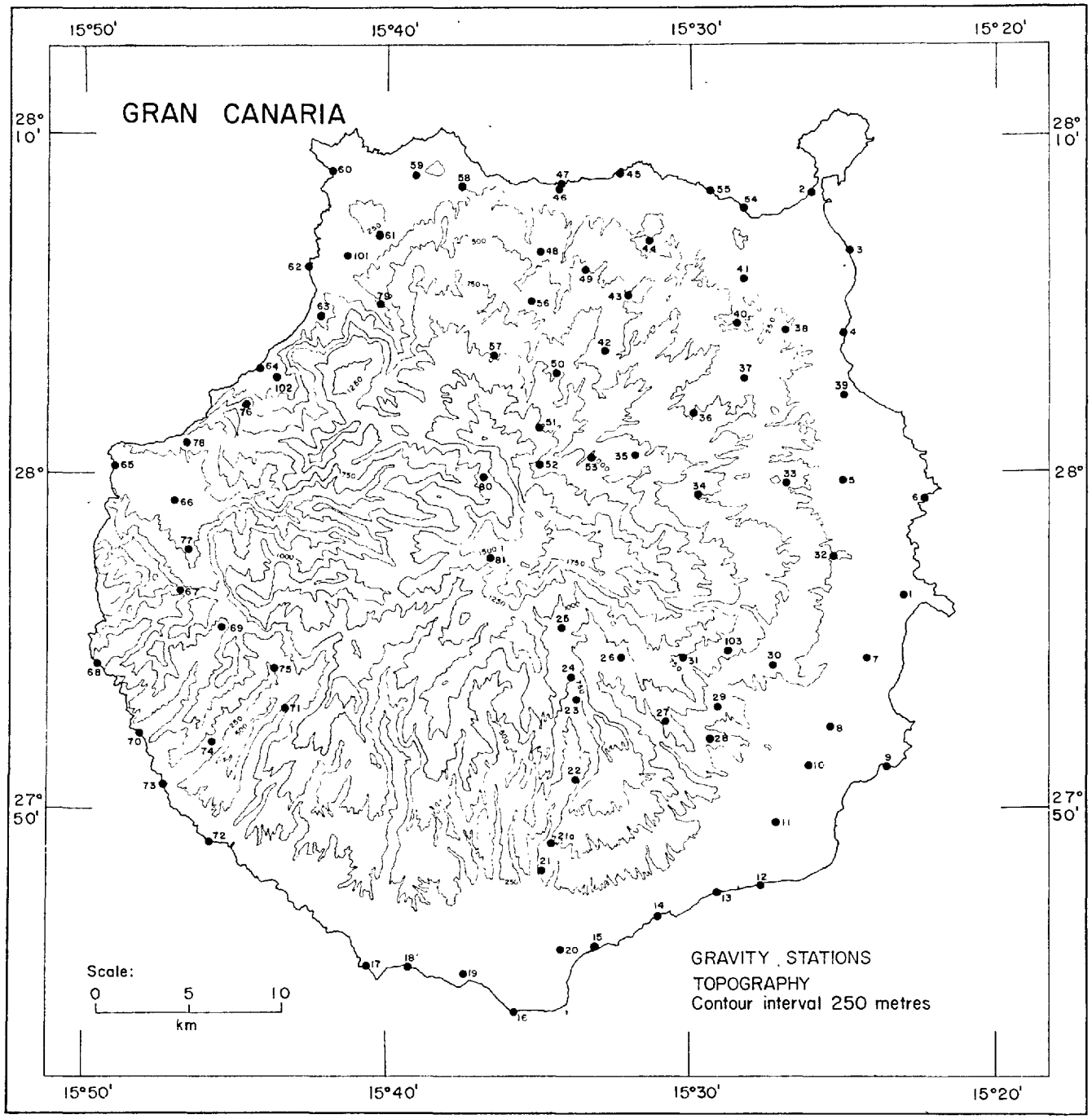
GRAN CANARIA
15°50'
15°40'
15°30'
15°20'
28° 10'
28°
27° 50'
Scale:
0 5 10
km
GRAVITY . STATIONS
TOPOGRAPHY
Contour interval 250 metres

FIG. 6.9

Hausen considers that these basalts are underlain by tilted dislocated trachytic lavas, but this latter formation has been reinterpreted by Schmincke (1967) as a swarm of trachytic dykes forming a concentric conical system within a 20 km diameter caldera in the west centre of the island. By this latter interpretation, the trachytes are much younger than the basalts which Hausen considered to overlie them. Both authors are agreed that the highly explosive salic phase of volcanism which succeeded the basalt sequence, had its centre in the region of this projected caldera. During this salic phase, tuffs, agglomerates and ignimbrites in vast quantities, together with smaller amounts of rhyolite and trachyte lavas were erupted. Schmincke (1967) considers that the caldera was actively subsiding during the emission of the ignimbrites, the total subsidence being at least 1000 m.

This sequence was followed by one of phonolitic lavas and tuffs which built up a great central cone between 9 and 14 MY ago (Abdel-Monem et al, 1967). The exact location of this centre has been obscured by great NW-SE faults which have since ruptured the island, and by floods of younger basaltic lavas which now cover much of the north and east of the island. The central volcano which Schmincke (1967) suggests arose inside the caldera may possibly have been the centre of the phonolitic volcanism, but little is left of

this supposed volcano except for its substructure which is exposed in the central part of the island.

More recent activity has taken the form of floods of basaltic lavas which have erupted in the centre, north and east of the island, beginning in the post-Miocene and continuing to the Present.

6.3.3 Details of Survey. Maps on a scale of 1:25,000 were available for part of the island and gravity stations in the areas covered by these maps were located to within 40 m and their elevations determined to within ± 10 m as on Lanzarote. For the remainder of the island, the 1942, 1:100,000 military map was used. Stations in this area, approximately half of the total number established, could only be located to within 100 m and their elevations had to be determined by altimeter except at coastal stations where reference could be made to sea-level. The error in the elevations determined by altimeter is ± 20 m which corresponds to an error of ± 4 mgal in the Bouguer anomaly. Other errors are negligible in comparison and can be neglected.

Because of the extremely rugged terrain and poor quality of the small-scale map, no attempt was made to calculate the terrain corrections. The contour map presented as Fig. 5.10 is therefore the simple Bouguer anomaly map and while it may be distorted due to topographic effects, the error in the simple Bouguer anomaly values is only ± 4 mgal.

6.3.4 Regional Anomaly. The marine gravity track GG' (Fig. 6.1) passes 15 km to the south of Gran Canaria. It can be seen in Fig. 6.3 that the free-air anomaly changes from small negative values at 30 - 50 km from the island to a large positive value nearer land. As discussed in the case of Ascension Island, this form is typical of an island which has some degree of regional compensation.

The large gravity anomaly practically disappears in the Bouguer anomaly profile. The regional field value of the Bouguer anomaly on Gran Canaria, calculated for a density of 2.4 gm/cc, can be estimated from the GG' and II' profiles and is approximately 160 mgal. There is only a very small east-west gradient of the regional field over the island.

The calculated depth to the Moho in Fig. 6.3 is probably distorted by attributing to irregularities in the Moho anomalies which are due to bodies within the crust. A smoothed and perhaps more realistic configuration of the Moho would have a depth of approximately 17 km to the south of Gran Canaria.

In a compilation of crustal structures at continental margins as deduced from seismic refraction and gravity data, Worzel (1965a) showed that the transition from continental to oceanic crust occurs over a distance of between 50 and 250 km. Gran Canaria lies some 180 km from the African continental shelf, and at such a distance one might expect

a depth to the Moho approaching that of the typical oceanic crust. The increased depth in this case may represent a form of isostatic compensation for Gran Canaria and the other islands. If the compensation is considered to take the form of a shallow depression of the Moho with a diameter of 100 to 200 km, the depth to the Moho under the island can be expected to be slightly greater than the 17 km calculated for the depth at 15 km south of the island.

It can therefore be said that the island is isostatically compensated in some degree but the gravity data available are insufficient to determine whether or not complete equilibrium has been achieved.

6.3.5 Local Anomaly. The island topography and distribution of gravity stations are shown in Fig. 6.9. The Bouguer anomaly values and contours are presented in Fig. 6.10 and show a large SE-NW gravity gradient across the island rising to a centre of high Bouguer anomaly of 276 mgal in the north-west of the island. Superimposed on this gradient in the south-east of the island is a second centre of high anomaly where the Bouguer anomaly reaches 260 mgal.

The distribution of gravity stations around the island nucleus of Hausen (1962) and the caldera of Schmincke (1967) is sparse, but the lack of any evidence for a major gravity anomaly in the area must cast some doubt on the interpretation that it represents the magmatic centre of the island. On the

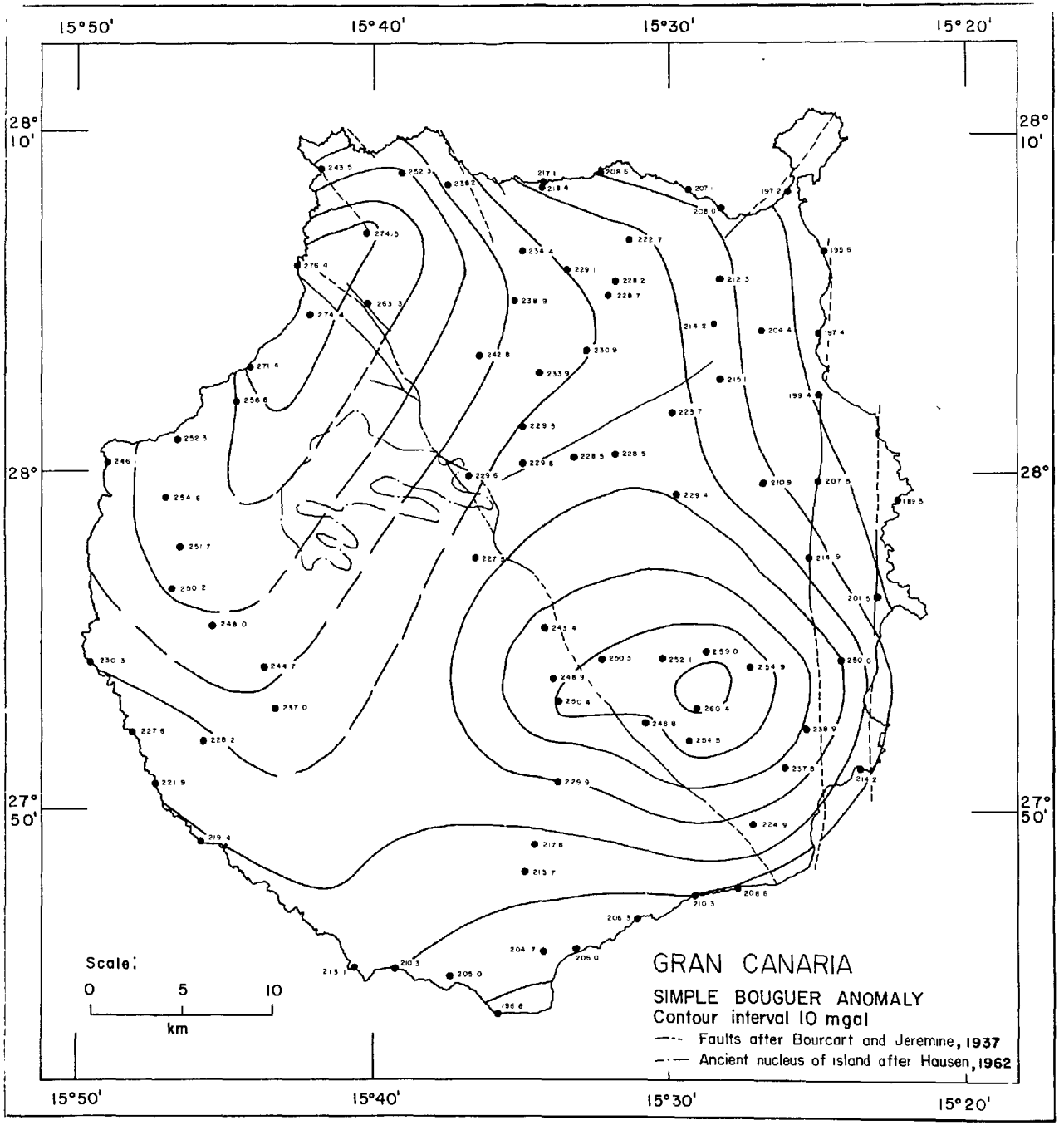
15°50'
15°40'
15°30'
15°20'
28° 10'
28°
27° 50'
Scale:
0 5 10
km
GRAN CANARIA
SIMPLE BOUGUER ANOMALY
Contour interval 10 mgal
Faults after Bourcart and Jeremine, 1937
Ancient nucleus of island after Hausen, 1962

FIG. 6.10.

other hand, the position of the major anomaly strongly supports the suggestion of Hausen (1962) that there was a major magmatic centre off the north-west coast of the island and that the structure associated with this centre has since collapsed into the sea. The shallow bathymetry in this region and the arc of sheer cliffs comprising the north-west coastline are consistent with the subsidence of such a centre.

The anomaly is possibly elongated in the direction of the NE-SW system but this may be due to the distorting effect of the topography and of the faulting in this area.

The real value of the main maximum is uncertain since it may continue to increase seawards, but as the isoanomaly contours appear to be closing, the observed value of 276 mgal is adopted as the maximum value. The amplitude of the anomaly can be estimated using the regional field determined from the marine gravity data, but before the marine and land anomalies can be compared, allowance must be made for the terrain correction of the land anomaly. The terrain correction for station 62 was calculated by manual methods and found to be 11 mgal. The background field of 160 mgal estimated from the marine gravity data then yields an amplitude of approximately 125 mgal for the main anomaly.

The eastern anomaly is much smaller, with steeper gravity gradients, which suggest a shallower depth to the disturbing body. A linear NW-SE gradient of 1.4 mgal/km was

subtracted in an attempt to remove the gravity gradient of the main anomaly. The amplitude and maximum gradient of the resulting anomaly was 72 mgal and 5.9 mgal/km respectively. There is little geological evidence for any major volcanic centre associated with this gravity anomaly but this may represent the centre for the phonolite formation as it is the only area where there is immediate superposition of the phonolites on the old weathered basalts (Hausen, 1962).

6.4 A Gravity Survey of Tenerife.

6.4.1 Introduction. At 28°15'N, 16°35'W, Tenerife is situated in the centre of the Canary chain of islands. It is also the largest, with an area of 2058 km^2 and the maximum elevation of 3718 m is almost twice as high as any other island in the archipelago. The island slopes fairly uniformly from this height down to sea-level and the slopes are continued in the bathymetry down to depths of 3700 m in the north and south. In the south-east it is connected to Gran Canaria by a narrow ridge at a depth of less than 1500 m and in the south-west it is separated from Gomera by depths of less than 1000 m.

6.4.2 General Geology. Tenerife is an immense volcanic structure of the central type resting on a much older base which is also volcanic. The base series can be seen in the north-east and west peninsulas, both of which are

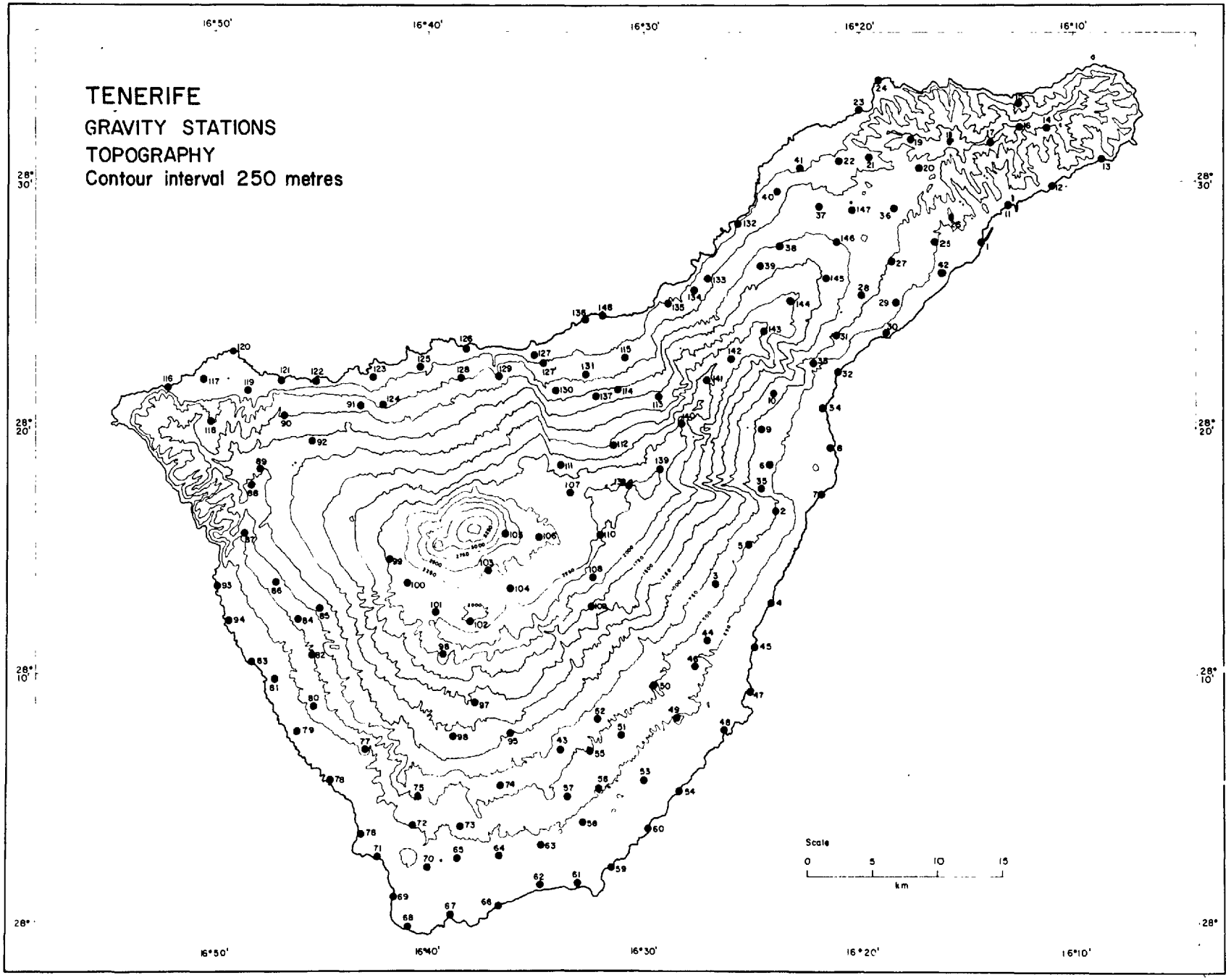
TENERIFE
GRAVITY STATIONS
TOPOGRAPHY
Contour interval 250 metres
16°50'
16°40'
16°30'
16°20'
16°10'
28° 30'
28° 20'
28° 10'
28°
Scale
0 5 10 15
km

FIG. 6.11.

characterized by mature erosion topography in marked contrast to the rest of the island. The base consists of massive piles of basaltic lavas, tuffs and agglomerates, mainly of the alkali-basaltic type, which Hausen (1956) suggests have been erupted along NNE-SSW fissures. Hausen (1956) also suggests that this series may be roughly contemporaneous with the rocks on Gomera.

After a period of quiescence, great eruptions of the central type commenced and built up the massive cone which now dominates the archipelago. The early phases of this eruption were of a salic character, succeeded in turn by olivine basalts and alkali basalts and terminating in pumice showers and great mud flows.

The summit of the central volcano is marked by a peak 3718 m high, which rises on the north-west edge of a vast caldera of about 16 km diameter with its floor at about 2000 m above sea-level. Only the southern walls of the caldera can be seen, and Ridley (1968) considers that it has been produced by a combination of exogenic and magmatic processes acting to produce lateral landslipping, in this case towaids the north, after foundering has been initiated along ring fractures following detumescence of the underlying magma chamber.

To the north of the caldera complex, lavas from non-central eruptions form a spine which joins the main structure

to the north-east peninsula. Two marked depressions on either side of this spine were attributed by Bravo (1962) to landslipping of lavas resting on water saturated argillaceous material. Numerous small cinder cones, of mainly basaltic type, are scattered over the slopes of the main volcano. The majority are of Quaternary age, but such eruptions have continued into historic times, the last being in 1909. No radiometric dates for any Tenerife rocks have been published but by comparison of palaeomagnetic data from Tenerife and Madeira, Watkins et al (1966) suggest that the base series is unlikely to be older than Miocene.

6.4.3 Details of the Survey. Field procedure and data reduction were as described for Lanzarote except that in the terrain correction by computer the contour interval used was 250 m instead of 100 m. This results in an increase of the error in the terrain correction to $\pm$ 3 mgal (see Table 2.4) and consequently the inaccuracy in the Bouguer anomaly is increased to $\pm$ 5 mgal.

6.4.4 Regional Anomaly. Marine gravity track GG' (Fig. 6.3) passes 16 km south of the island and the short track HH' (Fig. 6.4) starts 7 km east of Santa Cruz and heads eastwards to Las Palmas.

The free-air anomalies are typical of a regionally compensated island, as was discussed in the case of Ascension Island. The large positive values on and close to the

island decrease rapidly to small negative values at some distance away, where the effect of the island is small and the deeper and more extensive negative effect of the compensating mass predominates.

The Bouguer anomaly, calculated as described in Chapter 2, shows a slight east-west gradient of approximately 0.4 mgal/km. The regional Bouguer anomaly over the island can be estimated from the GG' and HH' profiles and for a density of 2.4 gm/cc is 170 mgal.

As mentioned in the case of Gran Canaria, the calculated depth to the Moho is probably distorted. If the configuration is smoothed, the depth to the Moho south of Tenerife is approximately 16 km and decreases towards the west. This figure is in reasonable agreement with 14.6 km obtained by Dash and Bosshard (1968) in a profile between Tenerife and Gomera. This is considerably deeper than the normal 11.5 km to the Moho in oceanic areas and Worzel (1965a) suggests that the isostatic compensation inferred from the free-air anomaly is obtained by a regional crustal thickening. As with Gran Canaria, the data are insufficient to determine whether or not complete isostatic equilibrium has been attained.

The existence of a regional east-west gravity gradient, the gravity increasing westwards, is confirmed by the Bouguer anomaly map of the island Fig. 6.12. The absence of

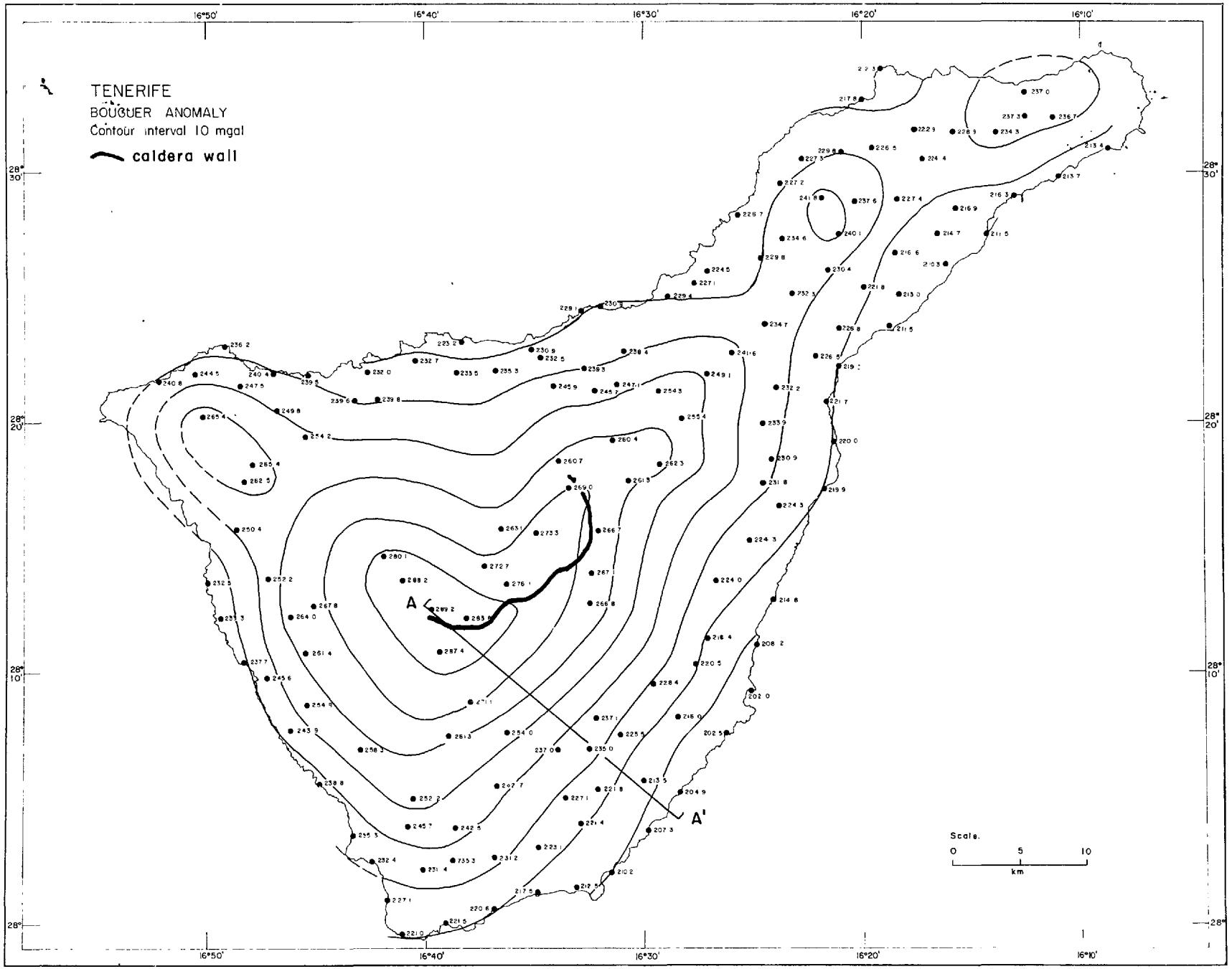
TENERIFE
BOUGUER ANOMALY
Contour interval 10 mgal
caldera wall
16°50'
16°40'
16°30'
16°20'
16°10'
28° 30'
28° 20'
28° 10'
28°
A
A'
Scale.
0 5 10
km

FIG. 6.12.

such a gradient on Gran Canaria is possibly a result of the counterbalancing of the gravity effect of the African continent by the effect due to the compensating mass under Tenerife.

6.4.5 Local Anomaly. The island topography and the distribution of the gravity stations are indicated in Fig. 6.11.

The Bouguer anomaly as contoured in Fig. 6,12 conforms closely to the island topography with the maximum value of 289 mgal occurring in the western summit caldera. This close correspondence of the Bouguer anomaly with the topography raises the question of whether or not the density value of 2.3 gm/cc used in the Bouguer and terrain corrections is correct. A higher density means a decrease in the elevation factor and a relative reduction of the Bouguer anomaly of the higher stations. In fact the bulk density of Tenerife calculated in Chapter 3 is 2.41 gm/cc but a difference of 0.11 gm/cc would reduce the Bouguer correction by only 9.2 mgal in 2000 m. It would require a density of 2.9 gm/cc, the value obtained by the Parasnis method (see Table 3.2) before the correlation between the topography and the Bouguer anomaly is reduced to a minimum; as discussed at length in Chapter 3, this is a quite unrealistic value. Furthermore, the Bouguer anomaly maps of Gran Canaria and Lanzarote (Fig. 6.7 and 6.10) where no such correlation between terrain and Bouguer anomaly is evident, both depict anomalies of

similar magnitude to that on Tenerife, and it seems quite reasonable in young topography for gravity anomalies due to volcanic centres to coincide with the volcanic structures to which the centres have given rise. Thus, while a density of 2.4 gm/cc might correctly be used for the Bouguer correction, the effect of using this different density is so small that it does not justify changing the density of 2.3 gm/cc adopted for all the other islands.

The Bouguer anomaly is triangular in shape, clearly indicating the rift zones which extend with angles of roughly 120° between them from the main anomaly to the north-east, north-west and south. In the north-east and north-west these rift zones terminate in old dissected headlands. While there is no similar headland in the south Hausen (1956) suggests that a mountainous outcrop in the lower flanks of the main volcano belongs to the same series.

The headland in the north-east is marked by two small gravity maxima and that in the north-west by one. These anomalies may represent old volcanic centres but their amplitudes, which are much smaller than the other volcanic centres in the Canary Islands, and their forms are similar to the volcanic centres found along the great fissure eruption of S. Jorge in the Azores. It is also worthy of note that these three maxima lie on a line which, if continued to the south-west, passes through Gomera and Hierro. It may be that

the headlands are the products of a great eruptive fissure and that Gomera represents a larger volcanic centre which has erupted along this same fissure.

The form of Tenerife is very similar to several of the Hawaiian shield volcanoes which, as pointed out by Macdonald (1965), are generally "lobate, resembling three-pointed stars in ground-plan, as a result of building by eruptions predominantly along the three rift zones." Macdonald suggests that the most probable cause of these rift zones is the inflation of the volcano by intrusion of magma into it.

Regrettably, no stations were established in the summit region to the north or west of the main peak so that the gravity field in the caldera region is poorly defined, but the large positive anomaly on the western side clearly indicates the presence of a large high-density subsurface mass. The volcanics in the surrounding region all display low-pressure mineralogy (Ridley, 1968) suggestive of an origin in a shallow level magma chamber and it may be this chamber which gives rise to the gravity anomaly.

The low values of the highest stations on the peak may be a reflection of its high pyroclastic content and consequent low density. There is no indication that the caldera represents a residual gravity low which, following the classification of Yokoyama (1963), one would expect if the caldera is of the Krakatoa type (Williams, 1941) as suggested by Machado

(1964). Although the stations are widely spaced and the inaccuracy too great to allow the detection of a small gravity low, the absence of any major gravity anomaly associated with the caldera strongly supports Ridley's (1968) theory of its formation.

The magnitude of the main anomaly can be estimated from the regional gravity field as determined from the marine gravity data. The regional value of 170 mgal calculated for a density of 2.4 gm/cc yields a value of approximately 120 mgal for the amplitude of the anomaly. The maximum gradient is 5 mgal/km.

6.5 A Gravity Survey of Hierro.

6.5.1 Introduction. Hierro is situated at $27^{o}45'N$, $18^{o}00'W$ at the extreme south-west of the Canary Archipelago. With an area of approximately 277 km^2 it is the smallest of the seven major islands in the group. The maximum elevation is 1500 m and land above 1000 m forms a large proportion of the surface for such a small island. The island slopes from these highlands down to sea-level as steep slopes or cliffs and these slopes are continued under the water where the depth increases rapidly with gradients of 1 in 4 to 1 in 5 down to 3000 m. Between Hierro and Gomera, the water depth is less than 3100 m but to the south and west the flanks continue down to 3700 m where the basal diameter is approximately

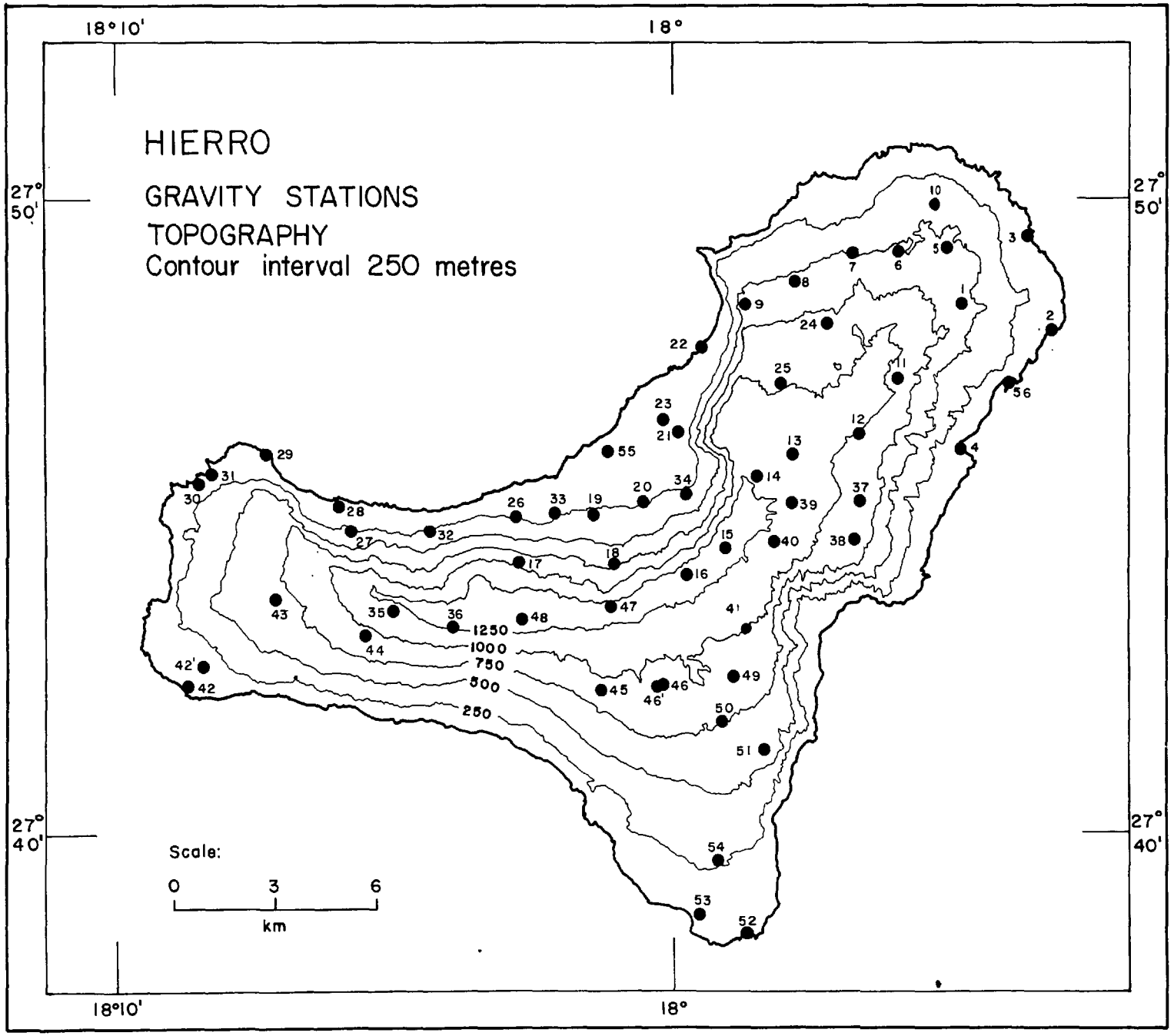
HIERRO
GRAVITY STATIONS
TOPOGRAPHY
Contour interval 250 metres
18°10'
18°
27° 50'
27° 40'
1250
1000
750
500
250
Scale:
0 3 6
km

FIG. 6.13.

100 km. The island is bordered in the west by the Canary Abyssal Plain and the water depth continues to increase to 4000 m and more slowly, from 4000m to 5200 m.

The bathymetry suggests that the southern headland of the island is continued southwards in the form of a submarine ridge which terminates 25 km south of Hierro in a small seamount.

6.5.2 General Geology. The island forms an arc open to the north-west with a peninsula extending southwards from its convex edge.

The oldest formation visible is a great series of lavas, at least 1000 m thick and cut by a multitude of dykes. The lavas rest almost horizontally with perhaps a slight dip away from the north-west bay except in the south of the western limb where there is an inclination of about 30^{o} towards the south. Hausen (1964) considers that the lavas represent the remnants of a great shield volcano which had its centre somewhere in the north-west bay, which is known as "El Golfo". The lavas are of trachy-basaltic composition (Hausen, personnel communication). On the basis of K-Ar dating and palaeomagnetic investigations in the Canary Islands, Abdel-Monem et al (1967) suggest that the series has probably been erupted entirely within the last 2 MY.

This earlier series is succeeded by a great number of adventive cones and more basaltic lavas. These cones are

largely uneroded and are clearly quite young, although there has been no historic eruption on this island.

The late volcanic products which cover much of the island, render it difficult to determine the geological history. The sheer cliffs around El Golfo have lead many geologists to consider the island as the remains of a much larger structure, part of which has disappeared in a gigantic explosion which formed the giant "caldera" of El Golfo (Von Kuebel, 1906; Navarro, 1908; Blumenthal, 1961). Others (Gagel, 1910; Hausen, 1964) dismiss this possibility on the grounds that there are no pyroclastic deposits to be found on the island, such as one might expect from such an explosion. Hausen (1964) considers that the original shield volcano has been broken up by faults, principally along WNW, NNE and NE directions, to leave the "horst" blocks of the island as it now stands. The southern peninsula he regards as an addition to the old block, formed by the emission of more recent lavas.

Ridley (1968) regards El Golfo as being an example of lateral collapse of the volcanic flank. Sub-aerial lava flows on oceanic islands are generally confined to the sub-aerial part of the cone or the shallow water around it, leading to a steepening of the sub-aerial flanks compared to those under-water and hence to an unstable structure. Ridley suggests that subsequent magmatic detumescence which might normally

lead to caldera formation will, because of this unstability, give rise to large-scale landslipping instead.

6.5.3 Details of the Survey. Field procedure and data reduction were carried out as described for Lanzarote except that, as for Tenerife, the contour interval used in the terrain correction by computer was 250 m instead of 100 m. This results in an increase of one milligal in the terrain correction error, bringing the total inaccuracy in the Bouguer anomaly to ± 5 mgal.

6.5.4 Regional Anomaly. The marine gravity track GG' (Fig. 6.1 and 6.3) passes 20 km to the north of Hierro but the island rises so abruptly from the sea-floor that the island finds little expression in the bathymetry or gravity field observed on the profile. The Bouguer anomaly at the longitude of Hierro shows an east-west gradient of some 0.5 mgal/km across the island. Using this profile to estimate the regional field over the island, a value of approximately 205 mgal is obtained for a density of 2.4 gm/cc.

The depth of the Moho obtained by seismic refraction profiles B and C of Dash and Bosshard (1968) is 11.3 km at a distance of 10 km west of the island of Hierro. The depth calculated from the gravity profile (Fig. 6.3) is 13 km which, in view of the inaccuracies in the two methods, is in reasonable agreement with the seismic result.

Whilst it is most probable that Hierro, like the other Canary Islands investigated, is regionally compensated, the regional data available are too few to confirm this.

6.5.5 Local Anomaly. The island topography and the distribution of the gravity stations are shown in Fig. 6.13. The inaccessibility of large sectors in the south of the island introduces considerable uncertainty in that area in the Bouguer anomaly contours as drawn in Fig. 6.14.

The Bouguer anomaly map shows a centre of high anomaly of value 260 mgal, with lobes extending along the three limbs of the island. The Bouguer anomaly centre appears to be located along the escarpment behind the north-west bay of El Golfo. The absence of indications of a gravity high offshore in El Golfo does not exclude the possibility that a volcanic centre may exist there as suggested by Hausen (1964) and others. The removal of the volcano by explosion as in Krakatoa-type caldera formation would produce a reduction in Bouguer anomaly (Yokoyama, 1963) as would its disappearance by drop-faulting or land-slipping. Such a reduction might be enough to counterbalance the high gravity value of a volcanic centre.

A depression in the gravity field crosses the centre of the island in a NW-SE direction and may represent a major fault across the island. This depression occurs slightly to the south-west of a narrow waist in the central uplands

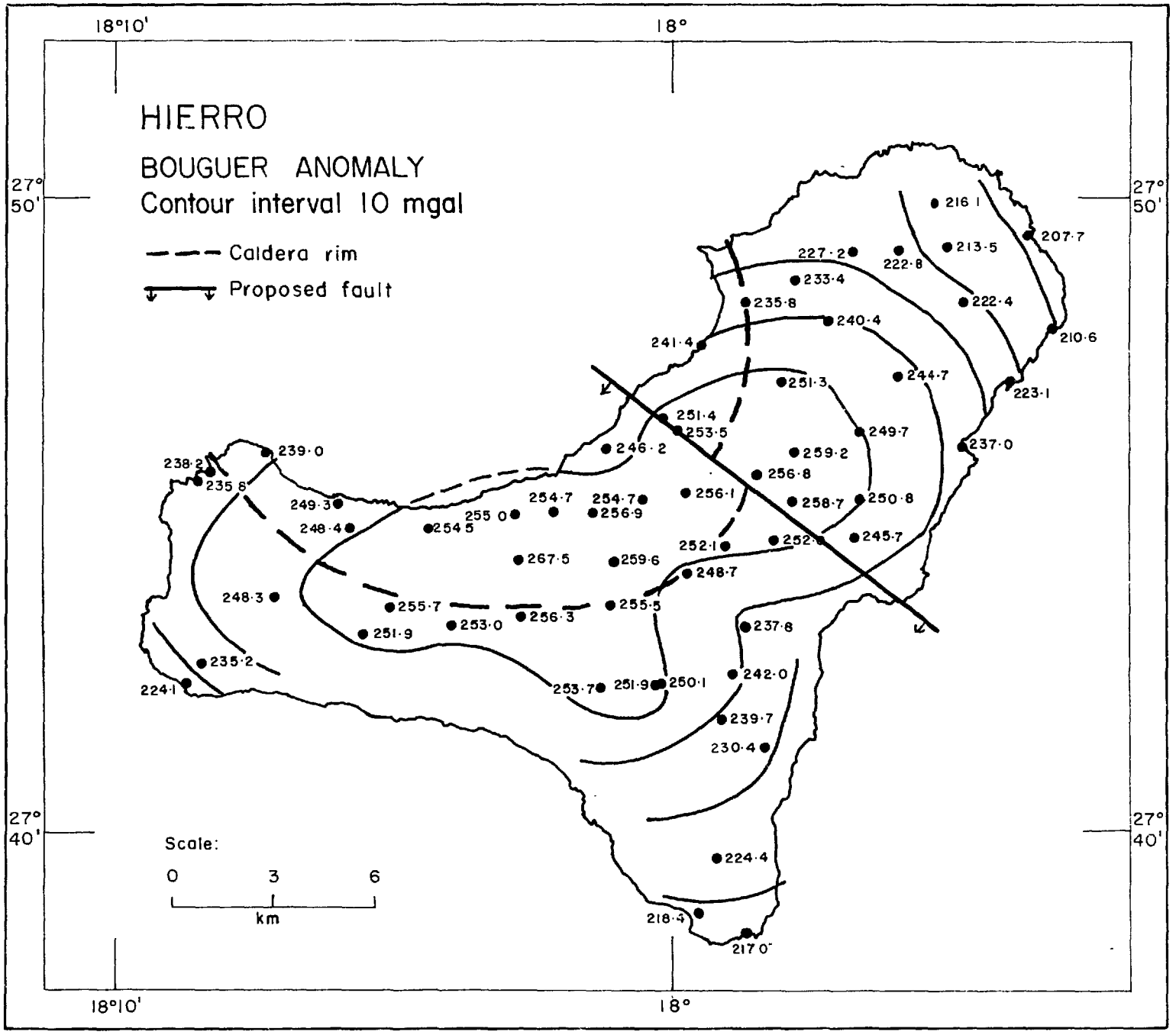
HIERRO
BOUGUER ANOMALY
Contour interval 10 mgal
Caldera rim
Proposed fault
18°10'
18°
27° 50'
27° 40'
216·1
207·7
213·5
227·2
222·8
233·4
222·4
235·8
240·4
210·6
241·4
244·7
251·3
223·1
251·4
253·5
249·7
239·0
246·2
259·2
237·0
238·2
235·6
256·8
249·3
254·7
254·7
256·1
258·7
250·8
248·4
255·0
256·9
254·5
252·1
252·
245·7
267·5
259·6
248·7
248·3
255·7
255·5
256·3
253·0
251·9
237·8
235·2
224·1
253·7
251·9
250·1
242·0
239·7
230·4
224·4
218·4
217·0
Scale:
0 3 6
km

FIG. 6.14.

produced by an eastward break in the El Golfo escarpment and a westward break in the eastern coastline. It seems probable that these topographic features may be the result of a NW-SE fault whereby the southern half of the island has dropped slightly and perhaps tilted towards the south-east as is suggested by the inclination of the lavas observed by Hausen (1964). The displacement of the gravity anomaly to the south-west of the topographic expression of the proposed fault line may indicate that the fault plane dips in that direction.

With the exception of the break due to the above fault, the El Golfo escarpment is very similar in both scale and curvature to the great arc of cliffs which forms the north-west coast of Gran Canaria (Fig. 6.9) and which is very clearly associated with a major volcanic centre (Fig. 6.10). None of the products of explosive eruption on Gran Canaria are attributed to this centre so that, like El Golfo, explosive activity has been dismissed as a possible cause of the disappearance of the central part of the volcano. It therefore seems probable that on Hierro as on Gran Canaria, the central portion of a major volcanic centre disappeared beneath the waves by down-faulting or slumping along radial fractures leaving behind only a section of the original shield. In one of the few sectors of the escarpment wall of El Golfo not inundated by recent lava flows, Hausen (1964) observed a columnar basalt which has slipped along a fault plane dipping

at some 45° and this must lend strong support to the down-faulting mechanism for the formation of the "caldera".

Faults in a NNE and WNW direction as suggested by Hausen may also have operated to produce the steep eastern and southern coasts of the island. The gravity data is insufficient to determine whether the peninsulas represent rift zones or horst blocks except in the case of the northern peninsula, where the east-west trend of the gravity contours is cut sharply by the coastline, suggesting that it represents the remains of a land surface of considerably greater extent.

It seem probable that the island is the remains of a great shield volcano centred on the bay of El Golfo. The central portion of the old volcano dropped below sea-level along radial fractures and further linear faults ruptured the flanks until only the present island remains.

Whilst it cannot be verified from the gravity data, the southern peninsula and the submarine ridge which extends southwards suggest a north-south rift zone. This trend if extended northwards passes through La Palma and it is possible that Hierro may owe its origin to the intersection of this fissure with the NE-SW trending fissure through Gomera and the old headlands of Tenerife mentioned above,

If the value of 205 mgal observed on the marine gravity track GG' is adopted for the regional field, the amplitude of the main anomaly is only 55 mgal, less than half as much

as is observed on the other Canary Islands investigated. Even if allowance is made for the down-faulting of the central block and the maximum value of the anomaly is considered as being about 270 mgal, the anomaly is still small by comparison, However, on the other three Canary Islands surveyed the regional field adopted is some 30 mgal lower than the minimum value observed on the island and, as seen on profile HH' (Fig. 6.4), the Bouguer anomaly continues to decrease as the island slopes down to the ocean floor. On this basis the regional field may be between 170 and 180 mgal but even so the amplitude of 90 - 100 mgal is less than on the other islands.

It must be noted that if the regional field is 180 mgal, the gravity field must first decrease as the island is approached, before increasing again rapidly to its maximum over the island itself. A similar Bouguer anomaly was observed over Santa Maria in the Azores and as discussed there, indicates a degree of regional isostatic compensation.

6.6 General Discussion.

The general map of the gravity surveys on the Canary Islands is presented as Fig. 6.15 and the results of the island surveys are summarized in Table 6.1. The regional values are estimated from the marine gravity tracks which pass between 15 - 30 km from the islands. If Tenerife is regarded as being typical, it can be seen from the HH'

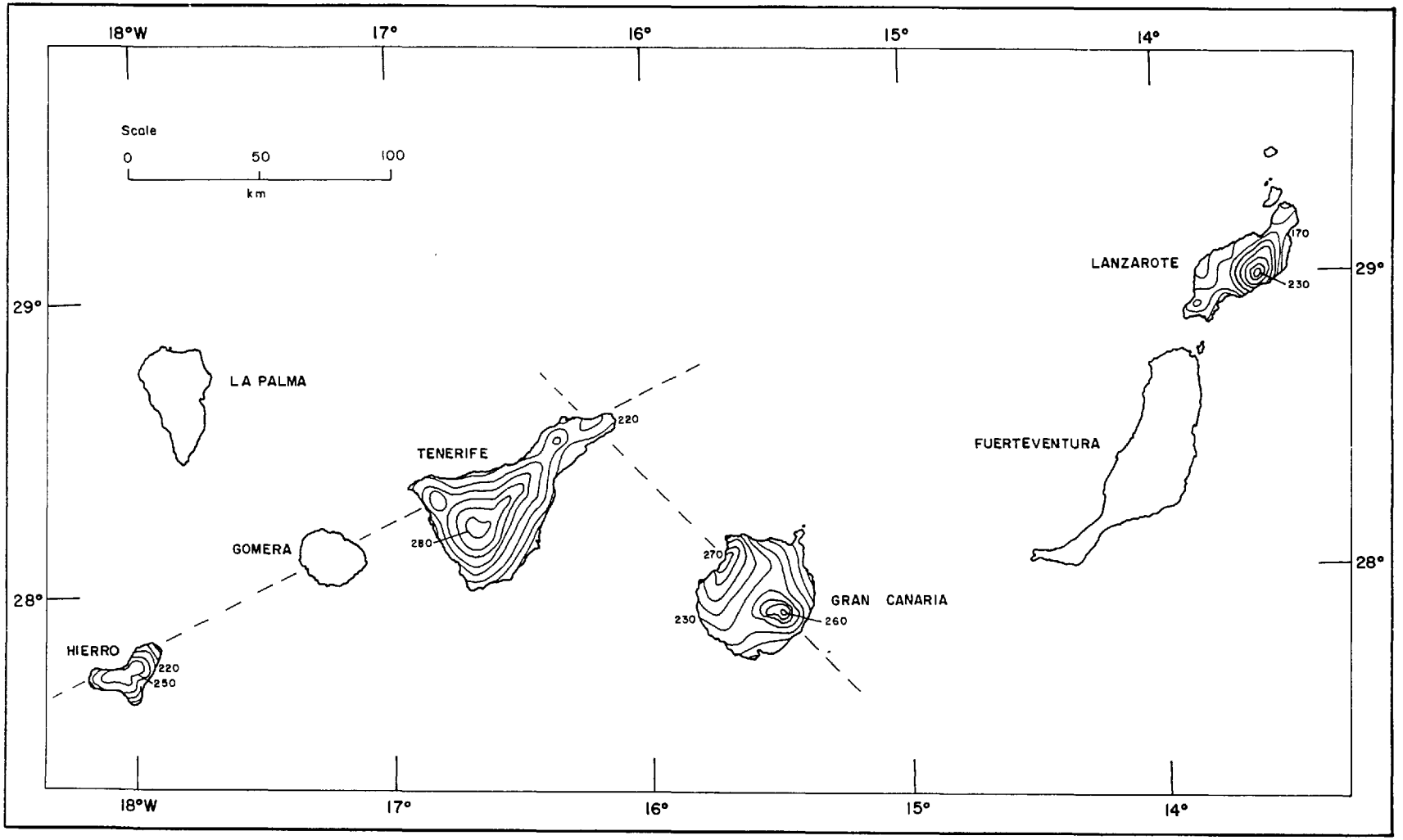

FIG. 6.15. Bouguer gravity anomaly map of the Canary Islands. Anomaly values in milligals. — — volcano tectonic lines

Summary of Gravity Results on the Canary Islands.

	1	2	3	4	5	6	7
Island Name	km	mgal	mgal	mgal	mgal	mgal/km	km
Lanzarote	90	230	155	120	115	6.5	15
*Gran Canaria E	185	270	198	160	72	5.9	10
*Gran Canaria W	215	287	198	160	127	6.5	16
Tenerife	285	289	202	170	119	5.0	20
Hierro	325	268	208	180	88	6.7	10

1 The distance from the continental shelf to the positive anomaly centre.

2 Maximum observed value of the anomaly at the centre.

3 Minimum observed value of the Bouguer anomaly on the island.

4 Estimated regional field at the position of the positive anomaly centre.

5 Estimated amplitude of the anomaly.

6 Maximum gravity gradient associated with the anomaly.

7 Maximum possible depth to the anomalous mass (after Bott and Smith, 1958).

Table 6.1

---

* The Gran Canaria values have been corrected for terrain effects.

profiles (Fig. 6.4) that the Bouguer anomaly attains its minimum value, which is the value adopted for the background field, within this distance. It is considered that the error in the regional field is less than ± 20 mgal.

The marine gravity data are inadequate for making any quantitative assessment of isostatic compensation. Qualitatively however, the form of the free-air anomaly profiles east and west of Gran Canaria indicates a certain degree of compensation. The Bouguer anomaly values along the GG' profile appear to increase much more slowly than is usual on continental margin traverses (Worzel, 1965a), suggesting that the Bouguer anomaly over the archipelago is low with respect to the gravity field in the north and in the south. Such a low Bouguer anomaly would indicate an anomalous mass deficiency under the island corresponding to the compensating mass indicated by the free-air anomaly, and suggests that all the islands are to some extent isostatically compensated. The mass deficiency is most probably induced by a thickening of the crust, as indicated by the seismic refraction studies and the calculated gravity section (Fig. 6.3). It may also represent low density material under the crust such as is found on the axial zone of the Mid-Atlantic Ridge, but such material must be localized since the seismic studies indicate normal mantle material. The extent to which isostatic equilibrium has been attained cannot be determined from the

present data. However if the islands were severely under-compensated one might expect to find geological evidence for subsidence of the islands, and no such evidence has been discovered.

The calculated depth to the Moho along the GG' track is in good agreement with the depth obtained by seismic-refraction studies at the western end of the profile, and ranges from about 13 km under Hierro to 19 km under Lanzarote. This compares with a crustal thickness of 27 km under the continental shelf. As discussed in Section 6.2.4, the crustal thickness under the islands is too small and the Bouguer anomaly value is too high to be consistent with suggestions that the Canary Islands represent the remnants of a continental headland (Hausen, 1956). It has been suggested (Tryggvason, 1965; Schienmann, 1964; Demenitskaya and Dibner, 1965) that Iceland and the Faroes may be underlain by a sialic sub-stratum and gravity surveys on these islands observed typically continental Bouguer anomaly values of -15 to +60 mgal and +23 to +38 mgal respectively (Einarrson, 1954; Saxov and Abrahamsen, 1964). The Canary Island gravity values are over 100 mgal higher and must indicate a quite different sub-structure and one which is certainly other than continental.

Radiometric dating (Abdel-Monem et al, 1967) indicates that sub-aerial volcanism has continued on the Canary Islands

from at least 12 - 16 MY ago until the present. The oldest rocks dated are from the eastern islands and although all the islands bear traces of recent volcanic activity, there does appear to be a tendency for the main sub-aerial shield-building eruptive phase to decrease in age westwards. On Hierro, the most westerly island, all the major sub-aerial lavas sampled appear to have been erupted in the last 0.7 MY (Abdel-Monem et al, 1967). This westward decrease in age of the islands is consistent with Wilson's (1963) postulate that volcanic islands are produced on mid-ocean ridges and swept outwards by the viscous drag of mantle convection currents. However, the ages of the exposed rocks would require an incredibly high drift-rate for the islands to reach their present position of 2000 km from the Mid-Atlantic Ridge. McBirney and Gass (1967) concluded from a study of the petrology of rocks from the Atlantic and the Pacific islands that the high pressure mineral assemblages of the Canary Island basalts are inconsistent with their formation on the crest of the Mid-Atlantic Ridge. The implication must be either that the islands have been built up in situ or that all the exposed rocks represent a reactivation of volcanism in Tertiary and Recent times as the islands have drifted against the African continent. Assuming an average drift rate of 1 cm/year the core of the islands must be Mesozoic in age, if they were first formed on the Mid-Atlantic Ridge. As

there is no evidence on the Canary Islands for rocks older than Miocene, it cannot be said that the age variations on the Canary Islands lend any real support to crustal spreading theories.

Whether or not the islands have an ancient Mesozoic basement, the problem of the continued volcanism remains. The evidence of the widespread tectonic activity on all the islands and the significant lineations of volcanic centres suggest that the islands have been built at centres along great linear fissures. The directions of faulting are various, but the principal features trend NW-SE and NE-SW, conformably with the two main trends on the near-lying coast of Africa. It seems probable that, as suggested by Hausen (1956), these fractures represent marginal tectonic activity associated with the Atlas Mountains. The great fractures may have tapped deep, high-pressure magma sources, perhaps generated by the same tectonic activity, to form the islands in their present position on the edge of the African continent.

Recent petrological studies (Ridley, 1968) reveal that the Canary Island basaltic rocks have a high-pressure mineral facies, suggesting that they were generated at depths of more than 35 km and the subordinate rock types, such as trachyte and rhyolite, have low pressure mineral assemblages, indicating a shallower origin at less than 15 km depth. It seems probable that the basalts are erupted mainly from fissures

which penetrate the crust and upper mantle while the subordinate lavas are derivative rocks, fractionated from the primary magma by processes of magmatic differentiation in high-level magma reservoirs. It is these reservoirs which are detected by the gravity surveys as major centres of high gravity field. The amplitudes of these anomalies range from 70 - 125 mgal and are similar to those observed in the Hawaiian Islands. There the existence of high density bodies was first suggested by Woollard (1951) from gravity data and later confirmed by seismic (Furumoto et al, 1965) and magnetic surveys (Malahoff and Woollard, 1966). In the Hawaiian Islands, these dense bodies have been interpreted as magma chambers or composite volcanic plugs with depths to the upper surface of between 0.3 and 9.3 km and areal dimensions ranging from 5 x 5 km^2 to 20 x 10 km^2. On Oahu the seismic velocities indicate a density of approximately 3.2 gm/cc. The parallel between the Hawaiian Islands and the Canary Islands is not an exact one, particularly in petrology, but it seems probable that the centres of high gravity represent reservoirs of accumulate magma, capped by a lighter fraction which gives rise to the low-pressure mineral assemblage trachytes and phonolites. It may be the movement of magma in these high-level reservoirs which gives rise to the fracturing and detumescence which lead to the formation of calderas.

6.7 Conclusions.

(1) The Canary Islands are great volcanic edifices located in the transition zone between the continental and oceanic-type crusts. They are truly oceanic in character but there is no evidence to support the theory that they originated on the Mid-Atlantic Ridge; neither is there any evidence that they did not.

(2) The islands are to some extent isostatically compensated by a regional thickening of the crust under the islands.

(3) The islands have arisen at centres along great volcanic fissures probably associated with the tectonic instability of the neighbouring Atlas Mountains.

(4) The islands are characterized by central-type anomalies of a high gravity with amplitudes ranging from 75 to 125 mgal and gradients from 5.0 - 6.5 mgal/km. These anomalies are attributed to high-level magma reservoirs within the crust and island body.

CHAPTER 7

GRAVITY SURVEYS OF TWO ISLANDS IN THE DEEP OCEAN

7.1 A Gravity Survey of Fernando de Noronha.

7.1.1 Introduction. In the summer of 1966, a network of 20 gravity stations was established on the island of Fernando de Noronha using a Worden Geodetic gravimeter. A gravity station at the landing strip (Woollard and Rose, 1963) could only be approximately reoccupied and a new primary base, connected to the Woollard station at Recife, was established and used in the course of the survey.

7.1.2 General Geology. Fernando de Noronha is a small archipelago in the Atlantic Ocean situated at $3^{\circ}50'S$ and $32^{\circ}25'W$, and having an area of 18.4 km^2. With a maximum elevation of 323 m, it is the tip of a great volcanic pile rising from the sea-floor at a depth of 4000 m, where it has a basal diameter of approximately 50 km.

On the main island, to which the present survey is restricted, two principal volcanic formations can be recognised (Almeida, 1958). The older, occupying a belt across the centre of the island, consists of various pyroclastic rocks cut by plugs of alkaline basalts and intrusive domes of

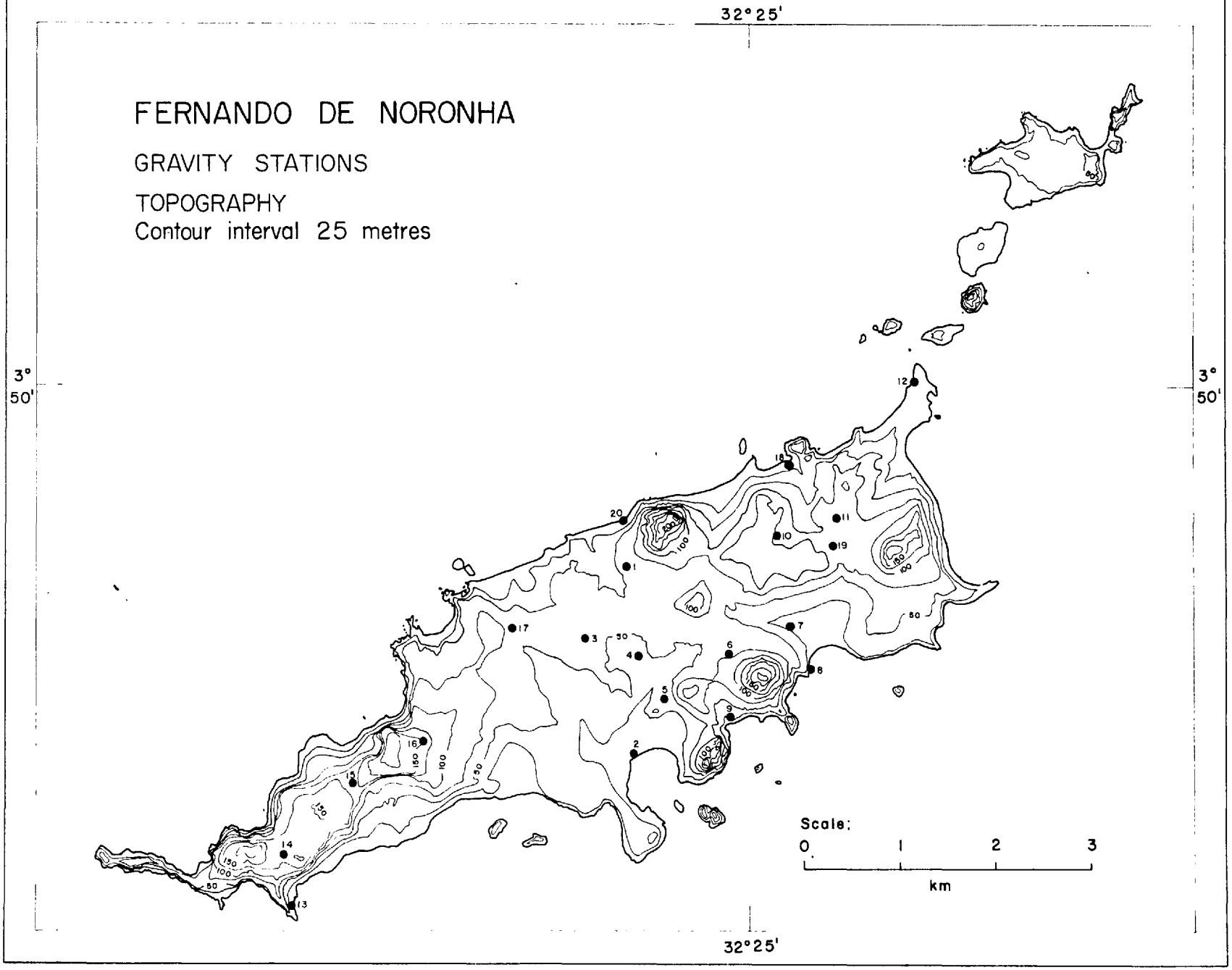
FERNANDO DE NORONHA
GRAVITY STATIONS
TOPOGRAPHY
Contour interval 25 metres
32°25'
3°
50'
Scale:
0 1 2 3
km

FIG. 7.1.

alkaline trachytes and phonolites. To the north-east and south-west of this area lies the second formation, comprised of ankaramite lava flows with associated tuffs, breccias and agglomerates. Sedimentary deposits are all of a superficial nature, but former positions of sea-level are indicated by beach levels at 40 m, 12 m and -6 m. These have been attributed to eustatic oscillations caused by the Pleistocene glacial phenomena, which dates the island as pre-glacial. From palaeomagnetic evidence, Richardson and Watkins (1967) suggest that the age of the visible rocks does not exceed the Miocene.

7.1.3 Details of the Survey. Stations were located to within 20 m using the 1964 military 1:10,000 map. Elevations were taken from the same map, which was contoured at 10 m intervals, or by reference to sea-level at coastal stations and are accurate to $\pm$ 5 m. Data reduction was carried out as detailed in Chapter 2 except that terrain corrections for each station were only made out to Hammer zone J (6.65 km), the bathymetric data (Admiralty Chart 388) available being insufficient to extend the correction further. By approximating the island to a truncated cone of upper radius 5 km at sea-level and lower radius 25 km at 4 km depth, the contribution of the neglected water layer to the terrain correction can be shown to be of the order of 27 mgal for a density of 2.4 gm/cc for the island body. This error will affect all

the stations practically equally but the relative error in the Bouguer anomaly due to terrain correction will not be more than 1 mgal. Maximum elevation errors correspond to an error in the simple Bouguer anomaly of ± 1 mgal and instrumental errors due to drift and neglecting tidal effects contribute a further 0.5 mgal, so that the Bouguer anomaly values are considered accurate to within 2.5 mgal.

7.1.4 Regional Anomaly. In so far as is known, there are no marine gravity data close enough to the island to provide any information regarding the regional field and regional trends over the island. However, the isolated position of the island, 300 km from the South American continental shelf, means that the only major influence is likely to be that of the transition from oceanic to continental crust, and at 300 km from the continent even this influence will be very small over an island of the size of Fernando de Noronha.

7.1.5 Local Anomaly. The Bouguer anomaly values and contours are shown in Fig. 7.2 which indicates a well marked gravity high in the east-centre of the island. The maximum observed value is 246 mgal but, as pointed out above, a more correct value would be some 25 - 30 mgal higher, i.e. 270 - 275 mgal. This value is similar to the maximum Bouguer anomaly values observed on several of the Canary Islands and on Madeira.

The Bouguer anomaly decreases only slightly to the north-east, so that an area of high Bouguer anomaly is formed

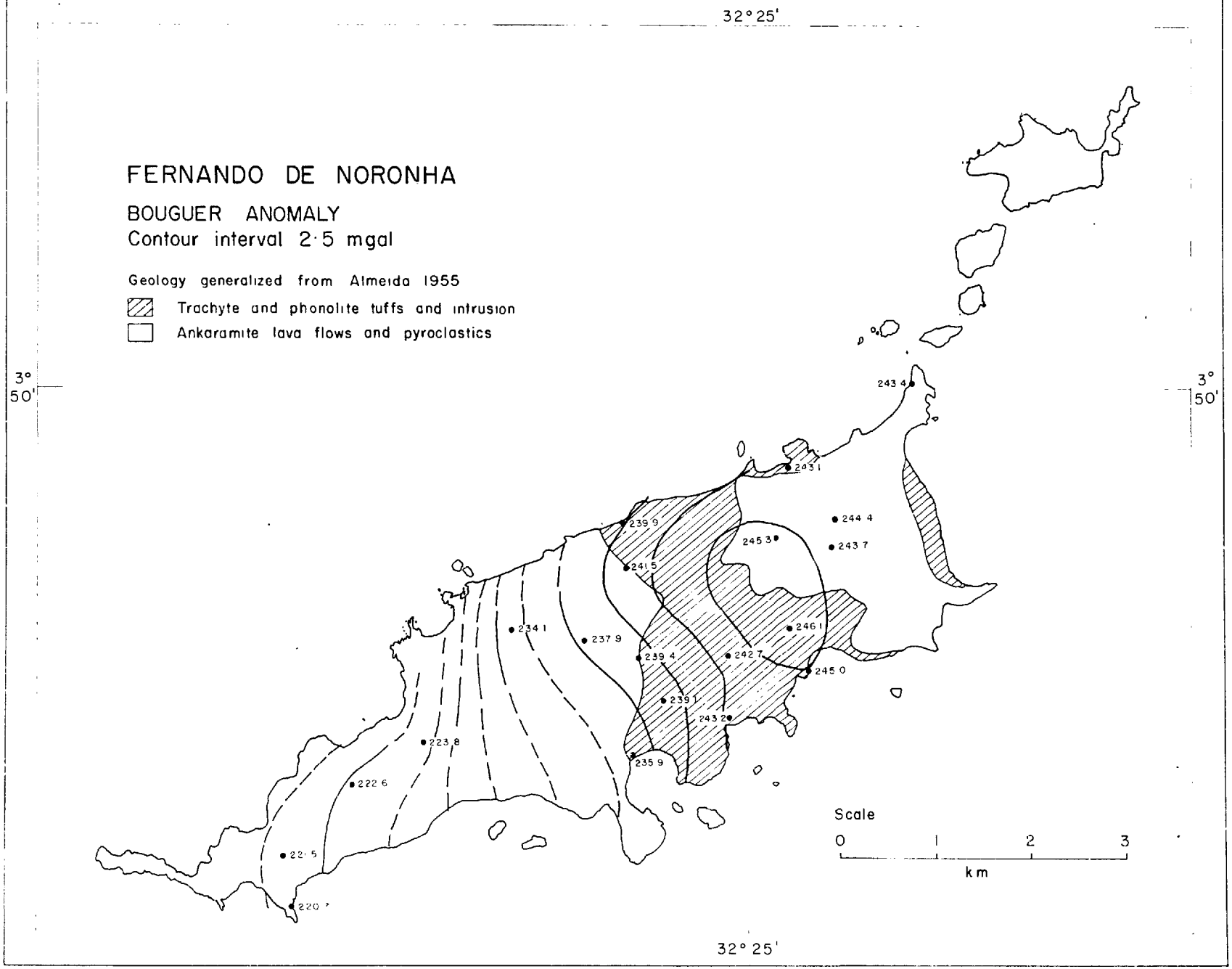
32° 25'
FERNANDO DE NORONHA
BOUGUER ANOMALY
Contour interval 2·5 mgal
Geology generalized from Almeida 1955
Trachyte and phonolite tuffs and intrusion
Ankaramite lava flows and pyroclastics
3° 50'
243 4
243 1
239 9
244 4
245 3
243 7
241 5
234 1
237 9
246 1
239 4
242 7
245 0
239 1
243 2
223 8
235 9
222 6
221 5
220 7
Scale
0 1 2 3
km
32° 25'

FIG. 7.2.

occupying the eastern end of the island. To the south-west the gravity field decreases sharply, with gradients in excess of 5 mgal/km. Gravity noses trend north-westwards and south-westwards from the main anomaly towards the trachytic domes which dominate the northern and southern coasts of the island, and suggest that these domes represent offshoots from the main volcanic centre. The location of the gravity high over the region of ostensibly less dense rocks, the trachytes and phonolites, and its large amplitude of over 25 mgal, indicate that the gravity anomaly must be associated with some massive structure at depth, and confirm its identification as the main volcanic centre.

It would be of great interest to determine the regional field in order to discover if the amplitude of the anomaly as well as the maximum value, was similar to the amplitudes of the Canary Island anomalies, but the present data are inadequate for this purpose. All that can be said is that the amplitude is greater than 30 mgal and that the maximum gradient is approximately 6.5 mgal/km.

7.2 Gravity Survey of Madeira Island.

The Instituto Geográfico e Cadastral of Portugal who carried out a gravity survey of the island of Madeira in April 1964, very kindly made their data available and granted permission for it to be used in this thesis.

7.2.1 Introduction. Madeira is the main island of the Madeira Archipelago (Fig. 7.3), which is situated in the North Atlantic some 500 km north of the Canary Islands and 700 km west of Morocco. The archipelago also comprises several much smaller islands, of which the principal are Porto Santo in the north-east and Deserta Grande in the south-east.

The maximum length of Madeira is in an east-west direction and is 58 km, the maximum width is 22 km, and the maximum elevation is 1861 m. Although the island is very rugged and marked by steep cliffs along much of the coastline, it is surrounded by a fairly wide, shallow marine shelf which extends ~~north~~ south-eastwards to include Deserta Grande. Beyond the edge of this shelf, at 150 m, the water depth increases rapidly, with slopes of up to 20°, to over 4000 m, except in the north-east where depths of less than 2400 m separate Madeira from Porto Santo. The basal diameter at 4000 m is approximately 130 km.

Madeira is at the southern end of a gentle rise which trends NNE towards Josephine Bank. It may also be considered

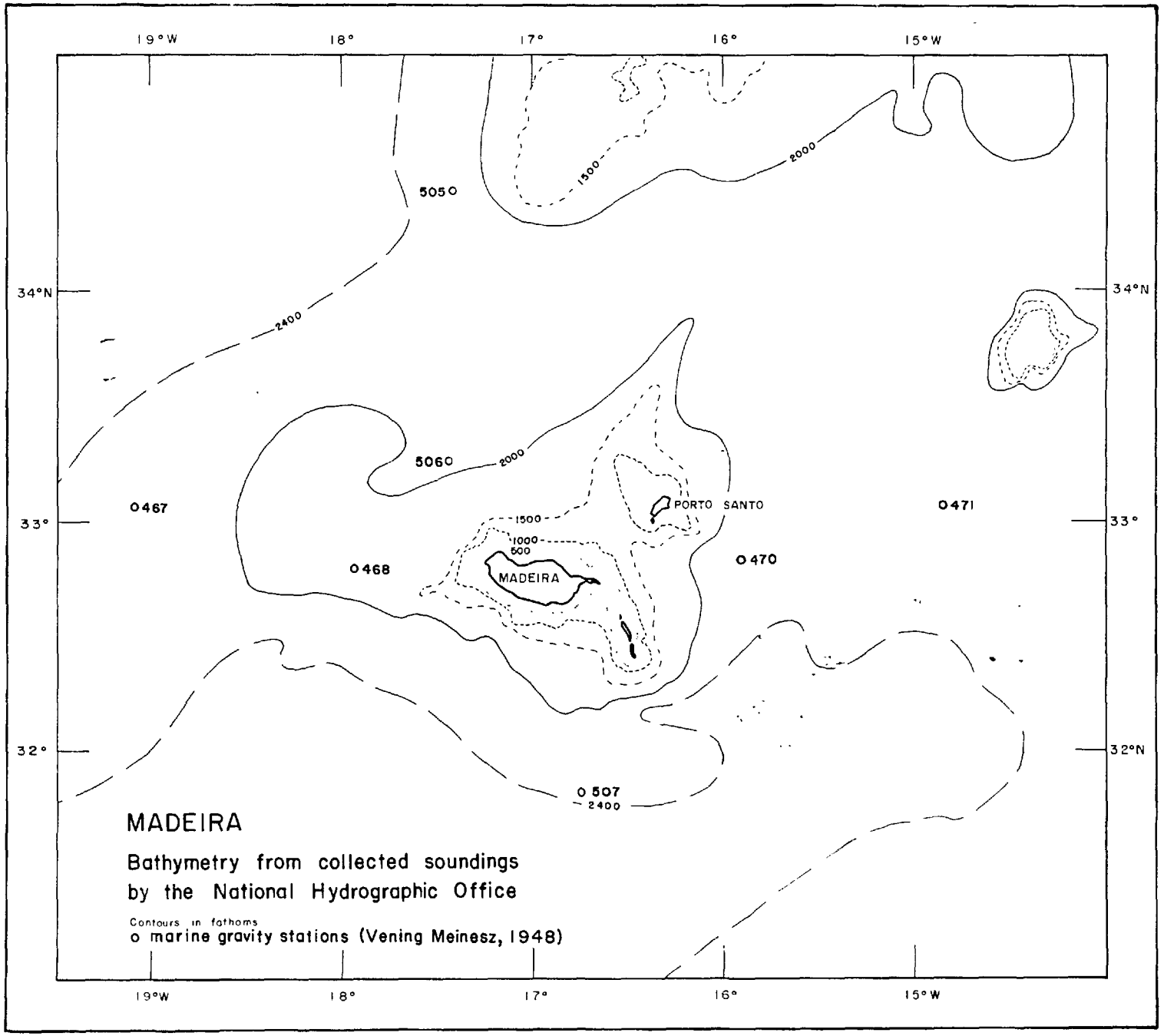
19°W
18°
17°
16°
15°W
34°N
33°
32°
5050
2400
1500
2000
5060
2000
0467
1500
1000
500
PORTO SANTO
0471
0468
MADEIRA
0470
0507
2400
MADEIRA
Bathymetry from collected soundings
by the National Hydrographic Office
Contours in fathoms
o marine gravity stations (Vening Meinesz, 1948)

FIG. 7.3.

as the westernmost limit of a NE-SW trending line of seamounts which ends near Lisbon in a series of lavas overlying Turonian carbonates (Krejci-Graf, 1964). To the south, Madeira is separated from the Canary Islands by the Madeira Abyssal Plain.

7.2.2 General Geology. The great piles of lavas and tuffs forming Madeira have been so deeply eroded that the main feature of the present relief is a basaltic range of mountains which runs east-west along the length of the island. The deep dissection of the island has been aided by the high proportion of soft tuffaceous sediments in the volcanic materials that comprise the island. The older parts of the island are characterised also by trachytes, trachydolerites, alkali-rich intrusives and coarse volcanic breccias. The younger volcanic products are primarily olivine-basalt and analcine-rich basalt (Krejci-Graf, 1955).

Evidence for considerable uplift of the island is provided by a richly fossiliferous reef deposit which outcrops at 330 m, separating the younger lavas from the older volcanic series.

Fossils from this reef have been dated as being of Miocene age (Joksimowitsch, 1910) which sets an upper limit to the age of the island. There is no evidence of any Recent volcanic activity, and the island volcanism is believed to

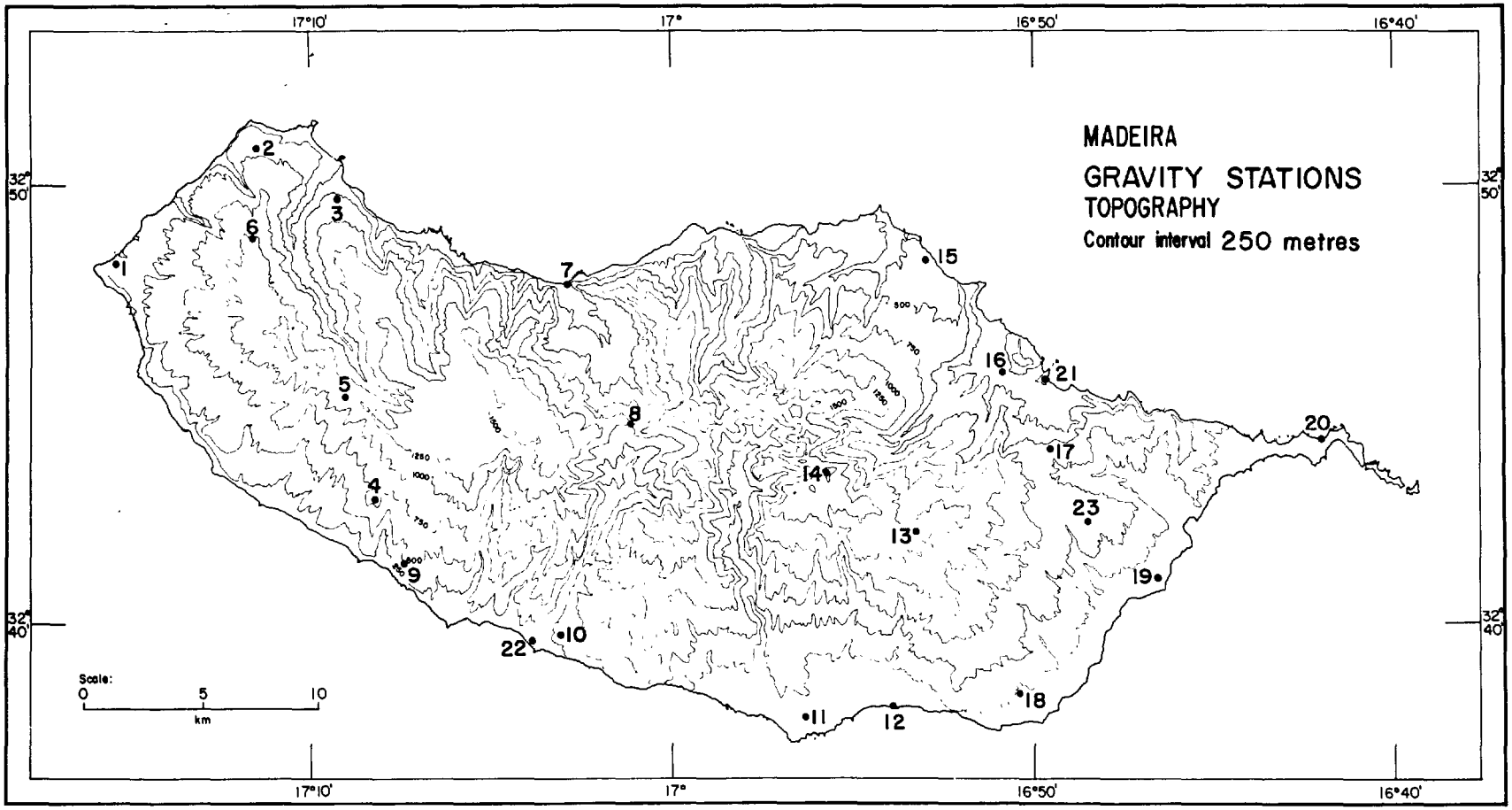
MADEIRA
GRAVITY STATIONS
TOPOGRAPHY
Contour interval 250 metres
17°10'
17°
16°50'
16°40'
32° 50'
32° 40'
Scale:
0
5
10
km
1
2
3
4
5
6
7
8
9
10
11
12
13
14
15
16
17
18
19
20
21
22
23

FIG. 7.4.

be extinct, but several severe earthquake shocks have been recorded since the island's discovery in 1351.

7.2.3 Details of Survey. The Portuguese survey was carried out using La Coste and Romberg gravimeter No. 86. Elevations were measured by trigonometrical levelling. The error in the observed value of gravity is unknown but is not likely to be greater than in the surveys using the Worden gravimeter. As surveying techniques were used, the errors in location and elevation are likely to be considerably less than in the surveys already described.

Data reduction was carried out as described in Chapter 2, using a density of 2.3 gm/cc. For the terrain correction by computer, contours at 250 m intervals on the 1958, 1:50,000 map of the island were approximated by polygons. The bathymetry was contoured from the Admiralty Chart No.1831 and from sheet No. 80 of the Plotting Sheets of collected soundings published by the National Hydrographic Office. As discussed in Chapter 2, the error in terrain correction is $\pm$ 3 mgal, and with the reduced errors in elevation the total inaccuracy in the Bouguer anomaly is $\pm$ 5 mgal.

7.2.4 Regional Anomaly. Vening Meinesz (1948) established several pendulum gravity stations in the seas around the island and these stations provide some evidence as to the regional gravity anomaly. The locations of the stations which are near the island are shown in Fig. 7.3 and these stations

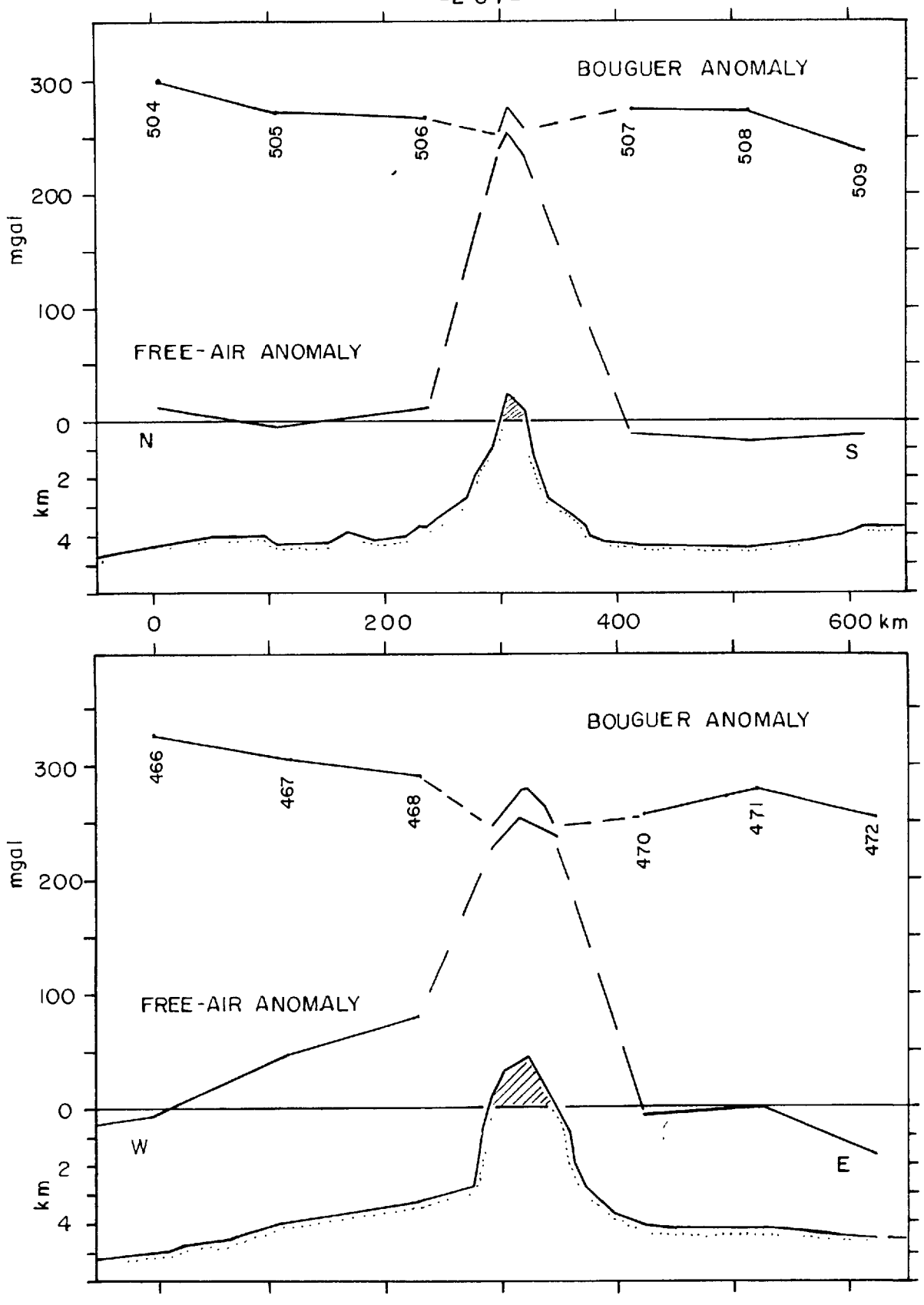

FIG. 7.5. Gravity profiles across Madeira from pendulum gravity stations. Station numbers are from Vening Meinesz (1948).

are used as the basis of the two profiles across the island, one roughly north-south, the other east-west, shown in Fig. 7.5.

In calculating the Bouguer anomaly for the marine stations, a density of 2.4 gm/cc was used for the island body and 2.6 gm/cc for the remainder of the ocean crust. The choice of these densities has already been discussed at length in Chapters 3 and 5. The gravity effect of the body of the island down to 2200 fathoms was calculated for a density of 2.4 gm/cc using the three-dimensional method of Talwani described in Chapter 2. To this is added the effect of the two-dimensional section taken below a constant depth of 2200 fathoms (4020 m) under the island area. The effect of the two-dimensional section is computed as described in Chapter 2, using a density of 2.6 gm/cc. The value of the Bouguer anomaly over the island is taken from the Bouguer anomaly map, Fig. 7.6.

If it is assumed that the centre of high Bouguer anomaly over the island as seen in Fig. 7.6 is due to a fairly local mass excess, it follows that the background value of the Bouguer anomaly over the island is probably less than 230 mgal. From the west-east Bouguer anomaly profile, the regional field over the island might be expected to be 295 mgal. That it appears some 20 mgal less in the north-south profile may reflect a north-south belt of lower anomaly associated with

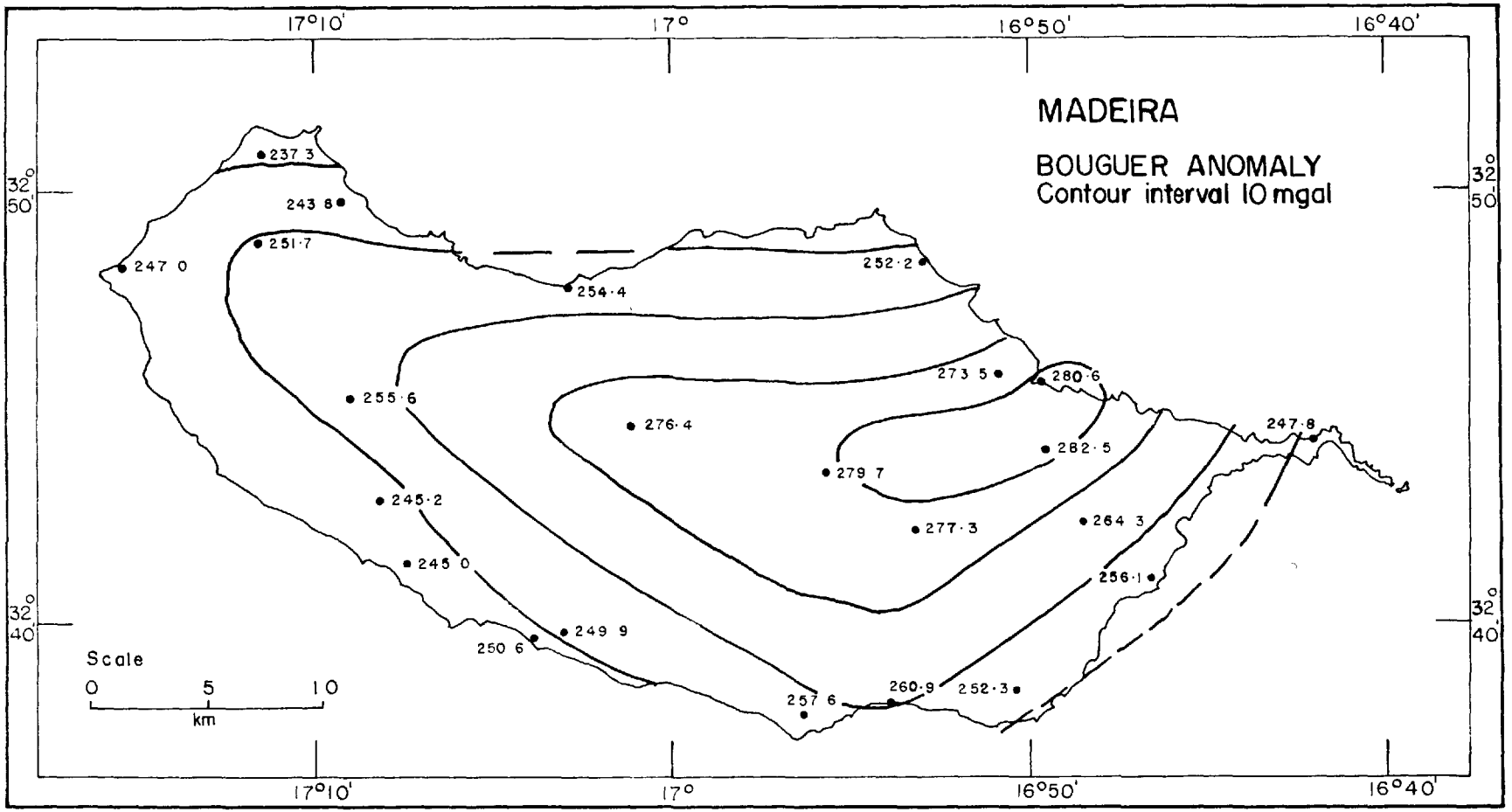
MADEIRA
BOUGUER ANOMALY
Contour interval 10 mgal
17°10'
17°
16°50'
16°40'
32° 50'
32° 40'
237 3
243 8
247 0
251·7
254·4
252·2
273 5
280·6
255·6
276·4
247·8
282·5
279 7
245·2
277·3
264 3
245 0
256·1
249 9
250 6
257 6
260·9
252·3
Scale
0 5 10
km

FIG. 7.6.

the NNE-SSW trending Madeira Rise. In both profiles it is clear that there is a broad regional gravity minimum associated with the island, of at least 50 mgal amplitude and 200-400 km diameter.

The Bouguer anomaly profile is very similar to the regional anomaly observed over Santa Maria. As discussed in that case, the mass deficit indicated by this minimum in the Bouguer anomaly must arise from a thickening of the crust or from some lower density material in the mantle. As the island is far from the axial zone of the Mid-Atlantic Ridge, which is the only region where such low density material has been observed, it seems more likely that the lower anomaly is caused by a thickening of the crust under the island such as has been observed in the Hawaiian Islands (Worzel and Harrison, 1963). If the densities of 2.9 gm/cc and 3.4 gm/cc are adopted for the lower crustal layer and mantle respectively and the thickening of the crust is considered to take the form of a bowl-shaped depression of the mantle, of diameter 300 km, then an anomaly of 50 - 60 mgal implies a crustal thickening of approximately 3 km.

This is a clear example of regional compensation but the regional gravity data are inadequate to determine whether or not complete isostatic equilibrium has been attained.

7.2.5 Local Anomaly. The topography of the island and the distribution of the gravity stations are shown in Fig. 7.4 and the Bouguer anomaly values and contours in Fig. 7.6.

There is a marked centre of high Bouguer anomaly of value 287 mgal in the east of the island, strongly elongated towards the west along the main topographic trend of the island. The gravity centre is interpreted as indicating the main volcanic and magmatic centre, and the westward extension of the anomaly as representing a rift zone which has given rise to the upland backbone of the island. Gravity stations in the area are few, but the Bouguer anomaly suggests that there is another rift zone trending southwards from the main centre.

If it is assumed that the volcanic centre gave rise to a mighty volcano above it, such as is observed on Tenerife, then the extension of the centre as indicated by the Bouguer anomaly beyond the present coastline implies that a considerable part of the volcanic structure has now disappeared. In similar situations which exist in Gran Canaria and Hierro, the disappearance of part of the volcano was attributed to tectonic displacement, and the same mechanism probably operated in this instance.

If the trend of the gravity anomaly is continued to the north-east, it is found to pass through Porto Santo, which lies 45 km away to the north-east. This may represent a rift zone, or it is possible that Madeira is only the western part of what was a much larger island which extended as far as

Porto Santo. The deep channel between the two islands must make this latter interpretation highly speculative.

The absolute value of the maximum Bouguer anomaly is similar to that observed on Fernando de Noronha, Gran Canaria and Tenerife. The amplitude of the island anomaly cannot be accurately determined but it must be greater than 45 mgal, the range of Bouguer anomaly observed on the island. Experience in the Azores and Canary Islands shows that the regional field as indicated by the marine gravity data is approximately 30 - 40 mgal less than the minimum value observed on the island. On this basis the amplitude of the anomaly may be as much as 90 mgal. This is less than the anomalies observed on the Canary Islands but greater than the maximum anomalies observed in the Azores.

CHAPTER 8

GRAVITY OBSERVATIONS BY THE PORTUGUESE SERVICO METEOROLÓGICO NACIONAL

The Portuguese Servico Nacional has kindly made available the results of their gravity surveys on the Cape Verde Islands. Gravity observations on the islands of S. Tomé and Príncipe in the Gulf of Guinea have already been published by the same Portuguese authority in their publication GEO No.107, 1966, and are included here with their gracious permission.

Lack of time and space forbids any detailed interpretation of these gravity data and they are included here primarily for the sake of comparison and completeness. With these islands we have gravity data for 25 of the 37 major oceanic islands in the Atlantic and gravity surveys on some islands in each of the Atlantic oceanic island groups.

8.1 The Cape Verde Islands.

8.1.1 Introduction. The Cape Verde Archipelago (Fig. 8.1) is situated in the Atlantic Ocean some 600 km west of Dakar on the coast of West Africa. The total area is 4055 km^2 comprising 10 major islands and 5 islets which form three sides of a square with the open side on the west.

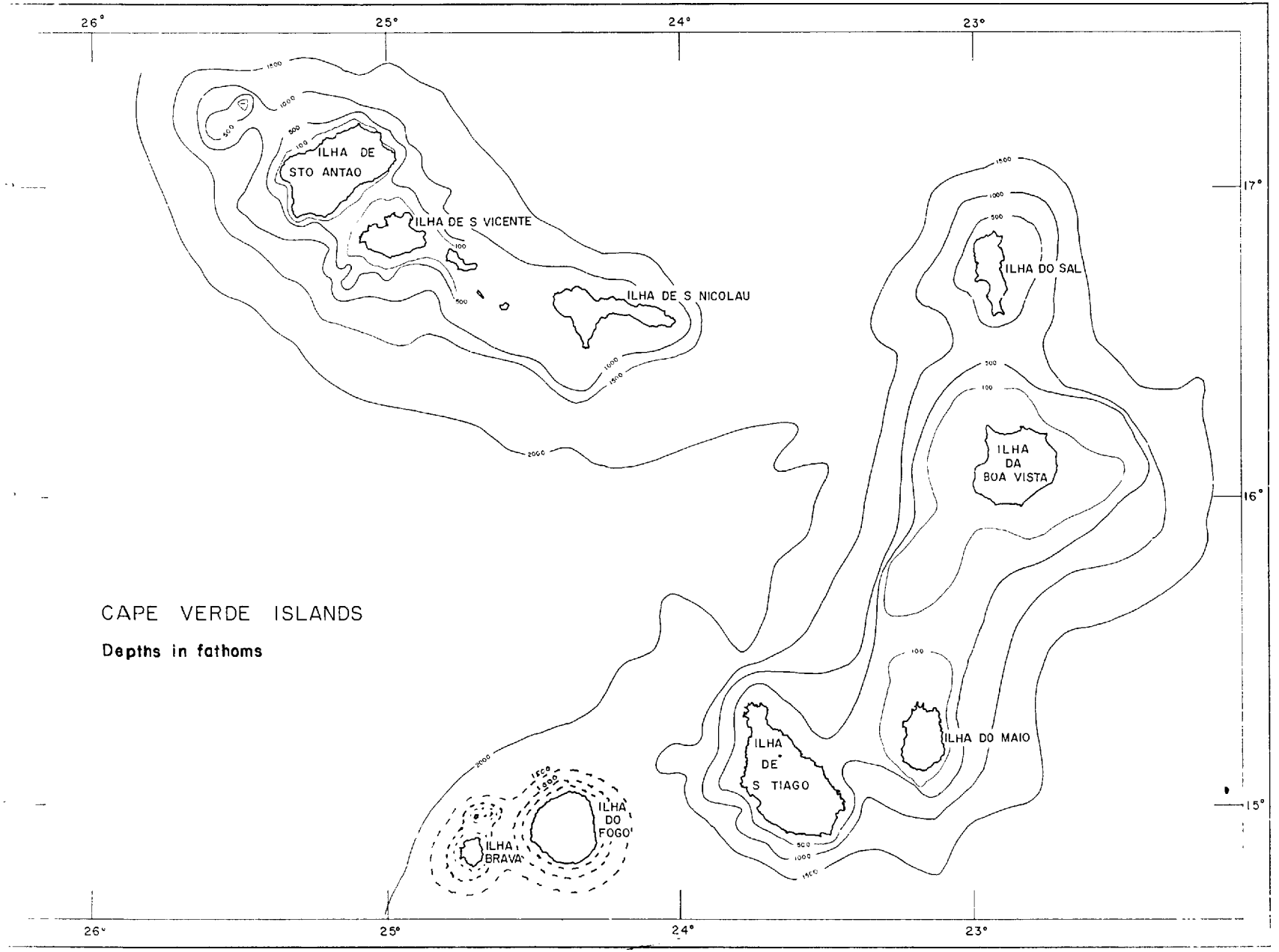
26°
25°
24°
23°
17°
16°
15°
ILHA DE STO ANTAO
ILHA DE S VICENTE
ILHA DE S NICOLAU
ILHA DO SAL
ILHA DA BOA VISTA
ILHA DE S TIAGO
ILHA DO MAIO
ILHA DO FOGO
ILHA BRAVA
CAPE VERDE ISLANDS
Depths in fathoms

FIG. 8.1.

The islands are separated from the African mainland by depths of over 3000 m and are surrounded on the other three sides by the Cape Verde Abyssal Plain at depths of over 4000 m which increase to over 6000 m in the west. The bathymetry in the vicinity of the islands as contoured in Fig. 8.1 is compiled from the Admiralty Chart No. 366 and the 1:1,000,000 plotting sheets of collected soundings Nos. 155 and 156, produced by the National Hydrographic Office. It shows that the islands can be sub-divided into three groups each enclosed by the 1500 fathoms (2740 m) contour.

8.1.2 General Geology. The geomorphology of the islands is very varied and ranges from the very young uneroded volcano of Fogo through the deeply dissected mountains of S. Antao and Santiago to the flat, low-lying islands of Maio, Boa Vista and Sal.

The islands are composed primarily of basic volcanic materials and are unique among the islands studied here in that marine sedimentary strata have been laid down between the successive stages of volcanic activity and been exposed by subsequent uplift. This uplift has been considerable. Friedlander (1913) described raised beaches at 150, 280, 350 and 500 m above sea-level.

The most comprehensive account of the islands is that of Bebiano (1932). In it, he described a general succession

for the island of Maio which appears to hold good, with minor local variations, throughout the archipelago (Part, 1950).

The oldest observed volcanic series, comprising slightly alkaline olivine-basalt and pyroclastics, is underlain by limestones and grits of the Cretaceous era (Stahlecker, 1935; Bebiano and Pires Soares, 1951) and overlain by clays and limestones of Miocene age (Sousa Torres and Pires Soares, 1946, 1950). Renewal of volcanic activity in the late Tertiary took the form of more basalts and also trachytes, phonolites and intrusions of other soda-rich rocks. After a period of quiescence, a reversion to more basic volcanic activity in Quaternary and Recent times brought the sequence to a close. Fogo, on which historic eruptions have occurred as recently as 1951, is the only island still volcanically active.

The markedly linear distribution of the islands, and evidence for folding on S. Antão and S. Nicolau, have lead Bebiano (1932) to suggest that the distribution of the islands may be controlled by a system of major faults and folds as drawn in Fig. 8.2. He considers that the main factor influencing the geological history of the archipelago has been isostatic crustal adjustment in a belt parallel to the coast following the great accumulation of sediments in the seas bordering on West Africa during and since Tertiary times.

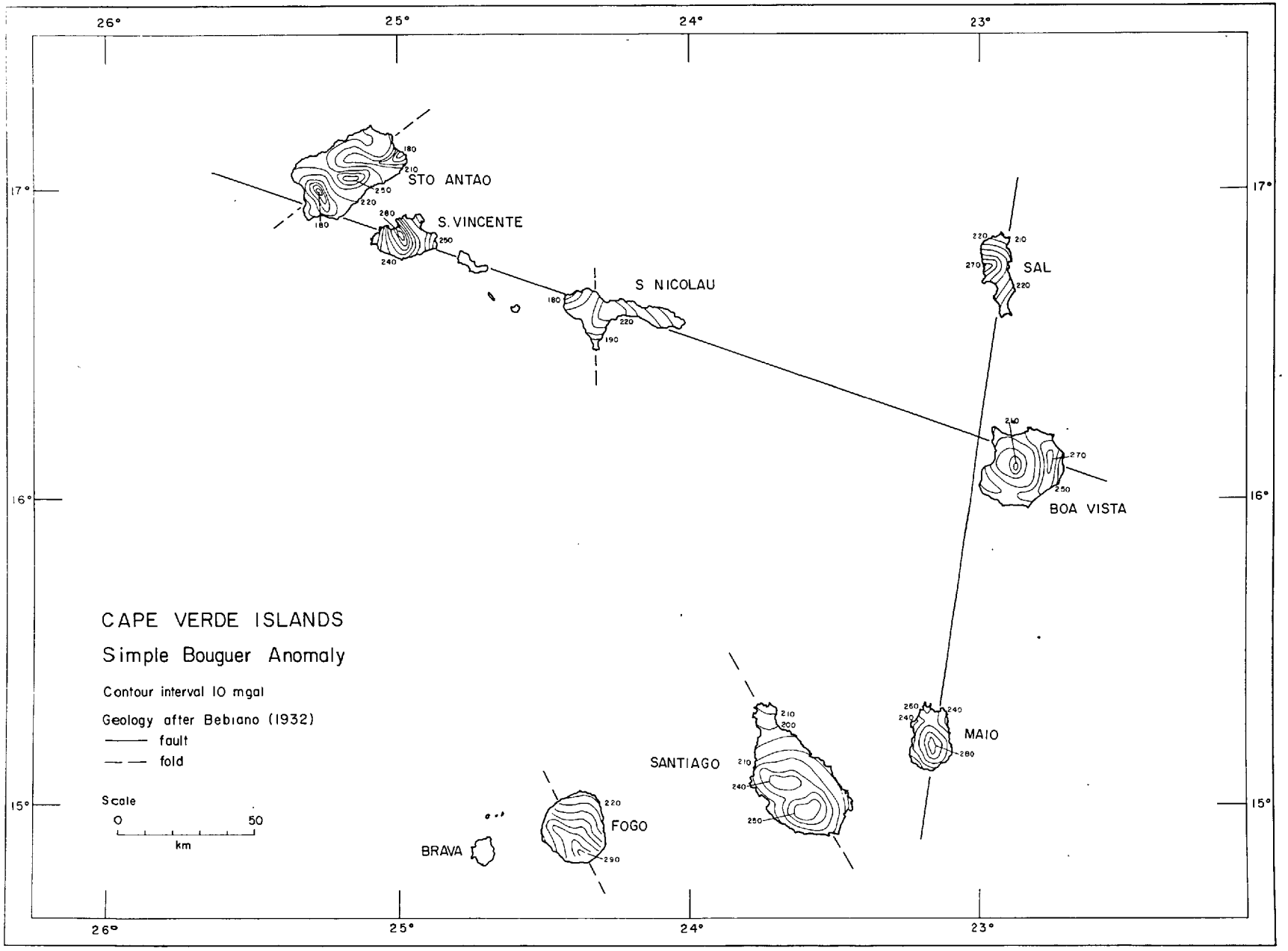
26°
25°
24°
23°
17°
16°
15°
STO ANTAO
S. VINCENTE
S NICOLAU
SAL
BOA VISTA
MAIO
SANTIAGO
FOGO
BRAVA
CAPE VERDE ISLANDS
Simple Bouguer Anomaly
Contour interval 10 mgal
Geology after Bebiano (1932)
fault
fold
Scale
0
50
km

FIG. 8.2

8.1.3 Details of the Data Reduction. The observed gravity values and the station elevations and locations are all as presented by the Servico Meteorológico Nacional. The station elevations were determined from triangulation points, from topographic maps and by barometric methods, and are estimated by the Portuguese to be accurate to ± 5 m. No error estimate is available for the observed gravity, but it is unlikely to be greater than 1 mgal.

No terrain correction has been applied and only the Simple Bouguer anomaly, calculated for a density of 2.3 gm/cc is presented for each island. The elevation error corresponds to an error of ± 1 mgal so that the total error in the Simple Bouguer anomaly is probably ± 2 mgal though terrain effects will introduce a distortion of the gravity picture which may be severe on some of the mountainous islands.

8.1.4 Regional Anomaly. Fig. 8.3 shows a gravity profile which crosses the archipelago between S. Antão and S. Vicente and extends 500 km NNE and 500 km south-west from S. Vicente. The profile is compiled from a line of pendulum gravity stations established by Vening Meinesz (1948).

The free-air anomaly has the familiar form of a small negative anomaly at some distance from the island changing rapidly to a large positive value on the island. As discussed in the chapter on Ascension Island, this can be interpreted

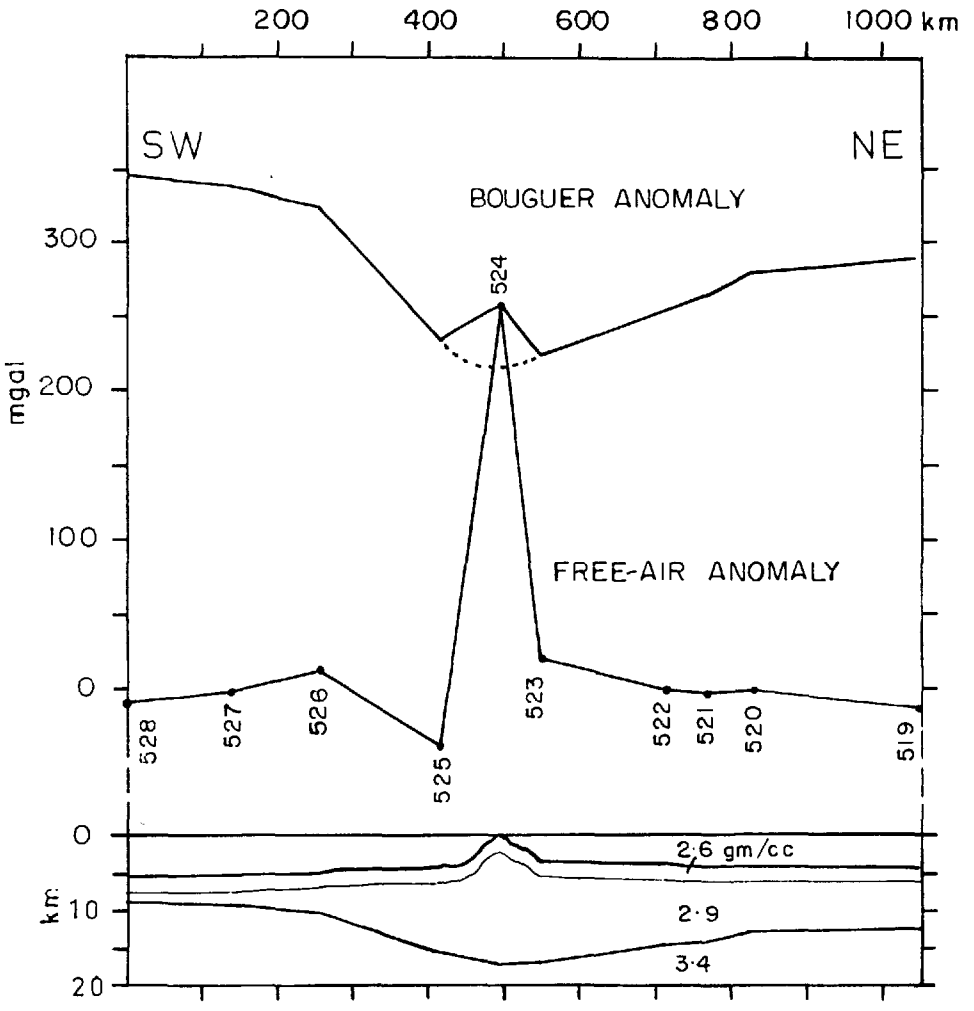

FIG 8·3. Gravity profile and possible structure across the Cape Verde Islands. Station numbers are from Vening Meinesz (1948).

as indicating some degree of regional isostatic compensation for the island.

The existence of a compensating mass is more clearly demonstrated by the Bouguer anomaly which was calculated by applying a two-dimensional correction for the water layer as described in Chapter 2, using a density of 2.6 gm/cc. The Bouguer anomaly decreases gradually as the continent is approached and superimposed on this regional trend a broad gravity low of approximately 90 mgal amplitude and 600 km diameter can be seen centred on the Cape Verde Islands.

The depth to the Moho was calculated, as described in Chapter 2, on the assumption that the isostatic compensation is achieved by a thickening of the crust. A simplified two-layer model of the crust was used, the upper layer of density 2.6 gm/cc and thickness 2 km and the lower layer of density 2.9 gm/cc. The complete structure section calculated is depicted in Fig. 8.3 and shows a depth to the Moho of 17 km under the islands.

The gravity data are insufficient for it to be possible to decide whether or not complete isostatic equilibrium has been attained but the history of emergence of the islands suggests that they are likely to be overcompensated rather than the reverse.

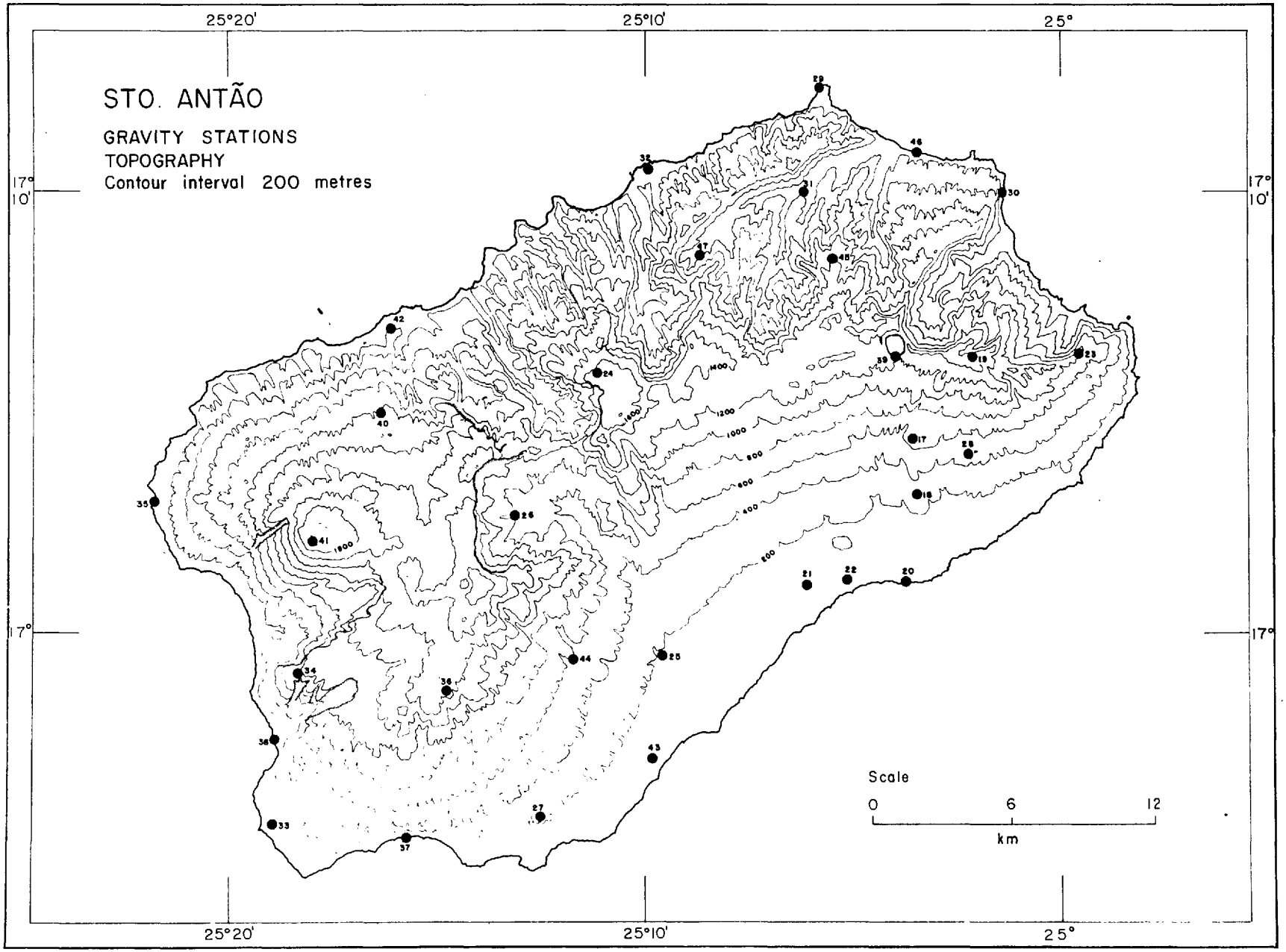
STO. ANTÃO
GRAVITY STATIONS
TOPOGRAPHY
Contour interval 200 metres
25°20'
25°10'
25°
17° 10'
17°
Scale
0
6
12
km

FIG. 8.4.

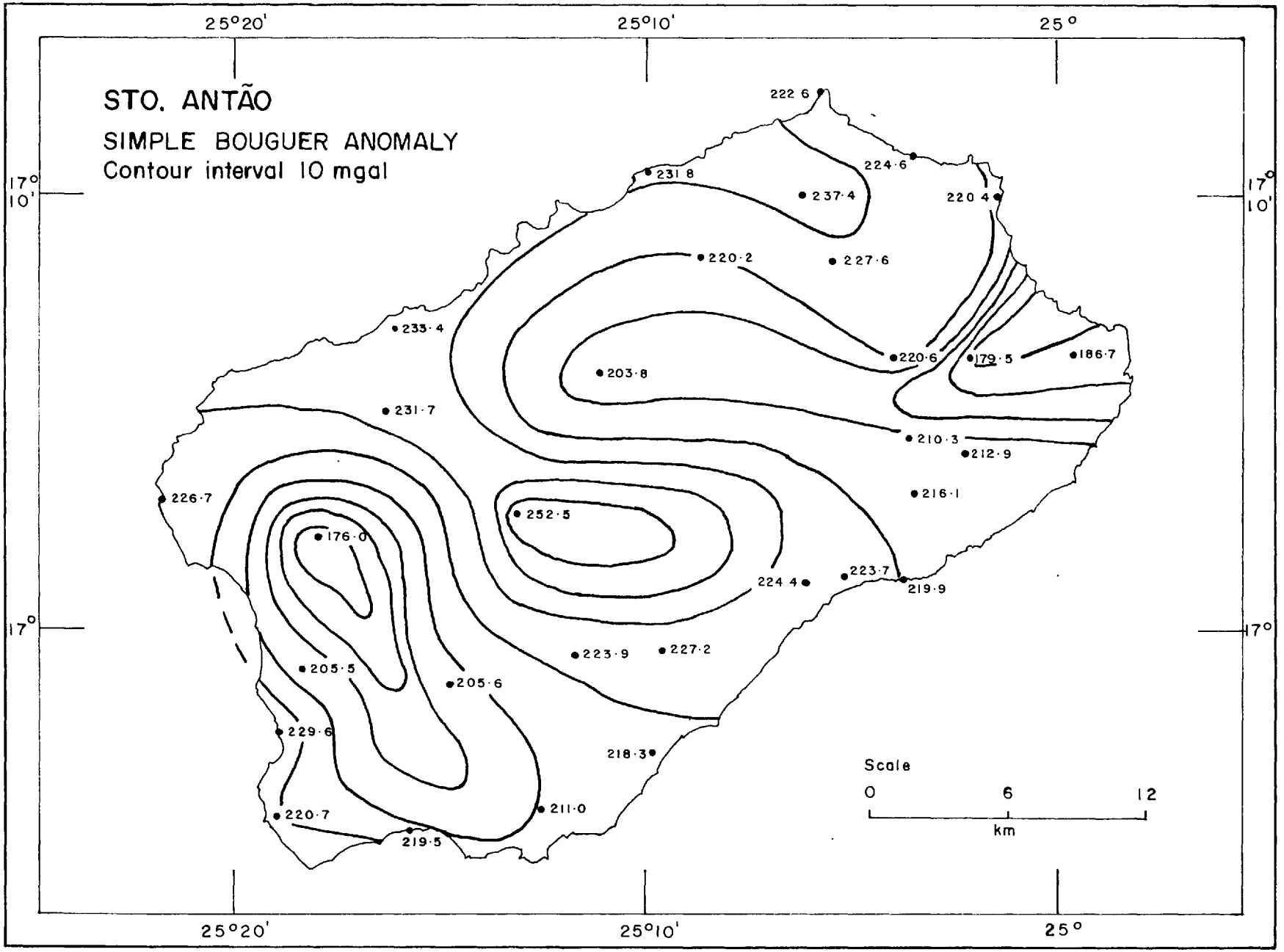
STO. ANTÃO
SIMPLE BOUGUER ANOMALY
Contour interval 10 mgal
25°20'
25°10'
25°
17° 10'
17°
222 6
224·6
231 8
237·4
220 4
220·2
227·6
233·4
220·6
179·5
186·7
203·8
231·7
210·3
212·9
226·7
216·1
252·5
176·0
224 4
223·7
219·9
223·9
227·2
205·5
205·6
229·6
218·3
220·7
211·0
219·5
Scale
0
6
12
km

FIG. 8.5.

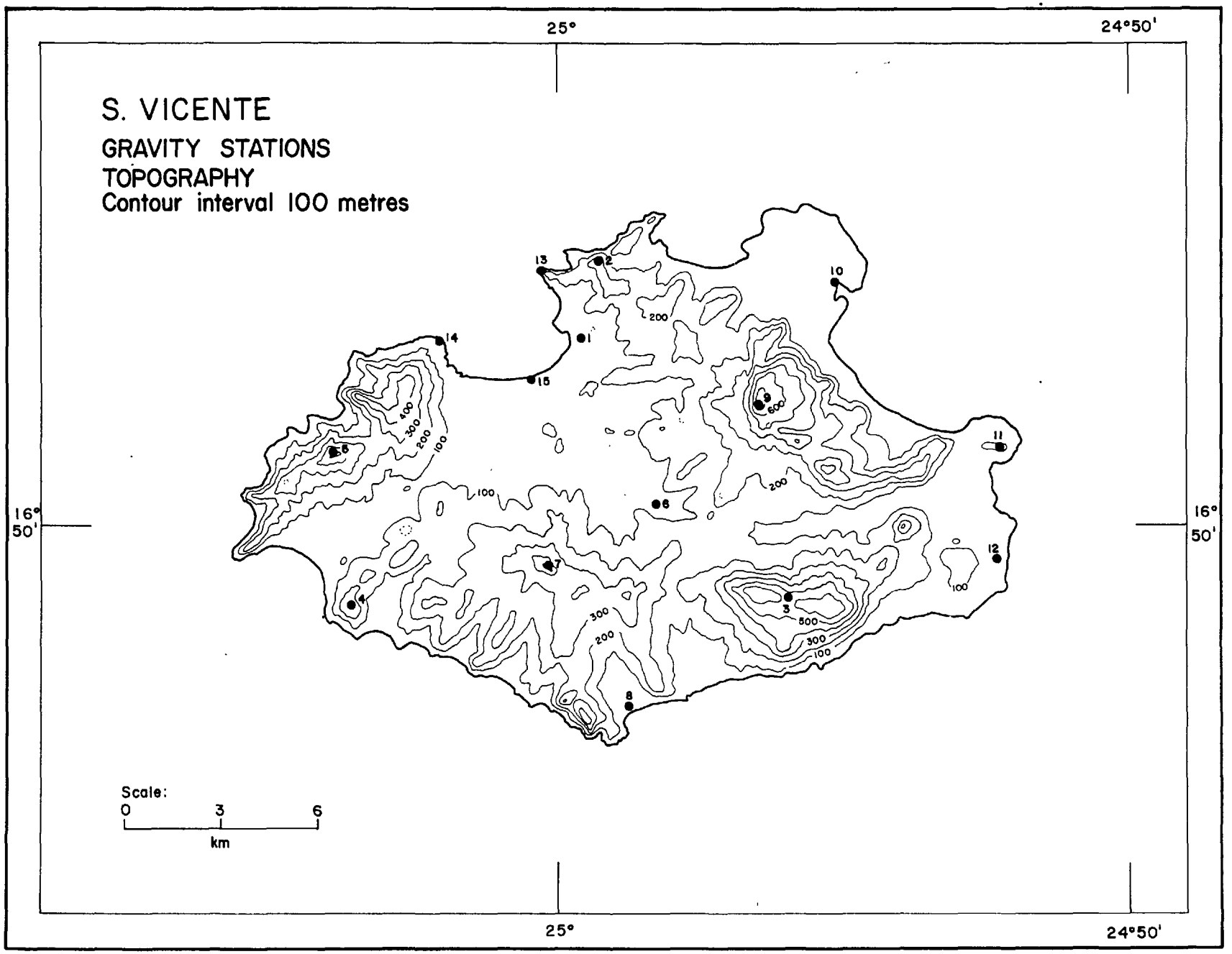
S. VICENTE
GRAVITY STATIONS
TOPOGRAPHY
Contour interval 100 metres
25°
24°50'
16°
50'
Scale:
0
3
6
km

FIG. 8.6.

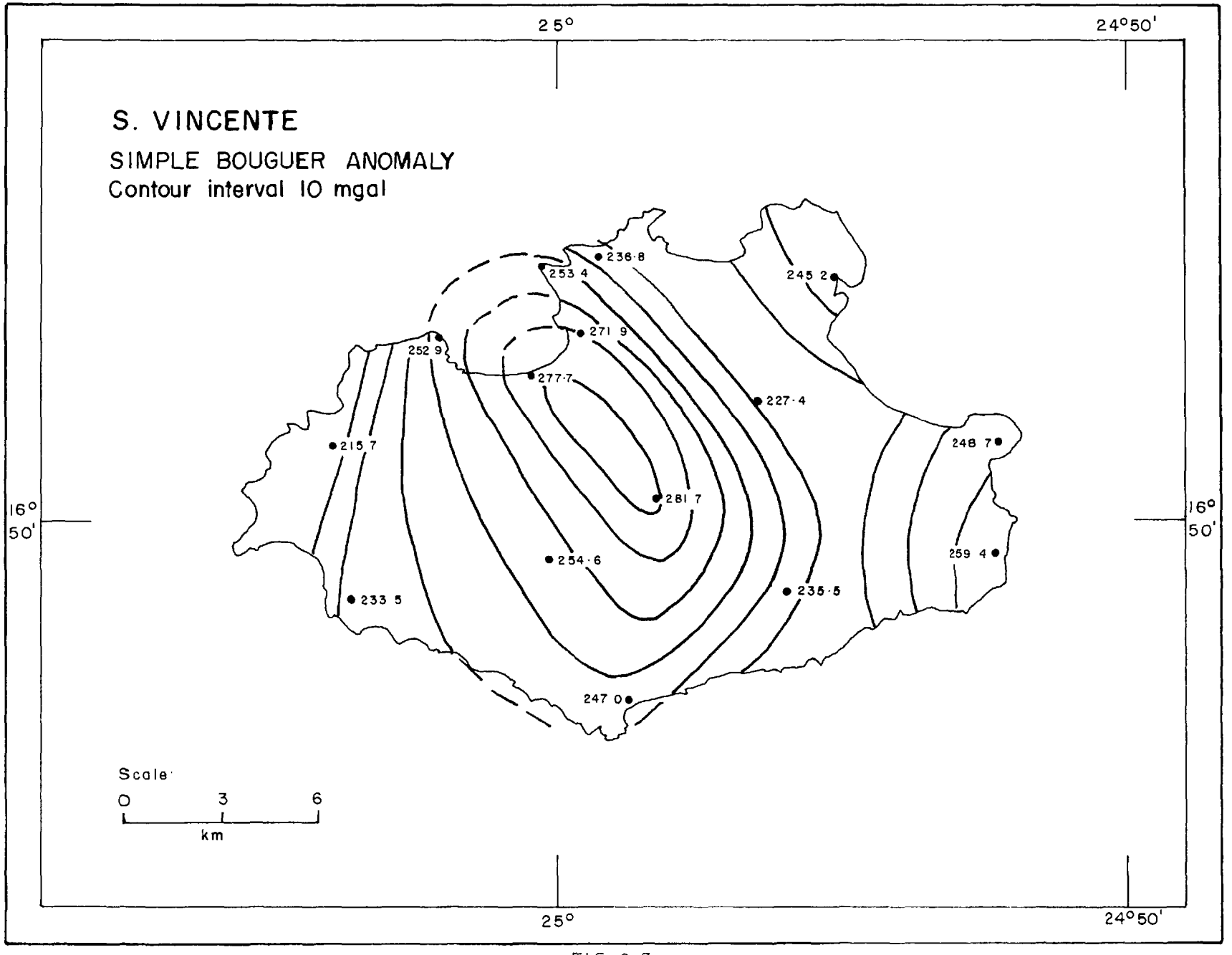
25°
24°50'
S. VINCENTE
SIMPLE BOUGUER ANOMALY
Contour interval 10 mgal
236·8
253 4
245 2
271 9
252 9
277·7
227·4
215 7
248 7
281 7
16° 50'
254·6
259 4
233 5
235·5
247 0
Scale
0 3 6
km
25°
24°50'

FIG. 8.7

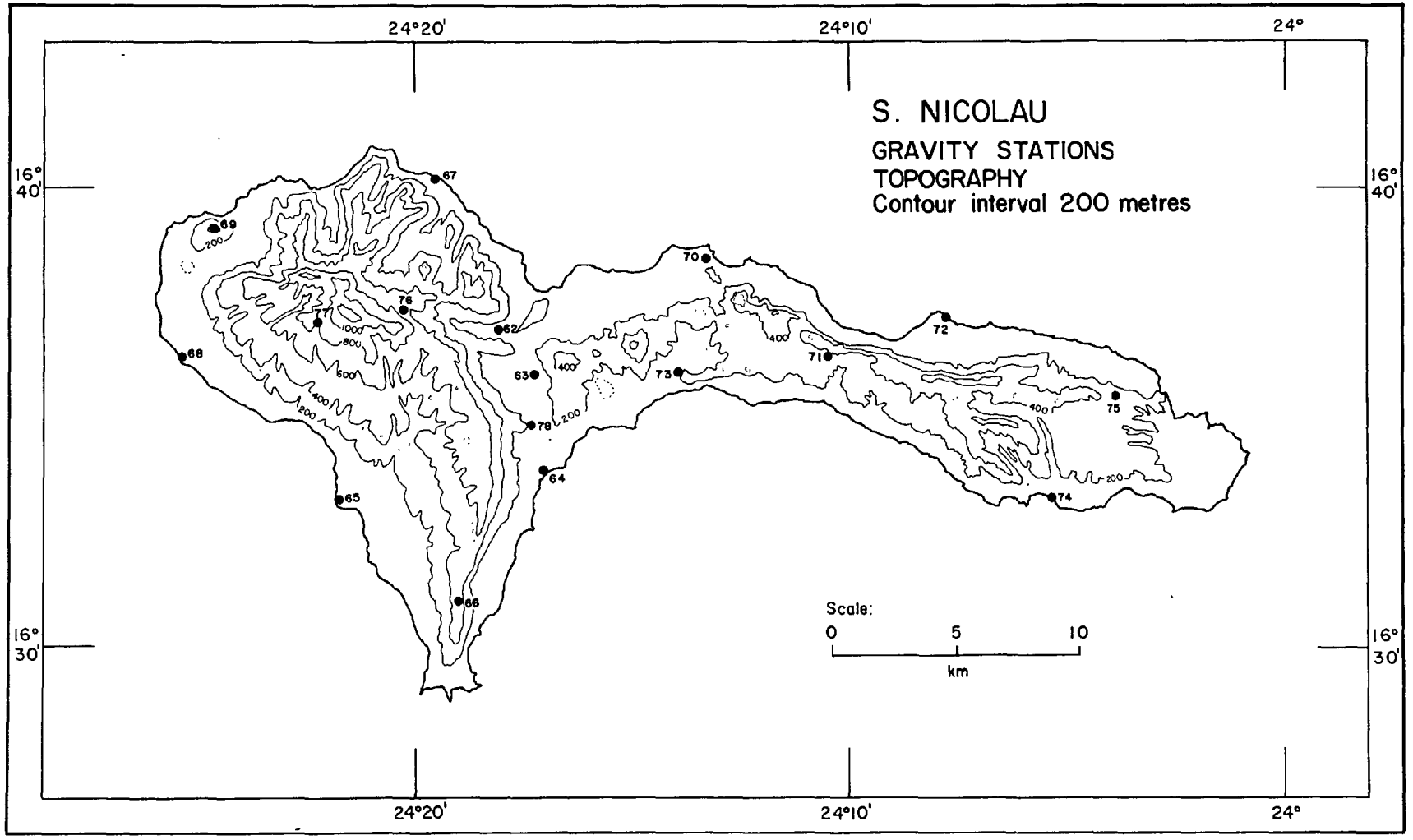
S. NICOLAU
GRAVITY STATIONS
TOPOGRAPHY
Contour interval 200 metres
24°20'
24°10'
24°
16° 40'
16° 30'
Scale:
0
5
10
km
67
69
70
76
77
62
72
68
63
71
73
75
78
64
74
65
66

FIG. 8.8.

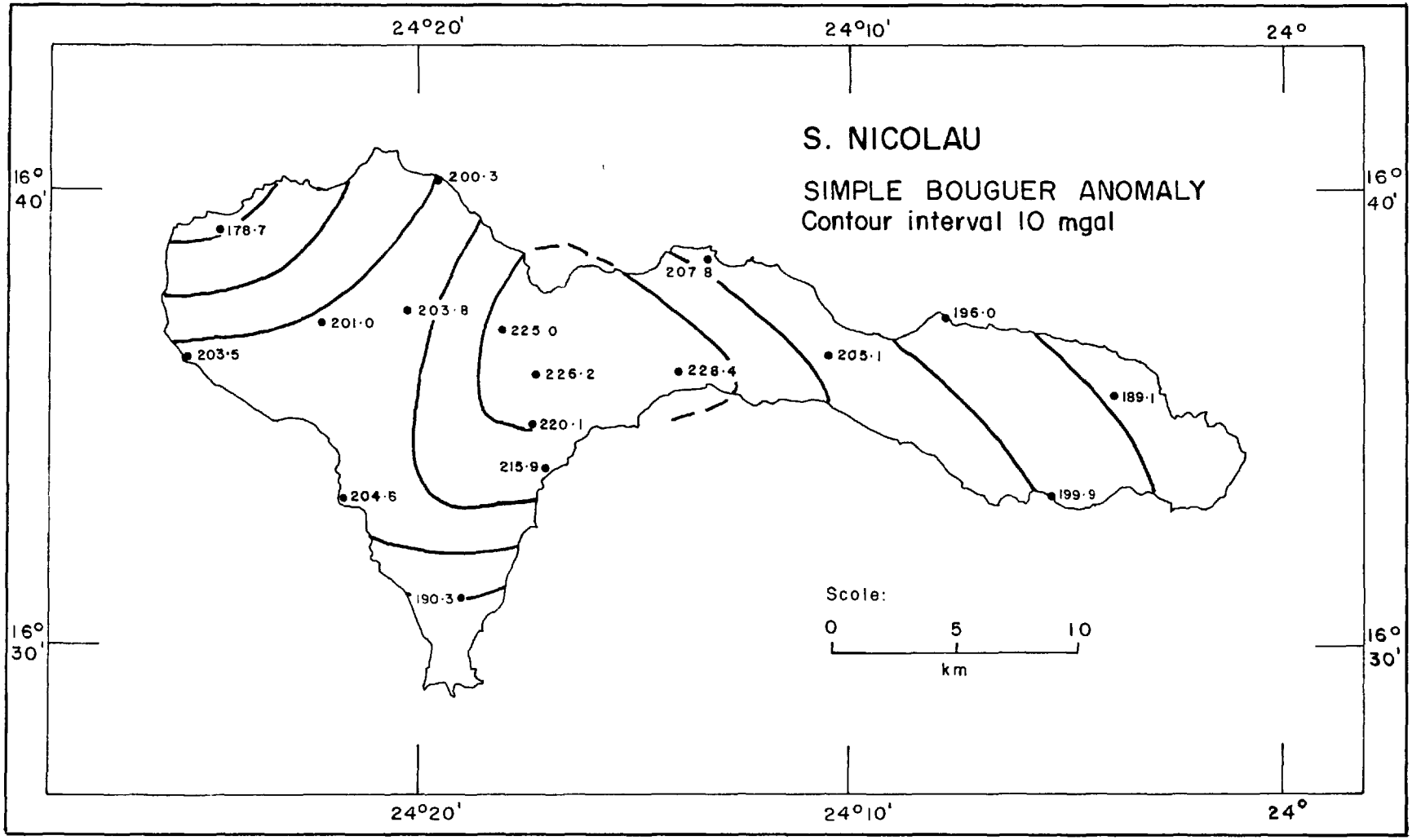
24°20'
24°10'
24°
16° 40'
16° 30'
S. NICOLAU
SIMPLE BOUGUER ANOMALY
Contour interval 10 mgal
200·3
178·7
201·0
203·8
225 0
207 8
196·0
203·5
226·2
228·4
205·1
189·1
220·1
215·9
204·6
199·9
190·3
Scale:
0
5
10
km

FIG. 8.9.

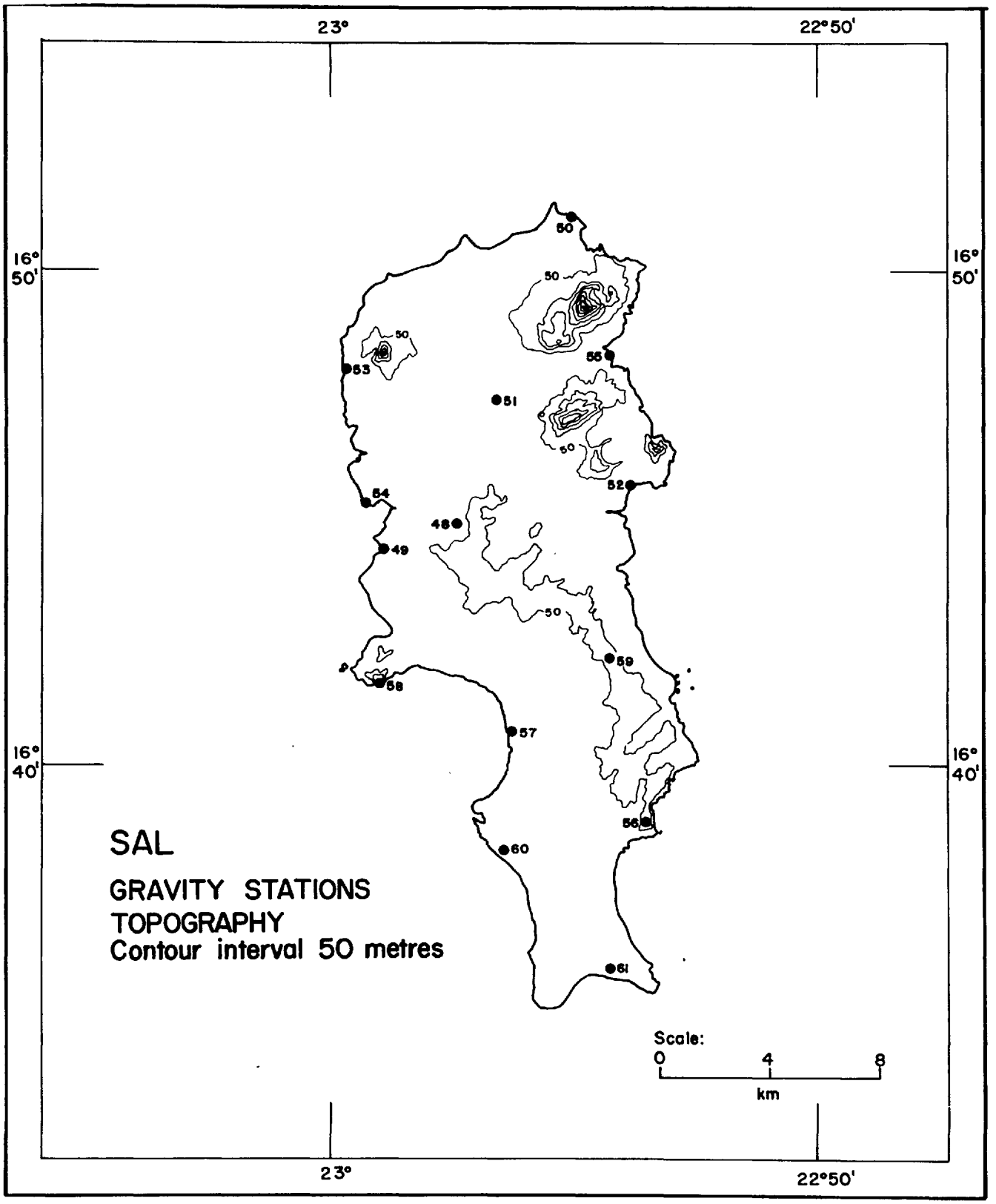
23°
22°50'
16° 50'
16° 40'
50
50
50
50
50
50
63
55
51
52
54
48
49
59
58
57
56
60
61
SAL
GRAVITY STATIONS
TOPOGRAPHY
Contour interval 50 metres
Scale:
0
4
8
km

FIG. 8.10.

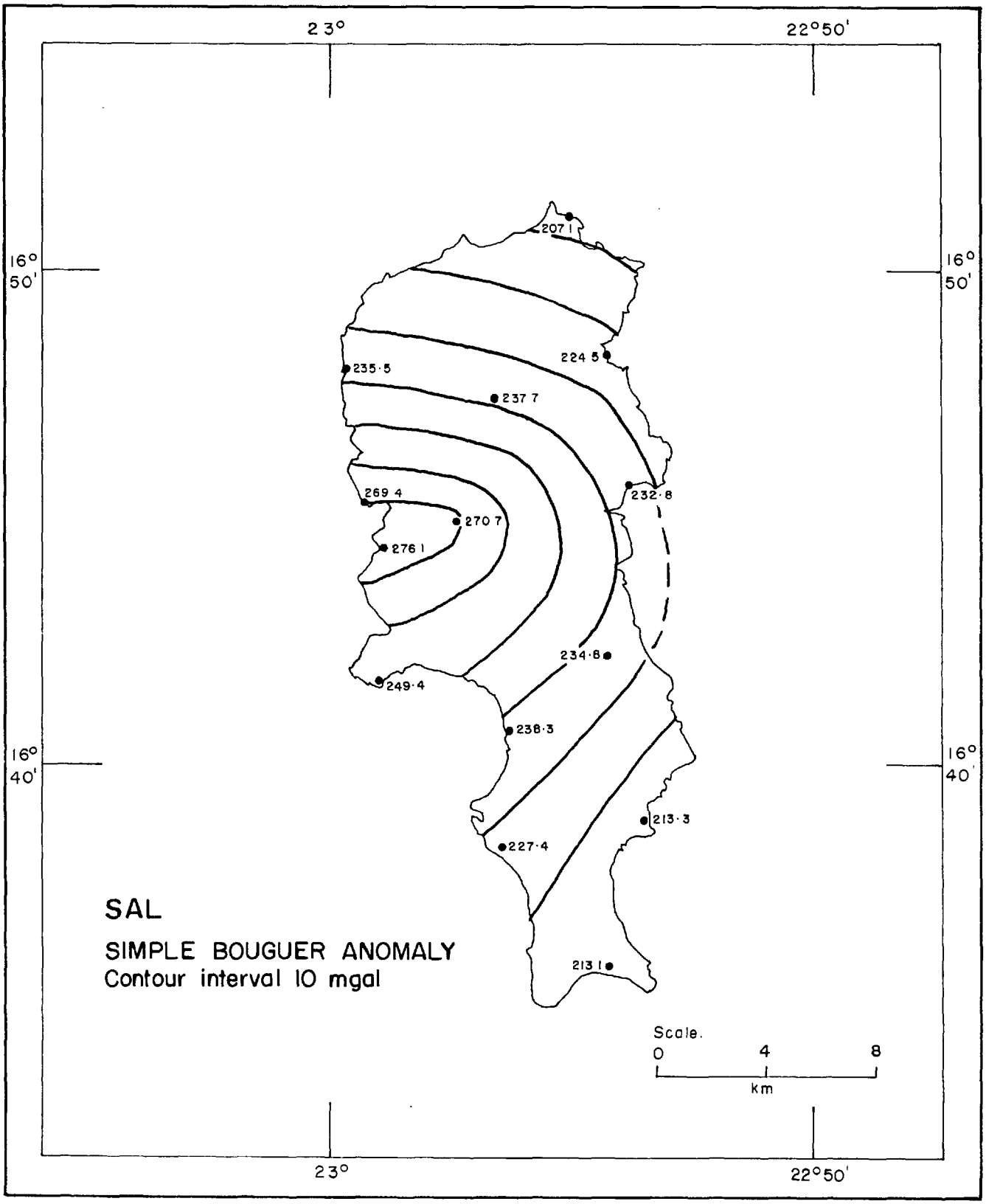
23°
22°50'
16° 50'
16° 40'
207·1
224·5
235·5
237·7
269·4
270·7
276·1
232·8
234·8
249·4
238·3
213·3
227·4
213·1
SAL
SIMPLE BOUGUER ANOMALY
Contour interval 10 mgal
Scale.
0
4
8
km

FIG. 8.11.

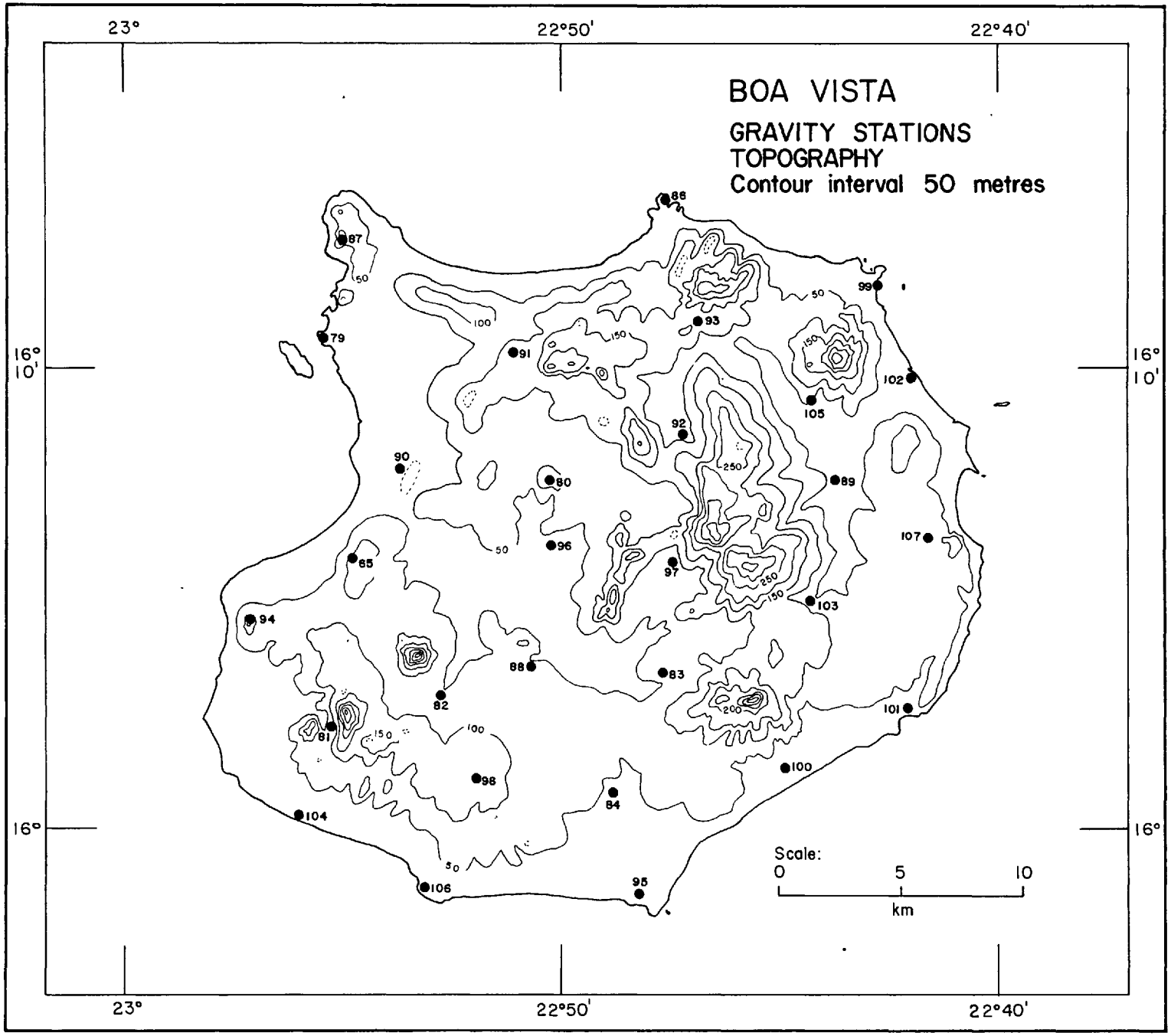
BOA VISTA
GRAVITY STATIONS
TOPOGRAPHY
Contour interval 50 metres
23°
22°50'
22°40'
16° 10'
16°
Scale:
0 5 10
km

FIG. 8.12.

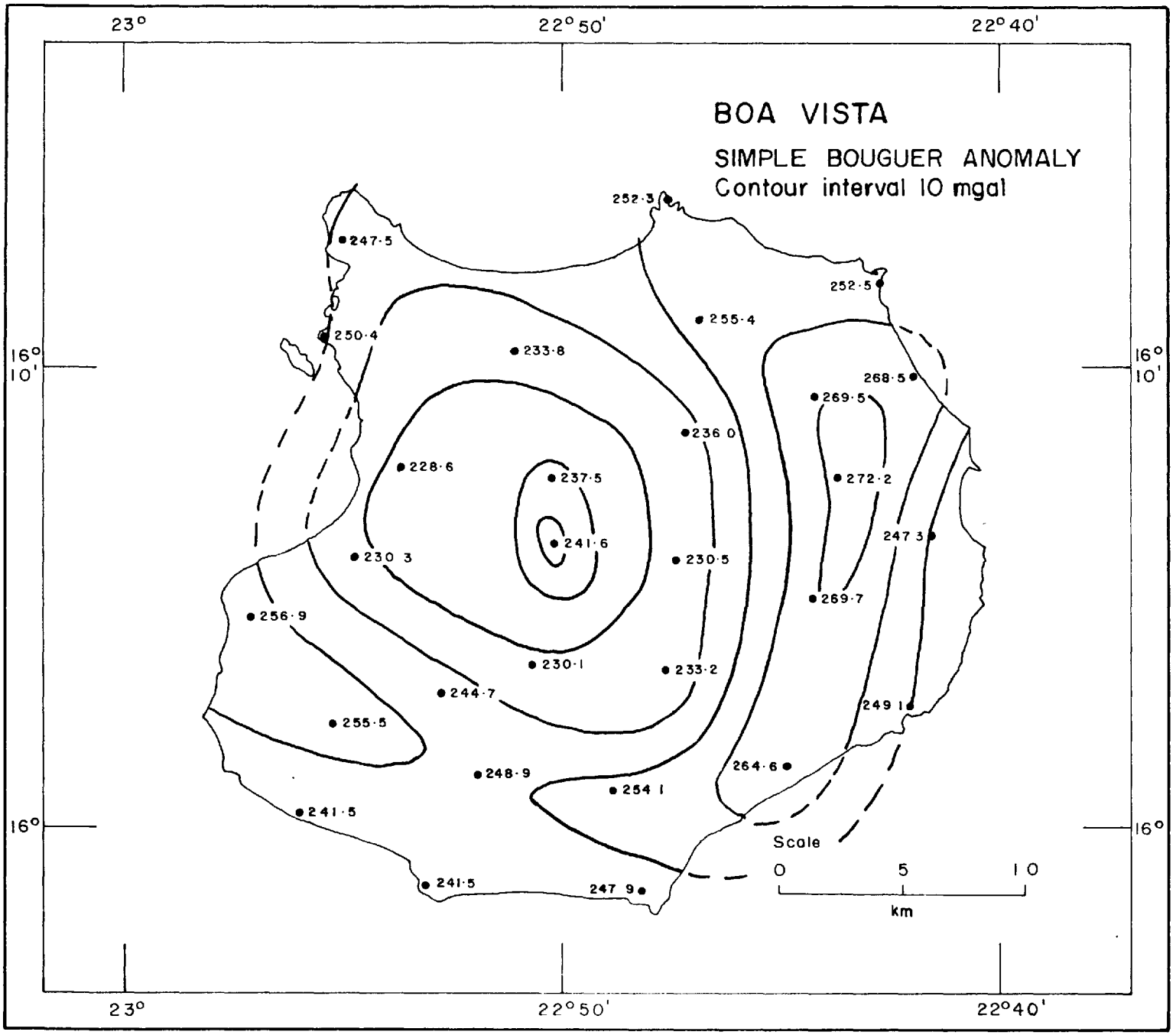
BOA VISTA
SIMPLE BOUGUER ANOMALY
Contour interval 10 mgal
23°
22°50'
22°40'
16° 10'
16°
252·3
247·5
252·5
255·4
250·4
233·8
268·5
269·5
236 0
228·6
237·5
272·2
241·6
247 3
230 3
230·5
269·7
256·9
230·1
233·2
244·7
249 1
255·5
248·9
264·6
254 1
241·5
241·5
247 9
Scale
0 5 10
km

FIG 8.13.

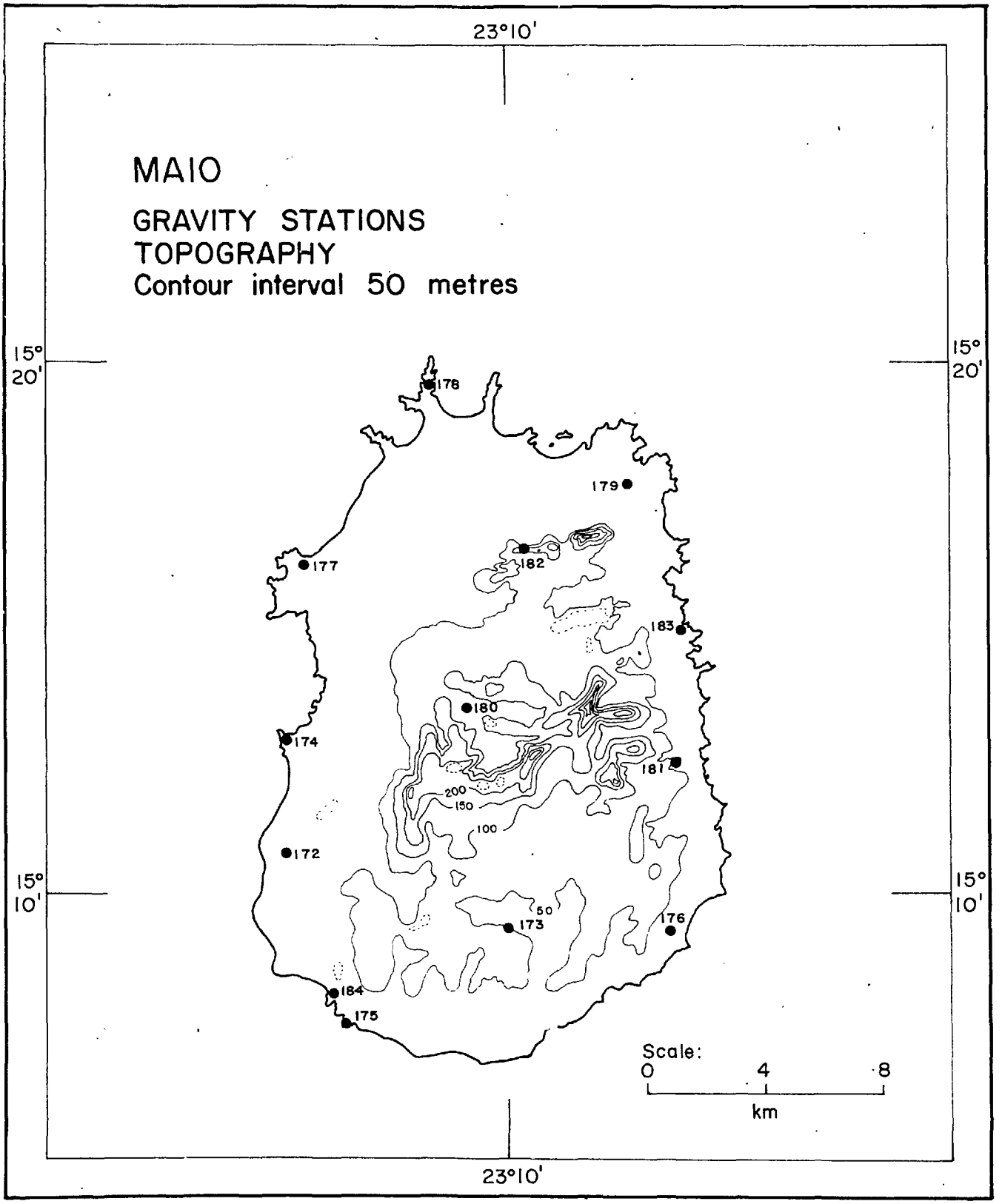
23°10'
MAIO
GRAVITY STATIONS
TOPOGRAPHY
Contour interval 50 metres
15° 20'
15° 10'
178
179
177
182
183
180
174
181
200
150
100
172
50
173
176
184
175
Scale:
0
4
8
km
23°10'

FIG. 8.14.

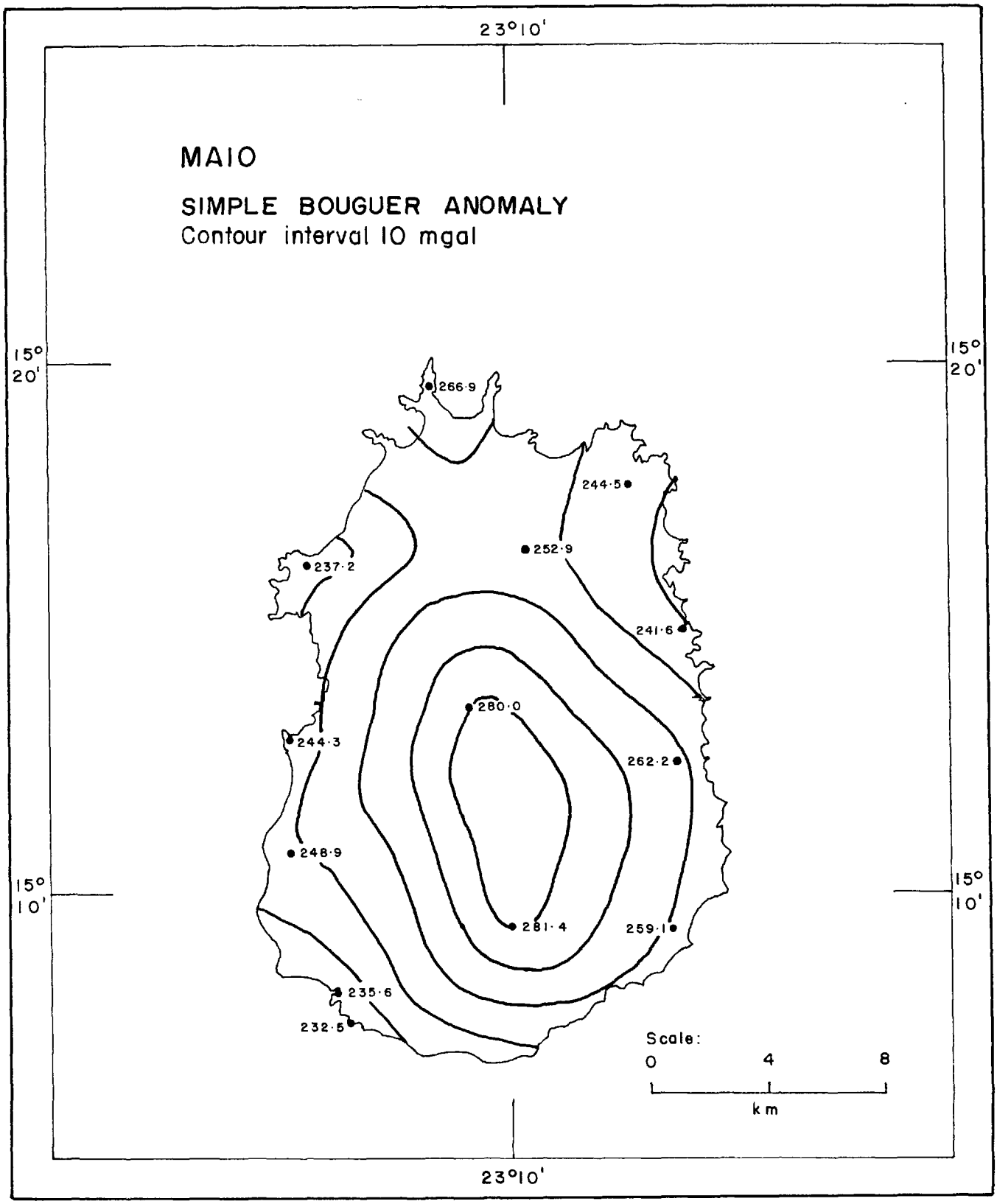
23°10'
MAIO
SIMPLE BOUGUER ANOMALY
Contour interval 10 mgal
15° 20'
15° 10'
266·9
244·5
252·9
237·2
241·6
280·0
244·3
262·2
248·9
281·4
259·1
235·6
232·5
Scale:
0
4
8
km
23°10'

FIG. 8.15.

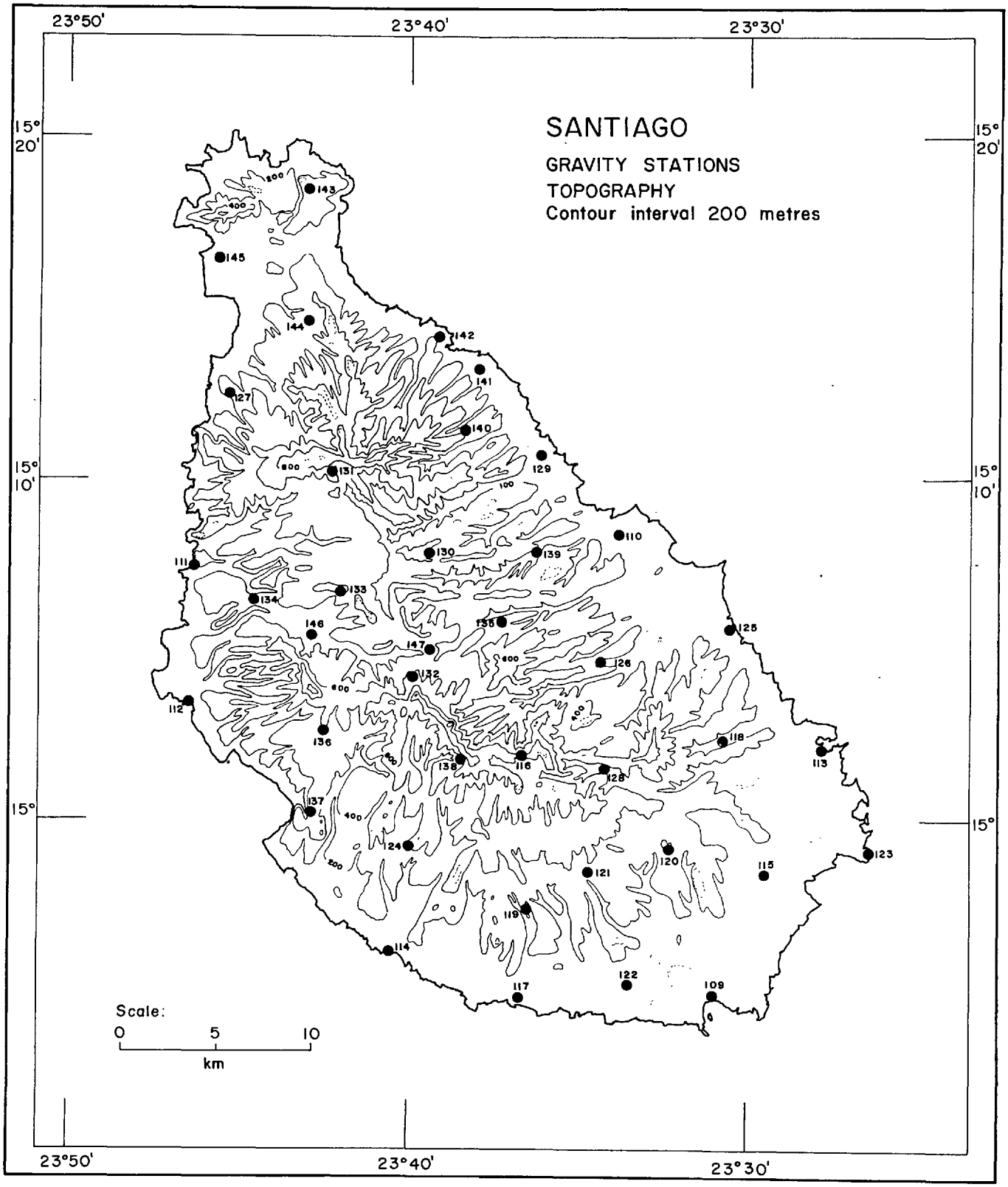
SANTIAGO
GRAVITY STATIONS
TOPOGRAPHY
Contour interval 200 metres
23°50'
23°40'
23°30'
15° 20'
15° 10'
15°
Scale:
0 5 10
km

FIG. 8.16.

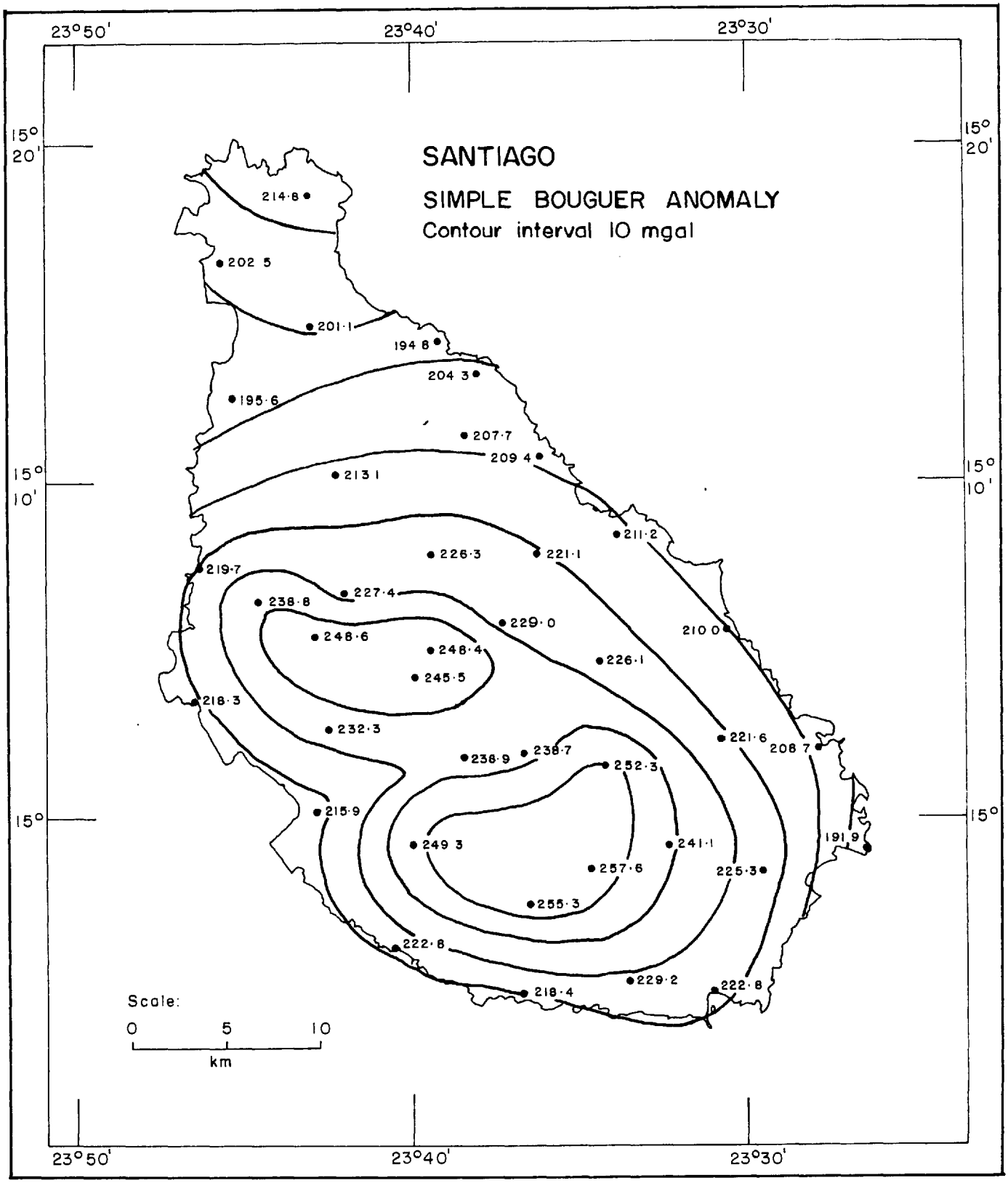
SANTIAGO
SIMPLE BOUGUER ANOMALY
Contour interval 10 mgal
23°50'
23°40'
23°30'
15° 20'
15° 10'
15°
214·8
202 5
201·1
194 8
204 3
195·6
207·7
209 4
213 1
211·2
226·3
221·1
219·7
227·4
238·8
229·0
210 0
248·6
248·4
226·1
245·5
218·3
232·3
221·6
208 7
238·9
238·7
252·3
215·9
249 3
241·1
191·9
257·6
225·3
255·3
222·8
229·2
222·8
218·4
Scale:
0 5 10
km

FIG. 8.17.

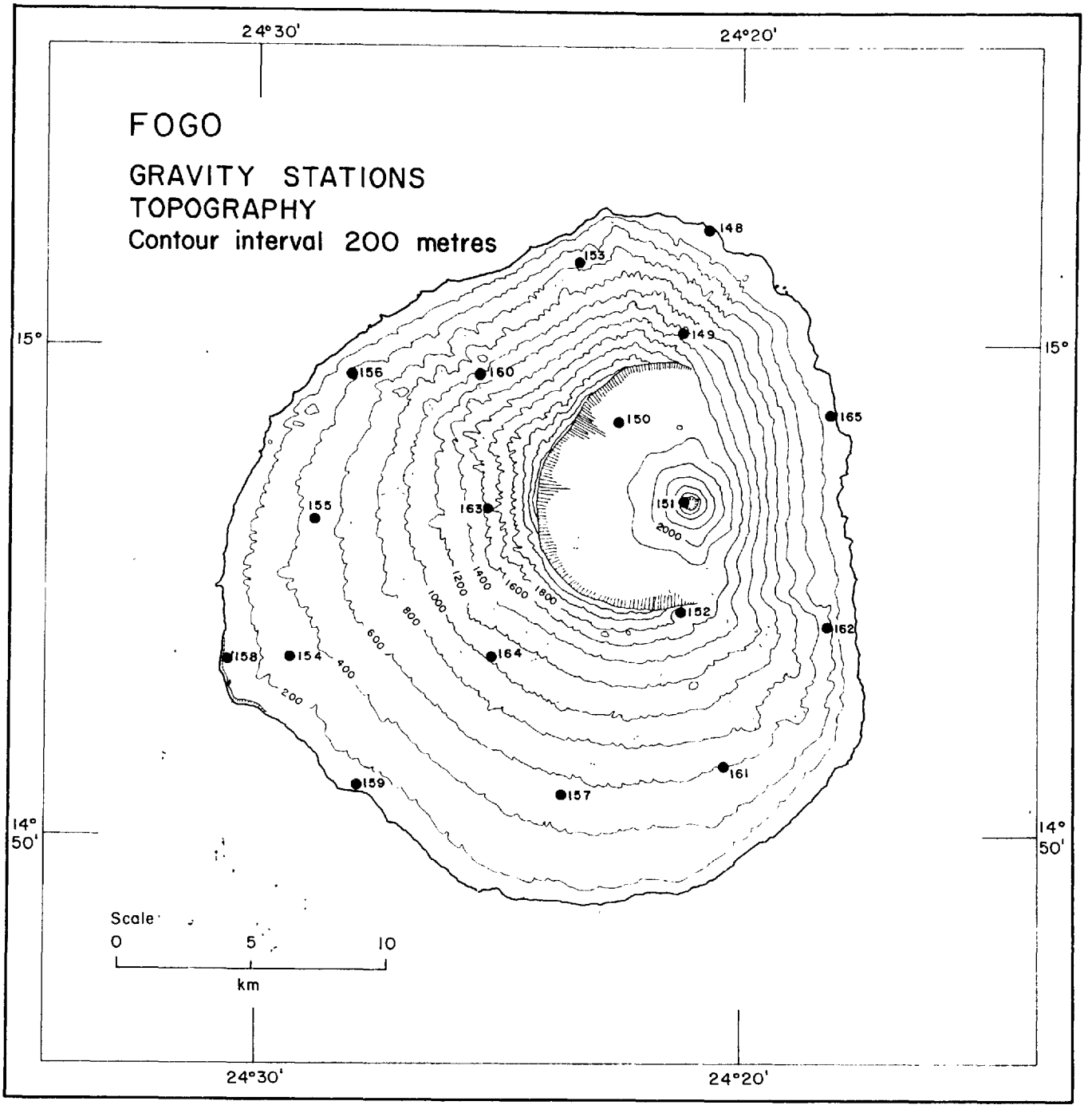
24°30'
24°20'
FOGO
GRAVITY STATIONS
TOPOGRAPHY
Contour interval 200 metres
15°
14° 50'
148
153
149
156
160
150
165
155
163
151
2000
1200
1400
1600
1800
1000
800
600
400
200
152
162
158
154
164
161
159
157
Scale
0
5
10
km

FIG. 8.18.

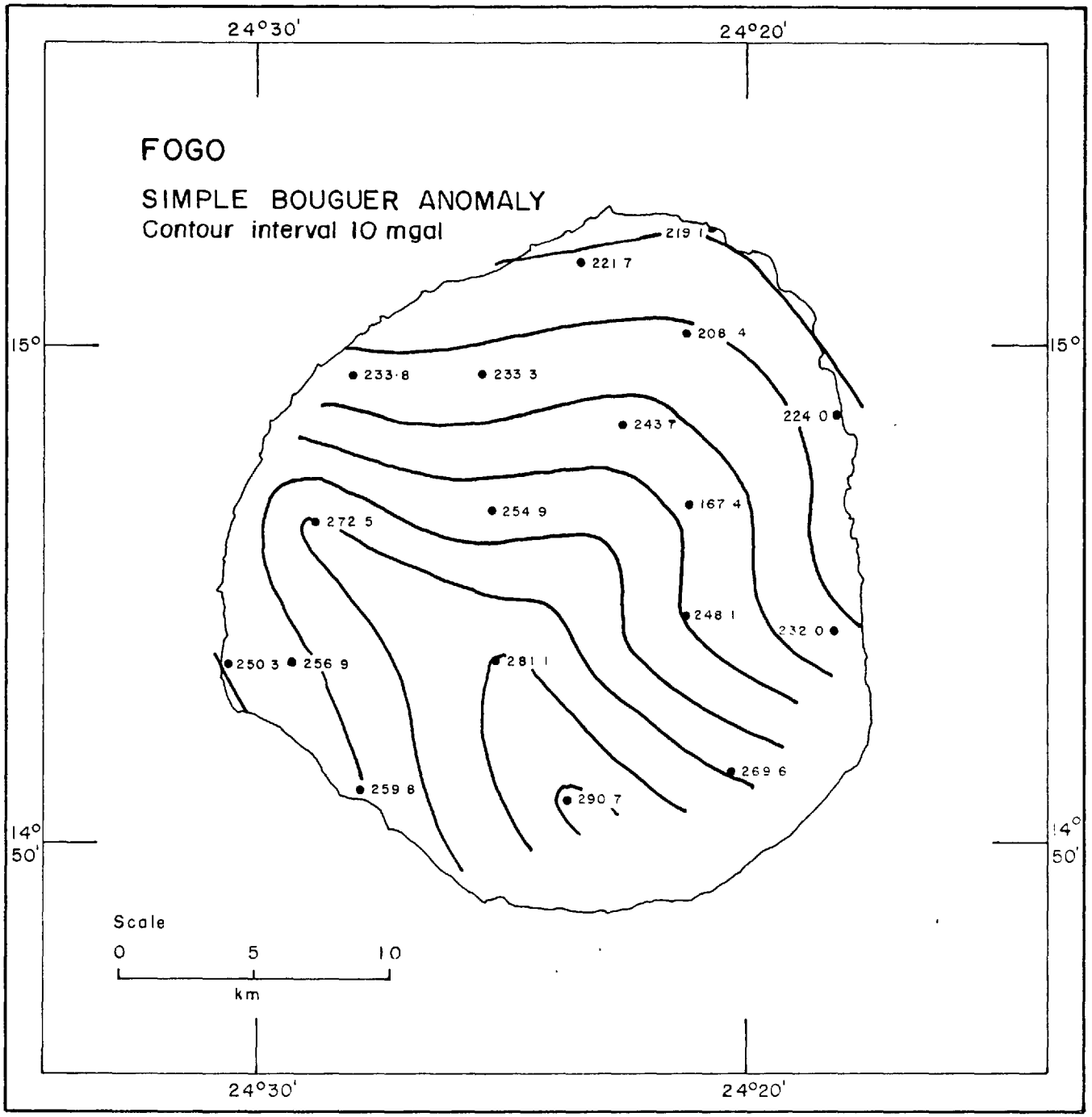
24°30'
24°20'
FOGO
SIMPLE BOUGUER ANOMALY
Contour interval 10 mgal
15°
14° 50'
219 1
221 7
208 4
233·8
233 3
224 0
243 7
254 9
167 4
272 5
248 1
232 0
250 3
256 9
281 1
269 6
259 8
290 7
Scale
0 5 10
km

FIG. 8.19.

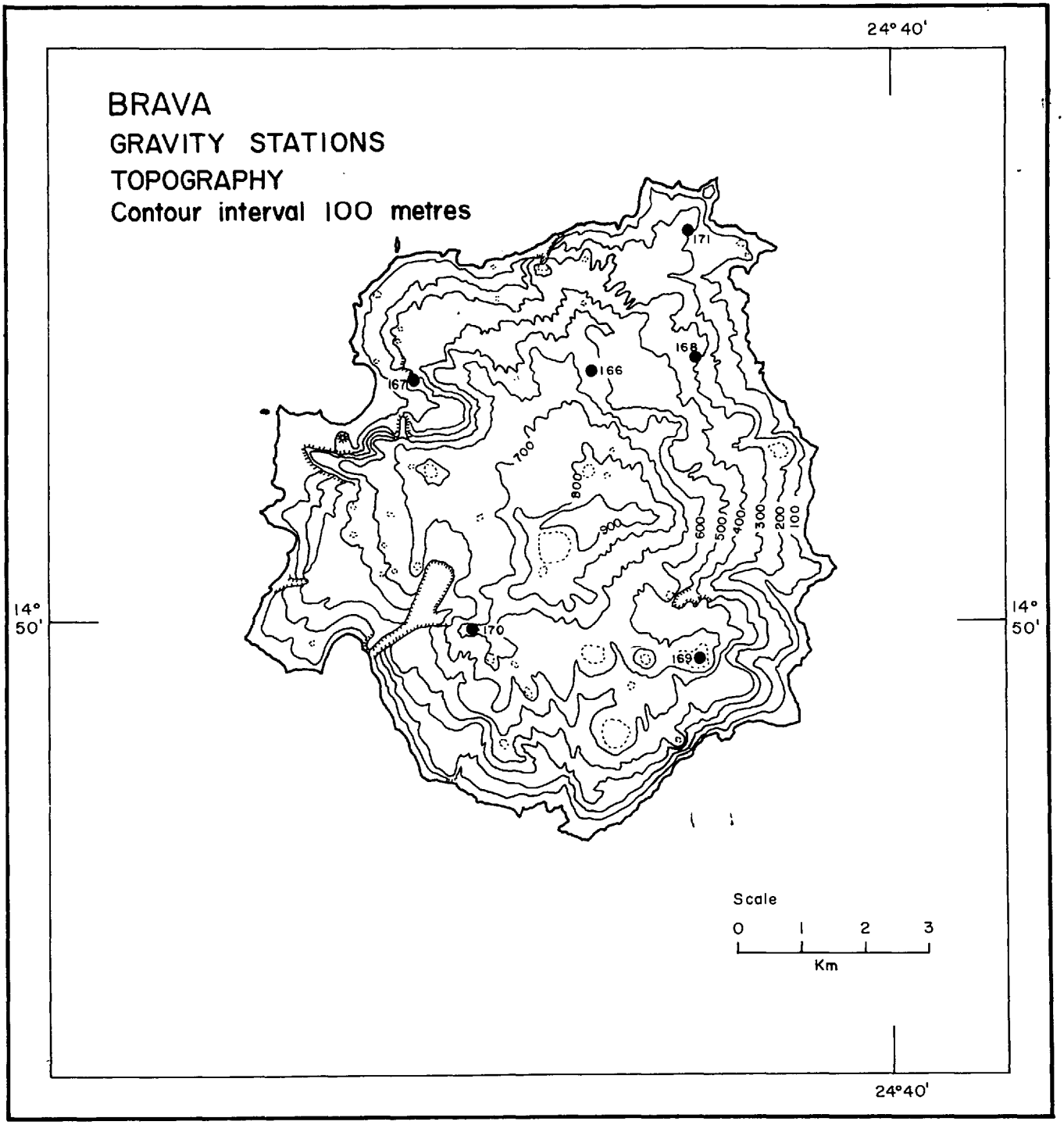
BRAVA
GRAVITY STATIONS
TOPOGRAPHY
Contour interval 100 metres
24°40'
14°
50'
171
168
166
167
170
169
100
200
300
400
500
600
700
800
900
Scale
0 1 2 3
Km

FIG. 8.20.

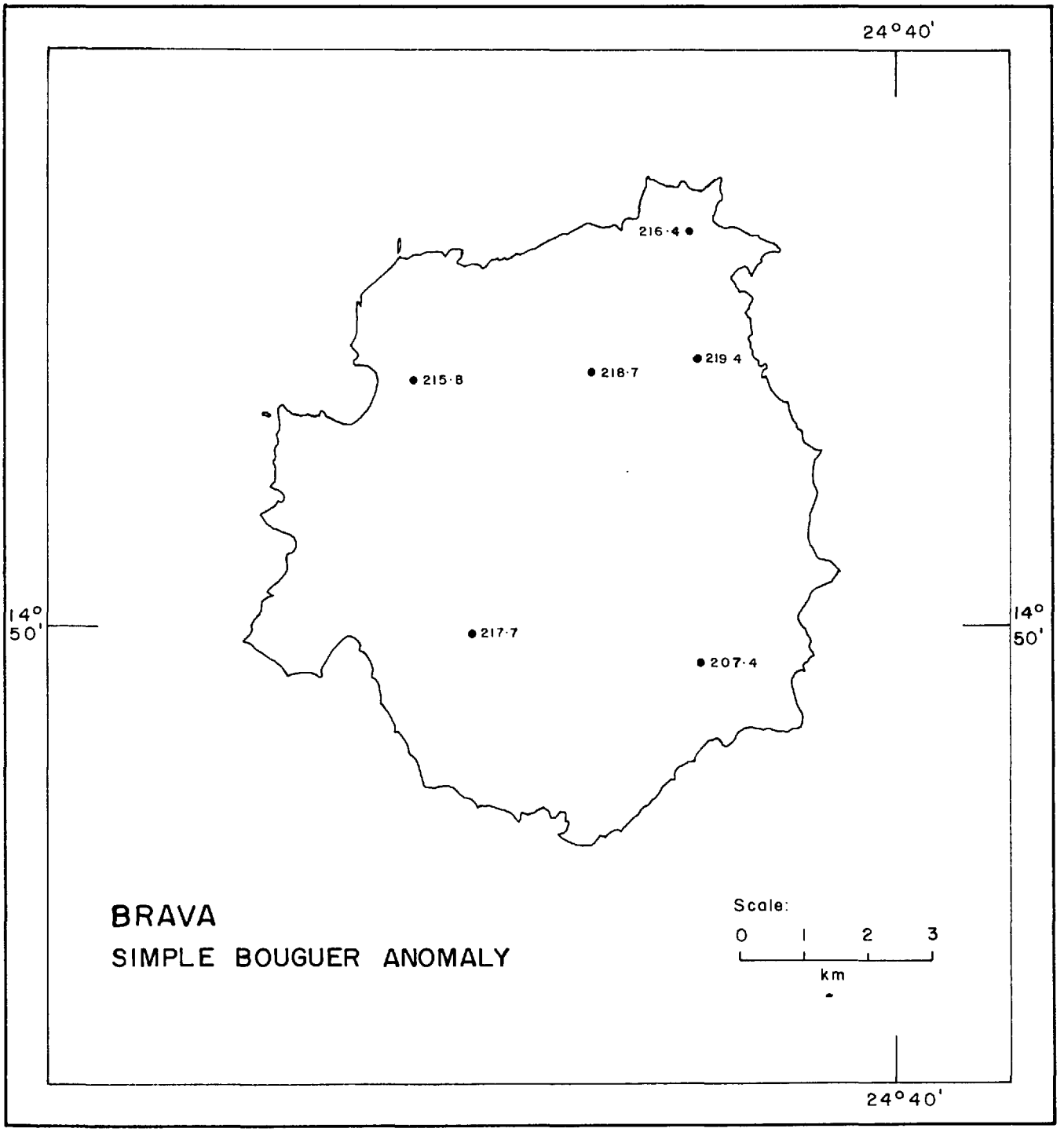
24°40'
216·4
219·4
215·8
218·7
14°
50'
217·7
207·4
14°
50'
BRAVA
SIMPLE BOUGUER ANOMALY
Scale:
0
1
2
3
km
24°40'

FIG. 8.21.

8.2 The Islands of São Tomé and Príncipe.

8.2.1 Introduction. São Tomé and Príncipe are the inner two islands of a chain of four which extends for 650 km across the Equator in the Gulf of Guinea. The islands lie on a NE-SW shelf and submarine ridge which may be continued south-westwards as a line of seamounts perhaps as far as St. Helena (Hall, 1966). The line of the islands can also be extended to the north-east through the Cameroons along a large tectonic trough and rift valley, (Furon, 1963).

With a surface area of about 950 km^2, the oval-shaped island of São Tomé is one of the two larger islands, while Príncipe, with an area of approximately 150 km^2, is the second smallest. Both islands are mountainous and deeply dissected.

8.2.2 General Geology. The islands are composed principally of basalt and phonolite lavas and tuffs cut by innumerable basalt dykes (Neiva, 1956a; 1956b). The basalts are mostly trachybasalts of a distinctly alkaline cast and the phonolites are associated with tiphrites. Both islands are basalt volcanoes cut by later phonolite and trachyte eruptions.

A small outcrop of Miocene limestone (G. Silva, 1956) is found on Príncipe at 130 m above the present sea-level, dating the volcanic rocks below it as being older than Miocene and the first eruptions of the island as being perhaps of late Cretaceous age (Neiva, 1956b). There is also

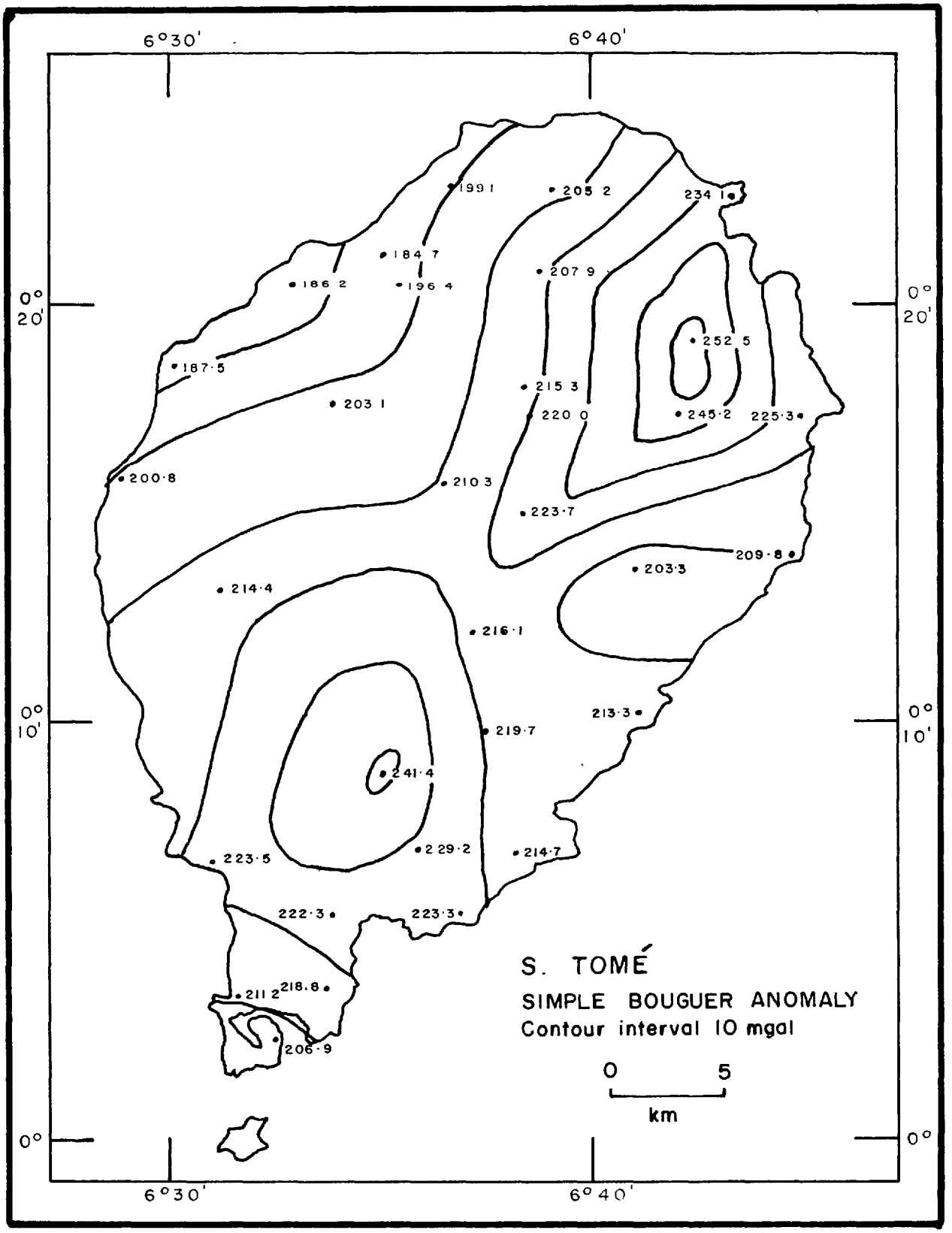
6°30'
6°40'
0° 20'
0° 10'
0°
199·1
205·2
234·1
184·7
207·9
186·2
196·4
252·5
187·5
215·3
203·1
220·0
245·2
225·3
200·8
210·3
223·7
209·8
203·3
214·4
216·1
213·3
219·7
241·4
229·2
223·5
214·7
222·3
223·3
211·2
218·8
206·9
S. TOMÉ
SIMPLE BOUGUER ANOMALY
Contour interval 10 mgal
0
5
km

FIG. 8.22.

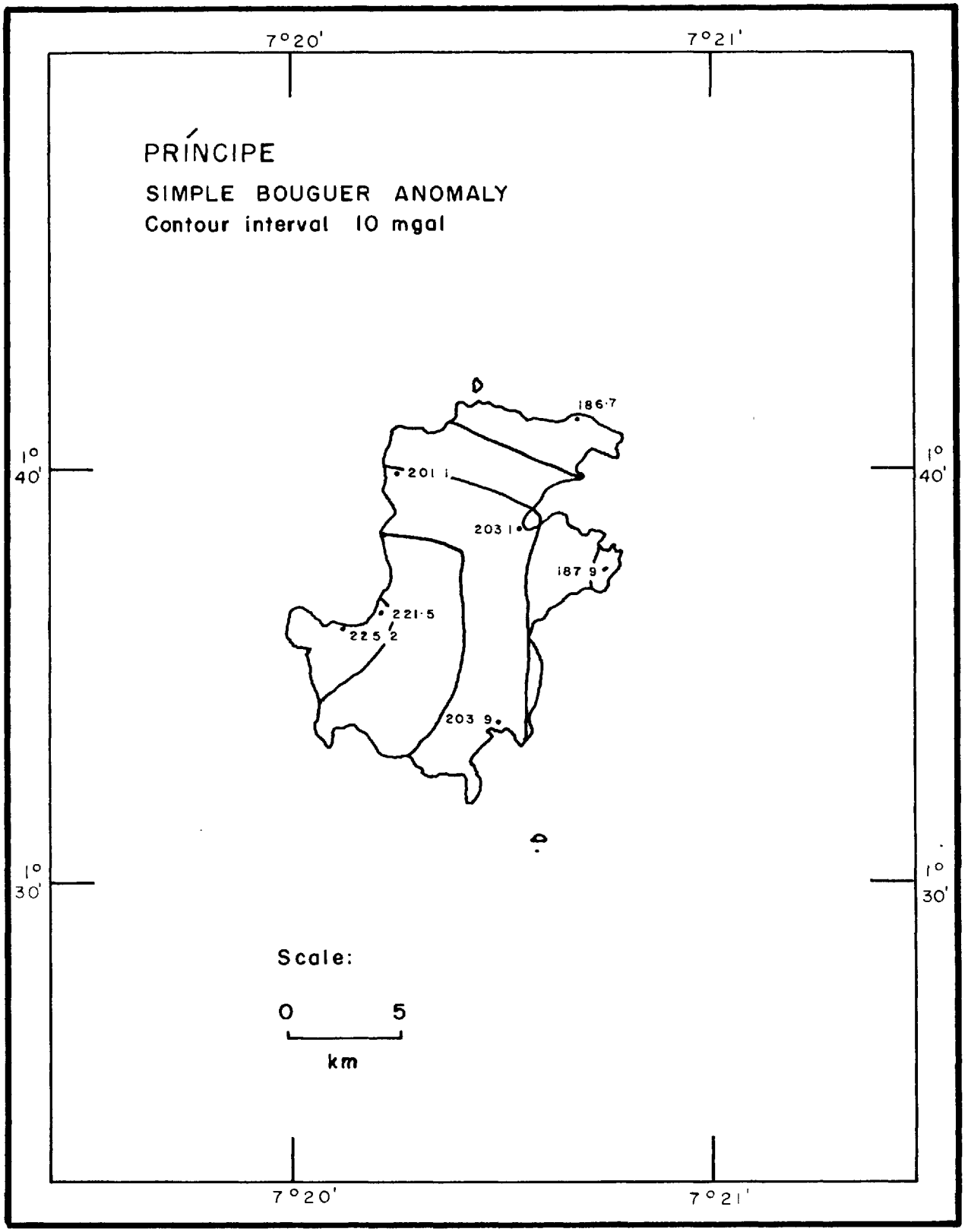
7°20'
7°21'
PRÍNCIPE
SIMPLE BOUGUER ANOMALY
Contour interval 10 mgal
186·7
201 1
203 1
187 9
221·5
225 2
203 9
1° 40'
1° 30'
Scale:
0 5
km

FIG. 8 23.

clear evidence that there has been some relatively recent volcanism. Raised beaches on São Tomé provide further evidence of recent epirogenic movement.

8.2.3 Details of the Data Reduction. As for the Cape Verde Islands.

8.3 Discussion.

The islands are characterized by centres of high Bouguer anomaly with maximum values in excess of 219 mgal. The amplitudes of the anomalies cannot be determined exactly from the surface gravity data but must, in most cases, be greater than 50 mgal. The maximum values and the amplitudes are subject to large error due to the absence of terrain correction; these corrections would increase the maximum anomaly by several milligals and might also increase the apparent amplitudes. The gradients of the Simple Bouguer anomaly are not very meaningful in rugged topography because of terrain effects, but on the flatter islands of Sal, Boa Vista and Maio, the maximum observed gradients are similar to those on the Azores and Canary Islands.

The gravity contours are frequently elongated in one direction or other and probably indicate rift zones. On several islands there are two volcanic centres, and the line of these two centres may indicate the trend of a major crustal fracture. This is particularly well illustrated in

the case of S. Tomé, which has two centres trending along the line of the Cameroon-St. Helena fracture.

The regions of gravity high are generally centred on an area where there are several outcrops of differentiated rocks and are consistent with the suggestion (Chapter 6) that these gravity centres represent high-level magma chambers in which the derivative rocks are fractionated from the primary magma by processes of magmatic differentiation.

CHAPTER 9

CONCLUSION

It is now possible to summarize the data presented on the Atlantic oceanic islands, to examine which features they have in common, and to see what differences exist between the different island groups.

The islands studied in this report are all steep-sided volcanic structures with rock types within any one group ranging from tholeiite through basalt-trachyte-phonolite to rhyolite but always with alkali-basalt strongly predominating.

Of the islands investigated, only the Cape Verde and Gulf of Guinea Islands are clearly older than Miocene, and recent volcanic activity is characteristic of all the island groups. The islands close to the crest of the Mid-Atlantic Ridge are very young, but so also are Hierro in the Canary Islands and Fogo in the Cape Verde Islands, both far distant from the mid-ocean ridge. The estimated ages of the oldest islands in the Azores and in the Canaries both fall within the Miocene period. Thus, although there is a tendency for the age of the main volcanic phase within an island group to decrease westwards, i.e. towards the Mid-Atlantic Ridge, the

contemporaneous volcanism on the ridge, in the ocean basin, and on the continental margin, is consistent with the conclusion of McBirney and Gass (1967), arrived at from petrological evidence, that the oceanic islands are likely to be related to zones of magma genesis within the underlying mantle and are not, as proposed by Wilson (1963), initiated at the axis of the ridge and carried outwards from it by the spreading crust.

The decrease in age of volcanism towards the Mid-Atlantic Ridge is readily understandable for islands on the ridge where generation of magma may be associated with the axial region only, and volcanism will peter out as the islands drift away from it. It is not so easy to explain in terms of crustal spreading for the other island groups, unless perhaps the underlying zone of magma genesis is deep in the mantle convection cell and is moving more slowly than the outer currents which carry the crust away from the mid-ocean ridge.

A feature of all the islands is the strong tectonic control on the volcanism. The Azores, Ascension Island and the Guinea Islands are all situated along major linear fissure systems and the geology of the Canary and Cape Verde Islands indicate major faulting in two or more directions. In the former group the crust is invaded by magma along the fissures, the islands arising at centres of volcanism at points of crustal weakness created perhaps by a slight change in

direction of the fissure trend. In the latter group, where no single tectonic trend predominates, the island may arise at points of weakness at the intersection of two fissure systems.

Crustal studies (Le Pichon et al, 1965) indicate that the crust under the islands on the Mid-Atlantic Ridge is likely to be much thinner than normal ocean crust and to be underlain by material with lower density than normal mantle. All the islands appear to have some regional isostatic compensation, but this difference in crustal structure may mean that the manner of compensation is different for islands on and off the Ridge. No pertinent seismic refraction data have yet been published for the Atlantic islands, but it is probable that the off-Ridge islands are compensated in the same manner as the Hawaiian Islands where seismic refraction studies have discovered a thickening of the crust under the islands to form a crustal root (Worzel and Harrison, 1963).

Bott (1965) suggests that the anomalous mantle under the axial zone of the mid-oceanic ridge is partially fused mantle material. While compensation for the islands on the Mid-Atlantic Ridge may be achieved by a thickening of the anomalous mantle layer, it could equally well be attained by a decrease in density within this anomalous mantle layer owing to increased fusion along the fissure system. This latter possibility is consistent with the interpretation of

Machado (1956; 1964) who suggests that seismological observations on the Azores indicate fluid magma at a depth of 5 km under the islands. As proposed in Section 5.9, this partial fusion of the mantle may have provided the magma for the Ridge islands. In support of this is the opinion of McBirney and Gass (1967) that the rocks of these islands are produced by melting at shallow depths.

The gravity data which form the main body of this report are summarized in Table 9.1.

All the islands are regions of high Bouguer anomaly, with maximum values ranging from 125 mgal for the island nearest the Mid-Atlantic Ridge to almost 290 mgal on islands in the ocean basins and continental margins. The maximum Bouguer anomaly value recorded on each island is markedly smaller for the islands on the Mid-Atlantic Ridge. As seen in the Azores (Fig. 5.25), the gravity field increases towards the edge of the Ridge, but on Santa Maria, the island at the edge, the maximum value of 242 mgal is still some 30 mgal less than on the off-Ridge islands. As terrain corrections will add 20 - 40 mgal to the Simple Bouguer anomaly of the Cape Verde Islands and Guinea Islands, these will have values similar to those of the Canary Islands, Madeira and Fernando Noronha. It should be noted that the maximum Bouguer anomaly is not much affected by the size of the island. Of the two isolated islands arising in the deep ocean, Fernando de Noronha, with

Summary of Gravity Results on the Atlantic Islands

	1	2	3	4	5	6	7	8	9
Ascension Is.	182	156	130	52	7.0	6	100	97	3.4
Flores	161	146			6.0		130	142	1.8
Faial	125	86	75	50	5.0	8	44	172	1.4
Pico West	140	104	85	55	5.0	9	68	433	1.5
Pico East	147	104	90	57	4.5	11	84		
S. Jorge	149	108	100	50	5.0	8	113	240	1.5
Terceira	140	116	100	40	6.0	6	225	398	1.8
S. Miguel W	175	140	115	60	4.9	10	309	746	1.8
S. Miguel E	203	140	145	60	5.0	10	360		2.3
Santa Maria	242	206	175	67	6.5	9	400	96	2.7
Hierro	267	208	180	87	6.7	10	2000+	277	3.7
Tenerife	289	202	170	119	5.0	20	2000+	2058	3.0
Gran Canaria W	287	198	160	127	6.5	16	2000+	1500	3.0
Gran Canaria E	270			72	5.9	10	2000+		
Lanzarote	235	155	120	115	6.5	15	2000+	796	2.4
Madeira	287	237	c.200	c.87	5.0	13		850	4.0
Fernando de Noronha	270	245			6.5			18	4.0
S. Antão*	253	180							3.5
S. Vicente*	282	216							3.5
S. Nicolau*	228	179							3.5
Sal*	276	207							3.5

Table 9.1 (continued overleaf)

Table 9.1 (continued)

Boa Vista*	272	229		3.5
Maio*	281	233		3.5
Santiago*	258	192		3.5
Fogo*	291	219		3.5
Brava*	219	202		3.5
S. Tomé*	252	186	950	
Príncipe*	225	187	150	

1 Maximum observed value of the positive Bouguer anomaly centre in milligals.

2 Minimum observed value of the Bouguer anomaly on the island in milligals.

3 Estimated regional Bouguer anomaly at the centre of the anomaly in milligals.

4 Estimated amplitude of the gravity anomaly in milligals.

5 Maximum gravity gradient associated with the anomaly in milligals/kilometre.

6 Maximum possible depth to the top of the disturbing body in kilometres.

7 Distance of the gravity anomaly from the Mid-Atlantic Ridge in kilometres.

8 Island Area in square kilometres.

9 Depth to surrounding sea-floor in kilometres.

---

* These are Simple Bouguer anomaly values.

and area of 18 km^2 has a maximum value only 17 mgal less than the many times larger island of Madeira.

The most conspicuous feature of the island gravity maps, and one which is common to almost every island, is a closure of high Bouguer anomaly. Marine gravity data are used wherever possible to separate the island gravity field into the regional anomaly and the local anomaly associated with the gravity closure.

The lower regional field prevailing over the Ridge islands reflects the anomalous crustal structure of the axial zone of the mid-oceanic ridge. The increase in regional field away from the axis of the Ridge (see Fig. 5.25) may indicate a decrease in thickness of the anomalous mantle layer, or an increase in its density. The westward increase in regional field in the Canary Islands is considered to result from the seaward thinning of the crust at the continental margin.

The amplitudes of the local high gravity anomaly range from 40 to 130 mgal. These anomalies clearly indicate large high-density masses, of considerable vertical extent, under the surface of the islands.

The estimated magnitudes of these anomalies average 55 mgal on the Ridge islands compared with three anomalies of over 115 mgal in the Canary Islands. This marked difference may be partly due to the smaller horizontal extent of the anomalous body, but is probably due also to the smaller

vertical distance of positive density contrast on the Ridge islands. The anomalous mass must have a higher density than the surrounding rocks, and as it is unlikely to have a higher density than the mantle, only the portion within the crust and body of the island will contribute positively to the gravity anomaly. Not only do the islands on the Mid-Atlantic Ridge rise from a shallower sea bottom but, as the seismic refraction results of Ewing and Ewing (1959), Le Pichon et al (1965) and Dash and Bosshard (1968) indicate, they are also underlain by a thinner crust than the islands in the ocean basins and continental margins. The net result is to reduce the vertical thickness of rock within which the anomalous body has a positive density contrast and hence to reduce the gravity anomaly.

The local gravity anomaly contours are approximately circular, though frequently somewhat elongated along one or more directions, and for the purpose of computing density models the anomalous mass is assumed to be radially symmetrical.

There are four restraints on any density model constructed to represent the anomalous mass. These are (1) the magnitude of the anomaly, (2) the shape of the anomaly, (3) the densities of the crust within which the density model is to be constructed, and (4) the geologically permissible densities for the anomalous body.

Models have been fitted to the gravity anomaly on Tenerife in the Canary Islands and on Pico in the Azores,

chosen as being well-defined anomalies typical of the off-Ridge and Ridge islands respectively.

The density models for Tenerife are fitted to the line AA' in Fig. 6.12, which is chosen as the best defined section least disturbed by rift zone effects. The crustal section corresponds to the seismic refraction results of Dash and Bosshard (1968), with densities estimated from the seismic compressional velocities by means of Nafe and Drakes' (1963) velocity-density curves. The density of the island body and the crust to a depth of 5.5 km is assumed to be 2.3 gm/cc. This is underlain by a 2.5 km thick layer of 2.8 gm/cc material. This in turn overlies the oceanic layer of density 2.9 gm/cc which extends from 10 km depth to the mantle, at a depth of 16 km.

There are many different mass distributions which reproduce the above anomaly and satisfy the above-mentioned restraints. Two such models are presented in Fig. 9.1. In both, the island body is assumed to be densely intruded by lava in the form of dykes, sills or laccoliths (Nayudu, 1962) to produce a dense core of average density 2.6 gm/cc, i.e. 0.3 gm/cc more than the pyroclastics and volcanic sediments which probably constitute the island flanks. The strongest evidence for such a core comes from seismic refraction studies of seamounts (Laughton et al, 1960; Le Pichon et al, 1964) and of atolls (Raitt, 1954; 1957), which show that the

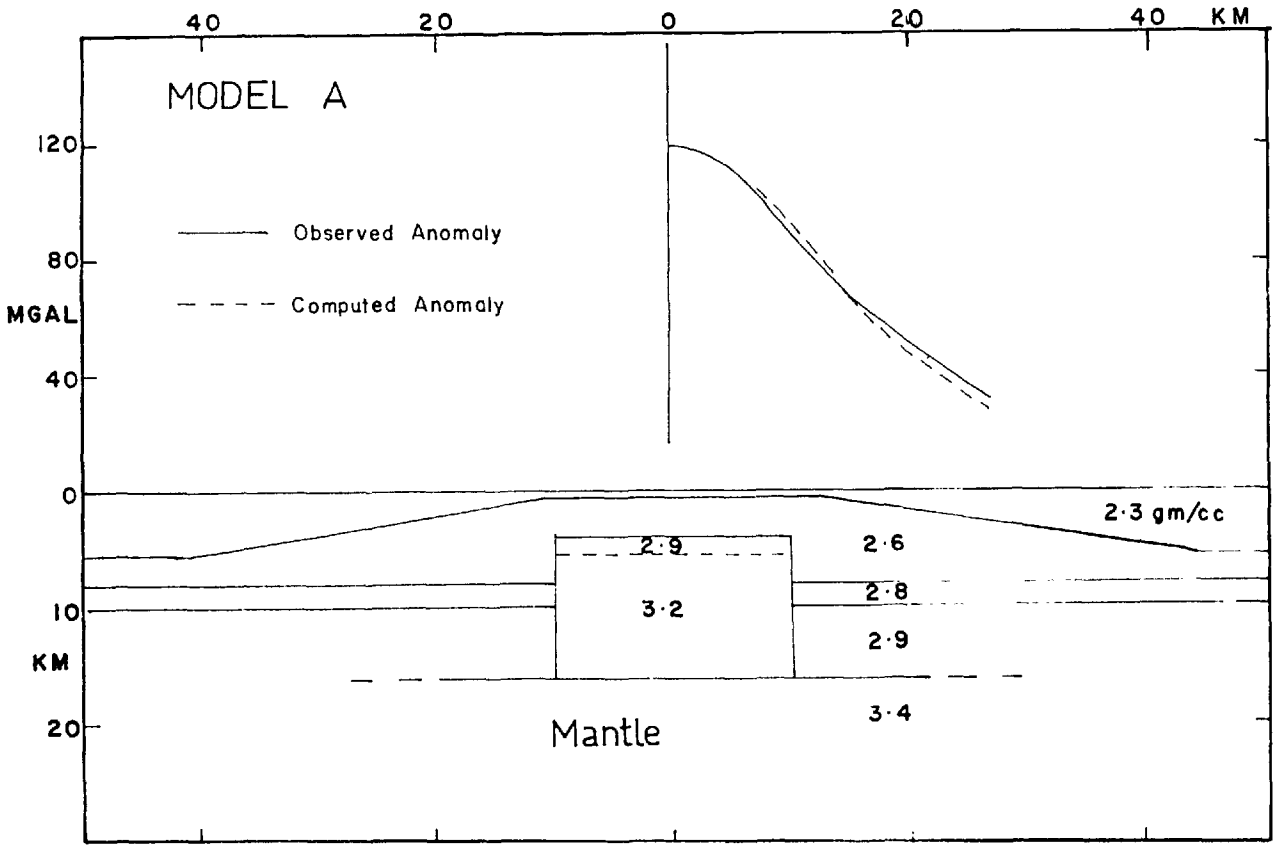

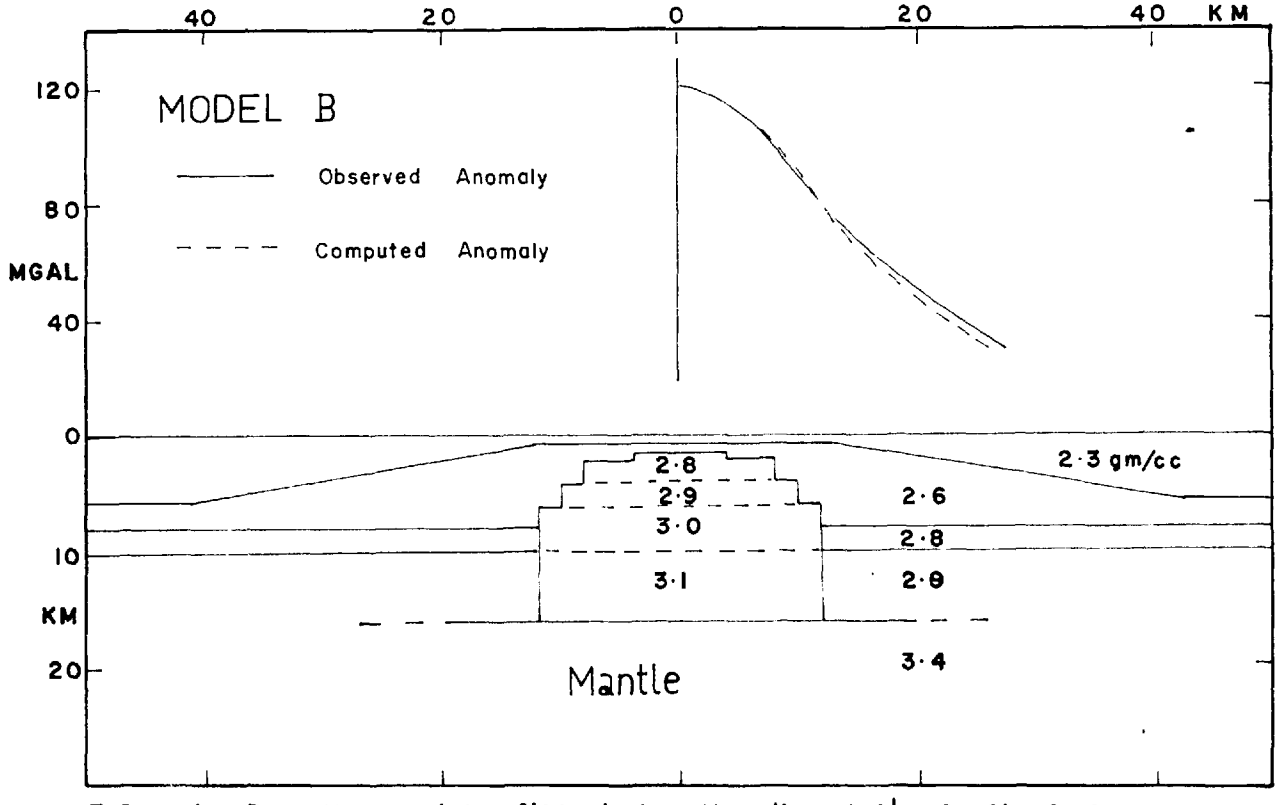

FIG. 9·1 Density models fitted to the line AA' of fig. 6·12

low-velocity upper layer is underlain by a layer of considerably higher velocity at a shallower depth than that of the surrounding ocean floor. This core is approximated mathematically by a cone, upper radius 12.5 km, extending from a depth of 0,5 km to the 2.6 gm/cc layer at 5.5 km. In constructing the models, the observed anomaly is considered as radially symmetrical and the gravity effect of the cone or cylinder, as the case may be, is computed by the method of Talwani and Ewing (1960).

Because of the similarity of the Bouguer anomaly in magnitude and shape to those observed on the Hawaiian Islands, the model fitted by Strange et al (1965) to the Oahu data is taken as the basis of model A. The anomalous body is regarded as an intrusion of mantle-like material, of density 3.2 gm/cc, into the crust and extending from the Moho to within about 4 km of the surface. The upper 1.5 km, of density 2.9 gm/cc, represents derivative rocks produced by fractionation.

The high pressure mineralogy of the bulk of the subaerial volcanics (Ridley, 1968) presents a major objection to a high level magma chamber comprising intruded mantle material. The parent magma may have been generated at depths greater than 35 km (Green and Ringwood, 1967; O'Hara and Yoder, 1967) and it is unlikely that this magma will be appreciably denser than the 2.9 - 3.0 gm/cc value of most basalt dykes. This is particularly so if the magma is generated by partial

fusion, which might lead to a reduction in density, as compared with normal mantle material, of up to 0.3 gm/cc (Daly, 1944). The second model, B, is based on the assumption that a high-level magma reservoir, fed from great depths in the mantle, has formed in the crust, that the original density of the magma in this reservoir is 3.0 gm/cc, and that variations in density will arise within the chamber as the denser minerals settle during gravity differentiation.

As mentioned above, crustal studies indicate a low density mantle material under the ridge islands, perhaps as the result of partial fusion. There is the evidence of McBirney and Gass (1967) for high-level magma generation for these islands and of Machado and Forjaz (1964) for fluid magma at high levels under the islands. It thus seems quite possible that it is the fused portion of the upper mantle that provides the magma for the islands on the Mid-Atlantic Ridge. This magma, in a differentiated form, will invade the crust along fissures and form central type volcanoes at points of crustal weakness along them. These volcanoes may be intruded by a core of fluid magma to form a structure very similar to that of Tenerife's model B.

The density model for the Ridge islands (Fig. 9.2) has been fitted to the line AA' on Pico, as shown in Fig. 5.17. The crustal section corresponds to the seismic refraction results of Le Pichon et al (1965). The density of the island

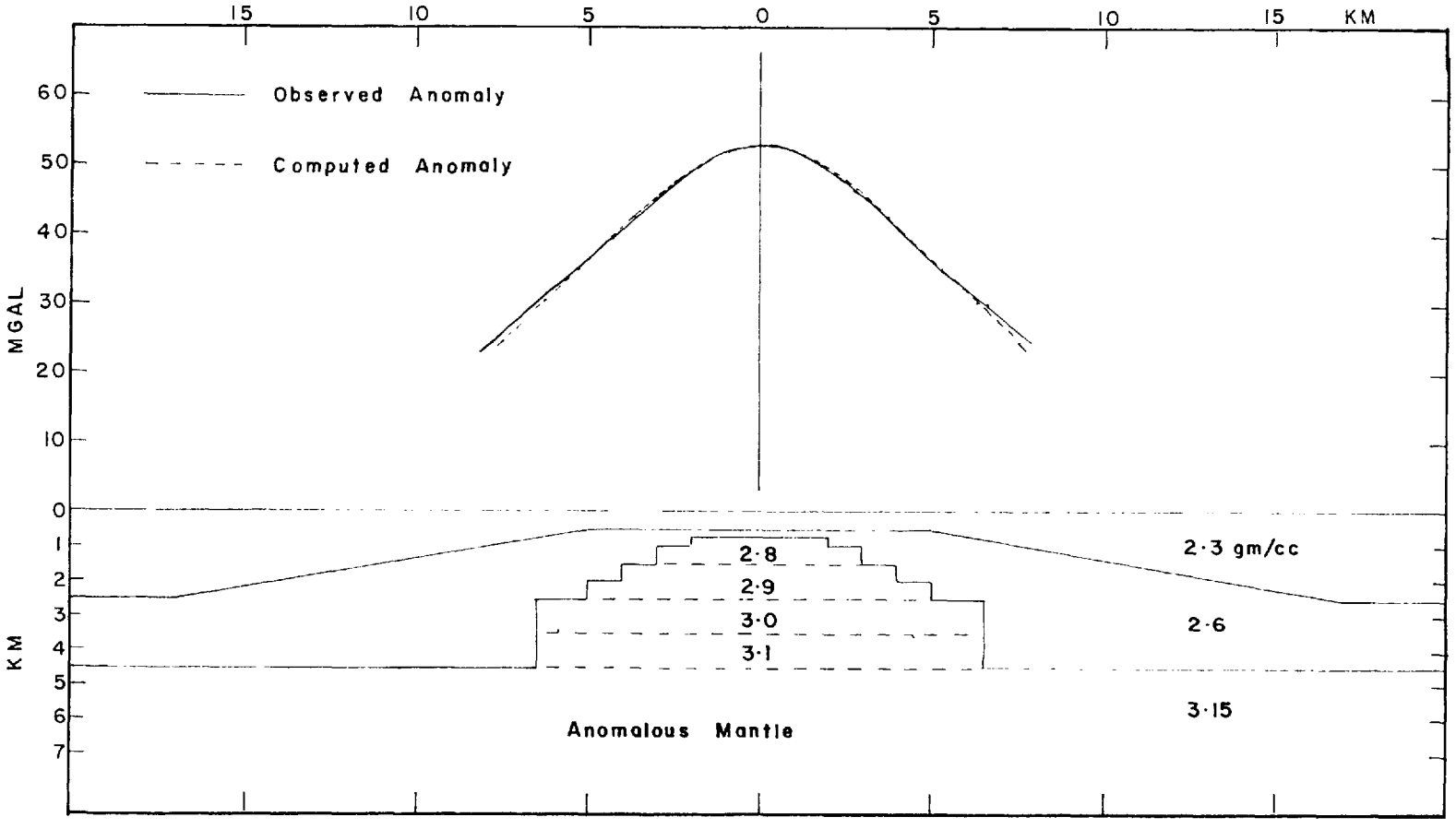

FIG. 9·2 Density model fitted to the line AA' of fig. 5·17

body and the crust down to a depth of 2.5 km is assumed to be 2.3 gm/cc corresponding to pyroclastics and volcanic sediment. This is underlain by a 2 km thick layer of density 2.6 gm/cc above the anomalous mantle of density 3.15 gm/cc. As for Tenerife, there is assumed to be a 2.6 gm/cc core of intrusives within the volcanic debris of which the island flanks are thought to consist, and within this core there is a high-level reservoir of magma varying in density from 3.1 gm/cc at the mantle to 2.8 gm/cc at 1.6 km below the surface.

The other main feature of the island gravity maps is the elongation of the gravity contours along the fissure systems which have controlled the growth of the islands. These gravity highs probably result from concentrations of dykes along these fissures rather than from elongate bodies of magma. In the proximity of a volcanic centre, the distension produced by the outward pressure of the dense magma chamber may lead to increased dyke formation. The outward pressure will lead to rifting, preferentially along existing trends, along which the magma may escape, leading to detumescence and perhaps sinking of the surface above the magma chamber. An excellent example of this proposed sequence of events is provided by Pico and Faial where recent eruptions have occurred on the flanks of the main volcanic centres, which are marked by collapse faulting. It may be that a similar mechanism operated on the other Azores islands to produce the calderas

and that these are collapse structures rather than explosive, as suggested by Machado (1964).

To sum up, the oceanic islands of the Atlantic are volcanic structures formed at centres along major fissures in the earth's crust. Alkali-basalt is the predominant rock type. In age, they range from Cretaceous to Recent, but Recent volcanic activity occurs in almost all the island groups. Some degree of regional isostatic compensation operates for all the islands.

The islands can be divided into two groups, differing in character of gravity field, crustal structure and depth of magma generation. The islands on the Mid-Atlantic Ridge have lower maximum and regional Bouguer anomaly values and smaller amplitudes of the local positive anomaly. They rise from shallower water depths, above a thinner crust which is underlain by lower density mantle. The magma for the Ridge islands is generated at shallow levels and volcanic centres are regarded as intrusions of differentiated, fused mantle material, while the volcanic centres of the other oceanic islands are simply high-level reservoirs for magma which is generated deep in the mantle.

This investigation of oceanic islands is based primarily on gravity surveys. In view of the ambiguity inherent in gravity data much of the above interpretation must be regarded as speculation. It will require detailed seismic refraction

work on and around the islands and aerial magnetic surveys over them, before the structure of oceanic islands can be conclusively determined. It is to be hoped however, that the ideas presented here will provide some framework for any such future investigations.

ACKNOWLEDGEMENTS

This study of the Atlantic islands was initiated by Prof. R.G. Mason and I am pleased to acknowledge his general supervision and his helpful criticism of the original manuscript.

I am grateful to Prof. R.G. Mason, Dr. B.P. Dash, P. Hadwen and L. Margherita for their practical help in the gravity surveys and to Dr. A. Richardson and Dr. N.D. Watkins who carried out the survey on Fernando de Noronha.

I am indebted to the Instituto Geográfico e Cadastral, Lisbon, for their kind permission to use the results of their gravity survey on Madeira and to the Servico Meteorológico Nacional, Lisbon, who graciously agreed to the inclusion of their data from the Cape Verde Islands, S. Tomé and Príncipe, in this report.

I wish to thank the Geodetic Institute of the Delft Technological University for the marine gravity data acquired by Hr. Neth. Ms. "Snellius" during the Navado III programme, 1965, the Department of Geodesy and Geophysics, University of Cambridge, for their "R.R.S. Discovery" marine gravity data in the Azores, and the Department of Geology, University of Birmingham, for the "H.M.S. Protector" marine gravity profile in the Canary Islands. I should emphasize that I must accept

sole responsibility for the use made of data acquired from all the above sources.

My thanks are due to the Instituto Nacional de Geofísica, Madrid, who gave me the results of their gravity surveys on the Canary Islands. Of these, only two gravity stations on Gran Canaria are included in this thesis, but the other results were of considerable value as an independent check of my own fieldwork.

Acknowledgement is made to my wife and to Mrs. J. Kelland for draughting many of the diagrams, and also to Mrs. J. Kelland for typing the thesis.

I wish to thank Royal Dutch Shell for the award of a three-year scholarship.

Finally, I wish to express my gratitude for the constant encouragement and practical assistance received from my wife, Margaret O. Macfarlane.

Duncan John Macfarlane.

The project was financed by the United Kingdom Natural Environment Research Council and I gratefully acknowledge its support.

BIBLIOGRAPHY

ABDEL-MONEM, A., N.D. WATKINS and P.W. GAST, 1967. Volcanic history of the Canary Islands. 14th Gen. Ass. I.U.G.G. Abs., 7:67.

ADAMS, W.M. and A.S. FURUMOTO, 1965. A seismic refraction study of the Koolau volcanic plug. Pacific Sci., 19:296-305.

AIRY, G.B., 1855. On the computations of the effect of the attraction of the mountain masses as disturbing the apparent astronomical latitude of stations in geodetic surveys. Trans. Roy. Soc. (London) Ser. B., 145.

ALMEIDA, F.F.M., 1958. Geologia e Petrologia do archipélago de Fernando de Noronha. Brazil Div. Geol. e Min. Mon. 13. English summary, 177-181.

ATKINS, F.B., P.E. BAKER, J.D. BELL and D.G.W. SMITH, 1964. Oxford expedition to Ascension Island, 1964. Nature, 204(4960):722-724.

BATH, M., 1960. Crustal structure of Iceland. Jour. Geophys. Res., 65:1793-1807.

BEBIANO, J.B., 1932. A geologia do Arquipélago de Cabo Verde. Comm. Serv. Geol. Port., 18.

BEBIANO, J.B. and J.M. PIRES SOARES, 1951. Notes on some supposed Senonian fossils from São Nicolau Island (Cape Verde Islands). Int. Geol. Cong. (18th, Great Britain) Rept., 14:186-189.

BELL, J.D., 1965. Eruption-mechanism on Ascension Island. Proc. Geol. Soc. of London, 1626:145-146.

BIBLE, J.L., 1962. Terrain correction tables for gravity. Geophysics, 27:715-718.

BLUMENTHAL, M.M., 1961. Rasgos principales de la geologia de las Islas Canarias, con datos sobre Madeira. Bol. del Inst. Geol. y Min. de Esp. Madrid.

BOTT, M.H.P., 1959. The use of electronic digital computers for the evaluation of gravimetric terrain corrections. Geophys. Pros., 7:45-54.

BOTT, M.H.P., 1965. Formation of ocean ridges. Nature, 207(4999):841-844.

BOTT, M.H.P. and R.A. SMITH, 1958. The estimation of the limiting depth of gravitating bodies. Geophys. Pros., 6:1-10.

BOURCART, J. and E. JEREMINE, 1937. La Grande Canarie. Bull. Volc. Ser. 2, 2:1-78.

BYERLY, P.E., 1965. Short note: Convolution filtering of gravity and magnetics maps. Geophysics, 30:281-3.

CAREY, S.W., 1958. The tectonic approach to continental drift. Continental Drift (Symp. Univ. Tasmania) 177-355.

COX, A. and R.R. DOELL, 1961. Palaeomagnetic evidence relevant to a change in the earth's radius. Nature, 189(4758):45-47.

COX, A., R.R. DOELL and G.B. DALRYMPLE, 1964. Reversals of the earth's magnetic field. Science, 144(3626): 1537-1543.

CREER, K.M., 1965. An expanding earth. Nature, 205(4971): 539-544.

DALY, R.A., 1944. Bull. Geol. Soc. Amer., 55:1363.

DARWIN, C., 1842. Coral Reefs. London.

DASH, B.P. and E. BOSSHARD, 1968. Crustal studies around the Canary Islands. Rep. Intnl. Geol. Cong. Prague.

DEAN, W.C., 1958. Frequency analysis for gravity and magnetic interpretation. Geophysics, 23:97-127.

DEMENITSKAYA, R.M. and V.D. DIBNER, 1965. Morphological structure and the earth's crust of the North Atlantic region. Geol. Sur. of Canada. Paper 66-15. Symposium 1965:63-79.

DIETZ, R.S., 1961. Continent and ocean basin evolution by spreading of the sea floor. Nature 190:854-857.

1962. Ocean basin evolution by sea-floor spreading. Jour. Oceanogr. Soc. Japan, 20th ann., 4-14.

EATON, J.P. and K.J. MURATA, 1960. How volcanoes grow. Science, 132:925-938.

EGYED, L., 1957. A new dynamic concept of the internal constitution of the earth. Sond. Geol. Rund., 46: 101-121.

EHRISMANN, W. et al., 1966. Topographic reduction of gravity measurements by the aid of digital computers. Boll. di Geofisica Teorica ed Appl., 8:3-20.

EINARRSON, T., 1954. A survey of gravity in Iceland. Soc. Sci. Isl. Reykjavik 22p.

ENGEL, A.E.J. and C.G. ENGEL, 1964. Composition of basalts from the Mid-Atlantic Ridge. Science 144:1330-33.

ENGEL, A.E.J., C.G. ENGEL and R.G. HAVENS, 1965. Chemical characteristics of oceanic basalts and the upper mantle. Bull. Geol. Soc. Amer., 76:719-734.

EWING, J. and M. EWING, 1959. Seismic refraction measurements on the Atlantic Ocean basins, in the Mediterranean Sea, on the Mid-Atlantic Ridge and in the Norwegian Sea. Bull. Geol. Soc. Amer., 70:291-318.

1967. Sediment distribution on the Mid-Ocean Ridges with respect to spreading of the sea floor. Science, 156(3782):1590-1592.

EWING, J., M. EWING, J.L. WORZEL and C. WINDISCH, 1966. Ages of horizon A and the oldest Atlantic sediments. Science, 154(3753):1125-1132.

FRIEDLANDER, I., 1913. Beitrage zur kenntnis der Kapverdischean Inseln. Berlin.

FURON, R., 1963. The Geology of Africa. Oliver and Boyd.

FURUMOTO, A.S., N.J. THOMSON and G.P. WOOLLARD, 1965. The structure of Koolau Volcano from seismic refraction studies. Pac. Sci., 19:296-305.

FURUMOTO, A.S. and G.P. WOOLLARD, 1965. Seismic refraction studies of the crustal structure of the Hawaiian Archipleago. Pac. Sci., 19:306-314.

GAGEL, C., 1910. Die mittelatlantischen vulkaninseln. Band VII Abt. 10.

GIMLETT, J.I., 1964. A computer method for calculating complete Bouguer corrections with varying surface density. Computers in the Mineral Industries Part 1. Stanford University Publications, Geological Sciences 9, Editor G.A. Parks.

GREEN, D.H. and A.E. RINGWOOD, 1967. The genesis of basaltic magmas. Cont. Min. Petrol., 15:103.

GRIGGS, D.T., 1939. American Jour. Sci., 237:11.

HADWEN,P and G.P.L. WALKER (in press). A geological review of the Azores.

HALL, G.P.D., 1966. Seamounts in the Gulf of Guinea. Nature, 212:1443.

HAMMER, S., 1939. Terrain corrections for gravimetric stations. Geophysics, 4:184-194.

1945. Estimating ore masses in gravity prospecting. Geophysics, 10:50-62.

HARRISON, J.C. and W.C. BRISBIN, 1959. Gravity anomalies off the west coast of North America : Seamount Jasper. Bull. Geol. Soc. Amer., 70:929-934.

HAUSEN, H., 1956. Contributions to the geology of Tenerife. Soc. Sci. Fenn. Comm. Phys. Math., V18.

1958. On the geology of Fuerteventura. Soc. Sci. Fenn. Comm. Phy. Math., V22.

1959. On the geology of Lanzarote. Soc. Sci. Fenn. Comm. Phys. Math., V23.

1962. New contributions to the geology of Grand Canary. Soc. Sci. Fenn. Comm. Phy, Math., V27 Helsingfors 1962.

1964. Rasgos geologicos generals de la isla de Hierro. Patronato de la Casa de Colon (Madrid) 10:547.

1965. Acta. Geog. (Helsinki), 18.

HAYFORD, J.F. and W. BOWIE, 1912. The effect of topography and isostatic compensation upon the intensity of gravity. U.S. C.G.S. Spec. Publ., 10, Washington.

HEEZEN, B.C., 1962. The deep-sea floor. Continental Drift. Editor, S.K. Runcorn. Academic Press:235-288.

HEEZEN, B.C., E.T. BUNCE, J.B. HERSEY and M. THARP, 1964. Chain and Romanche fracture zones. Deep Sea Res., 11:11-33.

HEEZEN, B.C. and M. THARP, 1961. Physiographic diagram of the South Atlantic Ocean. Geol. Soc. of Amer., New York 1961.

HEEZEN, B.C., M. THARP and M. EWING, 1959. The floors of the oceans. 1. The North Atlantic. Geol. Soc. Amer. Spec. Paper, 65.

HEIRTZLER, J.R. and Le PICHON, X., 1965. Crustal structure of the Mid-Ocean ridges pt. 3. Magnetic anomalies over the Mid-Atlantic Ridge. Jour. Geophy. Res., 70: 4013-4033.

HEISKANEN and F.A. VENING MEINESZ, 1958. The earth and its gravity field. McGraw-Hill Book Co.

HESS, H.H., 1962. History of ocean basins in Petrologic Studies, a volume to honour A.F. Buddington. Geol. Soc. Amer., 599-620.

1965. Mid-ocean ridges and tectonics of the sea-floor. Submarine Geology and Geophysics : Colston Papers, 17:317-332.

HULL, M.N., 1960. A median valley of the Mid-Atlantic Ridge. Deep Sea Res., 6:193-205.

HOLMES, A., 1928. Trans. Geol. Soc. Glasgow, 18:559.

HURLEY, P.M., 1968. The confirmation of continental drift. Sci. Amer., 218:52-64.

JEFFREYS, H., 1952. The Earth - its origin, history and physical constitution. Cambridge University Press, London.

JOKSUMOWITSCH, Z.J., 1910. Z. Deutsch. Geol. Gesellsch., 62.

JONES, J.G., 1966. Intraglacial volcanoes of south-west Iceland and their significance in the interpretation of the form of marine basaltic volcanoes. Nature, 212(5062):586-588.

JUNG, K., 1953. "Schweydarsche" Formeln für die Geländewirkung auf g. Zeit. f. Geophysik, 20:54.

KANE, M.F., 1964. A comprehensive system of terrain corrections using a digital computer. Computers in the Mineral Industries, Part 1. Stanford University Publications, Geological Sciences 9, Editor, Parks.

KEEN, M.J., 1963. Magnetic anomalies over the Mid-Atlantic Ridge. Nature, 197(4870):880-890.

KRAUSE, D.C., 1965. East and west Azores fracture-zones in the North Atlantic. Submarine Geology and Geophys. Colston Papers, 17, Butterworths :163-174.

KREJCI-GRAF, K., 1955. Vulkamissein and Inselvulkane. Natura un Volk, 85:40-51.

1964. Mitt. Geol. Gesellsch., 57.

LA FEHR, T.R., 1965. The estimation of the total amount of anomalous mass by Gauss's theorem. Jour. Geophys. Res., 70:1911-1919.

LAUGHTON, A.S., M.N. HILL and T.D. ALLAN, 1960. Geophysical investigations of a seamount 150 miles north of Madeira. Deep Sea Res., 7:117-141.

LEGGE, J.A., 1944. A proposed least squares method for the determination of the elevation factor. Geophysics, 9:175-179.

LE PICHON, X., R.E. HOUTZ, C.L. DRAKE and J.E. NAFE, 1965. Crustal structure of the Mid-Ocean Ridges 1) Seismic refraction measurements. Jour. Geophys. Res., 70: 319-339.

LE PICHON, X. and M. TALWANI, 1964. Gravity survey of a seamount near 35°N, 46°W in the North Atlantic. Marine Geol., 2:262-277.

LONCAREVIC, B.D., C.S. MASON and D.H. MATTHEWS, 1966. Mid-Atlantic Ridge near 45°N. 1. The median valley. Can. Jour. Earth Sci., 3:327-349.

McBIRNEY, A.R., 1963. Factors governing the nature of submarine volcanism. Bull Volc., 26:455-469.

McBIRNEY, A.R. and I.G. GASS, 1967. Relations of oceanic volcanic rocks to mid-oceanic rises and heat flow. Earth and Planetary Science Letters, 2:265-276.

MACDONALD, G.A., 1965. Hawaiian Calderas. Pac. Sci. 19:320-334.

MACDONALD, G.J.F., 1965. Continental structure and drift. Phil. Trans. Roy. Soc. Ser. A., 258:215-227.

MACHADO, F., 1954. Earthquake intensity anomalies and magma chambers of Azorean volcanoes. Trans. Amer. Geophys. Union, 35:833-837.

1964. Alguns problemas do vulcanismo de Tenerife. Bol. Soc. Port. Cien. Nat., 10:26-45.

1965. Vulcanismo das Ilhas de Cabo Verde e das outras ilhas Atlantidas. Estudos, Ensaios, e Documentos No. 117, Junta de Investigacoes do Ultramar, 83 pp.

MACHADO, F. and V.H. FORJAZ, 1964. Seismic swarm in the Azores, February 1964 (prelim. report). Geol. Soc. Port. Bol., 15:201-206.

MALAHOFF, A. and G.P. WOOLLARD, 1966. Magnetic measurements over the Hawaiian Ridge and their volcanological implications. Bull. Volc., 29:735-759.

MANGHNANI, M.H. and G.P, WOOLLARD, 1965. Ultrasonic velocities and related elastic properties of Hawaiian basaltic rocks. Pac. Sci., 19:306-314.

MARTINS, J. and C. MORELLI, 1962. Gravity tie Rome-Lisbon. Boll. Geofisica Teor. ed Appl., 4:278-285.

MASON, R.G. and A.D. RAFF, 1961. Magnetic survey off the west coast of North America, 32°N latitude to 42°N latitude. Bull Geol. Soc, Amer., 72:1259-1265.

MENARD, W.H., 1958. Development of median elevations in ocean basins. Bull. Geol. Soc. Amer., 69:1179-1186.

1964. Marine geology of the Pacific. McGraw-Hill Book Co. Inc. New York, 271 pp.

MESKÓ, A., 1965. Frequency analysis for gravity interpretation. Geophys. Pros., 13:475-488.

MILLER, E.T., and J.I. EWING, 1956. Geomagnetic measurements in the Gulf of Mexico and in the vicinity of Caryn Peak. Geophysics, 21:406-432.

MOORE, J.G., 1965. Petrology of deep-sea basalt near Hawaii. Amer. Jour. Sci., 263:40-52.

NAFE, J.E. and C.L. DRAKE, 1963. Physical properties of marine sediments. The Sea, Editor M.N. Hill. Interscience, New York, V3:794-815.

NAGY, D., 1966. The prism method for terrain corrections using digital computers. Pure and Applied Geophys., 63:31-39.

NAVARRO, L.F., 1908. Observaciones geologicas de la Isla de Hierro. (Canarias). Mem Soc. Esp. de Hist. Nat., V5, Madrid.

NAYUDU, Y.R., 1962. A new hypothesis for the origin of guyots and seamount terraces. The crust of the Pacific basin. Amer. Geophys. Union Geophysical Monograph No. 6.

NEIVA, J.M.C., 1965a. Contribuicão para o estudo geológico e geomorfologico da Ilha de S. Tomé e das ilheus das Rosas e das Cabras. Conf. Int. Afr. Ocid. Sess. 6. Sao Tome. Com., 2:147-153.

1965b. Contribuicão para e geologia e geomorfologia da ilha do Príncipe. Conf. Int. Afr. Ocid. Sess. 6. São Tomé, Com., 2:157-162.

NETTLETON, L.L., 1939. Determination of density for reduction of gravimeter observations. Geophysics, 4:176-183.

1940. Geophysical Prospecting for Oil. McGraw-Hill Book Co. Ltd., 444 pp.

1954. Regionals, residuals and structures. Geophysics, 19:1-22.

NICHOLLS, G.D., 1965. Petrological and geochemical evidence for convection in the earth's mantle. Phil. Trans. Roy. Soc. No. 1088:168-179.

OFFICER, C.B., M. EWING and P.C. WUENSCHEL, 1952. Seismic refraction measurements in the Atlantic Ocean. Part IV. Bermuda, Bermuda Rise and Nares Basin. Bull. Geol. Soc. Amer., 63:777-808.

O'HARA, M.J. and H.S. YODER, 1967. Formation and fractionation of basaltic magmas at high pressure. Scott. Jour. Geol., 3:67.

PÁLMASON, G., 1963. Seismic refraction investigations of the basalt lavas in northern and eastern Iceland. Jökull, Reykjavik, 13:40-60.

1965. Seismic refraction studies of basalt lavas, Faeroe Islands. Tectonophysics, 2:475-482.

PARASNIS, D.S., 1952. A study of rock densities in the English Midlands. Mon. Not. Roy. Astr. Soc. Geophys. Supp., 6:252.

PART, G.M., 1950. Volcanic rocks from the Cape Verde Islands. Brit. Mus. Nat. Hist. B. Miner., 1:27-72.

PITMAN, W.C. and J.R. HEIRTZLER, 1966. Magnetic anomalies over the Pacific-Antartic Ridge. Science, 154:1170-1171.

RAITT, R.W., 1954. Bikini and nearby atolls 3. Geophysics, seismic refraction studies of Bikini and Kwajalein Atolls and Sylvania Guyot. U.S. Geol. Surv. Prof. Pa. 260K:507-524.

1957. Seismic refraction studies of Eniwetok Atoll. U.S. Geol.Surv. Prof. Pap. 260-s.

RICHARDSON, A. and N.D. WATKINS, 1967. Palaeomagnetism of Atlantic islands: Fernando Noronha. Nature, 215 (5109):1470-1473.

RIDLEY, W.I., 1968. Geology of Las Canadas Area, Tenerife. Ph.D. thesis, London University.

RUNCORN, S.K., 1962. Palaeomagnetic evidence for continental drift and its geophysical cause. Continental drift, Editor S,K. Runcorn, Academic Press, 1-40.

ST.JOHN, V.P. and R. GREEN, 1967. Topographic and isostatic corrections to gravity surveys in mountainous areas. Geophys. Pros., 15:151-162.

SAXOV, S. and N. ABRAHAMSEN, 1964. A note on some gravity and density measuring in the Faeroes islands. Boll. di Geof. Teor. ed Appl., 6:249.

SCHEINMANN, Y.M., 1964. Duration of earth crust formation on the basis of data for the Northern Atlantic. Tectonophysics, 1:377-383.

SCHMINCKE, H.U., 1967. Cone sheet swarm, resurgence of Tejeda caldera, and the early geologic history of Gran Canaria. Bull. Volc., 31:153-162.

SHOR, G.G. and D.D. POLLARD, 1964. Mohole site selection studies north of Maui. Jour. Geophys. Res., 69: 1627-1638.

SHURBET, G.L. and J.L. WORZEL, 1955. Gravity anomalies associated with seamounts. Bull. Geol. Soc. Amer., 66:777-782.

SILVA, G.H. da., 1956. La faune Miocene de l'ile du Prince. Comm. Pres. au 20th Sess. du Cong. Geol. Inter. Mexico.

SIMPSON, S.M., 1954. Least squares polynomial fitting to gravitational data and the density plotting by digital computers. Geophysics, 19:255-269.

SKEELS, D.C., 1947. Ambiguity in gravity interpretation. Geophysics, 12:43-56.

1963. An approximate solution of the problem of maximum depth in gravity interpretation. Geophysics, 28:724-735.

SONSA TORRES, A. and J.M. SOARES, 1946. Formacoes sedimentaries do arquipélago de Capo Verde. Portugal Junta Min. Geog. e Inves. Col. Min. Ser. Geol., 3.

1950. A idade dos sedimentos do arquipélago de Capo Verde. Conf. Int. Afr. Ocid. Sess. 2 Bissau, 1:85-91.

SOUGY, J., 1962. West African fold belt. Bull. Geol. Soc. Amer., 73:871-876.

STAHLECKER, R., 1935. Neocom auf der Kapverden-Insel Maio. Neues Jahrb. Min. Geol. Paläont. Abt. B. Beil. Bd., 73:265-301.

STEARNS, M.T. and G.A. MACDONALD, 1946. Geology and ground water resources of the island of Hawaii. Hawaii Division of Hydrography Bull., 9.

STRANGE, W.E., G.P. WOOLLARD and J.C. ROSE, 1965. An analysis of the gravity field over the Hawaiian islands in terms of crustal structure. Pacific Sci., 19:381-9.

SUTTON, J., 1963. Long term cycles in the evolution of the continents. Nature, 198(4882):731-735.

TAKIN, M. and M. TALWANI, 1966. Rapid computation of the gravitational attraction of topography on a spherical earth. Geophys. Pros., 14:119-142.

TALWANI, M. and M. EWING, 1960. Rapid computation of gravitational attraction of three dimensional bodies of arbitrary shape. Geophysics, 25:203-225.

TALWANI, M., B.C. HEEZEN and J.L. WORZEL, 1961. Gravity anomalies, physiography and crustal structure of the Mid-Atlantic Ridge. Publ. Bur. Central Seismol. Intern. Ser.A. Trav. Sci. Fasc., 22:81-111.

TALWANI, M., X. LE PICHON and M. EWING, 1965. Crustal structure of the Mid-Ocean Ridges. 2) Computed model from gravity and seismic refraction data. Jour. Geophys. Res., 70:341-352.

TALWANI, M and J.L. WORZEL, 1962. Continuous gravity profile across the Romanche Trench. Jour. Geophys. Res., 67:3602.

TALWANI, M., J.L. WORZEL and M. LANDISMAN, 1959. Rapid gravity computations for two-dimensional bodies with application to the Mendocino submarine fracture zone. Jour. Geophys. Res., 64:49-60.

TINKLER, K.J., 1966. Volcanic chronology of Lanzarote (Canary Islands). Nature, 209(5028):1122-1123.

TOZER, D.C., 1965. Heat transfer and convection currents. Phil. Trans. Roy. Soc. Ser. A 258:252-271.

TRYGGVASON, T., 1965. Petrographic studies on the eruption of Hekla 1947-1948. The eruption of Hekla 1947-1948. Soc. Sci. Ist. Reykjavik IV, 6:13.

VACQUIER, V. and R. VON HERTZEN, 1964. Evidence for connection between heat flow and the Mid-Atlantic Ridge magnetic anomaly. Jour. Geophys. Res., 69:1093-1101.

VAN ANDEL, T.H. and C.O. BOWIN, 1968. Mid-Atlantic Ridge between 22° and 23°North latitude and the tectonics of mid-ocean rises. Jour. Geophys. Res., 73:1279-98.

VEIGA FERREIRA, O. de, 1961. Afloramentas de calcareo Miocenicos da Ilha de Santa Maria (Azores). Comm. Serv. Geol. de Port., 45:493-502.

VENING MEINESZ, F.A., 1948. Gravity expeditions at sea, 1923;1938. Vol. 4. Neth. Geod. Comm., Delft. 233 pp.

VINE, F.J., 1966. Spreading of the ocean floor: new evidence. Science, 154(3755):1405-1415.

VINE, F.J. and D.H. MATTHEWS, 1963. Magnetic anomalies over oceanic ridges. Nature, 199(4897):947-949.

VINE, F.J. and J.T. WILSON, 1965. Magnetic anomalies over a young oceanic ridge off Vancouver Island. Science, 150(3695):485.

VOGT, P.R. and N.A. OSTENSO, 1967. Steady state crustal spreading. Nature, 215:810-817.

VON HERZEN, R.P. and M.G. LANGSETH, 1966. Present status of oceanic heat-flow measurements. Phys. and Chem of the Earth, 6:365-407.

VON KNEBEL, W., 1906. Studien zur ober flachengestaltung der Inseln Palma und Hierro. "Globus" Band 89, Braunschweig.

WATKINS, N.D., A. RICHARDSON and R.G. MASON, 1966. Palaeomagnetism of the insular region: the Canary Islands. Earth and Planetary Science Letters, 1:225-231.

WESTOLL, T.S., 1965. Geological evidence bearing upon continental drift. Phil Trans. Roy. Soc. Ser. A, 258:12-26.

WILLIAMS, H., 1941. Calderas and their origin. Univ. Calif. Dept. Geol. Sci. Bull., 25:239-346.

WILSON, J.T., 1963a. Hypothesis of earth's behaviour. Nature, 198(4984):925-929.

1963b. Pattern of uplifted islands in the main ocean basins. Science, 139(3555):592-594.

WILSON, J.T., 1965. A new class of faults and their bearing on continental drift. Nature, 207(4995):343-347.

1966. Did the Atlantic close and then reopen? Nature, 211:676-681.

WOOLLARD, G.P., 1951. A gravity reconnaissance of the island of Oahu. Trans. Amer. Geoph. Union, 32:358-367.

1964. Comparative gravity measurements on Pacific ocean islands. Abst. Amer. Geoph. Union Trans., 45:641.

WOOLLARD, G.P. and J.C. ROSE, 1963. International gravity measurements. Soc. Exploration Geophysicists, 518pp.

WORZEL, J.L., 1959. Continuous gravity measurements on a surface ship with the Graf sea gravimeter. Jour. Geophys. Res., 64:1299-1315.

1965a. Deep structure of coastal margins and mid-oceanic ridges. Submarine Geol. and Geophys.: Colston Papers No. 17:335-359.

1965b. Pendulum gravity measurements at sea 1936-1959. J. Wiley and Sons, 422 pp.

WORZEL, J.L. and J.C. HARRISON, 1963. "Gravity at Sea." The Sea, 3. Interscience pp 134-174.

YOKOYAMA, I., 1963. Structure of calderas and gravity anomaly. Bull. Volc., 26:67-72.

ZBYSZEWSKI, G., F.M. D'ALMEIDA, O. da VEIGA FERREIRA and C.T. ASSUNÇÃO, 1958. Carta geológica de Portugal, noticia explicativa da fohla B, S. Miguel (Açores). Serv. Geol. de Port.

ZBYSZEWSKI, G., O. da VEIGA FERREIRA and C.T. ASSUNÇÃO, 1959a. Carta geológica de Portugal, noticia explicativa da fohla de S. Miguel (Açores). Serv. Geol. de Port.

1959b. Carta geológica de Portugal, noticia explicativa da fohla Ilha de Faial (Açores). Serv. Geol. de Port.

ZBYSZEWSKI, G., 1961. La fauna marine des basses plages quaternaires de Praia et de Prainha dans l'ile de Santa Maria. Comm. Serv. Geol. de Port., 45:467-78.

ZBYSZEWSKI, G., O. da VEIGA FERREIRA and C.T. ASSUNÇÃO, 1961. Carta geológica de Portugal, noticia explicativa da fohla de Ilha de Santa Maria (Açores). Serv. Geol. de Portugal, 25 pp.

ZBYSZEWSKI, G., C.R. FERREIRA, O. da VEIGA FERREIRA and C.T. ASSUNÇÃO, 1962. Carta geológica de Portugal, noticia explicativa da fohla de Ilha do Pico (Açores). Serv. Geol. de Portugal.

APPENDIX

SUMMARY OF GRAVITY OBSERVATIONS ON THE OCEANIC ISLANDS IN THE ATLANTIC OCEAN.

SUMMARY OF GRAVITY OBSERVATIONS ON ASCENSION ISLAND

STATION NUMBER	LATITUDE SOUTH	LONGITUDE WEST	ELEVATION (FEET)	OBSERVED GRAVITY	NORMAL GRAVITY	TERRAIN CORR.	BOUGUER ANOMALY	RESIDUAL ANOMALY
1	7 57.49	14 23.96	382	978281.6	978147.7	23.8	182.4	6.0
2	7 57.61	14 24.15	312	978288.3	978147.8	23.7	184.4	7.3
3	7 57.45	14 24.59	213	978296.4	978147.7	23.5	186.0	7.8
4	7 57.69	14 24.46	260	978293.3	978147.8	23.8	186.1	8.1
5	7 57.83	14 24.39	254	978294.5	978147.9	23.7	186.7	8.7
6	7 58.05	14 23.94	272	978291.0	978147.9	23.6	184.3	7.5
7	7 57.78	14 24.03	300	978289.1	978147.8	23.5	184.2	7.4
8	7 58.05	14 24.30	259	978294.3	978147.9	23.7	186.9	8.9
9	7 58.18	14 24.44	236	978298.8	978148.0	23.9	190.0	11.3
10	7 58.29	14 24.54	200	978301.5	978148.0	23.8	190.2	11.1
11	7 58.46	14 24.80	107	978310.5	978148.1	23.9	193.2	13.0
12	7 58.88	14 24.54	79	978312.9	978148.3	23.9	193.6	13.4
13	7 58.55	14 24.11	286	978291.1	978148.2	24.4	185.8	7.7
14	7 58.31	14 23.94	284	978289.5	978148.1	23.8	183.6	6.5
15	7 53.57	14 22.81	1	978302.2	978146.1	26.2	182.4	3.3
16	7 53.61	14 22.65	36	978300.0	978146.1	26.8	183.0	4.3
17	7 53.82	14 22.61	97	978297.0	978146.2	26.2	183.3	5.2
18	7 53.95	14 22.52	128	978296.2	978146.3	25.9	184.1	6.5
19	7 54.22	14 22.66	143	978297.2	978146.4	25.1	185.2	8.2
20	7 54.46	14 22.86	156	978297.7	978146.5	24.5	185.8	9.2
21	7 54.50	14 22.87	158	978297.6	978146.5	24.5	185.8	9.3
22	7 54.21	14 22.91	100	978299.3	978146.4	24.6	184.0	6.6
23	7 54.82	14 22.79	233	978292.8	978146.6	24.3	185.6	9.9
24	7 54.97	14 22.94	232	978292.8	978146.7	24.1	185.2	9.6
25	7 55.09	14 23.21	215	978293.8	978146.7	23.9	184.9	9.0
26	7 56.40	14 21.63	981	978230.9	978147.3	28.4	175.5	5.9
27	7 55.63	14 20.61	390	978270.7	978147.0	27.0	175.9	7.9
28	7 55.65	14 20.46	444	978264.8	978147.0	27.8	174.3	6.9
29	7 55.45	14 20.51	376	978269.9	978146.9	27.1	174.4	6.2
30	7 54.84	14 20.04	50	978284.4	978146.6	27.9	168.9	0.0
31	7 55.15	14 19.63	43	978282.8	978146.8	29.1	167.9	1.6
32	7 55.37	14 19.54	115	978278.9	978146.8	29.9	169.4	4.3
33	7 55.66	14 19.17	130	978274.6	978147.0	32.3	168.3	5.8
34	7 54.95	14 20.40	43	978290.9	978146.7	26.3	173.3	3.7
35	7 54.62	14 20.80	60	978292.5	978146.5	26.5	176.4	4.4

SUMMARY OF GRAVITY OBSERVATIONS ON ASCENSION ISLAND

STATION NUMBER	LATITUDE SOUTH	LONGITUDE WEST	ELEVATION (FEET)	OBSERVED GRAVITY	NORMAL GRAVITY	TERRAIN CORR.	BOUGUER ANOMALY	RESIDUAL ANOMALY
36	7 54.44	14 21.01	12	978297.2	978146.5	26.1	177.6	4.4
37	7 55.22	14 23.38	200	978294.5	978146.8	23.5	184.1	8.1
38	7 54.78	14 23.53	125	978300.1	978146.6	23.6	185.2	8.2
39	7 54.67	14 23.79	114	978300.4	978146.6	23.9	185.1	7.6
40	7 54.52	14 23.99	101	978301.8	978146.5	24.2	186.0	8.1
41	7 54.44	14 24.08	86	978302.6	978146.5	24.4	186.1	8.0
42	7 54.16	14 23.93	71	978302.8	978146.4	24.8	185.8	7.3
43	7 54.03	14 23.86	79	978302.0	978146.3	25.3	186.1	7.4
44	7 54.52	14 24.18	76	978302.8	978146.5	24.4	185.6	7.5
45	7 54.48	14 24.13	78	978303.2	978146.5	24.4	186.1	8.1
46	7 54.83	14 24.08	88	978301.3	978146.6	23.8	184.2	6.6
47	7 55.01	14 23.87	98	978302.2	978146.7	23.3	185.1	8.1
48	7 55.22	14 23.71	178	978296.1	978146.8	23.5	184.3	7.8
49	7 55.37	14 23.93	200	978295.1	978146.8	23.5	184.7	8.0
50	7 55.44	14 23.86	227	978293.5	978146.9	23.6	184.9	8.3
51	7 55.40	14 23.46	250	978290.8	978146.9	23.5	183.6	7.7
52	7 55.49	14 23.42	295	978287.5	978146.9	23.7	183.4	7.7
53	7 54.20	14 23.76	114	978300.8	978146.4	24.8	186.6	8.3
54	7 54.18	14 23.66	115	978301.1	978146.4	24.8	186.9	8.7
55	7 54.12	14 23.68	119	978300.4	978146.3	25.0	186.8	8.4
56	7 55.98	14 23.52	362	978282.5	978147.1	23.7	182.5	7.1
57	7 56.05	14 23.72	364	978282.3	978147.1	23.8	182.6	6.8
58	7 56.09	14 23.41	369	978281.1	978147.1	23.6	181.5	6.4
59	7 56.09	14 23.86	349	978283.1	978147.1	23.8	182.4	6.3
60	7 55.79	14 23.77	312	978286.1	978147.0	23.7	183.0	6.9
61	7 55.65	14 23.59	317	978286.4	978147.0	23.7	183.6	7.8
62	7 56.17	14 24.16	297	978286.5	978147.2	23.7	182.2	5.6
63	7 56.27	14 24.26	306	978286.6	978147.2	23.7	182.9	6.1
64	7 56.33	14 24.45	250	978290.1	978147.2	23.6	182.7	5.5
65	7 56.46	14 24.65	192	978294.6	978147.3	23.5	183.2	5.6
66	7 56.44	14 24.70	182	978295.4	978147.3	23.5	183.4	5.7
67	7 56.28	14 24.87	124	978298.6	978147.2	23.4	182.8	4.8
68	7 55.99	14 24.82	56	978303.2	978147.1	23.1	182.8	5.0
69	7 55.82	14 24.80	57	978303.9	978147.0	23.2	183.8	6.0
70	7 57.29	14 19.59	1765	978158.3	978147.6	42.4	167.3	8.1

SUMMARY OF GRAVITY OBSERVATIONS ON ASCENSION ISLAND

STATION NUMBER	LATITUDE SOUTH	LONGITUDE WEST	ELEVATION (FEET)	OBSERVED GRAVITY	NORMAL GRAVITY	TERRAIN CORR.	BOUGUER ANOMALY	RESIDUAL ANOMALY
71	7 57.09	14 19.65	1560	978176.6	978147.6	37.6	167.5	7.6
72	7 56.67	14 19.34	1365	978186.5	978147.4	38.0	165.4	5.7
73	7 56.99	14 19.77	1288	978199.4	978147.5	34.3	169.5	8.7
74	7 57.41	14 19.73	1759	978159.9	978147.7	42.4	168.4	8.8
75	7 57.32	14 19.79	1726	978167.8	978147.6	39.6	171.5	11.4
76	7 57.34	14 19.99	1692	978173.7	978147.7	38.0	173.5	12.5
77	7 57.05	14 20.03	1759	978167.9	978147.5	38.9	173.1	11.3
78	7 56.82	14 20.25	1848	978161.6	978147.4	39.3	173.1	9.7
79	7 56.54	14 20.83	1587	978180.5	978147.3	38.2	174.1	7.7
80	7 55.56	14 21.31	614	978259.0	978146.9	26.6	178.4	8.0
81	7 55.85	14 21.81	685	978252.9	978147.0	26.8	177.0	5.8
82	7 56.12	14 24.91	75	978302.1	978147.2	23.3	183.1	5.1
83	7 56.18	14 25.04	60	978302.8	978147.2	23.4	182.9	4.7
84	7 56.02	14 25.02	46	978304.2	978147.1	23.4	183.5	5.3
85	7 55.98	14 25.17	14	978306.5	978147.1	23.4	183.7	5.4
86	7 55.82	14 25.09	24	978305.6	978147.0	23.6	183.8	5.6
87	7 55.81	14 24.97	53	978303.3	978147.0	23.6	183.3	5.3
88	7 55.68	14 24.76	56	978303.4	978147.0	23.3	183.3	5.6
89	7 55.53	14 24.57	12	978307.4	978146.9	23.0	184.3	6.7
90	7 55.46	14 24.43	11	978307.6	978146.9	23.1	184.5	7.1
91	7 55.31	14 24.30	14	978307.3	978146.8	22.9	184.3	7.0
92	7 55.23	14 24.32	29	978304.9	978146.8	23.2	183.2	5.8
93	7 55.88	14 24.70	62	978303.3	978147.1	23.2	183.4	5.8
94	7 56.59	14 24.59	200	978294.2	978147.3	23.3	183.1	5.6
95	7 56.67	14 24.79	167	978296.0	978147.4	23.5	182.9	4.9
96	7 56.82	14 24.93	140	978299.0	978147.4	23.7	184.4	6.0
97	7 56.89	14 24.50	217	978292.4	978147.5	23.4	182.3	4.8
98	7 57.05	14 24.41	216	978291.8	978147.5	23.3	181.6	4.2
99	7 57.03	14 24.55	217	978292.4	978147.5	23.4	182.3	4.6
100	7 57.15	14 24.59	176	978297.4	978147.6	23.3	184.5	6.6
101	7 57.10	14 24.64	182	978297.1	978147.6	23.4	184.7	6.7
102	7 57.11	14 24.76	303	978289.0	978147.6	24.3	185.3	7.0
103	7 57.19	14 24.50	214	978293.5	978147.6	23.3	183.0	5.4
104	7 56.12	14 23.28	366	978281.4	978147.2	23.7	181.6	6.8
105	7 56.21	14 23.30	376	978280.0	978147.2	23.7	180.8	6.1

SUMMARY OF GRAVITY OBSERVATIONS ON ASCENSION ISLAND

STATION NUMBER	LATITUDE SOUTH	LONGITUDE WEST	ELEVATION (FEET)	OBSERVED GRAVITY	NORMAL GRAVITY	TERRAIN CORR.	BOUGUER ANOMALY	RESIDUAL ANOMALY
106	7 56.05	14 23.26	375	978280.8	978147.1	23.7	181.7	6.9
107	7 55.95	14 23.17	388	978279.6	978147.1	23.8	181.4	6.8
108	7 55.86	14 23.21	356	978282.5	978147.0	23.8	182.3	7.5
109	7 55.97	14 22.99	419	978277.2	978147.1	24.2	181.4	7.2
110	7 55.97	14 22.86	441	978275.0	978147.1	24.0	180.4	6.6
111	7 56.02	14 22.48	540	978267.6	978147.1	25.0	180.4	7.6
112	7 56.13	14 22.48	540	978267.0	978147.2	24.9	179.6	7.0
113	7 56.14	14 22.65	514	978269.1	978147.2	24.6	179.8	6.6
114	7 56.34	14 22.48	508	978268.3	978147.2	24.5	178.5	6.1
115	7 56.16	14 22.80	488	978271.3	978147.2	24.3	180.0	6.5
116	7 56.14	14 22.93	455	978274.1	978147.2	24.2	180.5	6.7
117	7 56.10	14 23.16	377	978279.7	978147.1	23.8	180.8	6.3
118	7 56.97	14 23.10	512	978269.9	978147.5	24.2	179.7	6.0
119	7 57.01	14 22.94	527	978267.8	978147.5	24.3	178.7	5.5
120	7 57.02	14 23.27	497	978271.0	978147.5	24.0	179.7	5.4
121	7 57.18	14 23.10	500	978270.2	978147.6	24.1	179.1	5.4
122	7 57.07	14 22.79	558	978265.3	978147.5	24.4	178.3	5.6
123	7 56.82	14 22.48	600	978262.4	978147.4	24.4	178.2	6.3
124	7 56.73	14 22.52	593	978262.9	978147.4	24.8	178.7	6.6
125	7 56.61	14 22.47	588	978263.2	978147.4	24.8	178.6	6.6
126	7 56.60	14 22.41	633	978259.7	978147.4	25.3	178.6	6.7
127	7 56.51	14 22.50	564	978264.1	978147.3	25.0	178.3	6.0
128	7 56.56	14 21.88	942	978234.0	978147.3	27.9	175.6	5.4
129	7 56.68	14 22.11	733	978251.4	978147.4	26.2	177.6	6.8
130	7 57.03	14 22.55	555	978264.8	978147.5	24.7	177.9	6.0
131	7 57.22	14 22.51	567	978263.4	978147.6	24.9	177.4	5.7
132	7 57.10	14 22.40	591	978262.0	978147.6	25.1	177.7	6.4
133	7 57.33	14 22.46	586	978262.1	978147.7	25.0	177.3	5.9
134	7 57.50	14 22.47	659	978256.1	978147.7	25.6	176.6	5.2
135	7 58.77	14 23.76	107	978301.6	978148.2	23.3	183.6	6.6
136	7 58.96	14 23.85	85	978303.5	978148.3	23.4	184.1	6.4
137	7 59.02	14 23.90	62	978305.7	978148.3	23.4	184.8	6.8
138	7 59.07	14 23.85	95	978302.3	978148.4	23.6	183.6	5.7
139	7 59.21	14 24.09	13	978309.6	978148.4	23.6	185.6	6.5
140	7 58.35	14 23.90	287	978289.3	978148.1	23.9	183.7	6.6

SUMMARY OF GRAVITY OBSERVATIONS ON ASCENSION ISLAND

STATION NUMBER	LATITUDE SOUTH	LONGITUDE WEST	ELEVATION (FEET)	OBSERVED GRAVITY	NORMAL GRAVITY	TERRAIN CORR.	BOUGUER ANOMALY	RESIDUAL ANOMALY
141	7 58.24	14 23.69	228	978292.3	978148.0	23.3	182.4	6.2
142	7 58.33	14 23.41	227	978290.3	978148.1	23.7	180.6	5.4
143	7 58.39	14 23.16	214	978291.2	978148.1	23.3	180.2	6.0
144	7 57.41	14 23.58	439	978275.6	978147.7	23.9	180.2	5.0
145	7 57.31	14 23.45	442	978274.3	978147.6	23.9	179.2	4.4
146	7 57.11	14 23.64	413	978277.4	978147.6	23.7	180.2	4.9
147	7 56.96	14 23.57	444	978275.4	978147.5	23.8	180.4	5.3
148	7 57.41	14 23.70	430	978276.7	978147.7	23.9	180.7	5.1
149	7 57.21	14 23.90	382	978280.9	978147.6	23.8	181.8	5.7
150	7 57.31	14 23.82	401	978279.8	978147.6	23.8	181.9	6.0
151	7 57.39	14 23.91	390	978280.6	978147.7	23.6	181.7	5.5
152	7 56.90	14 24.23	313	978285.9	978147.5	23.5	182.2	5.3
153	7 56.78	14 24.11	313	978285.3	978147.4	23.5	181.7	5.1
154	7 56.71	14 24.00	314	978285.3	978147.4	23.5	181.7	5.5
155	7 56.67	14 24.14	296	978286.4	978147.4	23.4	181.6	5.0
156	7 56.78	14 24.20	291	978287.1	978147.4	23.4	181.9	5.2
157	7 56.84	14 23.86	340	978283.6	978147.4	23.5	181.7	5.8
158	7 56.69	14 23.74	404	978278.4	978147.4	23.8	180.9	5.3
159	7 56.58	14 23.78	404	978278.8	978147.3	23.8	181.4	5.7
160	7 56.25	14 24.03	345	978283.2	978147.2	23.8	182.1	5.8
161	7 56.24	14 23.60	416	978278.7	978147.2	23.9	182.3	6.9
162	7 56.39	14 23.53	416	978278.1	978147.3	23.8	181.5	6.3
163	7 55.77	14 20.87	531	978262.7	978147.0	27.0	177.1	8.6
164	7 55.72	14 20.97	518	978264.1	978147.0	26.7	177.3	8.4
165	7 55.66	14 20.79	463	978266.7	978147.0	26.9	176.6	8.0
166	7 55.51	14 21.42	602	978260.5	978146.9	26.5	179.1	8.2
167	7 55.46	14 21.38	593	978261.7	978146.9	26.7	179.9	9.0
168	7 55.53	14 21.61	618	978260.3	978146.9	26.4	179.8	8.4
169	7 55.32	14 21.55	598	978262.6	978146.8	26.7	181.2	9.5
170	7 55.49	14 21.75	617	978260.3	978146.9	26.4	179.7	7.9
171	7 55.32	14 21.21	756	978248.2	978146.8	29.1	179.4	8.6
172	7 55.27	14 21.09	758	978246.2	978146.8	29.9	178.4	7.8
173	7 55.37	14 21.09	750	978249.0	978146.8	28.9	179.6	9.3
174	7 55.68	14 21.31	594	978260.7	978147.0	26.1	178.2	8.1
175	7 55.81	14 21.48	615	978258.4	978147.0	25.9	177.1	6.8

SUMMARY OF GRAVITY OBSERVATIONS ON ASCENSION ISLAND

STATION NUMBER	LATITUDE SOUTH	LONGITUDE WEST	ELEVATION (FEET)	OBSERVED GRAVITY	NORMAL GRAVITY	TERRAIN CORR.	BOUGUER ANOMALY	RESIDUAL ANOMALY
176	7 56.20	14 21.83	867	978240.9	978147.2	27.4	177.2	6.6
177	7 56.14	14 21.93	852	978243.7	978147.2	27.2	178.8	7.8
178	7 57.90	14 22.58	462	978270.1	978147.9	24.7	176.8	5.0
179	7 58.01	14 22.61	465	978271.3	978147.9	24.8	178.3	6.4
180	7 58.06	14 22.70	349	978281.1	978148.0	24.2	179.9	7.6
181	7 58.23	14 22.83	292	978284.8	978148.0	23.7	179.4	6.5
182	7 58.29	14 22.87	272	978286.2	978148.0	23.6	179.4	6.4
183	7 58.10	14 24.62	10	978316.9	978148.0	23.3	192.8	13.8
184	7 57.86	14 24.69	25	978313.6	978147.9	23.0	190.3	11.4
185	7 57.39	14 24.80	13	978312.9	978147.7	22.8	188.8	10.2
186	7 57.05	14 25.06	3	978311.5	978147.5	22.9	187.1	8.2
187	7 57.07	14 25.10	3	978312.5	978147.5	23.0	188.2	9.2
188	7 57.90	14 23.06	306	978280.5	978147.9	23.6	176.0	2.4
189	7 58.77	14 22.95	124	978295.4	978148.2	23.3	178.5	4.8
190	7 58.90	14 22.90	121	978294.1	978148.3	23.5	177.1	3.5
191	7 59.29	14 22.98	59	978298.0	978148.5	24.1	177.4	3.0
192	7 59.28	14 23.07	54	978298.6	978148.5	23.9	177.5	2.7
193	7 58.56	14 24.32	182	978302.6	978148.2	23.9	190.1	11.2
194	7 58.71	14 24.18	208	978298.1	978148.2	24.0	187.4	8.8
195	7 58.49	14 21.90	560	978261.6	978148.1	26.7	176.4	7.6
196	7 59.19	14 22.17	9	978297.5	978148.4	24.0	173.7	3.3
197	7 59.05	14 22.58	147	978290.5	978148.4	24.4	176.0	3.7
198	7 58.62	14 22.55	263	978283.5	978148.2	24.1	176.4	4.6
199	7 57.58	14 21.31	1608	978185.1	978147.8	35.7	177.1	10.4
200	7 57.98	14 21.15	1147	978214.5	978147.9	31.5	172.3	6.8
201	7 55.76	14 19.87	914	978227.1	978147.0	33.9	173.1	8.2
202	7 58.80	14 20.63	213	978275.6	978148.3	27.1	168.2	5.9
203	7 58.76	14 20.49	201	978275.9	978148.2	27.3	168.0	6.5
204	7 56.74	14 18.03	462	978240.0	978147.4	34.3	156.8	4.0
205	7 56.95	14 17.92	402	978245.1	978147.5	32.5	156.1	4.7
206	7 57.22	14 17.96	232	978258.2	978147.6	30.8	156.4	5.8
207	7 56.78	14 18.45	548	978240.2	978147.4	32.8	161.1	6.2
208	7 56.31	14 20.01	1589	978177.0	978147.2	38.6	171.2	7.5
209	7 55.90	14 20.11	979	978224.1	978147.1	32.8	173.2	7.8
210	7 55.71	14 20.28	777	978239.5	978147.0	31.3	174.1	7.5

SUMMARY OF GRAVITY OBSERVATIONS IN THE AZORES (1) SANTA MARIA

STATION NUMBER	LATITUDE NORTH	LONGITUDE WEST	ELEVATION (METRES)	OBSERVED GRAVITY	NORMAL GRAVITY	TERRAIN CORR.	BOUGUER ANOMALY
0	36 58.39	25 9.95	100	980117.3	979914.7	12.5	236.3
1	36 58.38	25 9.39	113	980115.1	979914.6	12.2	236.7
2	36 58.28	25 10.45	87	980118.0	979914.5	13.8	235.8
3	37 0.20	25 9.53	7	980142.6	979917.3	10.8	237.6
4	36 59.86	25 9.00	95	980123.4	979916.8	11.7	238.4
5	36 59.41	25 8.13	193	980100.3	979916.1	12.0	237.2
6	36 58.22	25 5.00	420	980045.7	979914.4	20.3	240.7
7	36 58.93	25 5.51	565	980010.0	979915.4	27.5	242.1
8	36 59.08	25 4.12	220	980093.4	979915.7	15.2	239.6
9	36 57.89	25 6.41	178	980102.5	979913.9	13.1	239.5
10	36 57.00	25 5.94	2	980129.1	979912.7	13.1	229.9
11	36 59.73	25 10.54	44	980135.6	979916.6	12.5	240.8
12	36 59.81	25 10.57	1	980145.6	979916.7	12.0	241.1
13	36 59.14	25 10.30	87	980122.7	979915.7	12.6	238.0
14	36 56.70	25 8.92	4	980124.9	979912.2	13.5	227.1
15	36 57.59	25 9.02	108	980110.9	979913.5	12.7	233.1
16	36 57.38	25 9.97	85	980111.8	979913.2	13.6	230.3
17	36 56.70	25 9.98	40	980113.4	979912.2	14.3	224.0
18	36 58.73	25 6.50	252	980089.2	979915.2	13.5	241.0
19	36 57.68	25 7.51	150	980104.3	979913.6	13.4	235.9
20	36 58.49	25 7.78	195	980098.9	979914.8	12.7	238.2
21	36 59.59	25 7.02	230	980093.0	979916.4	13.4	238.8
22	37 0.27	25 5.98	245	980094.1	979917.4	14.6	243.3
23	37 0.32	25 5.32	260	980084.4	979917.5	16.4	238.5
24	36 59.83	25 4.81	218	980095.8	979916.7	14.9	240.3
25	36 59.97	25 3.84	260	980080.2	979916.9	17.2	235.7
26	37 0.68	25 3.60	145	980104.2	979918.0	16.4	233.3
27	36 58.57	25 3.06	250	980074.6	979914.9	17.9	230.6
28	36 59.62	25 3.33	7	980133.8	979916.4	16.1	235.0
29	36 58.92	25 9.02	108	980119.8	979915.4	11.9	239.2
30	36 57.46	25 4.28	425	980037.1	979913.3	20.5	234.6
31	36 57.66	25 3.38	333	980057.4	979913.6	17.7	232.2
32	36 57.27	25 2.51	310	980052.6	979913.0	19.8	225.2
33	36 56.65	25 1.92	255	980056.3	979912.2	20.3	218.5
34	36 56.59	25 0.98	3	980105.5	979912.1	18.4	212.4

SUMMARY OF GRAVITY OBSERVATIONS IN THE AZORES (1) SANTA MARIA

STATION NUMBER	LATITUDE NORTH	LONGITUDE WEST	ELEVATION (METRES)	OBSERVED GRAVITY	NORMAL GRAVITY	TERRAIN CORR.	BOUGUER ANOMALY
35	36 56.14	25 1.30	230	980048.2	979911.4	24.6	210.2
36	36 56.08	25 2.76	237	980056.1	979911.3	20.3	215.4
37	36 57.64	25 2.14	275	980059.6	979913.6	20.2	224.6
38	36 56.73	25 4.31	273	980062.4	979912.3	18.6	226.6
39	36 58.43	25 5.45	298	980074.9	979914.7	18.1	241.6
40	36 55.65	25 1.09	1	980098.4	979910.7	18.5	206.4
41	36 56.14	25 3.79	205	980067.4	979911.4	18.6	218.1
42	36 59.73	25 5.64	481	980029.9	979916.6	26.0	241.4

SUMMARY OF GRAVITY OBSERVATIONS IN THE AZORES (2) SAO MIGUEL

STATION NUMBER	LATITUDE NORTH	LONGITUDE WEST	ELEVATION (METRES)	OBSERVED GRAVITY	NORMAL GRAVITY	TERRAIN CORR.	BOUGUER ANOMALY
0	37 43.92	25 39.69	3	980129.8	979980.7	6.8	156.5
1	37 45.86	25 44.15	200	980094.4	979983.5	9.5	162.8
2	37 48.19	25 48.10	101	980124.3	979986.9	9.8	168.7
3	37 49.27	25 49.78	84	980120.4	979988.4	9.7	159.6
4	37 52.05	25 50.34	227	980082.2	979992.5	16.7	154.6
5	37 53.73	25 49.23	20	980126.1	979994.9	11.2	146.7
6	37 51.54	25 47.87	270	980078.8	979991.8	11.0	155.3
7	37 53.76	25 45.31	125	980100.4	979995.0	13.3	145.2
8	37 51.43	25 42.13	45	980125.8	979991.6	10.0	153.7
9	37 49.78	25 40.10	4	980130.5	979989.2	7.6	149.8
10	37 49.19	25 36.67	29	980130.5	979988.3	7.1	155.4
11	37 48.49	25 33.62	46	980130.7	979987.3	7.2	160.3
12	37 49.30	25 30.90	50	980130.1	979988.5	7.7	159.9
13	37 49.14	25 27.76	214	980089.2	979988.3	15.7	162.0
14	37 48.95	25 23.60	250	980093.1	979988.0	11.1	169.2
15	37 51.08	25 19.54	140	980125.6	979991.1	11.4	175.6
16	37 51.27	25 15.87	158	980126.5	979991.4	12.5	181.1
17	37 51.11	25 11.28	166	980129.4	979991.1	13.5	187.1
18	37 49.73	25 8.84	142	980139.9	979989.1	13.1	194.0
19	37 45.97	25 12.18	447	980065.2	979983.6	17.3	193.8
20	37 44.73	25 14.93	110	980121.7	979981.8	13.1	176.3
21	37 44.54	25 14.73	3	980146.7	979981.6	9.9	175.6
22	37 46.16	25 18.72	208	980101.5	979983.9	13.0	174.8
23	37 42.89	25 22.22	102	980103.5	979979.2	11.9	157.8
24	37 42.57	25 26.11	1	980120.9	979978.7	8.0	150.4
25	37 43.32	25 31.43	130	980088.5	979979.8	9.0	145.3
26	37 45.14	25 36.60	36	980124.5	979982.4	7.1	156.8
27	37 44.19	25 40.14	5	980130.4	979981.1	6.5	156.8
28	37 45.19	25 17.08	365	980068.3	979982.5	14.4	177.7
29	37 46.32	25 13.94	274	980105.4	979984.2	14.9	194.2
30	37 44.30	25 11.64	3	980147.8	979981.2	14.2	181.4
31	37 47.22	25 12.12	658	980027.8	979985.5	20.6	202.6
32	37 45.43	25 9.32	285	980093.1	979982.9	18.4	189.1
33	37 48.24	25 8.53	213	980123.8	979986.9	15.2	197.3
34	37 49.97	25 13.02	463	980063.8	979989.5	15.9	188.5

SUMMARY OF GRAVITY OBSERVATIONS IN THE AZORES (2) SAO MIGUEL

STATION NUMBER	LATITUDE NORTH	LONGITUDE WEST	ELEVATION (METRES)	OBSERVED GRAVITY	NORMAL GRAVITY	TERRAIN CORR.	BOUGUER ANOMALY
35	37 50.70	25 14.04	265	980106.3	979990.5	14.2	186.2
36	37 44.89	25 24.45	496	980030.4	979982.1	11.8	165.4
37	37 45.03	25 24.69	510	980027.3	979982.3	11.9	165.1
38	37 43.92	25 28.51	325	980050.0	979980.7	12.6	150.9
39	37 44.41	25 33.65	63	980110.8	979981.4	7.7	150.5
40	37 45.41	25 32.64	222	980078.1	979982.8	9.5	151.9
41	37 47.40	25 32.76	152	980104.7	979985.7	8.7	159.9
42	37 47.49	25 30.14	217	980089.4	979985.9	10.3	159.9
43	37 49.16	25 25.72	2	980144.3	979988.3	10.2	166.6
44	37 51.78	25 46.26	260	980086.7	979992.1	13.1	162.9
45	37 51.13	25 47.37	261	980082.1	979991.2	10.8	157.1
46	37 50.65	25 47.90	284	980078.4	979990.5	11.5	159.7
47	37 51.51	25 48.55	281	980076.5	979991.7	11.6	156.0
48	37 50.59	25 50.03	167	980101.1	979990.4	10.5	156.7
49	37 46.97	25 46.13	279	980077.7	979985.1	14.2	166.0
50	37 47.05	25 21.98	525	980032.4	979985.2	12.1	170.8
51	37 46.95	25 36.30	177	980097.4	979985.1	7.7	157.6
52	37 46.32	25 39.35	198	980092.3	979984.2	8.0	158.1
53	37 48.00	25 38.70	198	980097.0	979986.6	8.3	160.8
54	37 48.43	25 41.90	275	980085.4	979987.2	9.3	165.9
55	37 46.00	25 41.50	196	980095.8	979983.7	8.0	161.8
56	37 44.65	25 42.22	104	980111.6	979981.7	7.6	159.6
57	37 44.35	25 21.71	475	980034.7	979981.3	12.3	166.5
58	37 43.84	25 17.80	4	980139.5	979980.5	11.4	171.3
59	37 47.92	25 44.04	475	980045.9	979986.5	12.2	172.4
60	37 49.03	25 44.15	640	980005.0	979988.1	15.4	168.2
61	37 49.92	25 45.51	790	979970.7	979989.4	19.5	168.5
62	37 54.24	25 46.88	126	980096.6	979995.7	12.7	140.4
63	37 52.46	25 43.70	275	980082.6	979993.1	12.6	160.5
64	37 47.22	25 17.59	711	979999.0	979985.5	19.2	183.6
65	37 45.89	25 23.16	560	980020.4	979983.5	12.9	168.7
66	37 46.38	25 34.56	186	980091.8	979984.2	8.0	155.0
67	37 47.84	25 9.66	569	980041.3	979986.4	19.6	195.3
68	37 48.43	25 17.59	580	980032.3	979987.2	14.4	182.7
69	37 50.05	25 17.99	280	980099.7	979989.6	11.8	181.3

SUMMARY OF GRAVITY OBSERVATIONS IN THE AZORES (2) SAO MIGUEL

STATION NUMBER	LATITUDE NORTH	LONGITUDE WEST	ELEVATION (METRES)	OBSERVED GRAVITY	NORMAL GRAVITY	TERRAIN CORR.	BOUGUER ANOMALY
70	37 48.92	25 46.67	452	980043.3	979937.9	14.3	165.7
71	37 50.08	25 43.26	432	980047.0	979939.6	12.6	161.8
72	37 47.92	25 14.45	940	979958.1	979836.5	24.0	195.1
73	37 49.59	25 15.46	505	980052.6	979968.9	17.5	188.4
74	37 44.62	25 39.80	31	980125.8	979951.7	6.7	157.4

SUMMARY OF GRAVITY OBSERVATIONS IN THE AZORES (3) TERCEIRA

STATION NUMBER	LATITUDE NORTH	LONGITUDE WEST	ELEVATION (METRES)	OBSERVED GRAVITY	NORMAL GRAVITY	TERRAIN CORR.	BOUGUER ANOMALY
0	38 46.33	27 5.73	55	980176.4	980071.9	5.3	121.5
1	38 39.12	27 12.92	2	980180.2	980061.3	5.2	124.5
2	38 39.39	27 11.23	97	980168.3	980061.7	5.7	132.9
3	38 39.51	27 10.12	135	980163.1	980061.9	6.2	136.1
4	38 39.46	27 8.67	182	980151.9	980061.8	5.7	134.4
5	38 38.89	27 7.10	2	980186.7	980061.0	4.8	130.9
6	38 38.78	27 4.85	8	980184.0	980060.8	4.1	129.0
7	38 40.27	27 4.57	2	980190.3	980063.0	4.4	132.1
8	38 41.56	27 4.98	128	980164.8	980064.9	5.4	132.5
9	38 41.26	27 3.03	7	980186.7	980064.4	3.9	127.7
10	38 42.63	27 3.62	1	980188.1	980066.4	4.4	126.3
11	38 43.87	27 3.61	2	980188.2	980068.3	4.7	125.0
12	38 43.22	27 5.35	90	980173.9	980067.3	5.6	131.3
13	38 44.29	27 6.19	136	980165.4	980068.9	6.8	132.2
14	38 44.04	27 7.16	276	980136.0	980068.5	6.5	132.6
15	38 42.75	27 6.93	545	980070.1	980066.6	15.1	134.3
16	38 43.59	27 8.69	392	980114.2	980067.8	7.5	137.1
17	38 40.36	27 6.76	274	980130.0	980063.1	6.2	131.3
18	38 44.89	27 5.02	63	980175.9	980069.8	5.4	124.9
19	38 45.38	27 3.95	47	980176.1	980070.5	5.7	121.3
20	38 46.22	27 5.14	49	980174.7	980071.7	5.9	119.3
21	38 46.02	27 6.24	60	980174.5	980071.4	5.6	121.4
22	38 47.09	27 6.90	1	980185.3	980073.0	5.4	117.9
23	38 45.05	27 7.48	115	980168.0	980070.0	5.6	128.0
24	38 45.40	27 9.34	173	980159.8	980070.5	5.7	131.8
25	38 46.30	27 10.64	150	980164.1	980071.8	6.5	130.6
26	38 46.88	27 9.41	82	980174.0	980072.7	5.8	124.5
27	38 46.63	27 7.92	53	980177.1	980072.3	5.5	121.5
28	38 47.21	27 11.56	118	980167.6	980073.2	6.5	125.9
29	38 47.57	27 12.74	88	980176.6	980073.7	6.4	128.0
30	38 47.53	27 14.07	88	980177.3	980073.6	6.3	128.7
31	38 47.62	27 15.79	82	980185.1	980073.8	6.5	135.2
31	38 48.08	27 15.64	1	980199.0	980074.4	5.6	130.4
32	38 46.45	27 17.42	331	980129.9	980072.0	8.4	136.6
33	38 47.48	27 18.03	132	980173.2	980073.6	7.8	135.4

SUMMARY OF GRAVITY OBSERVATIONS IN THE AZORES (3) TERCEIRA

STATION NUMBER	LATITUDE NORTH	LONGITUDE WEST	ELEVATION (METRES)	OBSERVED GRAVITY	NORMAL GRAVITY	TERRAIN CORR.	BOUGUER ANOMALY
34	38 46.48	27 18.75	330	980132.3	980072.1	10.1	140.3
35	38 47.30	27 19.83	128	980174.2	980073.3	8.0	136.0
36	38 43.62	27 21.69	341	980110.9	980067.9	13.4	128.8
37	38 40.45	27 9.88	284	980132.8	980063.2	6.0	135.9
38	38 40.97	27 8.12	291	980128.8	980064.0	5.7	132.3
39	38 42.12	27 8.17	334	980120.1	980065.7	6.0	131.3
40	38 42.50	27 7.37	329	980126.6	980066.2	6.5	136.7
41	38 41.48	27 7.31	308	980127.6	980064.8	5.9	134.1
42	38 39.85	27 6.09	159	980154.8	980062.4	5.1	131.3
43	38 40.15	27 11.78	191	980152.0	980062.8	6.2	135.9
44	38 41.34	27 11.34	334	980122.4	980064.5	6.7	135.5
45	38 42.57	27 9.69	375	980115.0	980066.4	6.4	134.6
46	38 43.71	27 9.69	329	980130.7	980068.0	6.5	139.0
47	38 42.84	27 11.13	444	980100.3	980066.7	7.5	135.4
48	38 42.37	27 12.77	461	980088.2	980066.1	7.8	127.8
49	38 43.30	27 13.26	537	980073.7	980067.4	8.8	129.2
50	38 43.58	27 14.98	530	980082.7	980067.8	10.3	137.8
51	38 44.54	27 15.93	513	980091.6	980069.2	8.9	140.2
52	38 42.88	27 17.77	547	980072.2	980066.8	12.5	134.0
53	38 43.20	27 16.81	491	980093.0	980067.3	9.3	139.2
54	38 42.24	27 14.66	460	980094.6	980065.9	9.3	135.6
55	38 40.68	27 14.46	183	980150.3	980063.6	6.8	132.4
56	38 40.61	27 13.07	167	980157.6	980063.5	7.4	137.0
57	38 38.82	27 13.58	164	980134.4	980060.9	10.5	118.8
58	38 39.37	27 14.21	6	980178.6	980061.7	5.1	123.3
59	38 40.12	27 15.84	97	980160.0	980062.8	7.6	125.4
60	38 40.36	27 17.48	109	980157.7	980063.1	8.0	125.7
61	38 40.98	27 16.27	174	980151.8	980064.0	7.3	132.1
62	38 41.71	27 17.69	325	980117.3	980065.1	9.6	130.8
63	38 42.32	27 15.89	422	980106.6	980066.0	8.1	138.3
64	38 41.45	27 15.25	437	980097.0	980064.7	10.3	135.4
65	38 44.38	27 14.63	530	980083.6	980069.0	8.7	135.8
66	38 45.64	27 16.09	425	980106.9	980070.9	8.7	134.9
67	38 45.78	27 14.79	382	980114.4	980071.1	9.0	133.4
68	38 42.69	27 19.44	517	980075.6	980066.5	13.7	132.6

SUMMARY OF GRAVITY OBSERVATIONS IN THE AZORES (3) TERCEIRA

STATION NUMBER	LATITUDE NORTH	LONGITUDE WEST	ELEVATION (METRES)	OBSERVED GRAVITY	NORMAL GRAVITY	TERRAIN CORR.	BOUGUER ANOMALY
69	38 42.91	27 20.71	462	980082.2	980066.8	16.3	129.8
70	38 39.22	27 16.57	13	980167.1	980061.4	7.3	115.7
71	38 41.08	27 19.12	128	980154.9	980064.2	9.2	127.1
72	38 41.46	27 20.61	147	980149.1	980064.7	10.6	126.2
73	38 42.74	27 21.71	215	980135.0	980066.6	12.6	126.6
74	38 45.00	27 21.95	283	980133.8	980069.9	12.7	136.7
75	38 45.87	27 22.40	106	980175.4	980071.2	9.9	136.6
76	38 46.77	27 21.62	157	980165.3	980072.5	10.9	137.0
77	38 45.90	27 21.14	383	980113.0	980071.2	13.1	136.2
78	38 43.28	27 19.91	640	980045.7	980067.3	17.2	131.4
79	38 46.30	27 13.77	476	980093.0	980071.8	9.6	131.8

SUMMARY OF GRAVITY OBSERVATIONS IN THE AZORES (4) SAN JORGE

STATION NUMBER	LATITUDE NORTH	LONGITUDE WEST	ELEVATION (METRES)	OBSERVED GRAVITY	NORMAL GRAVITY	TERRAIN CORR.	BOUGUER ANOMALY
1	38 36.03	28 0.97	2	980174.8	980056.8	11.2	129.7
2	38 40.76	28 12.32	2	980173.0	980063.7	10.9	120.6
3	38 43.07	28 15.04	232	980121.6	980067.1	11.8	115.5
4	38 44.23	28 16.36	415	980075.5	980068.8	17.2	112.0
5	38 45.14	28 18.44	266	980108.8	980070.1	19.0	114.2
6	38 44.16	28 15.86	408	980073.4	980068.7	17.1	108.4
7	38 42.24	28 13.66	158	980140.8	980065.9	11.8	120.2
8	38 43.02	28 12.86	426	980083.7	980067.0	15.1	122.3
9	38 36.16	28 0.36	126	980146.6	980057.0	11.1	127.4
10	38 35.78	27 58.86	78	980162.7	980056.4	9.7	132.6
11	38 35.60	27 57.23	235	980128.2	980056.1	16.3	138.3
12	38 36.56	27 58.74	269	980123.8	980057.5	11.4	134.8
13	38 36.10	27 55.91	735	980019.3	980056.7	21.9	140.6
14	38 35.30	27 54.66	674	980039.1	980055.7	19.2	145.7
15	38 34.67	27 53.22	731	980027.3	980054.6	20.1	148.0
16	38 33.89	27 51.42	644	980047.5	980053.6	18.0	148.7
17	38 32.85	27 50.48	424	980095.2	980052.1	13.5	146.6
18	38 33.08	27 49.29	379	980100.8	980052.4	10.9	139.7
19	38 32.63	27 48.95	308	980115.0	980051.8	10.4	139.0
20	38 32.63	27 47.29	222	980130.0	980051.8	9.4	134.7
21	38 32.90	27 45.84	118	980142.1	980052.2	8.3	123.3
22	38 36.45	27 59.91	268	980121.4	980057.4	11.9	132.8
23	38 36.86	28 0.32	367	980098.0	980058.0	12.5	130.4
24	38 37.21	27 59.93	442	980084.8	980058.5	12.2	132.3
25	38 38.11	27 59.80	505	980076.9	980059.8	12.7	137.0
26	38 38.60	27 59.86	475	980079.5	980060.5	12.4	132.2
27	38 38.81	27 59.60	437	980085.1	980060.8	15.2	132.3
28	38 39.16	28 1.03	481	980076.7	980061.3	13.5	131.1
29	38 39.72	28 2.33	386	980096.1	980062.2	13.3	129.1
30	38 37.67	27 59.93	501	980076.9	980059.2	12.1	136.2
31	38 36.35	28 2.05	1	980172.8	980057.2	11.7	127.5
32	38 36.98	28 2.24	322	980101.7	980059.2	17.1	128.9
33	38 37.65	28 3.71	499	980061.9	980059.4	20.7	129.1
34	38 38.34	28 5.13	376	980090.8	980060.1	17.1	127.6
35	38 37.91	28 5.96	2	980172.8	980059.5	12.2	124.9

SUMMARY OF GRAVITY OBSERVATIONS IN THE AZORES (4) SAN JORGE

STATION NUMBER	LATITUDE NORTH	LONGITUDE WEST	ELEVATION (METRES)	OBSERVED GRAVITY	NORMAL GRAVITY	TERRAIN CORR.	BOUGUER ANOMALY
36	38 38.63	28 7.78	2	980172.8	980060.6	11.2	123.9
37	38 39.19	28 8.75	112	980147.2	980061.4	12.1	121.7
38	38 39.86	28 9.84	78	980160.4	980062.4	11.8	126.3
39	38 41.52	28 12.90	156	980141.5	980064.8	11.4	121.2
40	38 41.07	28 11.10	343	980105.5	980064.1	13.3	127.5
41	38 40.77	28 9.91	475	980076.0	980063.7	14.7	127.8
42	38 40.18	28 11.02	96	980152.3	980062.8	12.4	122.3
43	38 41.80	28 12.40	269	980119.0	980065.2	12.0	122.9
44	38 41.99	28 12.09	323	980108.1	980065.5	12.3	123.5
45	38 42.31	28 12.03	363	980097.9	980066.0	12.6	121.6
46	38 42.48	28 11.83	400	980089.2	980066.2	13.4	121.4
47	38 42.54	28 11.40	409	980084.2	980066.3	14.3	119.1
48	38 42.03	28 9.71	464	980071.9	980065.6	16.7	121.5
49	38 41.59	28 8.67	571	980050.7	980064.9	18.0	125.0
50	38 41.26	28 7.33	564	980048.5	980064.4	20.3	124.1
51	38 40.76	28 5.83	533	980056.6	980063.7	18.3	124.4
52	38 40.53	28 4.88	458	980071.0	980063.4	18.4	123.2
53	38 40.68	28 3.19	33	980167.8	980063.6	10.7	121.9
54	38 40.20	28 3.70	340	980101.9	980062.9	15.1	126.3
55	38 38.63	27 58.00	4	980187.2	980060.6	8.9	136.4
56	38 37.94	27 56.71	4	980187.0	980059.6	12.1	140.4
57	38 37.69	27 55.72	3	980190.5	980059.2	8.7	140.6
58	38 38.05	28 1.05	565	980057.2	980059.7	14.1	131.5
59	38 40.23	28 7.05	775	980002.6	980062.9	21.9	126.2
60	38 43.51	28 13.97	415	980080.9	980067.7	18.5	119.8
61	38 33.82	27 47.89	382	980094.2	980053.5	13.0	134.8
62	38 34.00	27 50.33	568	980061.8	980053.8	14.1	142.7

SUMMARY OF GRAVITY OBSERVATIONS IN THE AZORES (5) PICO

STATION NUMBER	LATITUDE NORTH	LONGITUDE WEST	ELEVATION (METRES)	OBSERVED GRAVITY	NORMAL GRAVITY	TERRAIN CORR.	BOUGUER ANOMALY
1	38 32.06	28 31.73	8	980162.0	980050.9	4.1	116.9
2	38 33.52	28 28.96	5	980161.5	980053.1	6.2	115.7
3	38 32.38	28 27.81	109	980136.7	980051.4	5.9	114.4
4	38 33.36	28 26.88	9	980155.9	980052.8	6.3	111.3
5	38 32.57	28 26.43	120	980132.7	980051.7	6.9	113.4
6	38 32.49	28 24.98	139	980126.4	980051.6	8.9	113.2
7	38 33.48	28 24.67	14	980153.6	980053.0	7.3	110.9
8	38 32.69	28 23.66	134	980127.2	980051.9	8.4	112.2
9	38 32.71	28 21.95	114	980129.0	980051.9	9.5	110.8
10	38 32.13	28 20.17	2	980150.9	980051.0	9.6	110.0
11	38 31.41	28 19.19	37	980145.9	980050.0	10.2	113.9
12	38 30.18	28 17.35	165	980117.4	980048.2	14.0	118.2
13	38 29.46	28 15.22	229	980102.8	980047.1	14.7	119.0
14	38 28.97	28 14.17	200	980112.0	980046.4	13.0	121.1
15	38 28.32	28 12.01	2	980160.9	980045.5	10.3	126.2
16	38 27.41	28 11.31	83	980145.4	980044.1	13.8	132.7
17	38 27.38	28 10.07	2	980158.2	980044.1	13.5	128.1
18	38 26.64	28 6.78	369	980066.5	980043.0	20.1	121.9
19	38 27.33	28 9.17	27	980153.1	980044.0	14.5	129.3
20	38 28.32	28 18.02	720	980008.2	980045.5	14.0	129.5
21	38 28.67	28 17.83	745	979998.1	980046.0	14.9	125.1
22	38 29.13	28 17.44	605	980025.0	980046.7	16.5	123.3
23	38 30.24	28 19.31	210	980109.6	980048.3	14.4	120.3
24	38 28.81	28 16.69	600	980025.9	980046.2	16.0	123.1
25	38 27.54	28 16.06	785	979993.6	980044.3	17.1	133.0
26	38 27.37	28 15.22	810	979987.8	980044.1	17.9	133.5
27	38 26.91	28 14.67	864	979972.3	980043.4	19.7	132.1
28	38 27.90	28 17.29	730	980006.6	980044.9	15.1	131.8
29	38 27.27	28 18.59	596	980032.6	980043.9	11.7	126.9
30	38 26.76	28 18.83	545	980040.8	980043.2	11.6	124.9
31	38 25.65	28 17.49	273	980094.9	980041.6	11.3	122.6
32	38 24.86	28 18.36	81	980132.5	980040.4	11.6	120.9
33	38 25.00	28 16.88	73	980139.9	980040.6	8.1	122.9
34	38 24.77	28 15.62	100	980136.4	980040.3	11.7	129.0
35	38 23.65	28 15.31	2	980157.0	980038.6	10.7	129.5

SUMMARY OF GRAVITY OBSERVATIONS IN THE AZORES (5) PICO

STATION NUMBER	LATITUDE NORTH	LONGITUDE WEST	ELEVATION (METRES)	OBSERVED GRAVITY	NORMAL GRAVITY	TERRAIN CORR.	BOUGUER ANOMALY
36	38 23.54	28 13.30	179	980124.8	980038.5	14.2	138.5
37	38 24.08	28 12.41	148	980140.1	980039.3	14.4	146.6
38	38 24.35	28 11.34	5	980168.2	980039.7	15.8	145.4
39	38 24.69	28 9.96	132	980135.1	980040.2	19.0	141.9
40	38 24.58	28 8.49	220	980106.0	980040.0	19.3	132.0
41	38 24.54	28 6.94	235	980101.4	980039.9	17.5	128.9
42	38 24.89	28 5.00	20	980140.1	980039.3	11.6	116.6
43	38 24.74	28 4.27	212	980102.3	980040.2	11.7	118.8
44	38 24.78	28 1.88	10	980133.9	980040.3	7.9	103.6
45	38 25.28	28 3.09	130	980116.3	980041.0	10.0	112.9
46	38 26.35	28 3.40	3	980143.0	980042.6	8.7	109.7
47	38 25.38	28 4.74	312	980082.0	980041.2	12.5	119.5
48	38 25.24	28 5.29	352	980074.8	980041.0	14.1	122.6
49	38 26.41	28 5.52	201	980106.9	980042.7	13.4	120.2
50	38 27.84	28 18.49	639	980025.2	980044.8	12.7	128.8
51	38 26.12	28 18.61	430	980063.9	980042.2	11.4	124.4
52	38 24.96	28 20.30	46	980140.3	980040.5	12.6	122.1
53	38 25.07	28 21.91	89	980128.8	980040.7	13.1	120.1
54	38 25.26	28 23.19	47	980135.6	980041.0	13.7	118.3
55	38 25.67	28 24.36	52	980134.3	980041.6	15.1	118.9
56	38 25.58	28 26.08	56	980134.1	980041.5	12.4	116.9
57	38 26.14	28 25.74	171	980110.6	980042.3	18.0	122.6
58	38 25.85	28 27.75	4	980145.9	980041.8	11.7	116.6
59	38 26.83	28 28.92	173	980111.8	980043.3	10.3	115.5
60	38 26.77	28 30.17	6	980147.4	980043.2	8.5	114.0
61	38 27.73	28 30.83	75	980133.4	980044.6	7.0	111.7
62	38 28.39	28 31.14	91	980130.2	980045.6	6.4	110.3
63	38 28.94	28 31.48	97	980128.7	980046.4	5.7	108.6
64	38 29.59	28 31.84	66	980137.1	980047.3	5.5	109.3
65	38 30.39	28 31.82	50	980145.1	980048.5	4.9	112.1
66	38 30.99	28 32.03	16	980156.5	980049.4	4.5	115.0
67	38 31.56	28 31.82	33	980154.9	980050.2	4.8	116.5
68	38 31.64	28 30.12	118	980134.2	980050.3	5.5	114.4
69	38 32.59	28 31.28	5	980164.5	980051.7	4.4	118.3
70	38 32.99	28 30.57	3	980165.4	980052.3	4.9	118.6

SUMMARY OF GRAVITY OBSERVATIONS IN THE AZORES (5) PICO

STATION NUMBER	LATITUDE NORTH	LONGITUDE WEST	ELEVATION (METRES)	OBSERVED GRAVITY	NORMAL GRAVITY	TERRAIN CORR.	BOUGUER ANOMALY
71	38 32.42	28 29.38	93	980140.6	980051.5	5.6	114.4
72	38 31.07	28 21.51	433	980059.8	980049.5	12.2	114.4
73	38 31.56	28 23.81	331	980081.9	980050.2	10.5	112.5
74	38 31.86	28 26.00	252	980101.9	980050.5	10.5	115.4
75	38 28.89	28 19.18	762	979998.0	980046.3	14.9	128.3
76	38 29.15	28 20.36	800	979993.0	980046.7	15.5	131.6
77	38 29.74	28 22.04	860	979973.1	980047.5	18.3	126.5
78	38 28.61	28 22.14	1095	979924.4	980045.9	22.6	133.5
79	38 29.92	28 24.01	888	979961.2	980047.8	18.1	120.1
80	38 29.82	28 25.57	820	979977.1	980047.7	16.4	119.9
81	38 29.76	28 27.22	624	980019.7	980047.5	14.1	118.7
82	38 30.69	28 27.57	440	980061.0	980048.9	10.6	116.1
83	38 30.95	28 29.28	252	980102.9	980049.3	7.3	114.4
84	38 30.30	28 30.50	196	980109.8	980048.4	6.3	109.3
85	38 28.04	28 29.48	326	980079.3	980045.1	9.6	113.0
86	38 27.54	28 28.00	501	980042.5	980044.3	13.4	118.0
87	38 27.39	28 20.05	688	980012.5	980044.1	14.2	128.6
88	38 27.37	28 21.33	843	979984.0	980044.1	20.6	139.5
89	38 29.81	28 29.65	325	980078.1	980047.6	8.8	108.3

SUMMARY OF GRAVITY OBSERVATIONS IN THE AZORES (6) FAIAL

STATION NUMBER	LATITUDE NORTH	LONGITUDE WEST	ELEVATION (METRES)	OBSERVED GRAVITY	NORMAL GRAVITY	TERRAIN CORR.	BOUGUER ANOMALY	RESIDUAL ANOMALY
1	38 31.78	28 37.79	59	980143.7	980050.5	5.5	111.2	3.9
2	38 31.41	28 39.50	25	980150.1	980050.0	5.2	110.6	4.3
2	38 31.60	28 39.81	38	980149.7	980050.3	5.5	113.0	5.4
3	38 31.50	28 41.05	38	980147.8	980050.1	5.7	111.5	4.9
4	38 31.47	28 42.52	90	980132.4	980050.1	7.2	108.6	3.5
5	38 31.52	28 43.65	79	980135.4	980050.2	7.7	109.7	6.2
6	38 32.19	28 44.60	212	980108.8	980051.1	8.8	111.6	7.0
7	38 33.13	28 45.07	263	980095.7	980052.5	12.2	111.2	4.8
8	38 34.02	28 45.58	295	980093.0	980053.8	11.4	113.2	6.6
9	38 33.88	28 46.47	5	980156.0	980053.6	8.0	111.5	8.1
10	38 34.92	28 47.24	191	980112.9	980055.1	8.8	107.1	6.3
11	38 34.92	28 48.34	148	980114.4	980055.1	9.2	99.9	4.0
12	38 35.68	28 48.98	128	980117.1	980056.2	8.7	96.7	5.0
13	38 35.63	28 49.84	5	980139.7	980056.2	7.2	91.7	4.5
14	38 35.47	28 47.03	244	980103.3	980055.9	9.0	108.2	7.1
15	38 36.22	28 47.69	146	980121.5	980057.0	8.3	103.8	7.0
16	38 36.67	28 45.66	4	980158.6	980057.7	8.8	110.6	6.9
17	38 35.92	28 45.95	272	980099.8	980056.6	10.3	111.3	6.7
18	38 36.90	28 44.34	320	980089.2	980058.0	13.1	112.2	5.1
19	38 37.67	28 43.12	240	980112.5	980059.2	9.6	113.8	6.6
20	38 38.13	28 41.66	85	980147.3	980059.8	7.8	113.3	5.6
21	38 37.53	28 40.21	107	980146.1	980059.0	7.6	117.4	5.2
22	38 36.72	28 38.97	182	980128.8	980057.8	8.7	116.3	3.0
23	38 36.32	28 38.19	259	980112.6	980057.2	9.2	119.6	3.6
24	38 35.65	28 36.81	97	980150.9	980056.2	6.2	121.5	5.8
25	38 34.69	28 36.83	150	980138.5	980054.8	6.4	121.9	6.4
26	38 33.64	28 37.53	141	980139.3	980053.3	5.8	121.8	7.2
27	38 33.19	28 36.78	5	980167.5	980052.6	4.6	120.6	8.3
28	38 32.62	28 37.49	8	980162.6	980051.8	4.7	117.2	6.1
29	38 32.21	28 40.55	108	980136.6	980051.2	6.0	114.3	3.8
30	38 32.78	28 39.32	143	980132.4	980052.0	5.5	116.2	3.3
31	38 33.13	28 44.02	422	980066.1	980052.5	10.8	114.0	4.8
32	38 33.06	28 42.88	509	980046.6	980052.4	10.7	113.0	1.7
33	38 32.97	28 41.76	468	980055.5	980052.3	11.4	114.0	1.4
34	38 33.41	28 41.07	502	980051.5	980052.9	10.7	115.9	1.4

SUMMARY OF GRAVITY OBSERVATIONS IN THE AZORES (6) FAIAL

STATION NUMBER	LATITUDE NORTH		LONGITUDE WEST		ELEVATION (METRES)	OBSERVED GRAVITY	NORMAL GRAVITY	TERRAIN CORR.	BOUGUER ANOMALY	RESIDUAL ANOMALY
35	38	34.27	28	40.44	485	980061.3	980054.2	10.2	120.2	3.7
36	38	35.38	28	40.68	470	980066.5	980055.8	10.4	120.9	4.2
37	38	36.57	28	41.53	503	980055.5	980057.6	12.8	117.5	3.5
38	38	36.59	28	42.47	573	980039.0	980057.6	13.3	116.3	3.9
39	38	35.15	28	38.24	294	980108.6	980055.5	8.0	123.5	6.4
40	38	33.86	28	38.57	250	980116.3	980053.9	7.0	122.5	6.6
41	38	35.20	28	42.09	898	979961.5	980055.5	22.3	118.9	3.7
42	38	34.50	28	43.03	1014	979931.1	980054.5	25.2	117.1	3.5
43	38	35.23	28	42.81	572	980046.2	980055.6	13.2	125.2	11.2
44	38	34.87	28	42.07	870	979970.1	980055.1	18.8	118.5	3.1
45	38	34.29	28	41.62	655	980020.5	980054.2	13.2	118.5	3.0
46	38	31.96	28	42.26	207	980108.0	980050.8	8.2	109.4	1.4
47	38	31.59	28	44.82	73	980136.1	980050.3	8.5	109.8	8.6
48	38	35.04	28	45.16	570	980034.0	980055.3	13.9	113.6	5.3
49	38	34.93	28	44.53	724	980000.5	980055.1	16.1	115.2	5.1
50	38	35.80	28	39.57	454	980069.8	980056.4	9.3	119.1	2.1
51	38	36.40	28	44.14	511	980049.2	980057.3	13.7	114.1	4.9
52	38	35.06	28	46.36	354	980080.0	980055.3	11.3	111.2	7.0
53	38	32.24	28	37.60	4	980161.3	980051.2	4.3	115.3	5.8
54	38	33.11	28	37.60	183	980124.0	980052.5	7.8	118.1	5.1
55	38	35.16	28	36.85	135	980141.5	980055.5	6.4	121.0	5.2
56	38	36.11	28	37.16	181	980128.7	980056.9	7.7	117.9	2.3
57	38	34.22	28	37.31	135	980142.3	980054.1	5.4	122.3	6.7
58	38	35.78	28	49.99	114	980108.1	980056.4	10.2	86.1	0.0
59	38	35.95	28	49.77	149	980100.8	980056.7	13.0	88.7	1.8

SUMMARY OF GRAVITY OBSERVATIONS IN THE AZORES (7) FLORES

STATION NUMBER	LATITUDE NORTH	LONGITUDE WEST	ELEVATION (METRES)	OBSERVED GRAVITY	NORMAL GRAVITY	TERRAIN CORR.	BOUGUER ANOMALY
1	39 26.87	31 7.46	41	980260.7	980131.5	10.9	148.8
2	39 26.37	31 8.54	247	980209.4	980130.8	15.9	146.9
3	39 25.85	31 9.10	332	980195.2	980130.0	16.2	151.9
4	39 24.74	31 9.14	314	980198.2	980128.4	15.3	151.8
5	39 23.27	31 9.72	128	980237.8	980126.2	11.4	150.2
5	39 23.20	31 9.58	128	980232.3	980126.1	12.1	145.5
6	39 22.64	31 9.94	3	980260.4	980125.3	10.7	146.4
6	39 22.60	31 10.19	65	980245.9	980125.2	11.2	145.7
7	39 23.06	31 11.06	218	980215.9	980125.9	11.9	148.2
8	39 23.59	31 12.53	346	980196.2	980126.7	12.2	155.2
9	39 23.36	31 13.53	468	980164.9	980126.3	15.6	153.6
9	39 23.47	31 13.46	442	980170.6	980126.5	14.4	152.3
10	39 27.48	31 15.60	2	980271.5	980132.4	9.6	149.1
11	39 26.06	31 14.42	150	980243.4	980130.3	12.4	157.3
12	39 25.23	31 14.37	430	980180.5	980129.1	14.1	156.8
13	39 26.04	31 13.63	503	980161.5	980130.3	14.2	152.2
14	39 26.19	31 11.73	566	980152.2	980130.5	13.7	155.6
15	39 26.08	31 15.37	3	980273.5	980130.4	9.9	153.6
16	39 24.70	31 14.82	272	980217.1	980128.3	13.3	159.8
17	39 24.30	31 14.87	7	980270.3	980127.7	16.6	160.7
18	39 23.51	31 15.26	8	980266.2	980126.6	10.4	151.7
19	39 23.47	31 14.63	224	980222.9	980126.5	13.0	157.0
20	39 28.09	31 8.56	113	980254.0	980133.3	10.7	155.4
21	39 26.77	31 9.45	512	980157.0	980131.4	20.5	154.8
22	39 26.53	31 10.96	586	980147.4	980131.0	14.4	155.2
23	39 25.42	31 12.24	588	980144.2	980129.4	14.1	153.7
24	39 25.49	31 10.75	632	980135.5	980129.5	16.6	156.8
25	39 24.03	31 9.14	205	980218.2	980127.3	13.3	147.7
26	39 24.01	31 10.15	322	980195.6	980127.3	14.3	151.0
27	39 28.20	31 15.06	63	980256.3	980133.5	16.5	152.7
28	39 28.04	31 15.23	5	980269.6	980133.2	14.2	151.7
29	39 26.94	31 13.42	570	980150.9	980131.6	14.4	154.7
30	39 24.76	31 13.17	563	980148.6	980128.4	14.9	154.6
31	39 27.31	31 8.35	185	980233.8	980132.2	11.2	152.1
32	39 27.41	31 12.58	771	980106.3	980132.3	18.3	156.0

SUMMARY OF GRAVITY OBSERVATIONS IN THE AZORES (7) FLORES

STATION NUMBER	LATITUDE NORTH	LONGITUDE WEST	ELEVATION (METRES)	OBSERVED GRAVITY	NORMAL GRAVITY	TERRAIN CORR.	BOUGUER ANOMALY
33	39 27.31	31 9.81	280	980218.2	980132.2	11.6	157.0
34	39 28.42	31 9.46	170	980243.3	980133.8	12.8	158.4
35	39 28.58	31 10.38	573	980153.8	980134.0	16.8	158.2
36	39 28.61	31 11.48	670	980131.8	980134.1	17.6	157.5
37	39 29.28	31 10.34	489	980170.0	980135.1	16.9	155.6
38	39 29.68	31 9.43	292	980212.2	980135.7	15.5	154.0
39	39 29.97	31 12.31	446	980178.9	980136.1	16.4	153.9
40	39 31.10	31 12.16	3	980285.1	980137.8	7.2	155.1
41	39 31.27	31 12.23	36	980279.0	980138.0	7.3	155.9
42	39 30.96	31 13.55	104	980262.7	980137.6	8.4	155.6
43	39 29.88	31 13.89	337	980205.5	980136.0	13.3	154.3
44	39 28.69	31 13.89	725	980121.1	980134.2	19.0	159.8
45	39 27.18	31 7.33	12	980268.3	980132.0	9.6	148.4

SUMMARY OF GRAVITY OBSERVATIONS ON LANZAROTE

STATION NUMBER	LATITUDE NORTH	LONGITUDE WEST	ELEVATION (METRES)	OBSERVED GRAVITY	NORMAL GRAVITY	TERRAIN CORR.	BOUGUER ANOMALY
1	28 57.90	13 31.45	4	979442.0	979257.9	6.4	191.3
2	28 57.14	13 32.70	3	979449.1	979256.9	7.0	199.8
3	28 56.72	13 35.08	4	979458.4	979256.4	6.2	209.0
4	28 56.87	13 37.53	72	979435.9	979256.6	6.4	201.0
5	28 55.58	13 37.00	8	979433.2	979254.9	5.9	185.9
6	28 54.85	13 38.45	11	979412.6	979254.0	5.7	166.6
7	28 54.81	13 39.98	5	979405.0	979254.0	5.6	157.7
8	28 56.53	13 40.87	169	979387.0	979256.1	7.0	173.8
9	28 56.04	13 42.15	132	979386.5	979255.5	7.1	166.1
10	28 55.79	13 42.99	173	979374.3	979255.2	7.1	162.9
11	28 54.06	13 43.87	4	979401.0	979253.0	6.6	155.4
12	28 56.11	13 44.36	210	979370.1	979255.6	7.4	166.5
13	28 55.19	13 45.62	297	979351.2	979254.4	8.6	168.5
14	28 54.42	13 46.66	361	979337.2	979253.5	10.7	171.0
15	28 56.76	13 45.78	183	979380.8	979256.4	7.5	170.8
16	28 56.78	13 46.80	127	979391.0	979256.5	7.8	169.3
17	28 56.02	13 48.34	56	979407.8	979255.5	7.4	171.6
18	28 55.37	13 49.16	40	979414.1	979254.7	7.3	175.2
19	28 51.37	13 49.50	9	979411.4	979249.6	6.0	169.7
20	28 51.08	13 47.43	42	979397.2	979249.2	5.8	162.7
21	28 50.24	13 47.04	22	979397.2	979248.2	5.2	158.9
22	28 56.90	13 38.98	204	979390.4	979256.6	7.1	184.2
23	28 57.83	13 48.27	99	979394.3	979257.8	8.0	165.5
24	28 58.48	13 49.68	2	979412.2	979258.6	8.7	162.7
25	28 59.02	13 48.91	83	979392.4	979259.3	8.8	159.5
26	28 53.85	13 49.78	25	979423.0	979252.7	7.0	182.6
27	28 52.78	13 49.86	41	979413.3	979251.4	6.9	177.5
28	28 50.96	13 52.18	12	979404.3	979249.1	5.5	163.2
29	28 52.25	13 48.23	47	979406.5	979250.7	6.6	172.4
30	28 54.46	13 47.59	259	979361.9	979253.5	9.2	172.6
31	28 58.70	13 44.41	293	979358.0	979258.9	8.3	169.6
32	29 2.26	13 44.68	90	979404.3	979263.4	8.6	168.6
33	29 0.69	13 43.19	304	979359.1	979261.4	8.3	170.5
34	29 1.65	13 41.96	267	979373.2	979262.7	8.1	175.3
35	29 3.09	13 42.15	189	979386.2	979264.5	8.0	169.8

SUMMARY OF GRAVITY OBSERVATIONS ON LANZAROTE

STATION NUMBER	LATITUDE NORTH	LONGITUDE WEST	ELEVATION (METRES)	OBSERVED GRAVITY	NORMAL GRAVITY	TERRAIN CORR.	BOUGUER ANOMALY
36	29 4.17	13 42.91	59	979413.1	979265.9	7.9	167.6
37	29 1.33	13 40.99	310	979367.0	979262.3	7.9	178.4
38	28 59.88	13 40.99	352	979359.6	979260.4	8.1	182.0
39	28 58.45	13 41.35	315	979361.6	979258.6	7.8	177.7
40	28 57.32	13 43.52	238	979372.1	979257.1	7.8	173.3
41	28 58.14	13 40.02	328	979366.9	979258.2	7.9	186.2
42	28 59.15	13 38.62	337	979383.1	979259.5	8.1	203.2
43	28 58.44	13 37.08	188	979430.0	979258.6	7.1	216.4
44	28 58.08	13 35.59	119	979454.0	979258.1	6.6	227.8
45	28 59.70	13 36.68	277	979421.6	979260.2	7.6	227.8
46	28 58.34	13 34.35	64	979468.6	979258.4	6.5	230.3
47	29 12.34	13 28.60	444	979355.1	979276.3	13.6	186.7
48	29 10.56	13 28.02	281	979388.2	979274.0	9.0	182.9
49	29 13.00	13 27.00	3	979466.1	979277.1	7.3	196.9
50	29 11.49	13 26.90	91	979432.3	979275.2	7.6	184.0
51	29 11.36	13 28.85	378	979370.2	979275.0	10.1	185.5
52	29 9.72	13 29.47	317	979376.7	979273.0	9.6	180.6
53	29 8.43	13 29.76	278	979381.0	979271.3	8.6	177.3
54	29 9.36	13 27.44	135	979412.9	979272.5	7.5	176.6
55	29 9.09	13 25.57	1	979437.0	979272.1	7.4	172.5
56	29 7.55	13 27.43	4	979432.6	979270.2	6.9	170.1
57	29 7.25	13 28.72	85	979415.9	979269.8	7.9	172.0
58	29 5.80	13 28.02	41	979419.3	979267.9	7.3	167.4
59	29 4.05	13 28.58	97	979409.0	979265.7	7.3	171.2
60	29 3.03	13 27.79	3	979419.3	979264.4	7.3	162.8
61	28 58.96	13 32.44	64	979458.8	979259.2	6.7	219.9
62	29 0.43	13 32.62	131	979444.6	979261.1	6.8	218.1
63	29 1.46	13 31.18	144	979425.2	979262.4	7.1	200.5
64	29 0.89	13 29.17	65	979419.9	979261.7	7.4	179.4
65	29 2.95	13 29.72	142	979409.2	979264.3	7.4	182.4
66	29 7.13	13 30.74	570	979313.8	979269.6	15.7	180.9
67	29 6.03	13 31.55	605	979313.1	979268.2	17.5	190.8
68	29 5.70	13 30.54	507	979338.7	979267.8	11.8	190.3
69	29 3.18	13 33.45	305	979395.8	979264.6	8.0	204.0
70	29 3.17	13 31.41	259	979399.3	979264.6	7.8	197.5

SUMMARY OF GRAVITY OBSERVATIONS ON LANZAROTE

STATION NUMBER	LATITUDE NORTH		LONGITUDE WEST		ELEVATION (METRES)	OBSERVED GRAVITY	NORMAL GRAVITY	TERRAIN CORR.	BOUGUER ANOMALY
71	29	1.55	13	33.26	188	979432.8	979262.5	7.0	217.2
72	29	4.24	13	31.41	316	979388.6	979266.0	8.2	197.9
73	29	3.20	13	35.70	170	979419.9	979264.6	6.8	198.2
74	29	4.85	13	33.55	116	979426.0	979266.7	7.8	191.7
75	29	6.72	13	33.80	8	979438.5	979269.1	6.3	177.4
76	29	7.34	13	35.18	21	979431.0	979269.9	6.3	171.9
77	29	5.53	13	36.84	109	979412.6	979267.6	6.8	174.9
78	29	4.44	13	37.73	135	979410.8	979266.2	6.8	180.1
79	29	2.87	13	37.95	226	979395.8	979264.2	7.2	186.8
80	29	3.63	13	40.47	198	979384.9	979265.2	7.6	169.3
81	29	4.77	13	40.13	100	979409.8	979266.6	7.1	171.5
82	29	6.61	13	38.23	2	979431.3	979269.0	6.7	169.4
83	29	6.21	13	39.79	1	979430.7	979268.5	7.2	169.6
84	29	1.50	13	38.53	286	979385.0	979262.5	7.8	191.0
85	29	0.03	13	39.49	320	979378.8	979260.6	7.8	193.9
86	29	1.00	13	36.83	264	979415.1	979261.8	7.3	216.6
87	29	2.20	13	35.02	208	979426.3	979263.4	7.0	214.1
88	28	59.19	13	29.61	2	979426.9	979259.5	7.4	175.2
89	28	56.97	13	36.42	38	979451.5	979256.7	6.1	209.0

SUMMARY OF GRAVITY OBSERVATIONS ON GRAN CANARIA

STATION NUMBER	LATITUDE NORTH	LONGITUDE WEST	ELEVATION METRES	OBSERVED GRAVITY	NORMAL GRAVITY	BOUGUER ANOMALY
1	27 56.37	15 23.11	22	979377.3	979180.5	201.5
2	28 8.30	15 26.07	4	979391.8	979195.4	197.2
3	28 6.52	15 24.81	6	979387.5	979193.2	195.6
4	28 4.15	15 24.94	10	979385.5	979190.2	197.4
5	27 59.74	15 25.00	150	979360.4	979184.7	207.5
6	27 59.18	15 22.41	2	979372.9	979184.0	189.3
7	27 54.43	15 24.16	90	979389.0	979178.1	230.0
8	27 52.47	15 25.42	61	979401.6	979175.7	238.9
9	27 51.25	15 23.53	5	979387.3	979174.2	214.2
10	27 51.29	15 26.16	77	979395.7	979174.2	237.8
11	27 49.66	15 27.15	74	979381.4	979172.2	224.9
12	27 47.76	15 27.65	2	979378.0	979169.8	208.6
13	27 47.50	15 29.19	4	979379.0	979169.5	210.3
14	27 46.85	15 30.73	3	979374.4	979168.7	206.3
15	27 45.90	15 33.15	10	979371.4	979167.5	206.0
16	27 44.01	15 35.78	4	979361.2	979165.2	196.8
17	27 45.33	15 40.62	1	979379.7	979166.8	213.1
18	27 45.27	15 39.28	3	979376.5	979166.8	210.3
19	27 45.05	15 37.53	35	979364.1	979166.5	205.0
20	27 45.80	15 34.34	48	979361.9	979167.4	204.7
21	27 48.25	15 34.88	340	979311.9	979170.4	213.7
21	27 49.01	15 34.62	446	979294.5	979171.4	217.8
22	27 50.87	15 33.78	343	979330.8	979173.7	229.9
23	27 53.25	15 33.71	618	979295.8	979176.6	250.4
24	27 53.90	15 33.88	694	979277.1	979177.5	246.9
25	27 55.43	15 34.19	867	979238.7	979179.4	243.4
26	27 54.48	15 32.22	672	979285.8	979178.2	250.3
27	27 52.51	15 30.79	560	979305.6	979175.7	248.8
28	27 52.07	15 29.41	320	979361.8	979175.2	254.5
29	27 52.95	15 29.07	341	979364.3	979176.3	260.4
30	27 54.14	15 27.17	315	979365.8	979177.8	254.9
31	27 54.46	15 30.21	680	979284.9	979178.2	252.1
32	27 57.50	15 25.31	245	979344.8	979181.9	214.9
33	27 59.59	15 26.30	270	979338.1	979184.5	210.9
34	27 59.35	15 29.82	574	979291.7	979184.2	229.4

SUMMARY OF GRAVITY OBSERVATIONS ON GRAN CANARIA

STATION NUMBER	LATITUDE NORTH		LONGITUDE WEST		ELEVATION METRES	OBSERVED GRAVITY	NORMAL GRAVITY	BOUGUER ANOMALY
35	28	0.55	15	31.80	816	979239.0	979185.7	226.5
36	28	1.80	15	29.83	501	979304.6	979187.3	223.7
37	28	2.78	15	28.20	445	979309.1	979188.5	215.1
38	28	4.21	15	26.85	315	979327.8	979190.3	204.4
39	28	2.32	15	24.93	70	979372.4	979187.9	199.4
40	28	4.42	15	28.41	222	979357.6	979190.5	214.2
41	28	5.68	15	29.31	195	979363.0	979192.1	212.3
42	28	3.60	15	32.78	600	979293.0	979189.5	230.9
43	28	5.25	15	32.07	510	979311.9	979191.6	228.6
44	28	6.91	15	31.36	230	979367.5	979193.6	222.7
45	28	8.90	15	32.57	4	979403.9	979196.1	208.6
46	28	8.44	15	34.32	23	979409.1	979195.6	218.4
47	28	8.60	15	34.42	4	979412.1	979195.8	217.1
48	28	6.55	15	34.95	488	979324.0	979193.2	234.4
49	28	6.04	15	33.44	587	979297.1	979192.6	229.1
50	28	2.95	15	34.38	960	979218.8	979188.7	233.9
51	28	1.36	15	34.96	1360	979127.3	979186.7	229.3
52	28	0.27	15	34.95	1170	979166.6	979185.4	229.6
53	28	0.46	15	33.17	1035	979194.4	979185.6	228.5
54	28	7.80	15	29.30	5	979401.7	979194.8	208.0
55	28	8.37	15	30.35	4	979401.8	979195.5	207.1
56	28	5.10	15	35.19	649	979292.6	979191.4	238.9
57	28	3.47	15	36.43	965	979227.3	979189.4	242.8
58	28	8.55	15	37.50	197	979392.1	979195.7	238.2
59	28	8.82	15	39.24	143	979417.9	979196.0	252.3
60	28	8.95	15	41.67	2	979439.3	979196.2	243.5
61	28	7.06	15	40.26	205	979424.8	979193.8	274.5
62	28	6.18	15	42.62	2	979468.7	979192.7	276.4
63	28	4.63	15	42.22	115	979440.8	979190.8	274.4
64	28	3.14	15	44.23	4	979459.5	979188.9	271.4
65	28	0.18	15	48.94	3	979430.8	979185.3	246.1
66	27	59.20	15	47.02	56	979426.7	979184.0	254.6
67	27	56.53	15	46.80	555	979313.1	979180.7	250.2
68	27	54.34	15	49.57	3	979407.9	979178.0	230.5
69	27	55.44	15	45.45	430	979336.1	979179.4	248.0

SUMMARY OF GRAVITY OBSERVATIONS ON GRAN CANARIA

STATION NUMBER	LATITUDE NORTH	LONGITUDE WEST	ELEVATION METRES	OBSERVED GRAVITY	NORMAL GRAVITY	BOUGUER ANOMALY
70	27 52.28	15 48.14	2	979402.6	979175.4	227.6
71	27 52.96	15 43.32	245	979361.3	979176.3	237.0
72	27 48.99	15 45.73	2	979390.4	979171.4	219.4
73	27 50.76	15 47.36	3	979394.9	979173.6	221.9
74	27 52.03	15 45.74	70	979388.4	979175.1	228.2
75	27 54.20	15 43.66	265	979366.2	979177.8	244.7
76	28 2.01	15 44.69	680	979301.9	979187.5	258.8
77	27 57.77	15 46.53	261	979378.6	979182.3	251.7
78	28 1.07	15 46.61	435	979346.3	979186.4	252.3
79	28 5.00	15 40.14	190	979414.3	979191.3	263.3
80	27 59.93	15 36.78	1035	979197.6	979184.9	232.4
81	27 57.48	15 25.46	1280	979137.7	979181.9	227.5
101	28 6.40	15 41.28	130	979443.1	979193.0	277.7
102	28 3.07	15 43.79	80	979449.5	979188.9	277.6
103	27 54.70	15 28.83	585	979313.3	979178.5	259.0

SUMMARY OF GRAVITY OBSERVATIONS ON TENERIFE

STATION NUMBER	LATITUDE NORTH	LONGITUDE WEST	ELEVATION (METRES)	OBSERVED GRAVITY	NORMAL GRAVITY	TERRAIN CORR.	BOUGUER ANOMALY
1	28 27.48	16 14.26	6	979410.4	979219.4	19.2	211.5
2	28 26.68	16 23.76	470	979308.0	979205.9	22.4	224.3
3	28 13.67	16 26.72	650	979265.8	979202.1	22.3	224.0
4	28 12.74	16 24.20	3	979386.8	979200.9	28.3	214.8
5	28 15.27	16 25.08	494	979302.1	979204.1	21.4	224.3
6	28 18.44	16 24.11	289	979358.9	979208.1	18.7	230.9
7	28 17.23	16 21.79	4	979408.9	979206.5	16.7	219.9
8	28 19.27	16 21.24	4	979411.7	979209.1	16.6	220.0
9	28 19.89	16 24.51	463	979325.3	979209.9	20.2	233.9
10	28 21.35	16 23.98	640	979285.1	979211.7	22.9	232.2
11	28 28.99	16 13.00	7	979417.8	979221.3	18.3	216.3
12	28 29.60	16 10.88	3	979416.6	979222.3	18.8	213.7
13	28 30.87	16 8.54	3	979414.6	979223.7	21.9	213.4
14	28 32.18	16 11.10	465	979338.7	979225.3	24.6	236.7
15	28 33.14	16 12.44	163	979408.5	979226.5	20.4	237.0
16	28 32.22	16 12.47	722	979276.9	979225.4	32.5	237.3
17	28 31.66	16 13.80	825	979248.5	979224.7	35.4	234.3
18	28 31.62	16 15.75	984	979207.8	979224.6	36.8	228.9
19	28 31.69	16 17.55	842	979240.1	979224.7	28.7	222.9
20	28 30.53	16 17.15	618	979296.1	979223.2	20.3	224.4
21	28 30.91	16 19.58	399	979347.4	979223.7	18.1	226.5
22	28 30.68	16 20.93	290	979375.3	979223.4	16.3	229.8
23	28 32.88	16 20.04	2	979425.8	979226.2	17.8	217.8
24	28 34.12	16 19.07	2	979423.5	979227.8	16.2	212.3
25	28 27.54	16 16.43	295	979353.6	979219.5	18.0	214.7
26	28 28.55	16 15.63	505	979308.5	979220.8	22.0	216.9
27	28 26.76	16 18.50	492	979312.3	979218.5	18.3	216.6
28	28 25.35	16 19.98	612	979287.6	979216.7	21.0	221.8
29	28 25.09	16 18.27	318	979341.1	979216.4	20.8	213.0
30	28 23.78	16 18.77	141	979371.3	979214.8	25.1	211.5
31	28 23.61	16 21.07	445	979324.0	979214.5	22.8	226.8
32	28 22.29	16 21.04	3	979410.2	979213.0	21.7	219.5
33	28 22.58	16 22.06	340	979343.4	979213.3	24.2	226.5
34	28 20.80	16 21.56	4	979412.3	979211.0	19.6	221.7
35	28 17.57	16 24.40	322	979348.2	979207.0	22.2	231.8

SUMMARY OF GRAVITY OBSERVATIONS ON TENERIFE

STATION NUMBER	LATITUDE NORTH	LONGITUDE WEST	ELEVATION (METRES)	OBSERVED GRAVITY	NORMAL GRAVITY	TERRAIN CORR.	BOUGUER ANOMALY
36	28 28.85	16 18.40	545	979315.5	979221.1	17.3	227.4
37	28 28.97	16 21.83	617	979313.5	979221.3	18.6	241.8
38	28 27.35	16 23.62	799	979261.9	979219.2	22.3	234.6
39	28 26.52	16 24.58	881	979237.2	979218.2	23.8	229.8
40	28 29.46	16 23.75	403	979344.7	979221.9	13.8	227.2
41	28 30.55	16 22.75	221	979386.6	979223.3	17.1	227.3
42	28 26.30	16 16.07	141	979376.6	979217.9	21.7	210.3
43	28 7.06	16 34.01	654	979272.0	979193.8	20.0	237.0
44	28 11.41	16 27.10	378	979318.4	979199.3	19.1	218.4
45	28 11.11	16 24.81	3	979385.6	979198.9	20.9	208.2
46	28 10.45	16 27.68	330	979330.6	979198.1	17.9	220.5
47	28 9.34	16 25.10	3	979382.2	979196.7	15.9	202.0
48	28 7.61	16 25.95	3	979380.7	979194.5	15.7	202.5
49	28 8.20	16 28.56	281	979334.3	979195.3	17.3	216.0
50	28 9.49	16 29.47	558	979287.2	979196.9	19.6	228.4
51	28 7.59	16 31.11	450	979307.4	979194.5	17.1	225.5
52	28 8.25	16 32.19	654	979273.9	979195.3	19.7	237.1
53	28 5.78	16 30.03	166	979355.7	979192.2	14.8	213.5
54	28 5.16	16 28.39	4	979380.6	979191.5	15.0	204.9
55	28 7.18	16 32.58	541	979293.1	979194.0	21.0	235.0
56	28 5.38	16 32.23	288	979336.8	979191.7	15.6	221.8
57	28 5.12	16 33.58	391	979319.0	979191.4	16.5	227.1
58	28 3.99	16 32.84	203	979353.1	979190.0	15.0	221.2
59	28 2.08	16 31.48	4	979381.3	979187.6	15.7	210.2
60	28 3.74	16 29.86	4	979381.4	979189.7	14.8	207.3
61	28 1.45	16 33.03	5	979382.9	979186.8	15.3	212.5
62	28 1.30	16 34.79	21	979384.5	979186.7	15.2	217.5
63	28 3.07	16 34.85	205	979353.4	979188.9	15.1	223.1
64	28 2.67	16 36.84	161	979370.5	979188.4	14.9	231.2
65	28 2.54	16 38.71	165	979373.3	979188.2	15.2	235.3
66	28 0.61	16 36.85	4	979390.3	979185.8	15.5	220.8
67	28 0.04	16 39.05	2	979389.5	979185.1	16.7	221.5
68	27 59.57	16 41.09	21	979378.5	979184.5	22.5	221.0
69	28 1.00	16 41.70	1	979395.1	979186.3	18.1	227.1
70	28 2.07	16 40.18	80	979387.0	979187.6	15.0	231.4

SUMMARY OF GRAVITY OBSERVATIONS ON TENERIFE

STATION NUMBER	LATITUDE NORTH	LONGITUDE WEST	ELEVATION (METRES)	OBSERVED GRAVITY	NORMAL GRAVITY	TERRAIN CORR.	BOUGUER ANOMALY
71	28 2.52	16 42.42	4	979403.6	979188.2	16.2	232.4
72	28 3.93	16 40.88	276	979359.9	979189.9	17.1	245.7
73	28 3.89	16 38.64	312	979349.6	979189.9	16.6	242.5
74	28 5.39	16 36.58	619	979285.5	979191.7	19.4	242.7
75	28 5.03	16 40.58	558	979304.9	979191.2	20.0	252.2
76	28 3.47	16 43.28	6	979407.6	979189.4	16.8	235.3
77	28 6.82	16 42.88	285	979368.9	979193.5	20.4	256.3
78	28 5.55	16 44.77	2	979415.1	979191.9	15.2	238.8
79	28 7.72	16 46.20	99	979401.2	979194.7	16.4	243.9
80	28 8.67	16 45.33	375	979351.6	979195.8	19.5	254.9
81	28 9.76	16 47.37	118	979401.3	979197.2	16.4	245.6
82	28 10.77	16 45.45	546	979321.7	979198.5	22.3	261.4
83	28 10.35	16 48.27	11	979417.8	979197.9	15.5	237.7
84	28 12.15	16 46.10	612	979312.7	979200.2	21.6	264.0
85	28 12.62	16 45.11	865	979260.1	979200.8	24.7	267.6
86	28 13.65	16 47.17	672	979289.6	979202.1	22.0	252.2
87	28 15.68	16 48.55	585	979308.6	979204.6	22.2	250.4
88	28 17.56	16 48.32	940	979246.6	979207.0	23.3	262.5
89	28 18.34	16 47.73	1112	979210.1	979207.9	27.1	265.4
90	28 20.43	16 51.71	745	979278.2	979210.6	24.0	249.8
91	28 20.92	16 48.13	648	979290.0	979211.2	24.9	239.6
92	28 19.39	16 45.44	1073	979206.4	979209.3	26.3	251.2
93	28 13.54	16 49.90	1	979419.0	979201.9	15.2	232.5
94	28 12.04	16 49.39	22	979413.9	979200.1	14.8	233.3
95	28 7.53	16 36.25	1033	979203.9	979194.4	25.2	254.0
96	28 7.38	16 38.81	1223	979169.0	979194.2	26.9	261.3
97	28 9.03	16 37.73	1467	979126.8	979196.3	29.2	271.1
98	28 10.88	16 39.13	2085	979002.1	979198.6	41.3	287.4
99	28 14.46	16 41.90	2024	979015.4	979203.1	38.1	280.1
100	28 13.66	16 41.21	2087	979009.1	979202.1	38.1	288.2
101	28 12.46	16 39.63	2033	979021.5	979200.6	36.7	289.2
102	28 12.11	16 38.09	2015	979021.1	979200.1	35.0	283.8
103	28 14.22	16 37.17	2247	978958.0	979202.8	40.5	272.7
104	28 13.48	16 35.78	2212	978971.1	979201.9	37.3	276.1
105	28 15.69	16 36.44	2727	978830.1	979204.6	56.7	263.1

SUMMARY OF GRAVITY OBSERVATIONS ON TENERIFE

STATION NUMBER	LATITUDE NORTH	LONGITUDE WEST	ELEVATION (METRES)	OBSERVED GRAVITY	NORMAL GRAVITY	TERRAIN CORR.	BOUGUER ANOMALY
106	28 15.58	16 34.69	2298	978950.6	979204.5	39.3	273.3
107	28 17.45	16 33.34	2106	978991.0	979206.8	37.3	269.0
108	28 13.97	16 32.39	2166	978967.6	979202.5	42.2	267.1
109	28 12.77	16 32.46	1809	979045.9	979201.0	37.8	266.8
110	28 15.61	16 32.10	2281	978944.5	979204.5	42.4	266.7
111	28 18.50	16 33.72	1865	979036.8	979205.1	38.1	260.7
112	28 19.30	16 31.39	1573	979102.5	979209.1	33.1	260.4
113	28 21.27	16 29.35	1047	979215.4	979211.6	28.2	254.3
114	28 21.50	16 30.92	826	979256.9	979211.9	26.7	247.1
115	28 22.91	16 30.93	345	979357.8	979213.7	21.1	238.4
116	28 21.65	16 52.13	3	979433.0	979212.1	19.3	240.8
117	28 21.87	16 45.49	122	979413.9	979212.4	17.1	244.5
118	28 20.15	16 45.15	515	979345.4	979210.2	20.9	265.4
119	28 21.43	16 43.24	111	979417.2	979211.8	18.5	247.5
120	28 23.06	16 44.12	18	979428.5	979213.9	17.8	236.2
121	28 21.92	16 51.96	5	979432.1	979212.4	19.6	240.4
122	28 21.88	16 50.20	19	979425.5	979212.4	22.4	239.5
123	28 22.02	16 47.55	135	979395.7	979212.6	20.2	232.0
124	28 20.87	16 47.13	476	979327.2	979211.1	22.6	239.8
125	28 22.46	16 40.38	231	979374.6	979213.1	22.2	232.7
126	28 23.21	16 38.28	68	979403.0	979214.0	19.8	223.2
127	28 22.92	16 35.07	202	979380.5	979213.7	21.2	230.9
127	28 22.65	16 34.79	261	979368.5	979213.3	21.9	232.5
128	28 21.93	16 38.50	495	979318.4	979212.4	22.4	233.5
129	28 21.98	16 36.74	658	979281.3	979212.5	26.8	235.3
130	28 21.47	16 34.08	665	979291.7	979211.9	24.9	245.9
131	28 22.16	16 32.69	461	979332.8	979212.7	21.3	239.3
132	28 28.23	16 25.63	322	979350.4	979220.4	28.3	226.7
133	28 26.18	16 27.00	419	979331.1	979217.8	22.2	224.5
134	28 25.55	16 27.64	391	979339.6	979217.0	21.5	227.1
135	28 25.05	16 28.86	285	979363.8	979216.4	21.5	229.4
136	28 24.46	16 32.78	8	979427.1	979215.6	15.9	229.1
137	28 21.24	16 32.17	900	979239.8	979211.4	26.4	245.7
138	28 17.67	16 30.66	2293	978934.3	979207.1	47.3	261.3
139	28 18.46	16 29.28	2194	978956.6	979208.1	48.5	262.8

SUMMARY OF GRAVITY OBSERVATIONS ON TENERIFE

STATION NUMBER	LATITUDE NORTH	LONGITUDE WEST	ELEVATION (METRES)	OBSERVED GRAVITY	NORMAL GRAVITY	TERRAIN CORR.	BOUGUER ANOMALY
140	28 20.19	16 28.36	1977	978996.7	979210.3	49.3	255.4
141	28 21.96	16 27.10	1903	979005.0	979212.5	52.6	249.1
142	28 22.92	16 25.96	1706	979049.4	979213.7	43.7	241.6
143	28 24.04	16 24.46	1589	979068.6	979215.1	43.9	234.7
144	28 25.19	16 23.20	1317	979136.9	979216.5	32.3	232.3
145	28 26.04	16 21.54	958	979220.6	979217.6	24.0	230.4
146	28 27.52	16 21.07	764	979276.9	979219.5	20.5	240.1
147	28 28.81	16 20.31	630	979306.7	979221.1	14.3	237.6
148	28 24.63	16 31.96	7	979429.1	979215.8	16.1	230.9

SUMMARY OF GRAVITY OBSERVATIONS ON HIERRO

STATION NUMBER	LATITUDE NORTH	LONGITUDE WEST	ELEVATION (METRES)	OBSERVED GRAVITY	NORMAL GRAVITY	TERRAIN CORR.	BOUGUER ANOMALY
1	27 48.36	17 54.78	571	979234.9	979170.6	36.9	222.4
2	27 47.94	17 53.13	2	979351.9	979170.1	28.4	210.6
3	27 49.40	17 53.57	7	979349.2	979171.9	28.9	207.7
4	27 46.07	17 54.77	1	979370.8	979167.8	33.8	237.0
5	27 49.24	17 55.05	557	979229.4	979171.7	37.5	213.5
6	27 49.19	17 55.70	528	979246.8	979171.6	35.5	222.8
7	27 49.17	17 56.52	490	979258.9	979171.6	35.9	227.2
8	27 48.72	18 2.23	553	979250.8	979171.0	36.2	233.4
9	27 48.34	18 1.37	652	979225.3	979171.6	43.7	235.8
10	27 49.93	17 55.26	362	979277.2	979172.5	34.5	216.1
11	27 47.20	17 55.95	937	979168.6	979169.1	46.3	244.7
12	27 46.33	17 56.61	1000	979162.7	979168.1	42.8	249.7
13	27 46.00	18 2.22	1089	979152.1	979167.7	43.6	259.2
14	27 45.62	18 1.57	1208	979115.5	979167.2	51.7	256.8
15	27 44.51	18 0.91	1320	979081.8	979165.8	55.9	252.1
16	27 44.08	18 0.29	1332	979074.5	979165.3	56.7	248.7
17	27 44.27	18 2.78	960	979177.3	979165.5	51.9	267.5
18	27 44.24	18 1.04	705	979234.0	979165.5	41.4	259.6
19	27 45.04	18 1.42	282	979333.6	979166.5	29.9	256.9
20	27 45.23	18 0.49	241	979340.8	979166.7	29.4	254.7
21	27 46.36	18 0.14	85	979371.7	979168.1	31.9	253.5
22	27 47.75	18 0.56	7	979378.9	979169.8	30.8	241.4
23	27 46.55	18 0.12	51	979381.3	979168.3	27.6	251.4
24	27 48.03	17 57.21	799	979201.9	979170.2	39.1	240.4
25	27 47.10	18 1.98	975	979169.6	979169.0	43.7	251.3
26	27 45.04	18 2.81	255	979336.5	979166.5	30.9	255.0
27	27 44.78	18 5.76	285	979317.6	979166.2	36.5	248.4
28	27 45.16	18 5.96	48	979376.3	979166.6	29.4	249.3
29	27 46.04	18 7.21	1	979377.3	979167.7	29.2	239.0
30	27 45.53	18 8.53	48	979359.8	979167.1	32.9	235.8
31	27 45.68	18 8.26	30	979366.3	979167.3	32.8	238.2
32	27 44.81	18 4.43	255	979333.0	979166.2	33.6	254.5
33	27 45.05	18 2.11	232	979342.0	979166.5	29.9	254.7
34	27 45.37	18 0.27	284	979326.3	979166.9	36.4	256.1
35	27 43.51	18 5.03	1210	979104.2	979164.6	59.2	255.7

SUMMARY OF GRAVITY OBSERVATIONS ON HIERRO

STATION NUMBER	LATITUDE NORTH	LONGITUDE WEST	ELEVATION (METRES)	OBSERVED GRAVITY	NORMAL GRAVITY	TERRAIN CORR	BOUGUER ANOMALY
36	27 43.26	18 3.97	1296	979081.4	979164.3	60.8	253.0
37	27 45.27	17 56.62	863	979192.9	979166.8	41.5	250.8
38	27 44.65	18 3.28	857	979185.9	979166.0	43.9	245.7
39	27 45.24	18 2.18	1157	979132.6	979166.7	47.2	258.7
40	27 44.57	18 1.80	1164	979122.1	979165.9	48.7	252.0
41	27 43.25	18 1.37	998	979144.7	979164.3	45.5	237.8
42	27 42.30	18 8.70	110	979332.5	979163.1	31.3	224.1
42	27 42.65	18 8.45	141	979336.3	979163.5	32.5	235.2
43	27 43.71	18 7.27	718	979220.3	979164.8	42.1	248.3
44	27 43.13	18 5.70	994	979154.0	979164.1	51.0	251.9
45	27 42.26	18 1.38	890	979187.0	979163.0	48.8	253.7
46	27 42.32	18 0.16	956	979170.0	979163.1	48.2	250.1
46	27 42.32	18 0.26	929	979178.3	979163.1	39.5	251.9
47	27 43.58	18 1.12	1349	979074.9	979164.7	58.9	255.5
48	27 43.40	18 2.72	1390	979062.6	979164.4	65.0	256.3
49	27 42.47	18 1.10	900	979173.3	979163.3	48.9	242.0
50	27 41.75	18 0.94	761	979203.4	979162.4	37.1	239.7
51	27 41.33	18 1.65	602	979226.8	979161.9	34.7	231.4
52	27 38.34	18 1.27	2	979345.3	979158.2	29.5	217.0
53	27 38.68	18 0.47	112	979325.6	979158.6	27.6	218.4
54	27 39.55	18 0.83	269	979297.5	979159.7	29.5	224.4
55	27 46.04	18 1.16	70	979375.1	979167.7	23.9	246.2
56	27 47.04	17 53.95	4	979358.4	979169.0	32.9	223.1

SUMMARY OF GRAVITY OBSERVATIONS ON FERNANDO DE NORONHA

STATION NUMBER	LATITUDE SOUTH	LONGITUDE WEST	ELEVATION (METRES)	OBSERVED GRAVITY	NORMAL GRAVITY	TERRAIN CORR.	BOUGUER ANOMALY
1	3 51.00	32 25.68	55	978301.6	978072.3	0.5	241.5
2	3 52.04	32 25.65	5	978307.0	978072.4	0.2	235.9
3	3 51.40	32 25.92	54	978298.4	978072.3	0.3	237.9
4	3 51.50	32 25.61	41	978302.9	978072.3	0.1	239.4
5	3 51.72	32 25.48	36	978303.6	978072.4	0.3	239.1
6	3 51.48	32 25.11	74	978296.8	978072.3	0.5	242.7
7	3 51.33	32 24.76	19	978313.9	978072.3	0.5	244.1
8	3 51.57	32 24.65	1	978316.3	978072.3	0.8	245.0
9	3 51.82	32 25.10	52	978303.0	978072.4	1.6	243.2
10	3 50.83	32 24.84	93	978297.2	978072.2	0.6	245.3
11	3 50.73	32 24.51	85	978298.1	978072.2	0.5	244.4
12	3 49.97	32 24.06	16	978311.8	978072.0	0.2	243.4
13	3 52.86	32 27.58	2	978289.9	978072.6	3.0	220.7
14	3 52.59	32 27.62	133	978261.7	978072.5	4.1	221.5
15	3 52.20	32 27.23	116	978267.8	978072.5	2.7	222.6
16	3 51.96	32 26.84	148	978261.8	978072.4	3.0	223.8
17	3 51.34	32 26.34	65	978292.0	978072.3	0.6	234.1
18	3 50.44	32 24.77	18	978310.7	978072.1	0.7	243.1
19	3 50.88	32 24.53	86	978297.1	978072.2	0.5	243.7
20	3 50.74	32 25.70	4	978310.0	978072.2	1.3	239.9

SUMMARY OF GRAVITY OBSERVATIONS ON MADEIRA

STATION NUMBER	LATITUDE NORTH	LONGITUDE WEST	ELEVATION (METRES)	OBSERVED GRAVITY	NORMAL GRAVITY	TERRAIN CORR.	BOUGUER ANOMALY
1	32 48.72	17 15.12	392	979695.4	979563.0	31.3	247.0
2	32 51.40	17 11.25	479	979669.8	979566.7	32.6	237.3
3	32 50.15	17 9.02	597	979647.0	979565.0	35.1	243.8
4	32 43.33	17 7.98	846	979577.7	979555.7	43.5	245.2
5	32 45.67	17 8.80	1265	979496.4	979558.8	49.3	255.6
6	32 49.30	17 11.37	1022	979554.7	979563.8	43.8	251.7
7	32 48.22	17 2.67	6	979783.7	979562.3	31.7	254.4
8	32 45.03	17 0.90	992	979588.0	979558.0	35.8	276.4
9	32 41.87	17 7.20	479	979659.0	979553.7	38.0	245.0
10	32 40.22	17 2.88	370	979692.5	979551.4	30.2	249.9
11	32 38.33	16 56.12	261	979721.2	979548.8	29.8	257.6
12	32 38.55	16 53.67	18	979781.1	979549.1	25.2	260.9
13	32 42.50	16 52.97	1376	979496.1	979554.5	43.6	277.3
14	32 43.92	16 55.47	1818	979382.1	979556.5	68.2	279.7
15	32 48.63	16 53.32	347	979719.6	979562.9	21.8	252.2
16	32 46.98	16 50.87	54	979799.4	979560.6	23.2	273.5
17	32 44.42	16 49.25	598	979685.9	979557.1	26.8	282.5
18	32 38.82	16 50.22	227	979723.6	979549.5	29.9	252.3
19	32 41.28	16 46.22	50	979775.2	979552.9	23.1	256.1
20	32 44.68	16 41.77	165	979751.1	979557.5	19.3	247.8
21	32 46.20	16 49.35	7	979819.0	979559.6	19.8	280.6
22	32 40.02	17 3.63	6	979773.2	979551.1	27.2	250.6
23	32 42.80	16 48.30	752	979629.6	979554.9	29.9	264.3

GRAVITY OBSERVATIONS ON THE CAPE VERDE ISLANDS BY THE SERVICO METEOROLOGICO NACIONAL, PORTUGAL

(1) S. VICENTE

STATION NUMBER	LATITUDE NORTH	LONGITUDE WEST	ELEVATION METRES	OBSERVED GRAVITY	NORMAL GRAVITY	BOUGUER ANOMALY
1	16 53.10	24 59.60	8	978753.8	978483.6	271.9
2	16 54.40	24 54.40	280	978662.0	978484.6	236.8
3	16 48.80	24 56.00	484	978612.7	978480.0	235.5
4	16 48.70	25 3.60	302	978649.2	978479.9	233.5
5	16 51.20	25 3.90	571	978576.4	978482.0	215.7
6	16 50.40	24 58.30	61	978750.2	978481.3	281.7
7	16 49.60	25 0.20	535	978621.6	978480.7	254.6
8	16 47.00	24 58.80	6	978724.3	978478.5	247.0
9	16 52.00	24 56.30	750	978550.7	978482.6	227.4
10	16 54.00	24 55.10	5	978728.5	978484.3	245.2
11	16 51.30	24 52.20	140	978701.0	978482.1	248.7
12	16 49.50	24 52.30	38	978731.9	978480.6	259.4
13	16 54.20	25 0.30	57	978725.8	978484.5	253.4
14	16 53.10	25 2.10	84	978718.7	978483.6	252.9
15	16 52.40	25 0.30	1	978760.4	978483.0	277.7
(2) SANTA LUZIA						
16	16 44.70	24 45.20	7	978726.9	978476.6	251.8

GRAVITY OBSERVATIONS ON THE CAPE VERDE ISLANDS BY THE SERVICO METEOROLOGICO NACIONAL, PORTUGAL

(3) SANTO ANTAO

STATION NUMBER	LATITUDE NORTH		LONGITUDE WEST		ELEVATION METRES	OBSERVED GRAVITY	NORMAL GRAVITY	BOUGUER ANOMALY
17	17	4.40	25	3.60	612	978573.4	978493.0	210.3
18	17	3.20	25	3.40	323	978639.5	978492.0	216.1
19	17	6.40	25	2.10	1584	978337.8	978494.7	179.5
20	17	0.20	25	3.80	11	978707.1	978489.5	219.9
21	17	1.10	25	6.10	45	978705.1	978490.3	224.4
22	17	1.20	25	5.20	25	978708.7	978490.3	223.7
23	17	6.40	24	59.50	858	978499.3	978494.7	186.7
24	17	6.00	25	11.10	1657	978346.3	978494.4	203.8
25	16	59.50	25	9.60	172	978679.6	978488.9	227.2
26	17	2.70	25	13.10	754	978584.0	978491.6	252.5
27	16	55.90	25	12.50	292	978635.0	978485.9	211.0
28	17	4.10	25	2.20	616	978574.9	978492.8	212.9
29	17	12.40	25	5.90	3	978721.7	978499.8	222.6
30	17	10.00	25	1.50	40	978709.7	978497.7	220.4
31	17	10.00	25	6.20	109	978712.0	978497.7	237.4
32	17	10.60	25	9.30	48	978719.8	978498.3	231.8
33	16	55.70	25	19.00	89	978687.5	978485.7	220.7
34	16	59.10	25	18.40	916	978499.6	978488.6	205.5
35	17	3.00	25	21.80	34	978711.3	978491.8	226.7
36	16	58.80	25	14.80	1521	978371.1	978488.3	205.6
37	16	55.40	25	15.70	0	978705.0	978485.5	219.5
38	16	57.60	25	18.90	14	978714.0	978487.3	229.6
39	17	6.30	25	4.00	1294	978440.5	978494.6	220.6
40	17	5.00	25	16.30	1092	978493.4	978493.5	231.7
41	17	2.10	25	18.00	1979	978247.0	978491.1	176.0
42	17	7.00	25	16.10	212	978683.5	978495.2	233.4
43	16	57.40	25	9.80	50	978694.8	978487.2	218.3
44	16	59.60	25	11.80	572	978591.5	978489.0	223.9
45	17	8.50	25	5.50	999	978512.0	978496.5	227.6
46	17	10.80	25	3.50	6	978721.8	978498.4	224.6
47	17	8.60	25	8.70	312	978650.5	978496.6	220.2

GRAVITY OBSERVATIONS ON THE CAPE VERDE ISLANDS BY THE SERVICO METEOROLOGICO NACIONAL, PORTUGAL

STATION NUMBER	LATITUDE NORTH		LONGITUDE WEST		ELEVATION METRES	OBSERVED GRAVITY	NORMAL GRAVITY	BOUGUER ANOMALY
(4) SAL								
48	16	44.90	22	57.40	52	978736.4	978476.8	270.7
49	16	44.40	22	59.30	42	978743.5	978476.3	276.1
50	16	51.00	22	55.50	11	978686.6	978481.8	207.1
51	16	47.40	22	56.60	11	978714.2	978478.8	237.7
52	16	45.80	22	54.20	15	978707.1	978477.5	232.8
53	16	47.80	23	0.00	14	978711.7	978479.2	235.5
54	16	45.30	22	59.50	5	978745.4	978477.1	269.4
55	16	48.00	22	54.70	7	978702.3	978479.3	224.5
56	16	38.70	22	54.00	99	978663.9	978471.6	213.3
57	16	40.60	22	56.80	3	978711.0	978473.2	238.3
58	16	41.60	22	59.40	6	978722.2	978474.0	249.4
59	16	42.20	22	54.30	61	978696.4	978474.5	234.8
60	16	38.30	22	56.50	22	978694.0	978471.3	227.4
61	16	35.70	22	54.70	4	978681.4	978469.2	213.1
(5) S. NICOLAU								
62	16	36.90	24	18.10	90	978676.1	978470.2	225.0
63	16	35.90	24	17.30	184	978656.6	978469.3	226.2
64	16	33.80	24	17.00	44	978674.2	978467.6	215.9
65	16	33.20	24	21.70	11	978669.4	978467.1	204.6
66	16	31.00	24	19.00	540	978540.9	978465.3	190.3
67	16	40.20	24	19.60	24	978668.1	978472.9	200.3
68	16	36.20	24	25.30	4	978672.2	978469.6	203.5
69	16	39.10	24	24.60	436	978558.1	978472.0	178.7
70	16	38.50	24	13.30	111	978655.7	978471.5	207.8
71	16	36.30	24	10.50	347	978601.1	978469.7	205.1
72	16	37.20	24	7.80	24	978661.3	978470.4	196.0
73	16	36.00	24	14.00	138	978668.5	978469.4	228.4
74	16	33.20	24	5.40	10	978664.8	978467.1	199.9
75	16	35.50	24	3.90	445	978563.6	978469.0	189.1
76	16	37.30	24	20.30	721	978521.2	978470.5	203.8
77	16	37.00	24	22.20	784	978504.8	978470.2	201.0
78	16	34.80	24	17.30	184	978649.4	978468.4	220.1

GRAVITY OBSERVATIONS ON THE CAPE VERDE ISLANDS BY THE SERVICO METEOROLOGICO NACIONAL, PORTUGAL

(6) BOA VISTA

STATION NUMBER	LATITUDE NORTH	LONGITUDE WEST	ELEVATION METRES	OBSERVED GRAVITY	NORMAL GRAVITY	BOUGUER ANOMALY
79	16 10.70	22 55.40	4	978698.4	978448.9	250.4
80	16 7.60	22 50.30	134	978655.4	978446.4	237.5
81	16 2.20	22 55.20	85	978679.6	978442.1	255.5
82	16 2.90	22 52.80	50	978676.7	978442.7	244.7
83	16 3.30	22 47.60	52	978665.1	978443.0	233.2
84	16 0.80	22 48.80	42	978686.2	978441.0	254.1
85	16 5.90	22 54.80	74	978659.6	978445.1	230.3
86	16 13.60	22 47.60	10	978701.4	978451.2	252.3
87	16 12.70	22 55.00	146	978667.0	978450.5	247.5
88	16 3.50	22 50.70	49	978662.8	978443.1	230.1
89	16 7.60	22 43.70	29	978712.5	978446.4	272.2
90	16 7.80	22 53.70	13	978672.4	978446.6	228.6
91	16 10.30	22 51.10	139	978652.9	978448.6	233.8
92	16 8.60	22 47.20	75	978667.3	978447.2	236.0
93	16 11.10	22 46.80	70	978689.8	978449.2	255.4
94	16 4.60	22 57.10	167	978665.4	978444.0	256.9
95	15 58.60	22 48.20	28	978681.3	978439.2	247.9
96	16 6.10	22 50.20	40	978678.3	978445.2	241.6
97	16 5.60	22 47.40	76	978659.2	978444.8	230.5
98	16 1.20	22 52.00	96	978669.8	978441.3	248.9
99	16 11.80	22 42.80	0	978702.3	978449.8	252.5
100	16 1.30	22 44.90	5	978704.9	978441.4	264.6
101	16 2.60	22 42.00	54	978680.1	978442.4	249.1
102	16 9.80	22 42.00	13	978713.9	978448.2	268.5
103	16 5.00	22 44.30	78	978697.5	978444.3	269.7
104	16 0.30	22 56.00	3	978681.6	978440.6	241.5
105	16 9.40	22 44.30	25	978712.0	978447.9	269.5
106	15 58.70	22 53.20	15	978677.7	978439.3	241.5
107	16 6.30	22 41.60	71	978677.6	978445.4	247.3
108	16 10.70	22 55.40	16	978696.6	978448.9	251.0

GRAVITY OBSERVATIONS ON THE CAPE VERDE ISLANDS BY THE SERVICO METEOROLOGICO NACIONAL, PORTUGAL (7)

STATION NUMBER	LATITUDE NORTH		LONGITUDE WEST		ELEVATION METRES	OBSERVED GRAVITY	NORMAL GRAVITY	BOUGUER ANOMALY
109	14	54.90	23	31.00	27	978607.3	978390.2	222.8
110	15	8.40	23	33.80	199	978569.3	978400.4	211.2
111	15	7.50	23	46.30	4	978618.5	978399.7	219.7
112	15	3.40	23	46.50	29	978608.7	978396.6	218.3
113	15	2.10	23	27.90	16	978600.9	978395.6	208.7
114	14	56.20	23	40.60	39	978605.7	978391.2	222.8
115	14	58.40	23	29.50	146	978587.1	978392.8	225.3
116	15	1.80	23	36.60	826	978458.7	978395.4	238.7
117	14	54.80	23	36.70	124	978582.3	978390.2	218.4
118	15	2.30	23	30.80	64	978603.8	978395.8	221.6
119	14	57.40	23	36.50	302	978583.3	978392.1	255.3
120	14	59.20	23	32.30	437	978541.8	978393.4	241.1
121	14	58.50	23	34.70	311	978584.5	978392.9	257.6
122	14	55.20	23	33.50	73	978604.2	978390.4	229.2
123	14	59.00	23	26.40	8	978583.6	978393.3	191.9
124	14	59.30	23	40.00	391	978559.8	978393.5	249.3
125	15	5.60	23	30.60	136	978579.4	978398.2	210.0
126	15	4.70	23	34.40	184	978584.6	978397.6	226.1
127	15	12.50	23	45.30	386	978517.2	978403.5	195.6
128	15	1.20	23	33.90	250	978594.2	978394.9	252.3
129	15	10.70	23	36.10	45	978602.0	978402.1	209.4
130	15	8.00	23	39.40	423	978536.6	978400.1	226.3
131	15	10.40	23	42.40	706	978465.1	978401.9	213.1
132	15	4.00	23	39.90	666	978501.1	978397.0	245.5
133	15	6.70	23	42.00	718	978474.1	978399.1	227.4
134	15	6.40	23	44.70	362	978560.8	978398.8	238.8
135	15	5.80	23	37.30	310	978561.6	978398.4	229.0
136	15	2.70	23	42.50	585	978504.2	978396.1	232.3
137	15	0.20	23	42.90	453	978513.9	978394.2	215.9
138	15	1.80	23	38.70	908	978441.5	978395.4	238.9
139	15	8.00	23	36.30	54	978609.7	978400.1	221.1
140	15	11.40	23	38.40	256	978556.0	978402.6	207.7
141	15	13.20	23	38.00	105	978585.9	978404.0	204.3
142	15	14.20	23	39.20	165	978564.5	978404.8	194.8
143	15	18.50	23	43.00	182	978584.2	978408.0	214.8

GRAVITY OBSERVATIONS ON THE CAPE VERDE ISLANDS BY THE SERVICO METEOROLOGICO NACIONAL, PORTUGAL

(7) SANTIAGO (continued)

STATION NUMBER	LATITUDE NORTH	LONGITUDE WEST	ELEVATION METRES	OBSERVED GRAVITY	NORMAL GRAVITY	BOUGUER ANOMALY
144	15 14.60	23 42.50	306	978541.2	978405.1	201.1
145	15 16.50	23 45.60	25	978603.7	978406.5	202.5
146	15 5.30	23 42.70	233	978597.2	978398.0	248.6
147	15 5.00	23 39.40	581	978522.8	978397.8	248.4
(8) FOGO						
148	15 2.40	24 20.60	10	978612.9	978395.8	219.1
149	15 0.20	24 21.10	1342	978317.7	978394.2	208.4
150	14 58.40	24 22.60	1648	978286.7	978392.8	243.7
151	14 56.90	24 20.90	2829	977958.5	978391.7	167.4
152	14 54.40	24 21.50	1802	978255.4	978389.9	248.1
153	15 1.80	24 23.40	524	978505.8	978395.4	221.7
154	14 53.70	24 29.30	325	978577.1	978389.3	256.9
155	14 56.30	24 28.40	439	978570.6	978391.3	272.5
156	14 59.40	24 28.00	434	978535.2	978393.6	233.8
157	14 50.80	24 23.70	536	978564.1	978387.2	290.7
158	14 53.60	24 30.60	73	978624.1	978389.3	250.3
159	14 51.00	24 27.80	120	978621.6	978387.3	259.8
160	14 59.40	24 25.40	1078	978398.0	978393.6	233.3
161	14 51.40	24 20.30	536	978543.4	978387.6	269.6
162	14 54.40	24 18.20	544	978506.4	978389.9	232.0
163	14 56.50	24 25.70	1256	978379.7	978391.4	254.9
164	14 53.60	24 25.00	1040	978449.6	978389.3	281.1
165	14 58.60	24 18.20	71	978601.9	978393.0	224.0
(9) BRAVA						
166	14 52.20	24 42.60	535	978493.3	978388.2	218.7
167	14 52.20	24 44.10	338	978532.3	978388.2	215.8
168	14 52.30	24 41.70	336	978536.4	978388.3	219.4
169	14 49.70	24 41.60	673	978451.0	978386.4	207.4
170	14 50.00	24 43.60	764	978442.1	978386.6	217.7
171	14 53.40	24 41.70	237	978555.1	978389.1	216.4

GRAVITY OBSERVATIONS ON THE CAPE VERDE ISLANDS BY THE SERVICO METEOROLOGICO NACIONAL, PORTUGAL (10) MAIO

STATION NUMBER	LATITUDE NORTH	LONGITUDE WEST	ELEVATION METRES	OBSERVED GRAVITY	NORMAL GRAVITY	BOUGUER ANOMALY
172	15 10.80	23 14.20	15	978647.9	978402.2	248.9
173	15 9.40	23 10.00	51	978671.7	978401.1	281.4
174	15 12.90	23 14.10	9	978646.2	978403.8	244.3
175	15 7.60	23 13.00	20	978628.1	978399.8	232.5
176	15 9.30	23 6.80	53	978648.9	978401.0	259.1
177	15 16.30	23 13.80	19	978639.5	978406.4	237.2
178	15 19.60	23 11.40	7	978674.3	978408.9	266.9
179	15 17.80	23 8.60	24	978647.0	978407.5	244.5
180	15 13.50	23 10.80	50	978673.6	978404.2	280.0
181	15 12.30	23 7.10	36	978657.9	978403.3	262.2
182	15 16.50	23 9.70	82	978642.0	978406.5	252.9
183	15 15.00	23 6.60	19	978643.0	978405.4	241.6
184	15 8.10	23 13.20	21	978631.2	978400.1	235.6

GRAVITY OBSERVATIONS ON THE GUINEA ISLANDS BY THE SERVICO METEOROLOGICO NACIONAL, PORTUGAL

(1) S. TOME

STATION NUMBER	LATITUDE NORTH	LONGITUDE EAST	ELEVATION METRES	OBSERVED GRAVITY	NORMAL GRAVITY	BOUGUER ANOMALY
0	0 22.60	6 42.90	10.0	978281.2	978049.2	234.1
1	0 20.50	6 32.80	234.8	978185.5	978049.2	186.2
2	0 22.60	6 37.00	267.3	978191.6	978049.2	199.1
3	0 15.80	6 36.40	813.7	978086.7	978049.1	210.3
4	0 14.70	6 38.40	454.3	978176.4	978049.1	223.8
5	0 22.90	6 39.10	273.2	978196.4	978049.2	205.2
6	0 19.30	6 42.40	165.6	978266.5	978049.2	252.5
7	0 17.30	6 44.60	143.2	978244.0	978049.1	225.3
8	0 20.90	6 38.80	428.8	978176.1	978049.2	217.9
9	0 18.50	6 30.00	156.3	978203.5	978049.1	187.5
10	0 15.90	6 28.50	99.7	978228.8	978049.1	200.9
11	0 14.00	6 45.10	88.3	978240.1	978049.1	209.8
12	0 13.70	6 41.10	505.5	978145.1	978049.1	203.3
13	0 10.20	6 40.90	54.7	978250.8	978049.0	213.4
14	0 12.40	6 37.40	431.6	978173.5	978049.1	216.1
15	0 9.80	6 37.70	268.6	978211.7	978049.0	219.7
16	0 17.30	6 38.20	832.9	978092.3	978049.1	220.0
17	0 20.40	6 35.40	646.0	978108.4	978049.2	196.4
18	0 21.10	6 34.80	422.3	978144.2	978049.2	184.7
19	0 6.90	6 37.40	282.4	978203.8	978049.0	214.7
20	0 5.60	6 36.90	37.9	978264.2	978049.0	223.2
21	0 7.00	6 35.80	110.7	978254.7	978049.0	229.2
22	0 8.80	6 35.10	226.4	978242.3	978049.0	241.3
23	0 17.40	6 41.00	323.0	978225.8	978049.1	245.2
24	0 13.40	6 30.30	104.7	978241.3	978049.1	214.4
25	0 18.00	6 38.30	882.0	978077.2	978049.1	215.3
26	0 17.80	6 33.80	655.4	978113.1	978049.1	203.1
27	0 2.10	6 32.40	11.0	978253.5	978049.0	206.8
28	0 3.60	6 33.50	275.0	978209.4	978049.0	218.8
29	0 3.40	6 32.10	157.1	978226.9	978049.0	211.2
30	0 4.90	6 33.80	270.5	978213.9	978049.0	222.3
31	0 6.50	6 31.30	6.3	978271.1	978049.0	223.4

GRAVITY OBSERVATIONS ON THE GUINEA ISLANDS BY THE SERVICO METEOROLOGICO NACIONAL, PORTUGAL

(2) PRINCIPE

STATION NUMBER	LATITUDE NORTH	LONGITUDE EAST	ELEVATION METRES	OBSERVED GRAVITY	NORMAL GRAVITY	BOUGUER ANOMALY
1	1 38.60	7 25.40	3.0	978255.7	978053.2	203.1
2	1 39.80	7 22.40	153.8	978221.8	978053.3	201.1
3	1 36.10	7 21.30	67.0	978264.0	978053.0	225.2
4	1 36.40	7 22.00	10.0	978272.4	978053.0	221.5
5	1 41.40	7 26.70	108.8	978211.1	978053.5	180.7
6	1 33.60	7 25.20	3.6	978256.0	978052.8	203.9
7	1 37.70	7 27.60	97.4	978220.4	978053.2	187.9